Parametric Design for Optimized Concrete Through Girder Bridge Design

A case study

Author: P.L. van Westrienen
Date: March 8 2025

TU Delft

Witteveen + Bos

Parametric Design for Optimized Concrete Through Girder Bridge Design

A case study

By

P.L. (Peter) van Westrienen

In partial fulfilment of the requirements for the degree of:

Master of Science
in Civil Engineering

at the Delft University of Technology,
to be defended publicly on Monday March 17, 2025 at 11:00

Student number: 5173507

Supervisor:	Ir. B. Jongstra,	Witteveen + Bos
Thesis committee:	Prof. dr. ir. Y. Yang,	TU Delft
	Prof. dr. ir. M.A.N. Hendriks	TU Delft
	Prof. dr. Z. Li,	TU Delft

Cover image: Suspended through girder bridge Terneuzen (Van der Horst, n.d.)

Preface

In front of you lies the master thesis “Parametric Design for Optimized Concrete Through Girder Bridge Design; A case study” that concludes my academic journey at the Delft University of Technology. Completed between September 2024 and March 2025, this work fulfils the graduation requirements for the Master of Science in Civil Engineering.

For this research project I have been able to combine my interest and passion for civil engineering, design and programming. The resulting work not only showcases the knowledge acquired during my university years but also demonstrates its practical application. With a code repository of more than 16000 lines of code (equivalent to approximately 350 printed pages), I have also been able to apply my knowledge programming to create a final product that represents a significant personal achievement.

I want to thank Bert Jongstra, my daily supervisor at Witteveen + Bos for his invaluable support and the insights he was able to share with me not only during my time as graduate student, but also for his help with conceptualizing and structuring my research in the early stages of my thesis preparations. Next to that I want to thank Prof. Yuguang Yang, Prof. Max Hendriks and Prof. Zili Li for their academic expertise and perspectives that significantly improved this academic study.

It is my hope that you will find this research and its conclusions both interesting and inspiring.

Peter van Westrienen

Nijmegen, March 10 2025

Abstract

This master thesis explores the optimization of concrete through girder bridge design using a parametric design approach, focusing on reducing material usage and optimizing for costs and environmental performance through iterative design improvements. The research addresses a critical need in the Netherlands, where numerous bridges are approaching the end of their design life and require replacement or renovation, by allowing for rapid and efficient concrete through girder bridge design.

The primary objective is to develop a comprehensive parametric model that allows for systematic evaluation and iterative optimization of design parameters. By integrating python scripting, computational algorithms and external finite elements modelling software, the study aims to provide a parametric design tool that serves as a novel approach the bridge design that yields:

- Flexible tool for structural engineers
- Iterative optimization of structural designs by:
    - Minimization of material usage
    - Lower environmental impact
    - Lower construction costs
- Quicker design process
- Reduction of the cost of change during the design cycle

Key research features include focusing on single-span, single-track train bridges with spans of 25-45 meters and ensuring compliance with Dutch Eurocode and Prorail standards. To achieve this a comprehensive literature review is conducted and a case study of the train bridge spanning the channel 'nieuw Maximakanaal' is used.
The parametric model also computes an indication of environmental impact and material costs such that generated designs can be evaluated on these criteria.

To evaluate the effectiveness of the parametric model a reference design is considered that fits the scope constraints of the parametric model, namely the through girder bridge at the station of Bilthoven.
To optimize the design of this bridge three redesigns have been generated using the parametric model. The three considered redesigns are:

- Design featuring the same cross-section geometry as the reference design
- Design featuring a 'cut-out' in the centre of the cross-section to save material
- Design featuring an optimized geometry by reducing girder width

For each redesign the pre-stressing and reinforcement layout has been iteratively optimized by getting material usages as close as possible to 100%.

From the three considered redesigns, the optimal redesign manages to reduce material costs by 10.78% and environmental impact costs 11.07%. This is achieved by reducing the thickness of the girder cross-section from 1500 mm as in the reference design to 1200 mm and iteratively optimizing the reinforcement and pre-stressing layout.

The study concludes that the developed parametric model successfully optimizes concrete through girder bridge designs, resulting in significant reductions in material usage and environmental impact for a preliminary design. The model demonstrates the potential for achieving more sustainable and cost-effective bridge designs while meeting all the requirements.
By addressing the combination of structural engineering, computational modelling and sustainability, this thesis contributes to a novel approach of bridge design that can potentially change infrastructure development practices in the Netherlands.

Contents

1 Introduction

Concrete through girder bridges are commonly used in the Netherlands for railway crossings with spans ranging from 25 to 45 meters. A notable example is the bridge connecting the Westerscheldetunnel to the freight rail line serving Dow Benelux in Terneuzen, as shown in Figure 1. This bridge demonstrates an innovative design combining steel and concrete elements to suspend the concrete through girders by steel arch frames.

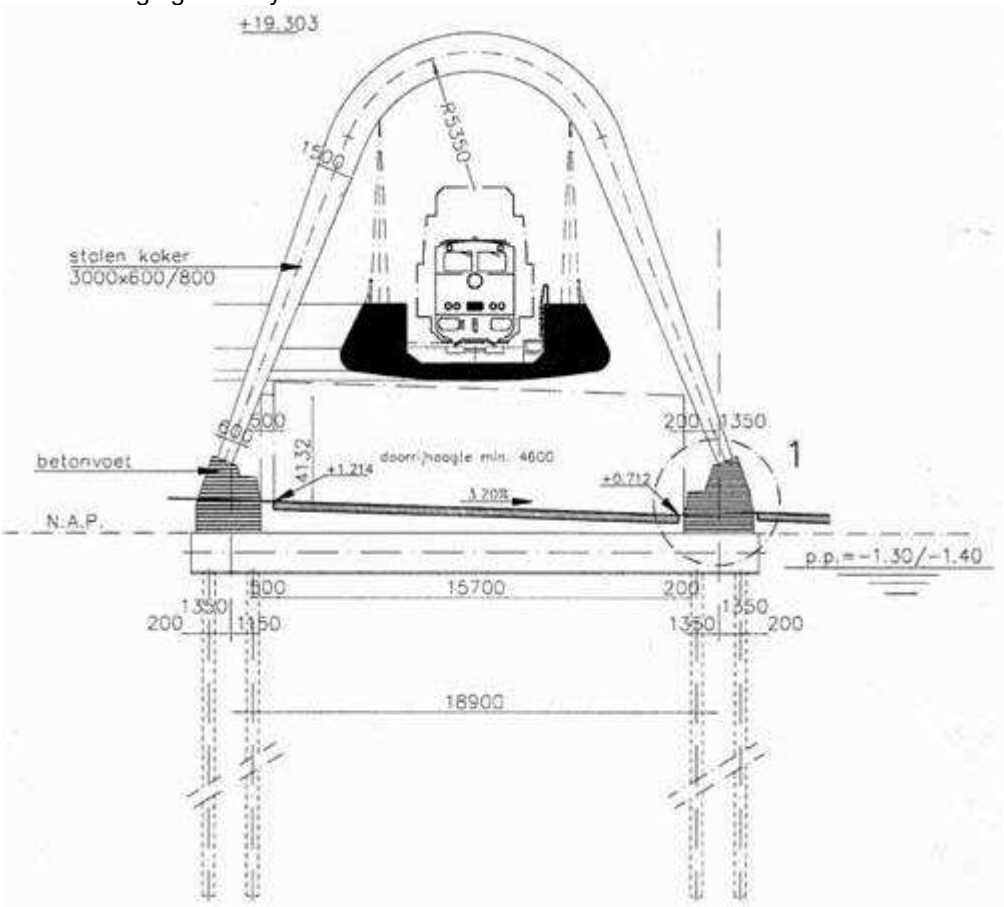

Figure 1: Cross-section concrete through girder bridge Terneuzen (Ossendrijver, n.d.)

Concrete through girder bridges provide the advantage of maintaining a low required free height, even for long spans, due to their slender decks.
However, these bridges are characterized by robust construction. The primary loads are supported by prestressed girders, which are reinforced with stirrups to effectively resist shear and torsion forces. The deck itself can also be prestressed, contributing to a more slender profile. Additionally, extensive suspension reinforcement is necessary to ensure structural integrity. Lastly, the prestressing anchors and reinforcement located near the supports require considerable space, resulting in large girder cross-sections.

1.1 Research problem

While these design choices ensure the structural robustness of the bridges, they also lead to an increased use of materials. This in turn impacts both the affordability and sustainability of the bridge construction.
Knowing that 25 bridges under management by the Ministry of Infrastructure and Water Management in the Netherlands have already passed the end of their design life, and 543 have already passed two thirds of the design life, there will be significant maintenance and construction of new bridges in the coming years (Kompeer & Schellevis, 2021). Combining this with the aim of the ministry to operate in a circular manner by 2030 and their responsibility in renovation and construction of bridges (Ministerie van Infrastructuur en Waterstaat, 2024), there is a clear and pressing need to optimize bridge designs. This optimization should reduce material usage without compromising structural performance, addressing both environmental and financial concerns.

At the moment, there is a lack of generic integral models that can systematically evaluate and optimize design parameters to minimize material usage while maintaining structural integrity. Developing a parametric design model could fill this gap, providing a powerful tool for engineers to create more efficient and sustainable bridge designs. Reducing the modelling and calculation time for engineers can also open up the door for more computationally expensive models, because the model is less prone to errors. The advantage of this increase in complexity is that it can yield more accurate long term results for FEA models (Canestro et al., 2021).
Within this context Fu & Wang (2014) state that the future task of the bridge engineer should not be to determine which models are appropriate or how they should be created. The routine work of establishing mechanic models and redoing calculations should be automated to leave the engineer to the creative work for finding solutions to the design problems at hand.
This research aims to address this underexplored potential for optimizing concrete through girder bridges by developing an integral way of designing bridges.

1.2 Research objective

The objective of this research project is to develop a parametric tool that can systematically evaluate the effect of changing design parameters. This would allow an engineer to achieve more efficient and sustainable bridge designs.
By integrating programming and construction techniques into the parametric model, this study provides a comprehensive tool for engineers to balance the demands of structural performance, cost-effectiveness, and sustainability. By incorporating automation algorithms, parametric models can allow for quick iterative design optimization. Also, they can be easily adjusted to accommodate different span lengths and design requirements, making it versatile tool for various bridge projects.
This approach not only builds on existing structural analysis and pre-stressing techniques but also pushes the boundaries by introducing a systematic method to minimize material usage. Thus, the research aims to add a new dimension to the existing body of literature by focusing on material efficiency and sustainability for concrete through girder bridges.
The novelty lies in the potential development of new design methodologies and the application design techniques that have not been fully explored for concrete through girder bridge design.

1.3 Scope

The project aims to deliver a functional parametric model, focusing on practical improvements rather than theoretical advancements at the detail level of a preliminary design.
This research is focused on optimizing the design of the superstructure of a concrete through girder bridges for single track train traffic, specifically targeting span lengths ranging from 25 to 45 meters that are not on a high speed line and feature a ballast track. This research limits itself to single span bridges.
The main challenge will be to develop a parametric model that systematically evaluates and optimizes various design parameters to minimize material usage and enhance sustainability while adhering to structural performance requirements. The model will be developed to comply with the Dutch Eurocode norms and the Prorail OVS norms. Key features of the model will include the automation of FEM model creation, cross-section and detail calculations, as well as the ability to optimize material usage and sustainability by refining reinforced cross-sections and pre-stressing layouts.

1.4 Research questions

The main research question for this project is '*How can a parametric model be set-up to allow for optimal design of concrete through girder bridges in terms of sustainability and costs?*'. To answer this research question multiple sub-questions are identified:

- What are the requirements a concrete through girder bridge should meet to be built in the Netherlands?
- What are the specific requirements that train bridges in the Netherlands have to meet that might affect the structural design of the bridge?
- How can a concrete through girder bridge be modelled in a parametric way?
- How can the results from a parametric model be evaluated based on the requirements it should meet in a generic way?
- What are methods to optimize the traditional design of a concrete through girder bridge?
- How can the designs be evaluated in terms of costs and sustainability?
- To what extent can a parametric design model improve traditional bridge designs?

1.5 Methodology

The main steps that will be taken to answer these questions can be summarised as follows:

1. Gathering the requirements for the bridge through a literature review (answering the first two sub questions)
2. Modelling the case study as the basis for the parametric model (partly answering sub question 3 and 4)
3. Identifying and deciding what the design parameters and criteria are
4. Expanding the design model to make it parametric (answering sub question 3)
    - User interface for the engineer to input the parameters
    - A finite elements structural model
    - A resistance model calculating the strength of the design
5. Create a method to test the design based on the requirements (answering question 4)
6. Find and evaluate methods of optimization and add them to the model (answering question 5)
7. Create multi-criteria evaluation method of different designs (answering question 6)
8. Create redesigns of a reference design to evaluate and compare the different designs

1.5.1 Literature review

The literature review will provide an in-depth examination of concrete through girder bridges' structural mechanics and specific design considerations. This part of the literature review serves as the basis for the design methodology and is used to identify potential optimization methods.
This is followed by an in depth study on specific requirements for concrete bridges in the Netherlands with a part two that comprises of a detailed analysis featuring all the requirements that are specific to railway bridges in the Netherlands.
The next part of the literature review covers some literature that considers the best ways to model a concrete through girder bridge.
The review concludes with a discussion on where the knowledge gap lies regarding parametric models and why it is relevant to study this topic.

1.5.2 Case study

The research will mainly focus on how to model and evaluate concrete through girder bridges in a parametric way. This will be based on the findings of the literature study and a case study.
For the case study a calculation report of a traditional concrete through girder bridge design will be used. From this case study the main steps and focus points of the design will be gathered. The calculations of this report will be used as common thread for the parametric model.

1.5.3 Modelling

To construct a structural model based on the inputs of the engineer a python project will be built to convert user input into a FEM model using the software RFEM. In this way the flexibility of python can be utilized, yet the FEM calculations can be performed in the powerful RFEM software.
The calculations in regards of the strength of the bridge will be written in python and will not use an external software, to keep complete control over how the bridge is analysed and increase the speed over which optimizations can be evaluated.
The applied optimization methods will be explicitly discussed in chapter 3.2.3.
For the evaluation of the designs a cost and sustainability comparison will be made using, on the one hand a cost indication calculation to get an approximation for the costs of design and on the other hand an environmental cost indication calculation. These two factors together can evaluate the value of a design. This whole process can be simplified to the flowchart in Figure 2 which represents the general working of the optimization model.

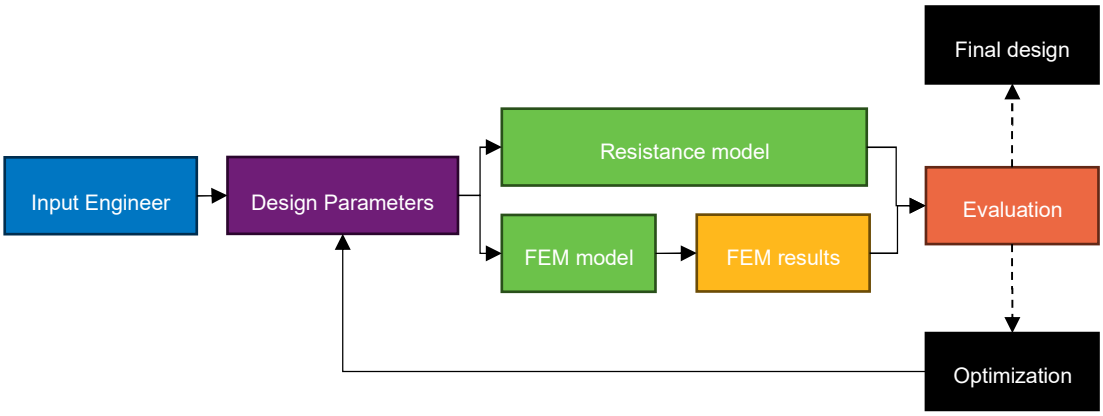

Figure 2: Flowchart methodology parametric model

1.5.4 Comparison

To evaluate the performance of the parametric model, redesigns will be made for an existing concrete through girder bridge reference design that was designed in a traditional way. Comparing the environmental impact and material costs of the redesigns it can be evaluated to what extend the parametric model allows for optimization of traditional design.

1.6 Reference design and case study

For this study, two bridge designs are studied. The first design is the basis for comparing optimized designs and is called the ‘reference design’ as described in paragraph 1.6.1. The second bridge design is a more complicated design that features multiple spans and two train tracks. This design is used as a ‘case study’ for the calculations as described in paragraph 0.

For the reference design there are no extensive calculations available to the research team, however for the case study there is a calculation report available that can be used as a guide for the calculations made in the report. Also this design uses more a more complex design due to the multiple spans and two-track bridges, which allows for a more comprehensive understating of the design of the bridge. This makes the through girder bridge crossing the ‘Maxima kanaal’ a good choice as case study.

However, because this design does not comply to all scope constraints it can not be used to compare the redesigns made, as this would be comparing apples to oranges. This is why the reference design is used as this particular bridge design does fit to all the scope constraints posed by this research. The comprehensive pre-stressing and reinforcement sketches allow for in-depth review of the material usage.

1.6.1 Reference design Bilthoven

The reference design is of the concrete through girder bridge built for the renovation of the station Bilthoven as depicted in Figure 3.

Figure 3: Concrete through girder bridge Bilthoven (BDP, n.d.)

The bridge features a single track and it is also only single span. The most northern bridge has a length of 33 meters and is only pre-stressed in longitudinal direction. The cross-section of the bridge is shown in Figure 4. For reinforcement sketches please see appendix B.

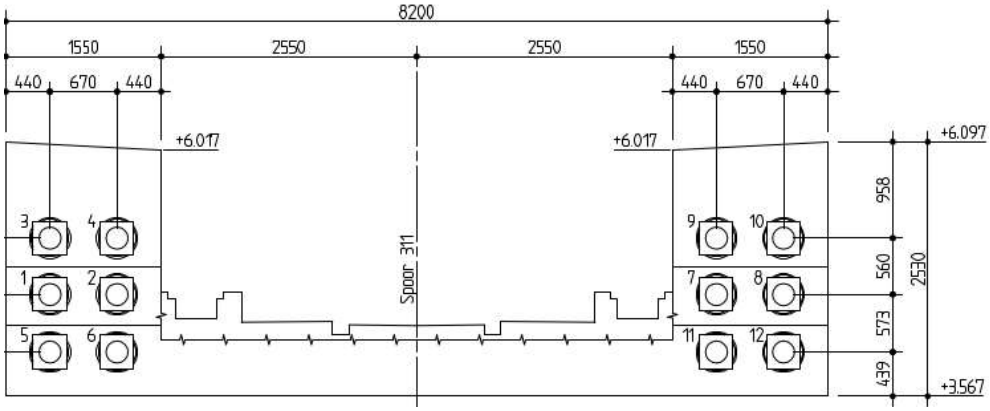

Figure 4: Cross-section of single-span single track bridge

C55/67 is used together with 6x22xØ15.7 FeP1860 pre-stressing strands and ducts with an outer diameter of 107 mm and an inner diameter of 100 mm. The profile of the pre-stress is shown in Figure 5.

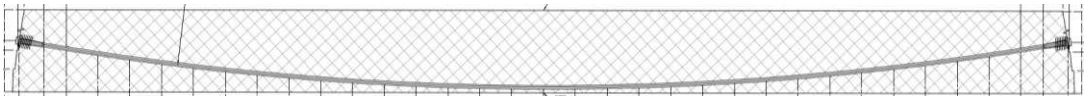

Figure 5: Pre-stressing profile single span bridge

1.6.2 Case study Maxima Kanaal

The case study that is used for modelling setting up the parametric model is the bridge spanning the 'Maxima kanaal' in Den Bosch as described in Cement (2013). Both the adjacent pedestrian and cyclist bridge and the car bridge visible in Figure 6 are not considered for the design.

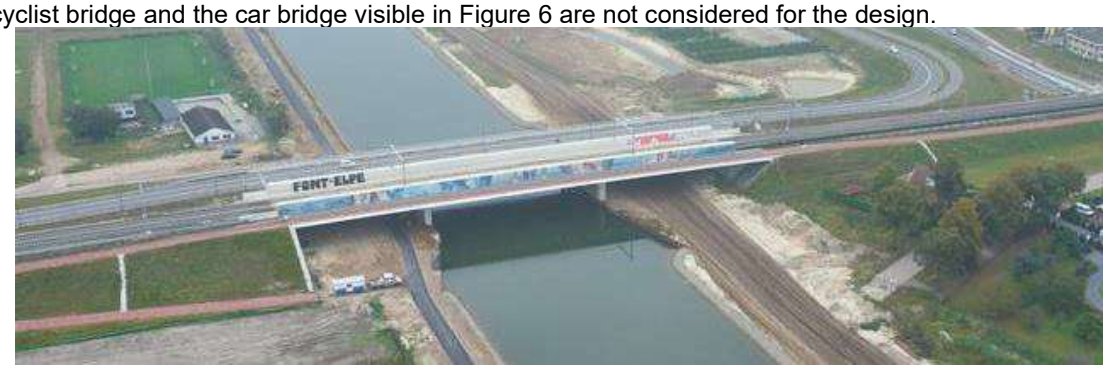

Figure 6: Concrete through girder bridge Maxima Kanaal (De Bekker, 2016)

This bridge features two pre-stressed girders, connected with a pre-stressed floor. It features two train tracks in opposite directions, a slab track railway and a straight stretch of track. It is a three span bridge with spans of 32, 43 and 35 meters. The cross-section and the length profile of the bridge are shown in Figure 7 and Figure 8.

C35/45 concrete is used together with FeB500 HWL steel for the super structure of the bridge. The pre-stress steel used is FeP1860 with up to 31 strands of Ø15.7 mm for the girders, and up to 22 strands of Ø15.7 mm for the floors using parabolic tendon profiles.

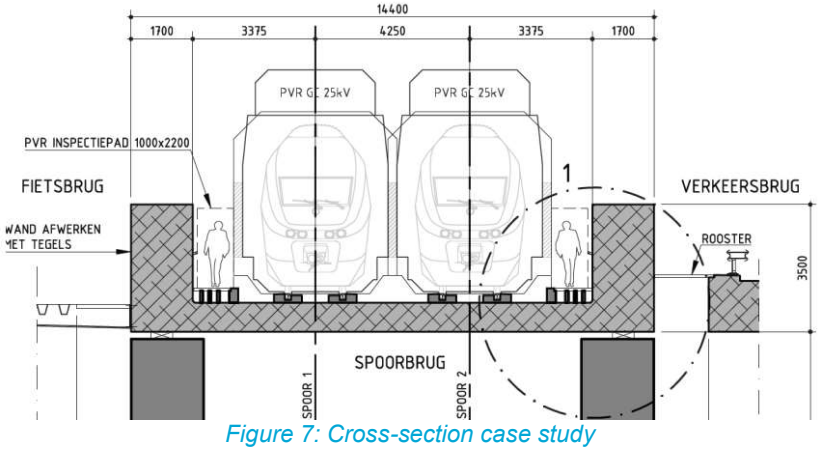

Figure 7: Cross-section case study

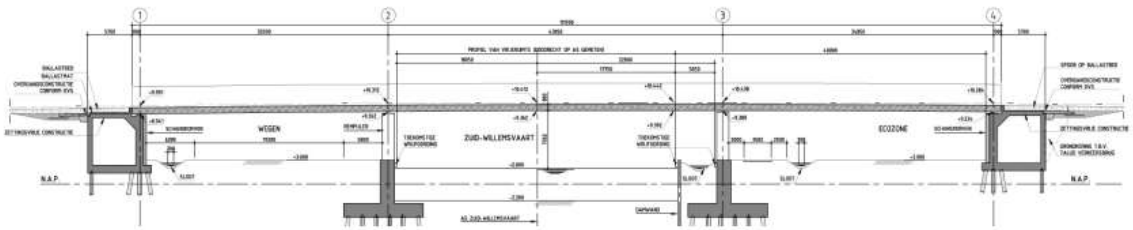

Figure 8: Length profile case study

As this design is used for the calculations it is important to note that the current Eurocode norms did not apply during the design of this bridge. This design uses the old NEN 6720 norms for the concrete resistance calculations.

2 Literature study

Historically, it has mainly been researched how to improve the efficiency of designs through structural analysis. Where the focus of this research used to be mainly for cost reduction, recently the aim of this research has also shifted towards multiple objective optimization, incorporating both sustainability and structural performance criteria. (Zaheer et al., 2022).
Improvements in computing power and finite-element modelling techniques have led to a great increase in potential computer technology application for bridge engineering since the 1970s. These technologies have made it possible to model increasingly more complex structures without using large approximations or simplifications (Fu & Wang, 2014). This has contributed significantly to the understanding and development of current bridge design. However, they often prioritize ease of design and construction over material efficiency, leading to designs that are material-intensive and less sustainable.
Parametric modelling offers a promising new solution for addressing these challenges in bridge design. Parametric modelling allows for the rapid generation and evaluation of multiple design alternatives by manipulating key parameters, enabling engineers to explore a wider range of solutions and optimize for multiple objectives simultaneously (Sharma, 2023).
Furthermore, parametric modelling can facilitate the integration of sustainability criteria into the design process from the beginning of the design. By incorporating material usage and life cycle performance, engineers can develop more environmentally friendly bridges without compromising structural integrity or functionality. Since the optimal design for a bridge will always be dependent on multiple optimization criteria, a multi-criteria decision making problem can be considered (García-Segura et al., 2018) for which these sustainability criteria can also be used.

2.1 Concrete through girder bridges

From the online article by Van der Horst (n.d.) in which he explains specific design concepts for concrete through girder bridges certain points of attention can be gathered. The first conclusion is that this type of bridge is almost exclusively used as train bridge. This is because of the well-known effect car traffic generally slowing down near walls or in tunnels. The reduced space and sight due to the girders of a through bridge would make drivers uncomfortable.
Next to this it is also noted that these bridge typically don't have spans of more than 55 meter and are often used when a low construction height is needed.
A trough bridge is constructed using large main girders with longitudinal prestressing that span between supports, with a relatively thin floor in between that can be prestressed or reinforced. The floor's thickness is independent of the girder span as it only spans in transverse direction. Between the main girders and the floor there are sloped sections to ensure even stress distribution and proper transfer of suspension forces between the floor and girders. Support blocks are placed directly under the main girders, with two per support.
Due to the relatively high flexibility in placing supports under the main girders, asymmetrically supported through bridges can be used to achieve highly skewed crossings. Additionally, they provide a noise-reducing function, which is particularly beneficial in urban areas.
By prestressing the relatively tall main girders of a trough bridge along their length, large spans can be achieved. Since large spans and, consequently, high prestressing forces are often used, careful consideration must be given during the design phase to the dimensioning of end and splitting reinforcement in the main girders and transverse prestressing in the floor. The floor thickness can be minimized, as the floor only spans the distance between the centrelines of the main girders.

Due to the eccentric load from the floor on the main girders, these girders are subjected to a suspension force from the floor, leading to large torsional moments in the main girders. Besides prestress the girders are equipped with stirrups and longitudinal reinforcement in order to transfer the shear forces and bending moments.
End cross-sections can be used to increase the effective width of the cross-section, however this does come at the cost of additional torsional moment (Wouterlood, 2018).

An interesting point to note is the location of shear and tension failure of a concrete through girder bridge. In contrast to different bridge types, where shear and tension failure often occurs at the top or bottom of a cross-section, this type of failure occurs at the upper side of the connection between the floor and the girder as shown in Figure 9 (Jongstra, 2015).

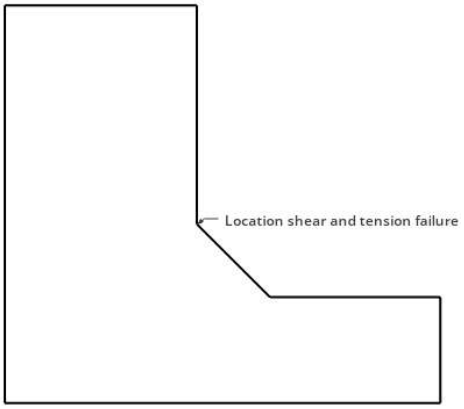

Figure 9: Location shear and tension failure

Another important design aspect is the tension reinforcement in the floor at the introduction of the pre-stress. As the tension is introduced in the girders a tension zone is created in the floor as depicted in Figure 10. (NS Railinfrabeheer, 1997).

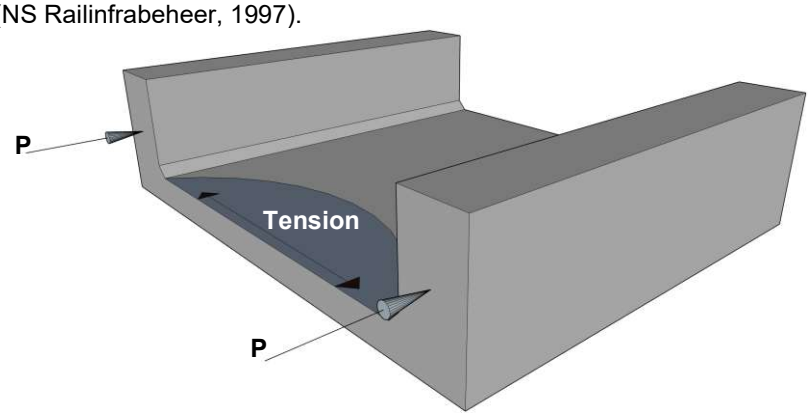

Figure 10: Introduction tension force in cross-section

NS Railinfrabeheer (1997) also proposes 4 ways to design stirrups in the through girder. The options are of course not limited to these designs however they provide a good starting point for stirrup design. Figure 11 shows these designs and also which stirrups will carry which loads.

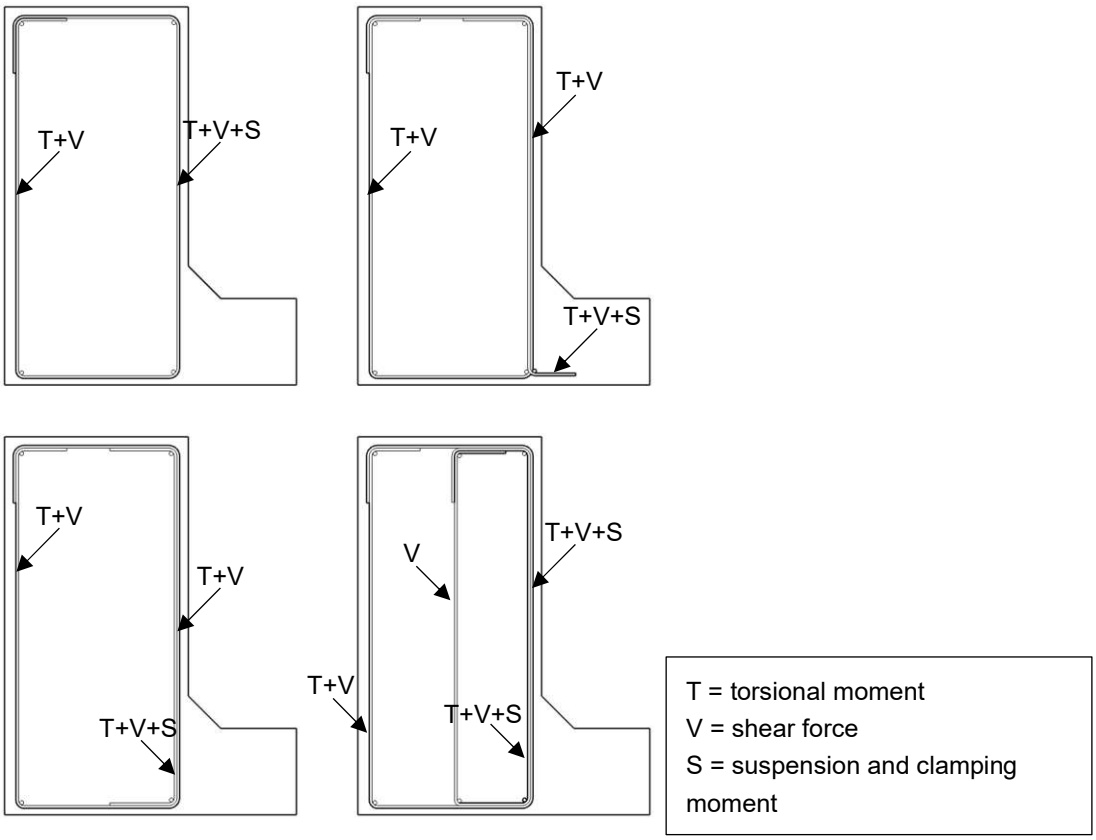

Figure 11: Different possible layouts reinforcement

Because of the large suspension forces, shear forces and torsional moments the girder requires heavy stirrup reinforcement. To achieve this different stirrup zones can be introduced, that each carry different kind of loads.

2.2 Specific requirements for concrete bridges in the Netherlands

For concrete bridges to be built in the Netherlands there are many norms that apply. First and foremost the design should met be conform the calculations in de European Eurocode standards:

- Eurocode 0 (NEN-EN 1990+A1+A1/C2:2019): Grondslagen van het constructief ontwerp
- Eurocode 1 (NEN-EN 1991) Belastingen op constructies
    - Deel 1 Algemene belastingen
        - 1 Volumieke gewichten, eigen gewicht en gebruiksbelasting bij gebouwen
        - 4 Windbelasting
        - 5 Thermische belasting
        - 7 Buitengewone belasting
    - Deel 2 Verkeersbelasting op bruggen
- Eurocode 2 (NEN-EN 1992) Ontwerp en berekening van betonconstructies
    - Deel 1-1 Algemene regels en regels voor gebouwen
    - Deel 2 Betonnen bruggen - Regels voor ontwerp, berekening en detaillering

Specifc Dutch standards must also be applied in addition to these norms. Furthermore, there are Dutch-specific guidelines such as ROK, CUR, OVS, and CROW that apply to bridges. The OVS guidelines are issued by ProRail, the organization responsible for railway infrastructure in the Netherlands. Meanwhile, the ROK (Richtlijnen Ontwerp Kunstwerken, or Guidelines for the Design of Civil Engineering Structures) is a specific design standard from Rijkswaterstaat, the government agency responsible for the design, construction, management, and maintenance of the main infrastructure facilities in the Netherlands.

Using a FEM model of a bridge calculations can be performed that result in the internal forces and deflections. These should be checked with the methodology described in the beforementioned norms. Any concrete bridge design should at least fulfil the requirements for the applicable norms. For concrete through girder bridges these can be summarized as:

- Main girder
    - ULS
        - $M_{Ed}<M_{Rd}$
        - Rotational capacity should be sufficient
        - Stirrups reinforcement for shear forces, torsional forces, suspension forces and clamping moment forces between floor and girder
    - SLS
        - No tension in concrete due to pre-stress at t=0
        - Max concrete compression strength should not be exceeded due to pre-stress at t=0
        - Decompression requirement regarding tension stresses in the concrete at t=∞, according to OVS must be fulfilled.
        - Main tension stresses (σ_{xx}, τ and σ_{zz}) should not exceed capacity
- Floor
    - ULS
        - $M_{Ed}<M_{Rd}$
        - Splitting forces tension zone due to pre-stress should be resisted
    - SLS
        - Crack width

- General
    - Shear between floor and girder
    - Splitting forces caused by introduction of pre-stress should not cause failure
    - Fatigue loading should not cause structural damage to the bridge
    - Deflection of the bridge should not exceed threshold curvature, there is required pre-camber

2.3 Specific requirements for train bridges in the Netherlands

As mentioned in the previous subchapter the OVS00030-1-V004 (ProRail, 2016) and OVS00030-6-V005 (ProRail, 2018) norms are applicable to all train structures built in the Netherlands. These norms describe specific requirement that have to be met for train infrastructure design.

Assuming a ballast track without high speed lines and only looking at the superstructure of the bridge, the key differences found in these OVS norms between traffic and railway concrete bridge design are summarized in this chapter.

2.3.1 OVS00030-6

For NEN-EN 1990 (CEN, 2019a) the most important changes are that the bridge should be designed with service life class 4 and a theoretical lifespan of 100 years. Next to that load model SW/0 should always be considered and is not dependent on the project and the multiplier for the train load models is α = 1.21.
Also, some additional requirements for maximum rotations are given. For the transition between the bridge deck and the open track behind the abutment the maximum rotation is $\phi = 6.5 \cdot 10^{-3}$ and for two consecutive bridge decks the maximum rotation is $\phi_1 + \phi_2 = 10 \cdot 10^{-3}$.

As the volumetric weight of the superstructure (ballast material, including the embedded concrete sleepers and rails with fastening structures), an average $\gamma_{superstructure}$ = 22 kN/m³ should be assumed. For the thickness, calculations should be based on a layer from the top of the deck plate (TDP) to 0.15 m below the top of the rail (BS -0.15 m).
For the cross-section of the bridge and the NEN-EN 1991-2 (CEN, 2015b) train load models the following dimensions are given in the OVS norms.

- The distance between two train wheels in transverse direction r = 1.5 m
- The distance between sleepers a = 0.6 m
- The schematised dimensions of NS-90 sleepers are 2.52 x 0.26 m
- The height of the top of the UIC54 rail to the bottom of the sleeper is 0.38 m.

Calculating the wind loads on the bridge with NEN-EN 1991-1-4 (CEN, 2011b) it should be assumed that the terrain category is ‘area II - Unbuilt area’, unless ‘area 0 - Sea or Coastal area’ is applicable. Next to that the wind load F_w in x direction may be limited by 1.5 kN/m^2 under the conditions that:

- Wind area I H < 5 m
- Wind area II H < 10 m
- Wind area III H < 15 m

The temperature differences on which concrete bridges should be designed are also governed by this norm, they are as prescribed in Table 1.

Table 1: Temperature differences for railway bridges

Construction element	Minimum	Reference	Maximum
Rail	-23 °C	25 °C	55 °C
Construction without cover	-20 °C	10 °C	40 °C
Construction with cover due to ballast or concrete flange	-15 °C	10 °C	35 °C

Re-railing load is considered as an incidental load and must be combined with one of the derailment loads. For each jack, the following load must be considered: F_{jack} = 500 kN with $A_{jackplate}$ = 0.70 * 1.60 m². The jack load must be applied at the most unfavourable location(s), within a distance of 2.20 m from the centre of the track. In the length direction the loads should be at least 5 meters apart as shown in Figure 12.

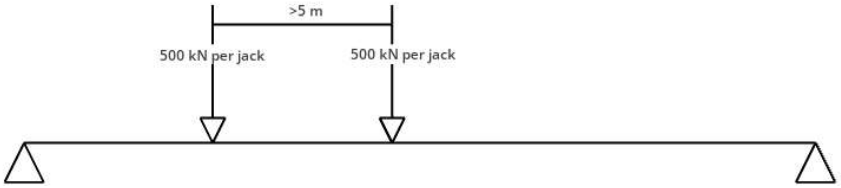

Figure 12: Rerailing loads in length direction

Furthermore there are some extra conditions that the concrete should meet for train bridge design in the Netherlands
The maximum strength class (C_{max}) to be considered for cast-in-place structural concrete is C55/67. For the ULS (Ultimate Limit State) testing, the bi-linear concrete and reinforcement steel deformation diagram should be used. And redistribution is not allowed.

Because concrete through girder bridges are pre-stressed in longitudinal direction the decompression requirements of the cross-section should be fulfilled in all SLS limit states:

- For the quasi-permanent combination, the de-tensioning requirement applies to the entire cross-section (no concrete tensile stress allowed).
- For the frequent load combination, the de-tensioning requirement applies to the zone where prestressing is present. For the side where no prestressing steel is present, concrete tensile stress σb < 0.5 fctk,0.05 with an upper limit of σb < 1.5 N/mm².
- For the characteristic load combination, in the zone where prestressing is present, the concrete tensile stress σb < 0.5 fctk,0.05 with an upper limit of σb < 1.5 N/mm². For the side where no prestressing steel is present, the concrete tensile stress σb < 0.75 fctk,0.05 with an upper limit of σb < 2.25 N/mm².

Finally, crack width checking is performed under the frequent load combination. For reinforced structures directly subjected to railway traffic loads, the crack width requirement based on the environmental classes (XD-3 / XA-2) is w = 0.2 mm. If the transverse reinforcement is located within a de-tensioning zone, a crack width requirement of w = 0.1 mm must be assumed.

2.3.2 OVS00030-1

This norm provides mostly boundary conditions that are important for train structures. For this specific project the most important aspects are summarized in this paragraph.

For single track railways a passing path should be provided along the track. The distance of the path to the centre of the track is dependent on the design speed of the railway. For this study speeds of up to 140 km/h are considered meaning that this distance should be 2250 - 4000 mm. The width of the path should be 1000 mm.

The minimum free height for bridges should be 4.6 m and if that is not possible other measures should be taken to prevent collisions unless it concerns walking or cycling traffic, than it is 2.6 m. This free height is calculated by rounding the free height to 100 mm and then subtracting 200 mm.

A guide structure for derailed trains should be placed at least 2000 mm and max 2150 mm from the centre of the track. To allow a derailed train to pass over a bridge without obstruction, the space up to 3000 mm from the centre of the adjacent track must be free of obstacles. Also, for single track rails, handrails should be installed on both sides of the track.

In regard to stray currents, all conductive parts that are connected to the system grounding (rails, overhead contact line support structure, mesh frames, etc.) from the reinforcement of the structure (≥1kΩ) should be isolated.

2.4 Modelling concrete through girder bridges

Firstly, it is noteworthy that current standards for modelling bridges often underestimate their actual strength. When tests are conducted on real concrete bridge models and compared (FEM) models, the FEM models generally underestimate the bridge's capacity. Research by Yang et al. at TU Delft (2023) suggests that bridges may be significantly stronger than initially assumed based on standard predictive models. In some extreme cases, the actual capacity of bridge components was found to be approximately twice as high as calculated using current models.

Wouterlood (2018) proposes three ways to model a concrete through girder bridge using FEM software.

- Plate model: Using only 2D plate elements with rigid connections.
- Beam model: Using 2D plate elements for the floor and 1D elements for the girders.
- Beam model with 2D haunch, this is a combination of both models, however compared to model two, the haunch is now modelled as 2D element explicitly such that the full cross-section is correctly modelled. The girder is still modelled as a 1D element.

To account for cracking the E-modulus of the floor is reduced to 1/3 of its normal value.

In this research the FEM model results are compared to the analytical solution:

- Plate model: 10-15% lower
- Beam model: 40% lower
- Beam model with 2D haunch: 10% lower

The large deviation for the beam model compared to the plate model or beam model with 2D haunch is attributed to the lack of rigid connections between girder and floor, resulting in reduced bending and torsional stiffness of the girder.
This research concludes that the analytical solution is a safe upper limit as it neglects the longitudinal load distribution in the floor. In reality this effect is better calculated in FEM models. It does however become clear that to accurately model this bridge, the connections are a very important factor. Only modelling the bridge with rigid connections between 1D girders and 2D floor elements will not yield accurate results and will overestimate the strength of the bridge. However when explicitly modelling a rigid connection between the floor and the girder, more reliable results are obtained.

Lantsoght et al. (2019) shows aspects that need to be considered for FEM modelling concrete bridges. In this article a concrete bridge is modelled to make predictions about the strength of this bridge. These results are later compared to the results of a proof load test.

- The slab/deck was modelled using quadratic shell elements, 500 x 500 mm in size, with variable thickness (470-870 mm).
- Non-structural elements (sidewalks and barriers) were not explicitly modelled but represented as equivalent permanent loads.
- Supports were modelled as rigid and ideal supports.
- Cracking effects were accounted for by using orthotropic behaviour with different Young's moduli in cracked (14 GPa) and uncracked (36 GPa) directions.

After an initial FEM model this study tries to optimize the FEM model, it uses multiple optimization methods:

- Using quadratic solid elements instead of quadratic shell elements.
- Including the elastic properties of the supports to better capture the support conditions.
- Explicitly modelling non-structural elements such as the curb to better capture the stiffness of the bridge. This should however be done with care as modelling the these elements with full stiffness may not correspond to actual behaviour as this concrete is poured in a different phase and it is connected to the structural elements with limited reinforcement.
- Lastly also the actual reinforcement layout is introduced to the FEM model.

It can be concluded that using these optimization techniques, the design moment M_{Ed} is reduced and is closer to the proof load results. That means that these optimization techniques might be suitable for modelling concrete through girder bridges as well.

2.5 Parametrically modelling bridges

In the traditional way of civil engineering design a trial and error approach is used. The designer chooses and evaluates a design which is than adjusted based on the evaluation results. In this way ensures a feasible design is found that fulfils the requirements, however this is often not the optimal solution. Using optimization algorithms, bridge designs can be optimized in terms of environmental impact and investment cost, however using algorithms like Genetic Algorithm (GA) (Biswas, 2025) and Pattern Search algorithms might lead to infeasible solutions (Chalouhi, 2019).

Using these algorithms the traditional trial and error approach does not have to be used, rather automatic design generation might be possible. Correctly steering the algorithms to feasible solutions might be a way to optimize bridge design.
For this study the focus lies mainly on parametric design that allows the engineer to create and optimize their designs using the trial and error approach. This means that the parametric model does not rely on automatic algorithms, but rather on rapidly evaluating different designs such that the engineer can optimize the design.

The paper by Salamak, (2024) also focuses on the streamlining of the design process of bridges using computational techniques. This study uses a visual programming language that has an interface for the engineer to input the design parameters. This study provides good insight into how a bridge can be parametrized and how the parameters can be optimized. It also describes how FEA is done within the parametric environment and not in an external FEA tool.
The study than uses a generative algorithm to create multiple designs giving good insight in the usage of the material and the material costs over the iterations of the algorithm. This highlights the potential of integrating FEM computations with a parametric model as this allows for rapid iterations that allow GA algorithms to find optimal design solutions. The results also show very promising optimizations that reduce the material costs of a case study.
The applications are however limited as an increase in design complexity can drastically increase the complexity in FEM and automatic solution generation by a GA. The implications of adding more design aspects such as dynamic response, more design parameters and a broader spectrum of design approaches will increase the complexity of a more complete parametric model.

2.6 Conclusion

This literature study reveals a research gap in the development of parametric models for concrete through girder bridges. Historically, bridge design research has focused on improving efficiency through structural analysis, primarily targeting cost reduction. However, recent shifts towards multi-objective optimization now incorporate sustainability and structural performance criteria (Zaheer et al., 2022). Despite advancements in computing power and finite-element modelling techniques since the 1970s (Fu & Wang, 2014), traditional models often prioritize ease of design and construction over material efficiency, leading to less sustainable designs.

Parametric modelling offers a promising solution by making it possible to rapidly generate and evaluate multiple design alternatives through the manipulation of key parameters. This approach allows engineers to explore a wider range of solutions and optimize for multiple objectives simultaneously (Sharma, 2023). Importantly, parametric modelling facilitates the integration of sustainability criteria from the outset, allowing for the consideration of material usage and life cycle performance to develop environmentally friendly bridges.

While there is substantial research on general bridge modelling techniques, there is limited focus on parametric modelling specifically for concrete through girder bridges. These bridges are predominantly used as train bridges due to their structural characteristics and the barriers (Van der Horst, n.d.). The unique design aspects, such as large main girders with longitudinal prestressing and specific failure modes (Jongstra, 2015), necessitate specialized modelling approaches that can accurately capture their complex behaviour.

The main challenges associated with parametrically modelling concrete through girder bridges, are modelling shear and tension failures at the connection between the floor and girders, optimizing pre-stress configurations and optimizing reinforcement layouts to manage torsional moments effectively. By addressing these gaps, parametric models can significantly contribute to more efficient and sustainable bridge designs, ultimately extending the service life of infrastructure while minimizing environmental impact.

The potential of parametric modelling is highlighted in Salamak (2024). Parametric design provides a promising alternative to traditional trial and error approaches, allowing rapid evaluation of designs with the potential implementation of automatic algorithms. Integrating Finite Element Analysis within parametric models can lead to significant cost reductions. However, increasing design complexity poses challenges. Despite these challenges, parametric and optimization-driven design hold considerable promise for more efficient and innovative bridge designs.

3 Modelling and design

This chapter discusses the way the model is built to allow for optimal design of concrete through girder bridges. The most important design aspects will be highlighted and the main calculation methods will be explained further.

3.1 Design

The most important design aspects of a concrete through girder bridge in the context of parametric modelling can be summarised as geometry, loads, modelling and reinforcement. This chapter shows the most important aspects for this part of the design.

3.1.1 Geometry

The first step of designing a through girder bridge is the geometry. In the context of this research to most important parameters next to bridge length are the width and height of the girder and floor cross-sections. These dimensions are dependent on many factors and are often decided in an iterative trial and error process.

The most important factor is the required span length of the bridge. Depending on this length a certain pre-stress and reinforcement layout is required that should be able to fit inside the girders and the floors with appropriate covers. A longer span means more reinforcement and pre-stress is required which leads to larger cross-sectional dimensions.
Next to that another important consideration is the required width of the bridge for the required track system. Depending on the amount of railway tracks on the bridge, the required width of the deck is altered. The OVS norms (ProRail, 2016, 2018) describe all the required components that should be fitted on the bridge such as rails derailment guards and inspection paths as mentioned in the literature study.
A typical cross-section of a single track cross-section is given in Figure 13.

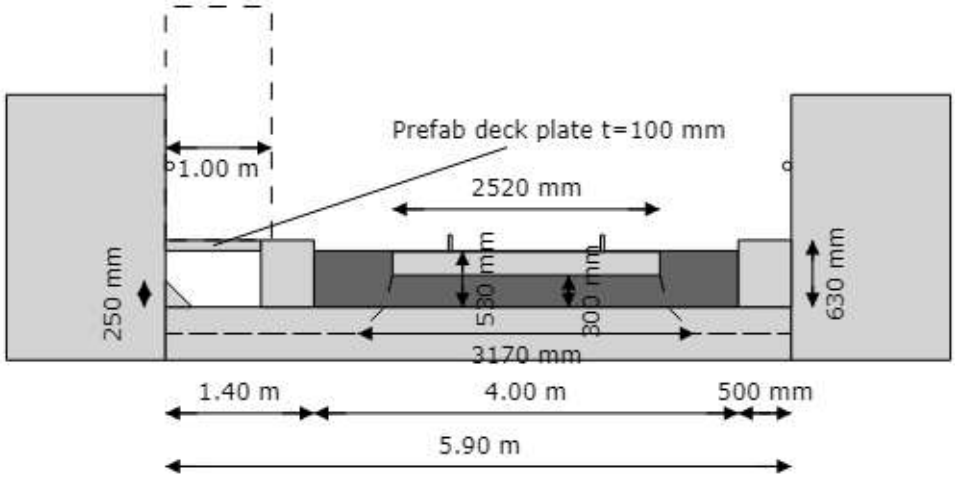

Figure 13: Typical through girder cross-section

Allowing the engineer to parametrically adjust the dimensions of the cross-section allows for optimization of the geometry of the cross-section.

3.1.2 Loads

This chapter showcases how the loads for a bridge are calculated and how this can be implemented into a parametric model. A reference calculation report is given in appendix C which shows the calculation of the loads for a specific design.

Permanent loads

Permanent loads are simply calculated as the self-weight of the structure. These can be calculated from the input geometry and track system. The automatic calculation of these loads aid the engineer in quickly determining the new permanent loads for an adjusted geometry.

In regards to the parametric model, the self-weight of the structural components is calculated automatically. The permanent loads of the non-structural components are modelled as additional loads, for which free rectangular surface loads are applied on the locations of these components on the deck. An example of the permanent load for a bridge is in the FEM model is provided in Figure 14.

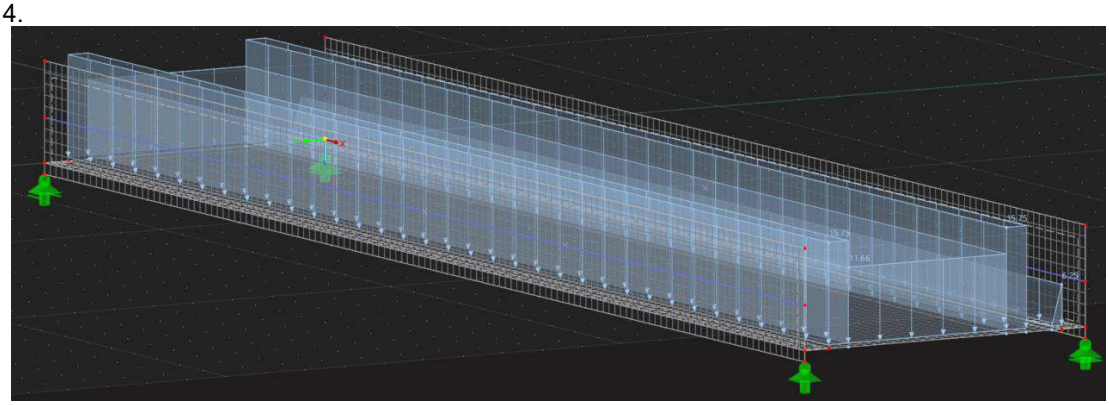

Figure 14: Example additional permanent loads FEM model

Pre-stress loads

Pre-stress is generally incorporated into bridge design as equivalent loads. From the pre-stressing profile and stress in the cables the equivalent load can be calculated. This means that the engineer only has to input the parameters such as height of cable at the introduction of the pre-stress and the lowest point of the cable, which are determined by the required cover and the proposed pre-stressing profile by the engineer.

From these parameters the parabolic tendon profile is calculated using geometric relations. For example the tendon profile of a girder with a height of 2500 mm, pre-stress introduction at 1250 mm and a minimum tendon height of 155 mm is automatically determined in Figure 15.

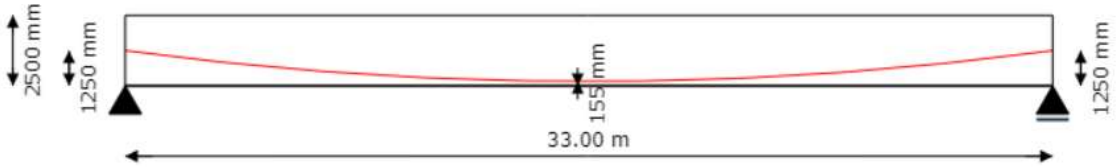

Figure 15: Example tendon profile in girder

Using the calculated tendon profile and the vertical displacement of the cable Δz due to the tension in the cable, the radius of the tendons can be approximated. This radius is used to calculate the horizontal and distributed pre-stressing forces:

$$F_P = A_p \sigma_{pw};\ q_P = \frac{F_P}{R}$$

The pre-stress losses need to be accounted for, these are calculated in the next chapter.

The area of the pre-stress also needs to be calculated for this step. This can all be done automatically when the amount of pre-stressing cables, strands per cable and the diameter of the strands are used.

The maximum stress in the cables is limited by:

- The maximum stress during stressing: min(0.8f_{pk},0.9$f_{p0,01k}$)
- The maximum stress at t=0: min(0.75f_{pk},0.85$f_{p0,01k}$)
- The limitation that no tension stresses can occur in the concrete due to pre-stress at t=0

So the maximum stress in the cable can also be computed using the pre-stress geometry. This means that by only inputting the physical parameters of the pre-stressing system the loads can automatically be determined which allows the engineer to optimize the pre-stressing system without having to redo these time consuming calculations as this can be done automatically. This way the pre-stress can be designed such that it used the steels full potential.

The equivalent pre-stress line loads are applied as free line loads acting on the girders and the loads at the introduction of the pre-stress are applied as free concentrated loads. An example of pre-stress loading is provided in Figure 16.

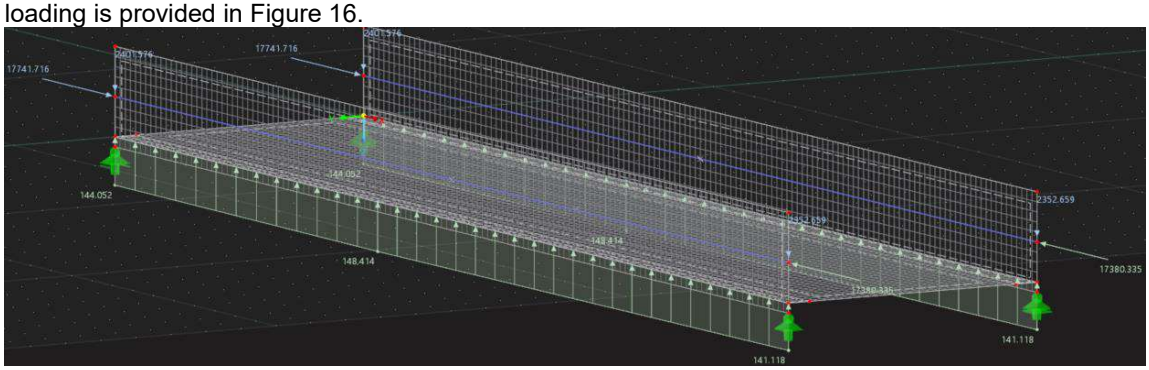

Figure 16: Example pre-stressing loads in FEM model

Setting
The parametric model is limited to single span statically determined bridge due to the scope of this research. This means that nodal displacements will not lead to loads.

Inspection path
Due to the inspection path that is considered as a non-public footpath there is a variable load of 5 kN/m^2 acting on the bridge at the location of the inspection path following NEN-EN 1991-2 (CEN, 2015b). It is applied in the same manner as the additional permanent loads in Figure 14, using free rectangular loads.

Braking and accelerating forces
These loads are not considered for the design as these will be mostly important to the substructure of the bridge, while only the superstructure is considered due to the scope of the research.

Wind loads
Wind loads are very complex to determine as they are dependent on a lot of boundary conditions. In the Netherlands wind loads can be estimated using the methodology in NEN-EN 1991-1-4 (CEN, 2011b). The important parameters for the engineer to determine are the free height required under the bridge, the location of the bridge which results in the 'wind area' that the bridge is in and the 'terrain category' which are both defined in NEN-EN 1991-1-4.
A complete calculation of for wind loads can be found in appendix C. The main idea behind this calculation is to determine extreme hydrostatic pressure that might occur in every direction and multiplying this with the reference area of the bridge in this direction to find the ultimate load that can act on the structure.
This calculation can be very time consuming, however due to the automatic calculation of the parametric model these loads can be quickly calculated when the geometry or other boundary conditions change.
The wind load should be applied in positive and negative y and z direction. It is assumed that wind in x direction will not be governing.
The loads are applied as surface loads on the deck and as line loads on the girders such that the eccentricities can be correctly modelled. An example of a load case in x direction is provided in Figure 17.

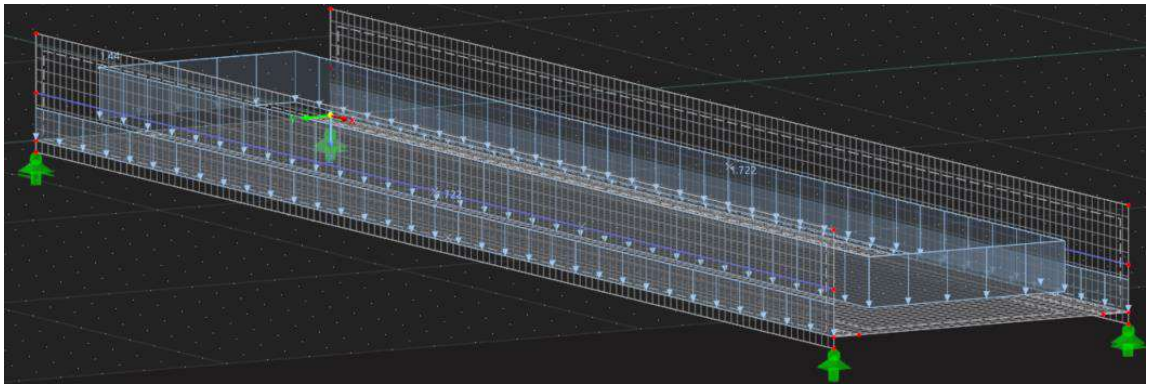

Figure 17: Example of wind loads in x direction in the FEM model

Train loads

NEN-EN 1991-2 (CEN, 2015b) considers four different train load models. Because only the super structure of single span bridges is considered, load models LM71 (Figure 18) and SW/2 (Figure 19) have to be considered.

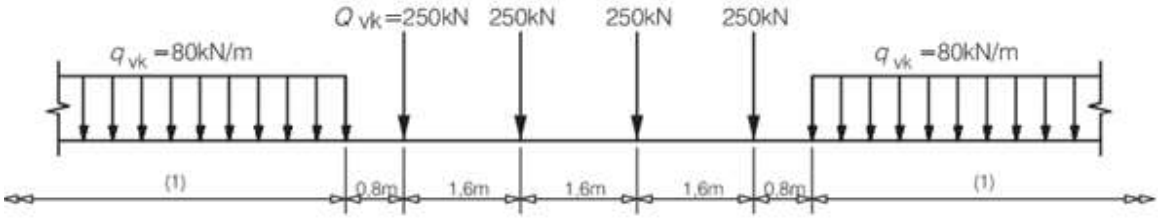

Figure 18: Train load model LM71

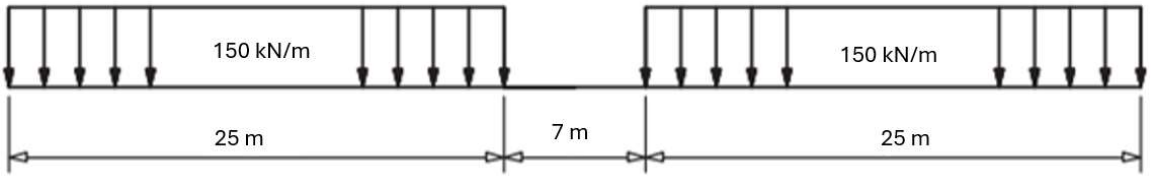

Figure 19: Load model SW/2

On both these load models an α factor of 1.21 which is found in the Dutch national annex is applied. In addition also a dynamic factor Φ_2 is applied. This factor is dependent on the span of the deck:

$$\Phi_2 = \min(\max(\frac{1.44}{\sqrt{L_\Phi} - 0.2} + 0.82; 1); 1.67)$$

Where L_Φ is twice the span of the deck.

These loads may be spread over an effective width that can be calculated at the height of the middle of the floor. Starting from the width of the sleeper the load is spread under an angle of ¼ in the ballast and ½ in the concrete floor:

$$W_{load} = W_{sleeper} + 2\left(\frac{h_{ballast}}{4} + \frac{h_{floor}}{2}\right)$$

This situation is sketched in Figure 13.

When applying these load models engineering judgement is used to find the location of the dynamic load that will cause the largest load effects. To find these locations 'influence lines' can be used which systematically place the loads on different locations on the bridge an calculate the load effects. For an influence line the x axis shows the location of the middle of the load model. The y-axis shows the maximum resulting force.

For example the influence line of the SW/2 load model for bending moment for a bridge with a length of 33 m, looks like Figure 20:

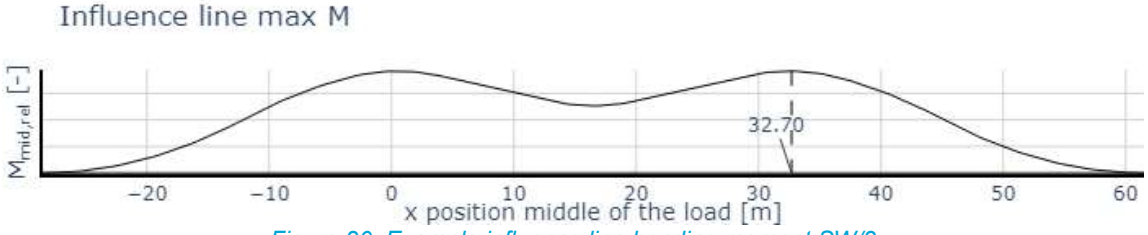

Figure 20: Example influence line bending moment SW/2

From this influence line it can be concluded that the load should be placed with the midpoint of the load at x = 32.7 m as this will result in the highest bending moment. This results in the load shown in Figure 21.

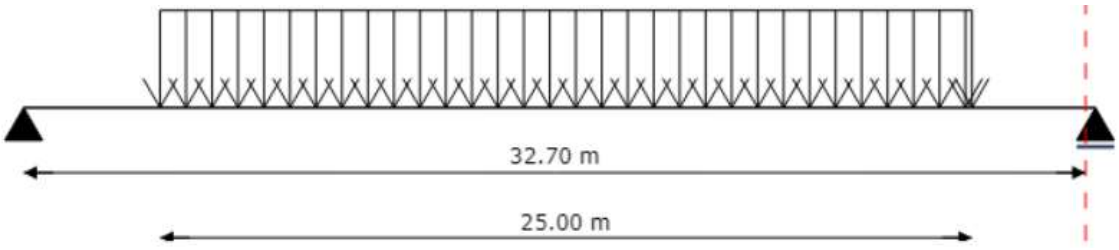

Figure 21: SW/2 load model resulting in the maximum bending moment

This load translates the following load case in the FEM model, depicted in Figure 22.

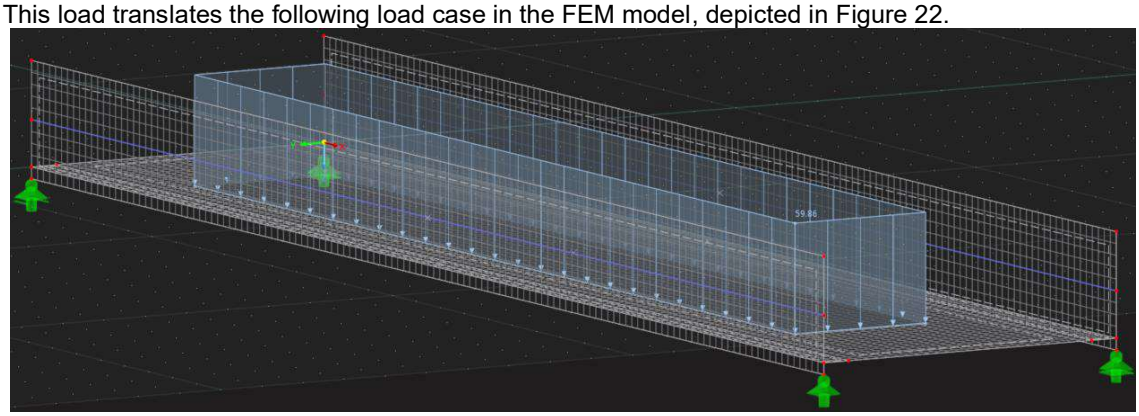

Figure 22: Example of train load SW/2 in the FEM model

Using these influence lines the decisive load positions are determined automatically and correctly, this means the engineer does not have to do these calculations anymore. This increases the speed of the design process and lowers the error sensitivity.

Temperature loads

Temperature loads are not considered in this research due to scope limitations.

Accidental loads

Next to these loads there are some special loads such as derailment, rerailing and impact loads. These loads however mostly have a local impact. Since this design model is used to create a preliminary design for a bridge these effects will not be considered.

3.1.3 Load combinations

The load combinations are derived from NEN-EN 1990 (CEN, 2019a), where special attention has to be paid to the load groups considered for train bridges. These groups determine how different train load models should be combined. The limit states ULS, SLS-Characteristic, SLS-Frequent, SLS-Quasi Permanent need to be considered for the calculations. The governing load combinations for these limit states are summarised as follows, for ULS is the least favourable of NEN-EN 1990 form. 6.10a, 6.10b:

$$\sum_{j\geq 1} \gamma_{G,j} G_{k,j} + \gamma_P P + \gamma_{Q,1} \Psi_{0,1} Q_{k,1} + \sum_{i>1} \gamma_{Q,i} \Psi_{0,i} Q_{k,i}$$

$$\sum_{j\geq 1} \xi_j \gamma_{G,j} G_{k,j} + \gamma_P P + \gamma_{Q,1} Q_{k,1} + \sum_{i>1} \gamma_{Q,i} \Psi_{0,i} Q_{k,i}$$

For SLS-Characteristic the decisive load combination is governed by 6.14b:

$$\sum_{j\geq 1} G_{k,j} + P + Q_{k,1} + \sum_{i>1} \Psi_{0,i} Q_{k,i}$$

And for SLS-Frequent the decisive load combination is governed by 6.15b:

$$\sum_{j\geq 1} G_{k,j} + P + \Psi_{1,1} Q_{k,1} + \sum_{i>1} \Psi_{2,i} Q_{k,i}$$

Finally for SLS-Quasi Permanent the decisive load combination is governed by 6.16b:

$$\sum_{j\geq 1} G_{k,j} + P + \sum_{i\geq 1} \Psi_{2,i} Q_{k,i}$$

The γ factors for consequence class 3 are determined from NEN-EN 1990 table NB.17 and are summarized in Table 2:

Table 2: Gamma factors load combinations

$\gamma_{G,j,sup}$ 6.10a	1.40
$\gamma_{G,j,sup}$ 6.10b	1.25
$\gamma_{G,j,inf}$	0.90
$\gamma_{G,i}$ Train load gr16, gr17, gr26, gr27	1.25
$\gamma_{G,i}$ Train load other groups	1.50
$\gamma_{G,i}$ Wind load	1.65
$\gamma_{G,i}$ Other variable loads	1.65

The Ψ combination factors for the different load combinations are obtained from NEN-EN 1990 table A2.3. This results in the load combinations shown in Table 3. For the full calculation of the load combinations please refer to appendix C.

Table 3: Load combinations

Load	ULS 6.10a			ULS 6.10b			
Permanent	1.40	1.40	1.40	1.25	1.25	1.25	1.25
Passing path	1.32	1.32	1.32	1.32	1.32	1.32	1.32
Wind	1.24			1.24			1.65
LM71	1.20			1.50			1.20
SW/2		1.00	1.00		1.25	1.25	

Load	SLS-char				SLS-freq			SLS-quasi
Permanent	1.00	1.00	1.00	1.00	1.00	1.00	1.00	1
Passing path	0.80	0.80	0.80	0.80				
Wind	0.75			1.00				
LM71	1.00			0.80	0.8			
SW/2		1.00	1.00			0.8	0.8	

3.1.4 Creep, shrinkage, relaxation and friction losses

Concrete through girder bridges are pre-stressed in longitudinal direction. Creep, shrinkage, relaxation and friction losses are therefore very important. These losses can add up to more than 20%. An example of the elaborate calculation preceded by these losses is given in appendix C.

To automate this calculation and allow the engineer to rapidly incorporate the losses into the pre-stress they are calculated in the method described below. This optimizes the design process for the engineer as next to the pre-stress system and the geometry, the only input for this calculation is: the type of pre-stress duct, the age of the concrete at end of life, the age of the concrete at the introduction of the pre-stress, the relative humidity and the relaxation loss percentage.

Friction losses

Friction losses are determined by using the pre-stressing profile according to NEN-EN 1992-1-1 (CEN, 2011a). The following formula may be used to calculated the pre-stress profile after friction losses are taken into account:

$$\sigma_{\text{PMi}}(x) = \sigma_{\text{PMi,max}} e^{-\mu(\theta + k \cdot x)}$$

The friction parameters μ and k are given by the manufacturer of the pre-stressing ducts. θ is the sum of the angular displacements over the distance x, irrespective of direction or sign.

Wedge set

For pre-stressing strands it should be assumed that the wedge set is 7 mm, according to the Dutch ROK norm (Rijkswaterstaat, 2021). The accumulation of this wedge set over the length of the bridge is calculated by discretizing the length of the bridge into Δx's. For the each dx and $\Delta\sigma_{\text{slip}}$ the total Δl is calculated using:

$$\Delta l = \frac{\Delta\sigma_{\text{slip}}}{E_{\text{P}}} \cdot \Delta x$$

Using a calculation algorithm the actual stress losses can be calculated by finding the $\Delta\sigma_{\text{slip}}$ values such that $\Sigma\Delta l$ =7 mm using the following rule:

$$\Delta\sigma_{\text{slip},x=i+1} = \max(\Delta\sigma_{\text{slip},x=i} - \max(2(\sigma_{\text{PMi},x=i} - \sigma_{\text{PMi},x=i+1}),0),0)$$

Subtracting the calculated slip losses from σ_{PMi} yields the pre-stress stresses at t=0 σ_{PM0}.

Creep loss

These losses are calculated using NEN-EN 1992-1-1 (CEN, 2011a). For this calculation it is important to know the time at which the pre-stress is applied to the concrete and the relative humidity of the environment.

With these parameters the creep coefficient $\phi(\infty, t_0)$ is approximated using the calculation methodology in appendix B of NEN-EN 1992-1-1. An important factor for the creep calculation is fictitious thickness h_0 which is twice the area of the cross-section divided by its perimeter.

Using the creep coefficient the creep loss is calculated using formula 3.6:

$$\varepsilon_{\text{cc}}(\infty, t_0) = \phi(\infty, t_0) \cdot \frac{\sigma_{\text{c}}}{E_{\text{c}}}$$

Where the stress in the concrete σ_{c} is calculated by the pre-stress compression:

$$\sigma_{\text{c}} = \sigma_{\text{P}} \cdot \frac{A_{\text{P}}}{A_{\text{c}}}$$

This loss is spread over the whole length of the pre-stressing cable.

Shrinkage

Drying shrinkage ε_{cd} strain is calculated with formula 3.9 from NEN-EN 1992-1-1 (CEN, 2011a).

$$\varepsilon_{cd}(t) = \beta_{ds}(t, t_s) k_h \varepsilon_{cd,0}$$

Here,

k_h is a factor dependent on the fictitious thickness h_0.

$\beta_{ds}(t, t_s)$ is also dependent on the fictitious thickness however this is also influenced by age of the concrete.

$\varepsilon_{cd,0}$ is the nominal drying shrinkage and is calculated in appendix B of NEN-EN 1992-1-1 (CEN, 2011a).

Autogenous shrinkage loss can be calculated using formula 3.12:

$$\varepsilon_{ca}(\infty) = 2.5(f_{ck} - 10) \cdot 10^{-6}$$

These losses together form the shrinkage loss and are also spread equally over the length of the bridge.

Relaxation

The specific relaxation loss calculation can also be found in NEN-EN 1992-1-1 (CEN, 2011a). ROK (Rijkswaterstaat, 2021) prescribes that the relaxation after 1000 hours of tensioning is 2.5% and that the steel should be assumed to be relaxation class 2. With these assumptions the relaxation loss can be calculated using formula 3.29:

$$\Delta\sigma_{PR} = 0.66\sigma_{Pi}\rho_{1000}e^{9.1\mu}\left(\frac{t}{1000}\right)^{0.75(1-\mu)} \cdot 10^{-5}$$

Where:

$$\mu = \frac{\sigma_{Pi}}{f_{pk}}$$

Using the same discretization as before $\Delta\sigma_{PR}$ can be calculated for each Δx.

These losses are summarized in the loss plot, showing the losses over the length of the bridge. For Figure 23 an example is used that shows the difference between σ_{Pi}, σ_{P0} and σ_{Pw}.

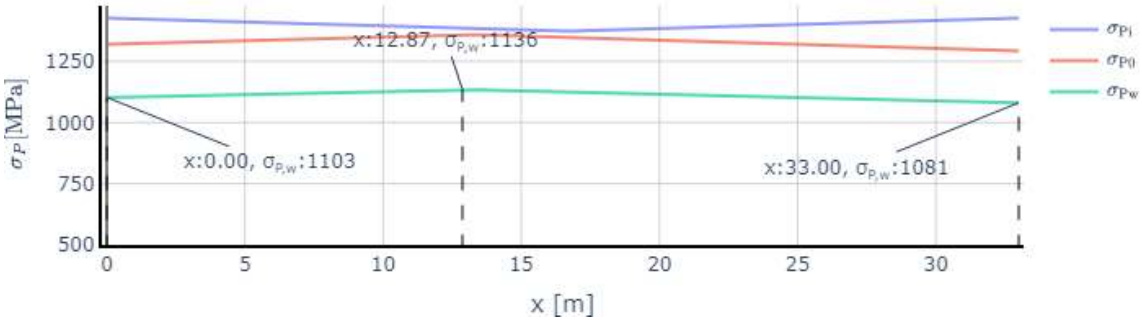

Figure 23: Pre-stress loss plot

An example of resulting pre-stress forces shown in Figure 24 where the effective pre-stress stress over the length is used to calculate the pre-stress forces.

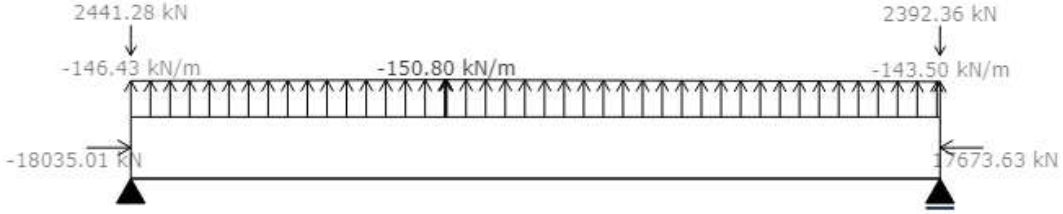

Figure 24: Resulting forces from pre-stress and losses

3.1.5 Finite Element Modelling

This paragraph will explain how the bridge will be modelled in RFEM (Dlubal, n.d.). A 3 dimensional FEM model is used and a view of the model and its geometry is shown in Figure 25.

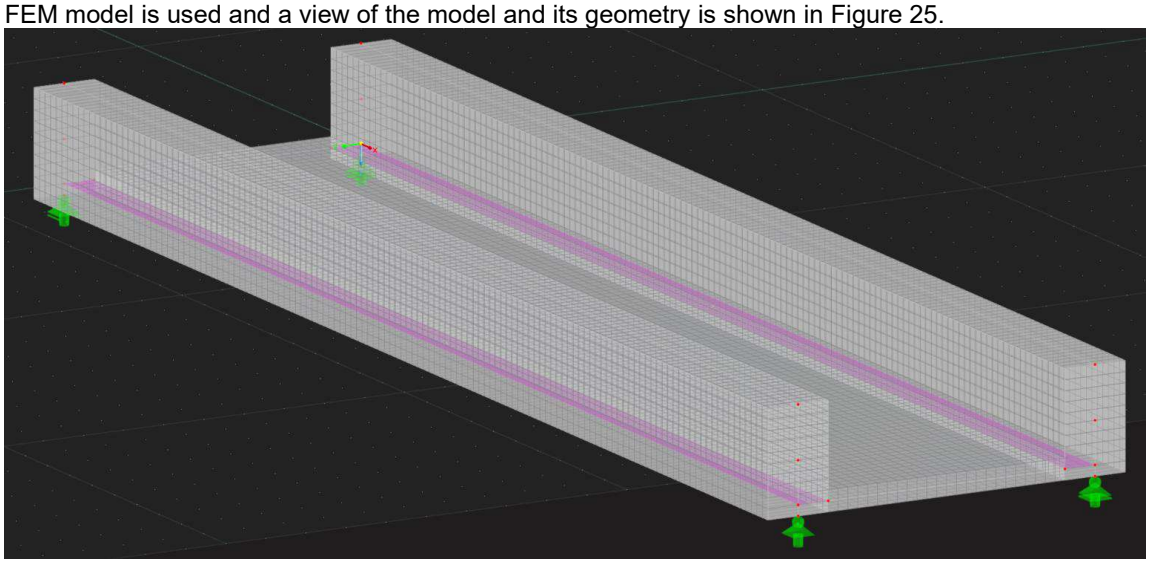

Figure 25: 3D view FEM model

The dimensions of the girders and floor are dependent on the input of the engineer in the parametric model and therefore only serve as a demonstration. For both the floor and the girder planar 2D plate elements with uniform thickness are used.

Supports

The bridge is supported at the ends of both girders where all the supports restrict movement in z-direction. To make sure the model is stable and not over constrained the following support conditions are applied as depicted in Figure 26. In this figure the arrows depict the directions for which the supports are allowed movement. Rotation is not restricted in any direction.

Figure 26: Support conditions of the FEM model

Mesh

The shell elements used for the floor and girder have a uniform thickness and carry both membrane forces and bending moments. The calculation uses a linear parallelized Cholesky solver.

As can be seen in Figure 25 the mesh uses quadrilateral elements for the shell elements. These mesh elements can be schematized as Figure 27.

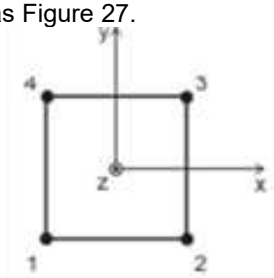

Figure 27: Schematized representation mesh element (Dlubal Software, 2024)

Modelling the girders as plate elements instead of 1D member elements is a result from section 2.4. Here three different options of modelling the girders are described from which modelling them as surfaces yield the most reliable results.

The properties of the FEM model and mesh are summarized in Table 4.

Table 4: Summary of the FEM properties

Plate bending theory	Mindlin / Reissner
Interpolation	Linear
Nodes	4
Degrees of freedom	$u_x, u_y, u_z, \varphi_x, \varphi_y, \varphi_z$
Mesh size	0.25 m
Total elements	Dependent on geometry

Floor-girder connection

The floor and girders are connected via a rigid planar surfaces with zero mass density such that the self-weight is not doubled in this area. This surface rigidly connects the floor and the girder and correctly models the behaviour of load transfer between these elements. Figure 28 shows how the elements are modelled by side view.

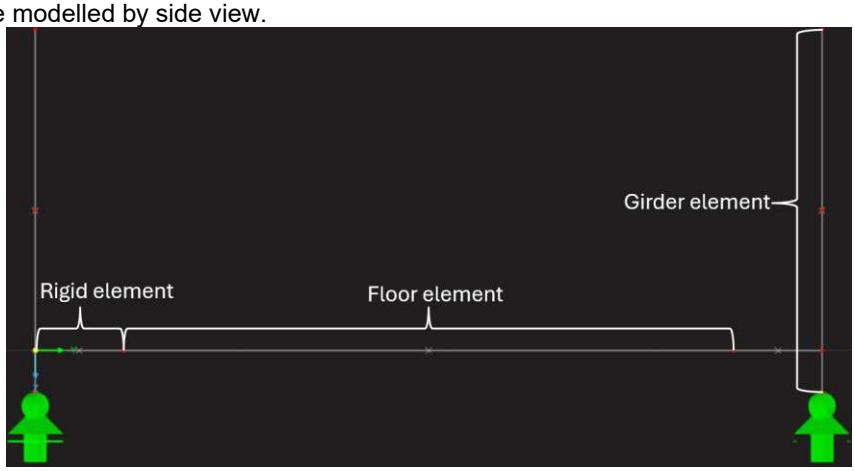

Figure 28: Connection between floor and girder RFEM

Surface integration

To correctly capture the internal forces of the girder, the 2D plane internal forces should be integrated to get the equivalent 1D forces. In RFEM this can be achieved through 'result beams', which integrate the forces of 2D elements to a 1D member element.

This is shown in the 3D representation of the FEM model in Figure 29. The marked 'result beam' is a member type that integrates all 2D forces in its volume to 1D member forces, in this way the 1D girder forces are converted from the 2D forces.

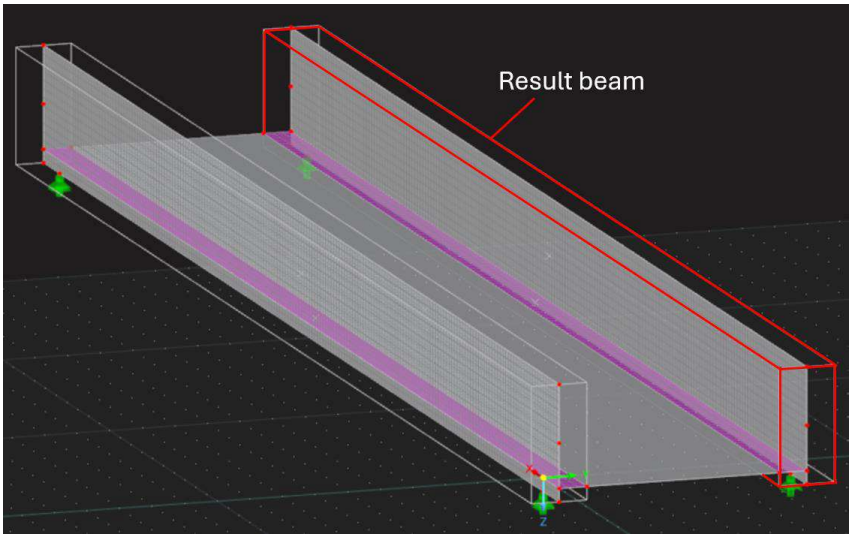

Figure 29: Result beam in 3D model

Model verification

To verify that the FEM of the girders is working as expected, they are verified by a simple hand calculation. The girder is modelled in RFEM and the properties are shown below:

- q = 100 kN/m
- l = 100 m
- h = 2500 mm
- W = 1500 mm
- E = 34000 MPa

To compare the torsional results the load q is acting with an arm a = 1 m on the girder using the same way of rigidly connecting the floor and girder as mentioned above.

Table 5: FEM results and hand calculation results

Calculation	FEM result	Hand calculation	Difference
Midspan moment	124951 kNm	125000 kNm	0.039 %
Midspan deflection	1962.6 mm	1960.8 mm	0.091 %
Quarter span torsional moment	2444 kNm	2500 kNm	2.244 %

For these calculations the following formulas have been used:

$$M = \frac{1}{8}ql^2$$

$$w = \frac{5}{384}\frac{ql^4}{EI}$$

$$T = 0.25qla$$

Comparing the results of the FEM calculations and the hand calculations in Table 13 shows that the differences between the results are insignificant. The relatively large difference in torsional moment is due to the fact that the FEA incorporates direct load transfer to the supports, instead of the hand calculation which assumes all load will be distributed to the girder. The model is therefore accepted.

3.1.6 Reinforcement

With the obtained FEM results the reinforcement can be designed. For the girders it should be noted that there is pre-stressing present in the cross-section which positively impacts the resistance.
For both the floor and the girders longitudinal reinforcement should be designed. The floor might require additional reinforcement for crack-width management. Next to that stirrups for the girder should also be designed for the shear force, torsional moment and suspension forces.
Additional attention for splitting reinforcement at the ends of the deck is required because a tension band is developed here due to the pre-stress forces.

Splitting reinforcement for the introduction of the pre-stress near the anchors is not considered in this research as it there is little room for design improvements for this reinforcement, because applying this reinforcement is not unique to concrete through girder bridges.
Next to that practical reinforcement will not be considered since this should be determined by the engineer and is not subject to design calculations.

Longitudinal reinforcement

Due to the decompression requirements in the OVS (ProRail, 2018) norm the girders will be uncracked in longitudinal direction. This way only ULS reinforcement has to be designed for the girder. Both the reinforcement for the longitudinal forces of the torsional moment that should be present all around the cross-section and the reinforcement for the ultimate moment which should be present at the bottom of the cross-section.
However for the floor this does not hold true as it is not pre-stressed. For the floor additional crack-width reinforcement might be required and it is also reinforced both in x and y direction. The reinforcement layout of the girder (a) and floor (b) might look like Figure 30.

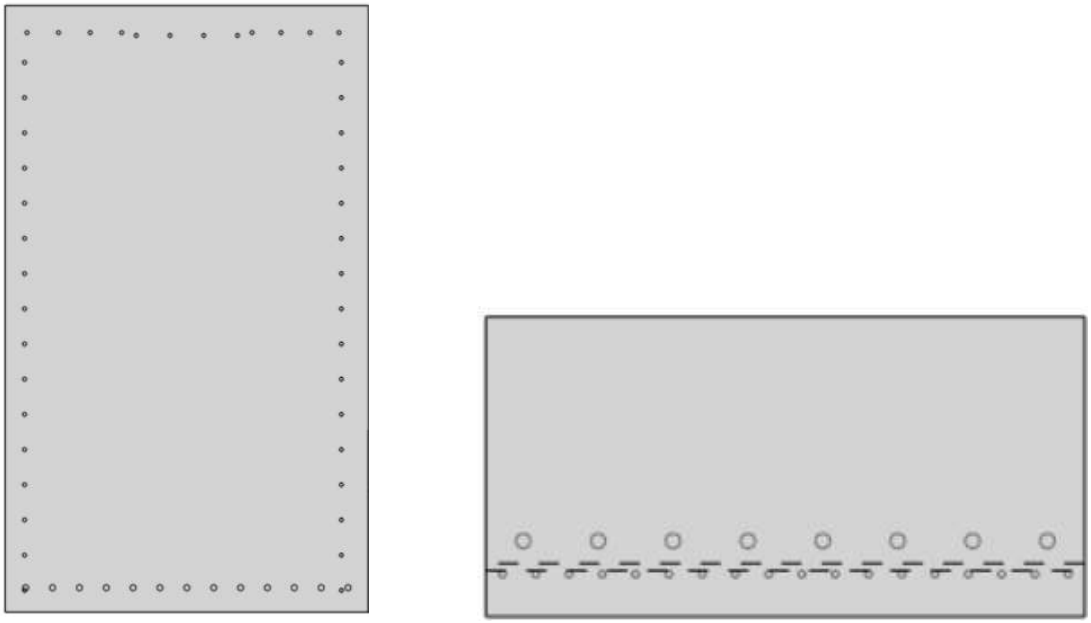

Figure 30: a) Longitudinal reinforcement girder, b) Longitudinal reinforcement floor, section in y direction

The longitudinal reinforcement of the floor is determined per meter, while the reinforcement of the girder is determined per girder.

Stirrups girder

The stirrup design for the girder has been divided in three zones that each carry different type of loading:

- I Shear and torsion
- II Shear
- III Shear torsion and suspension

The stirrup configuration is shown in Figure 31.

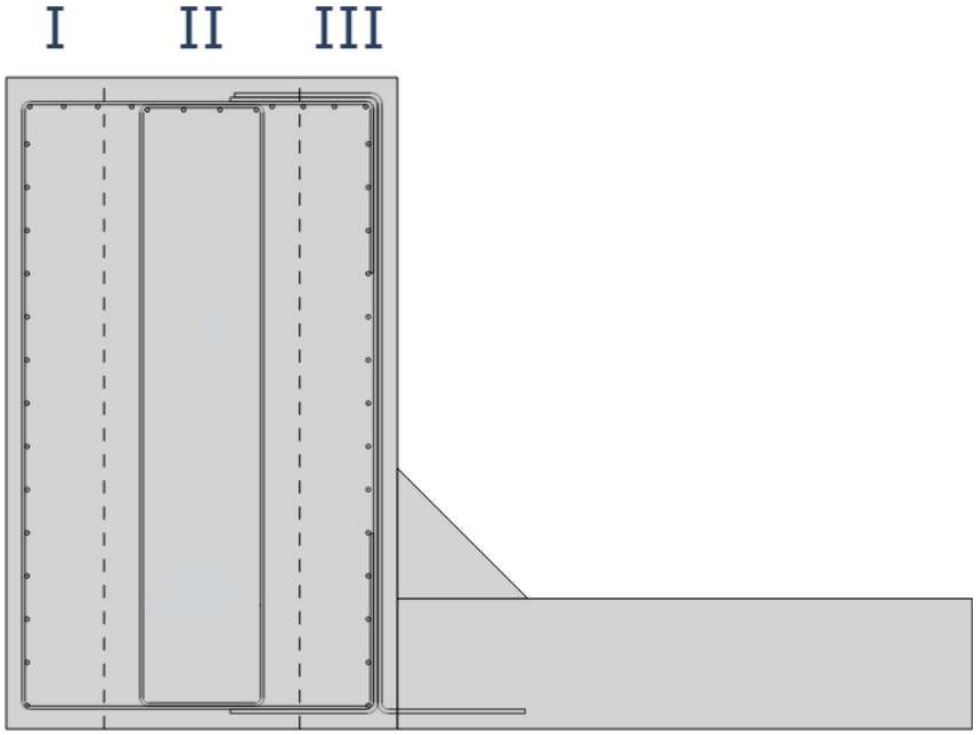

Figure 31: Stirrup configuration

This design allows for heavier reinforcement in zone III where suspension forces will be acting while also fulfilling the requirements in NEN-EN 1992-1-1 which requires a maximum centre to centre distance of 500 mm for stirrup webs.

Splitting reinforcement

Splitting reinforcement should be applied as shown in Figure 32, where an end of the deck is shown. In the tension zone of the deck the tension stresses should be carried by this reinforcement.

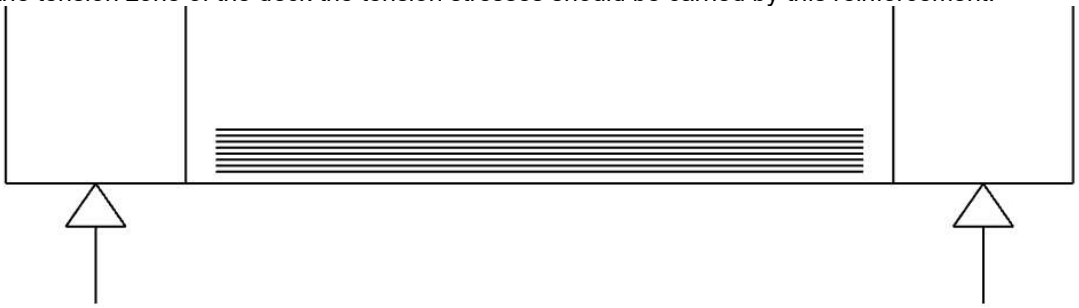

Figure 32: Splitting reinforcement at the end of the deck

3.1.7 Conclusion

Using the relation between the different input parameters, a design like this can be parametrized such that the model poses an generic way to design a concrete through girder bridge. Automating the intermediate calculations and design steps gives a significant time advantage for designing concrete through girder bridges and leaves space for optimizing the design in terms of sustainability and cost-efficiency.

3.2 Parametrizing

To turn the design steps from the previous chapter into a parametric model, first the design parameters should be determined. Thereafter the parametric model can be set-up.
It is important to make use of a chain of responsibility and mediator design patterns (Refactoring.Guru, n.d.) for the flow of the model, such that the inputs can be processed correctly and in clear manner where the 'Single Source of Truth' principle is obeyed (Ruslanova, 2024). This way a maintainable, robust and reuseable parametric model can be built.

3.2.1 Input parameters

This paragraph will summarize all the input parameters for the parametric model. First the geometry parameters summarized in Table 6 will be discussed.

Table 6: Input parameters geometry

Symbol	Unit	Description
L	m	Bridge length
H_{gir}	mm	Height of the girder
W_{gir}	mm	Width of the girder
H_{floor}	mm	Height of the floor
W_{floor}	mm	Width of the floor
a_{haunch}	mm	Height of the haunch

These parameters complete the geometry of the cross-section. They are very important as they will be used in almost all the steps of the design.
Using these parameters the cross-sectional parameters of the girder such as the area and moment of inertia can be determined with these parameters. The effective width can also be computed using NEN-EN 1992-2 (CEN, 2011b) with these design parameters.

The design parameters that are considered to calculate the loads on the bridge are listed in Table 7.

Table 7: Input parameters pre-stress loads

Symbol	Unit	Description
General parameters		
$t_{ballast}$	mm	Thickness of the ballast layer underneath the rail tracks
Concrete		Type of concrete used
Pre-stress parameters		
$c_{applied}$	mm	Applied cover on the reinforcement
f_{pk}	MPa	Characteristic tensile stress pre-stress
n_{cable}		Number of pre-stress cables per girder
$n_{strands}$		Number of strands per pre-stress cable
$Ø_{strands}$	mm	Diameter of strands
y_{low}	mm	Lowest point of the centreline of the pre-stress profile
$y_{top,left}$	mm	Height of the centreline of the pre-stress on the left side of the girder
$y_{top,right}$	mm	Height of the centreline of the pre-stress on the right side of the girder

These parameters determine the full pre-stress system, as these parameters allow determine the selection of pre-stress duct, geometry, full pre-stress profile over the length of the bridge and the forces resulting from the pre-stress.

In addition to this the pre-stress losses can now be computed using the parameters presented in Table 8.

Table 8: Input parameters pre-stress loss

Symbol	Unit	Description
ΔL_w	mm	Wedge set resulting from the tensioning of pre-stress steel
Pre-stress duct		Type of used pre-stressing duct
t	days	Age of the concrete for the decisive moment of the design
t_0	days	Age of the concrete when the pre-stress is applied
RH	%	Relative humidity of the environment around the bridge
ρ_{1000}	%	Relaxation after 1000 hours of tensioning

Using these parameters an in depth calculation for the pre-stress loads can be made.

The only load parameters remaining are the input parameters for the wind load presented in Table 9.

Table 9: Input parameters wind loads

Symbol	Unit	Description
h_{gl}	m	Height between the bridge and ground level
Wind area		Wind area as defined in NEN-EN 1991-1-4 (CEN, 2011b) NB. Figure 1
Terrain category		Terrain category as defined in NEN-EN 1991-1-4

With these parameters and the previously defined geometry parameters the wind loads acting on the bridge can be calculated.

The last required input parameters to fully parametrize the design of the superstructure are the parameters defining the reinforcement summarized in Table 10.

Table 10: Input parameters for reinforcement

Symbol	Unit	Description
General parameters		
Steel		Steel material used for the reinforcement
θ	°	Angle of concrete strut
c	mm	Cover of the reinforcement
Stirrups		
$Ø_{long,stirrup}$	mm	Diameter of the longitudinal reinforcement for torsion
$s_{long,stirrup}$	mm	Spacing of the longitudinal reinforcement for torsion
$Ø_{stirrup,left}$	mm	Diameter of the left stirrup
$s_{stirrup,left}$	mm	Spacing of the left stirrup
$Ø_{stirrup,middle}$	mm	Diameter of the middle stirrup
$s_{stirrup,middle}$	mm	Spacing of the middle stirrup
$Ø_{stirrup,C}$	mm	Diameter of the inverted C stirrup in zone III
$s_{stirrup,C}$	mm	Spacing of the inverted C stirrup in zone III
$Ø_{stirrup,Z}$	mm	Diameter of the inverted Z stirrup
$s_{stirrup,Z}$	mm	Spacing of the inverted Z stirrup
Girder longitudinal		
$Ø_1$	mm	Diameter of the longitudinal reinforcement
n_1		Number of longitudinal bars
Floor		
$Ø_{main,y}$	mm	Diameter of the main reinforcement in longitudinal direction
$n_{main,y}$		Number of main reinforcement bars per meter in longitudinal direction
s_{layers}	mm	The distance between two reinforcement layers in longitudinal direction
$Ø_{add,y}$	mm	Diameter of the additional reinforcement in longitudinal direction
$n_{add,y}$		Number of additional reinforcement bars per meter in longitudinal direction
$Ø_{main,x}$	mm	Diameter of the main reinforcement in transverse direction
$n_{main,x}$		Number of main reinforcement bars per meter in transverse direction
s_{layers}	mm	The distance between two reinforcement layers in transverse direction
$Ø_{add,x}$	mm	Diameter of the additional reinforcement in transverse direction
$n_{add,x}$		Number of additional reinforcement bars per meter in transverse direction
Splitting reinforcement		
$Ø_{spl}$	mm	Diameter of the splitting reinforcement
n_{spl}		Number of splitting reinforcement bars

With these design parameters the reinforcement model posed in paragraph 3.1.6 can be constructed, giving the engineer full freedom to optimize the reinforcement design.

3.2.2 Parametric model creation

The structure of the parametric model is very important as it can become quite difficult to manage the different sources of data. Not only does the model have many inputs, there are a lot of intermediate calculations that also generate more data that should be stored and managed in a structured manner. It is therefore crucial to use structured and clear models to handle the data.

To handle the input data multiple data models are created, which store the data and generate additional data by performing analysis and calculations. The flowchart in Figure 33 shows which input parameters are used for the models.
A brief description of the models is given below.

- Geometry model
    - The geometry model stores all the info about the dimensions and the dependent variables such as cross-sectional parameters.
- Load model
    - Train loads
        - Stores the loads and data from the train load models
    - Wind load model
        - Stores the data about wind and computes the loads on the bridge together with the geometry model.
    - Creep shrinkage and relaxation model
        - Stores the data about these effects and computes the strains that they cause. These can be translated to the pre-stress losses.
    - Pre-stress model
        - Stores all data about pre-stressing and also possesses calculation for the data dependent on the input such as the pre-stress profile and forces.
- Resistance model
    - The resistance model saves all the data about the reinforcement, however it does not include the calculation engines for the resistance. These are separate engines.
    - Durability model
        - The durability model is a simple model that calculates the required cover, crack width and stores the data about durability classes.

The load model and the geometry model are input for the FEM model that is created in RFEM (Dlubal software, n.d.), which in turn returns the internal forces results that can be used for the calculation engines, which will be further explained.
Figure 33 shows the flowchart for the data streams of the model.

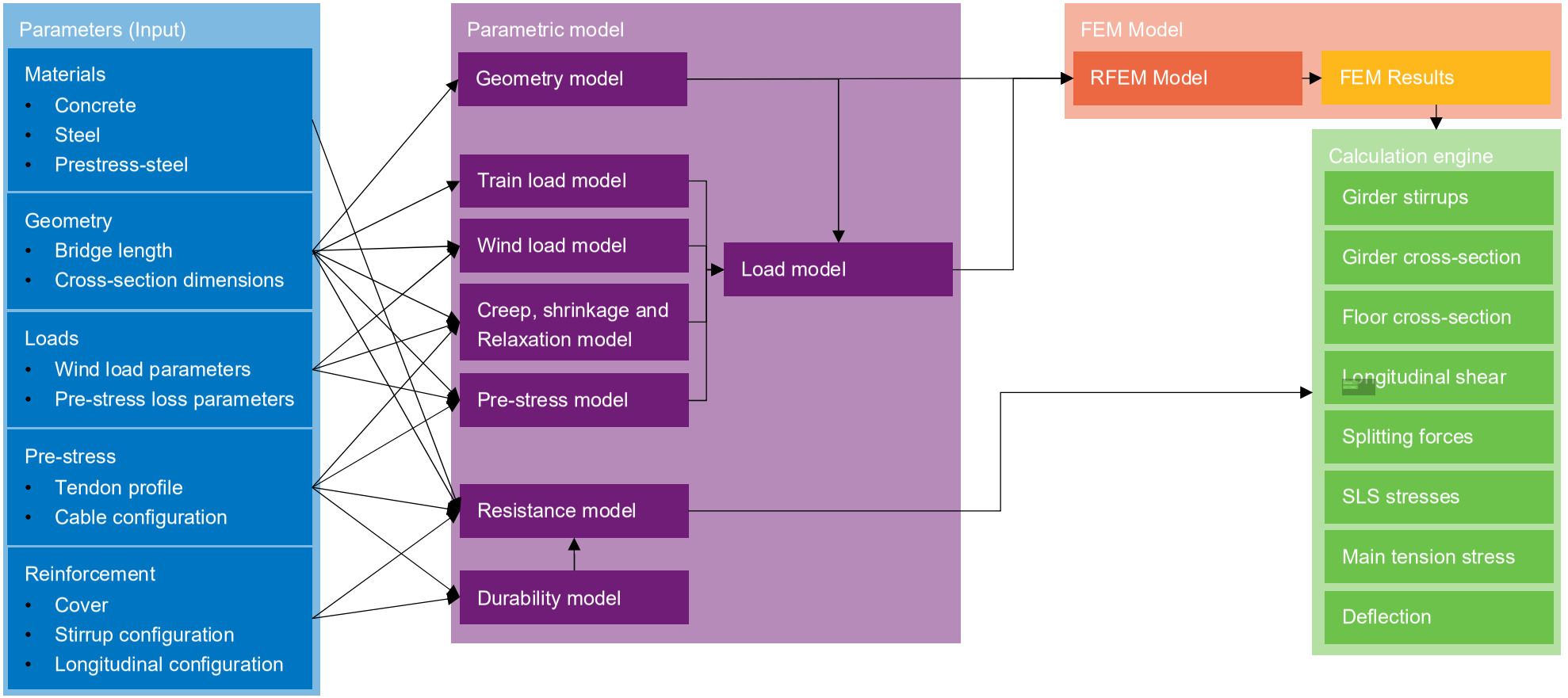

Figure 33: Flowchart working of the model

3.2.3 Resistance checks

Each design should adhere to the requirements mentioned in the literature study. With the collected internal forces of the girders and the floor these can be checked. This is done with the calculation engine shown in green in Figure 33. Please see the calculations in the appendix C for the complete calculations. Here the main idea of the calculations is highlighted.
All the calculations below are incorporated into the parametric model using an automatic calculation, which saves the engineer a lot of time and allows for optimization of reinforcement and geometry design.

Girder stirrups

The stirrups in the girder are checked on shear and torsion using NEN-EN 1992-1-1.
Section 6.3 covers the calculation for torsion. For the torsion calculation the effective wall thickness t_{eff} of the girder is very important, which can be calculated with formula 6.27. With this effective width the area A_k and perimeter u_k of the area enclosed by the centrelines of the connected walls, including the enclosed hollow parts can be calculated. With these parameters the required longitudinal and stirrup reinforcement can be calculated. The shear reinforcement is required in both zone I and III of the stirrups reinforcement.

$$A_{sl,T,req} = \frac{u_k T_{Ed} \cot(\theta)}{2 A_k f_{yd}}$$

$$A_{sw,T,req} = \frac{T_{Ed} z_y}{2 A_k f_{yd} \cot(\theta) z}$$

Section 6.2 of NEN-EN 1992-1-1 covers the shear stress calculations. For the parametric model the stirrups are designed such that 40 % of the shear force is distributed to the stirrups in zone I and III and the other 60 % is distributed to zone II. Before designing the stirrups it can be checked whether the pre-stressed concrete is strong enough to withstand the shear forces using:

$$V_{Rd,c} = \frac{I b_w}{S} \sqrt{f_{ctd}^2 + \alpha_l \sigma_{cp} f_{ctd}} > V_{Ed}$$

It should be noted that V_{Ed} in this case is sum of 0.2 V_{Ed} from the FEM results and V^*_{Ed} which is the equivalent shear force from the torsional moment that can be calculated using:

$$V_{Ed,T} = \tau_T t_{eff} z_y$$

If the concrete is not strong enough to withstand the torsional forces the stirrups should be checked to have enough area:

$$A_{sw,I,req} = \frac{0.2 V_{Ed}}{z f_{yd} \cot(\theta)}$$

$$A_{sw,II,req} = \frac{0.6 V_{Ed}}{z f_{yd} \cot(\theta)}$$

$$A_{sw,III,req} = \frac{0.2 V_{Ed}}{z f_{yd} \cot(\theta)}$$

Suspension forces from the floor acting on the girder are also considered as these have to be resisted by stirrups. These forces in the floor cause both a suspension force and a fixed end moment as shown in Figure 34.

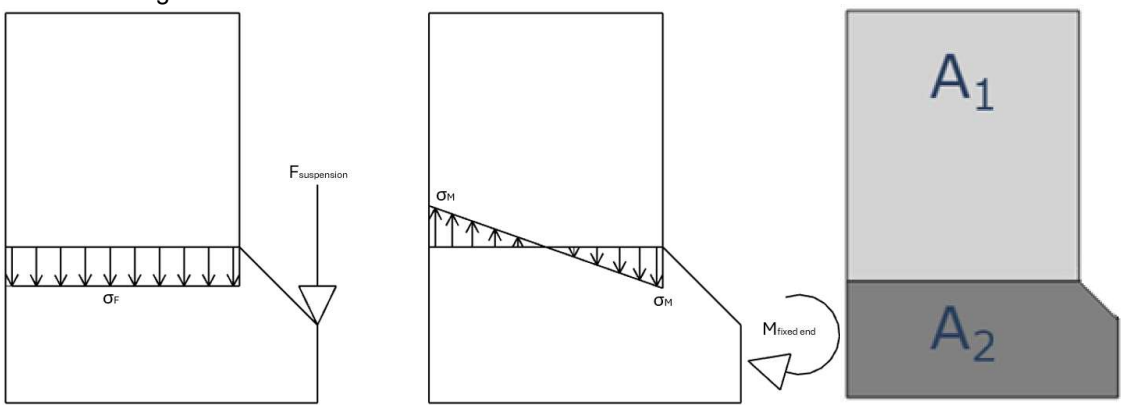

Figure 34: Suspension forces and fixed end moment for stirrups

These stresses need to resisted by stirrups in the girder. Because the critical line for the connection of the girder and the floor is along the top of the haunch. This way only the load that needs to be carried by the top part of the girder needs to be accounted for because this needs to be carried to the top part of the cross-section. This is translated to a reduction factor based on the area of the cross-section, as described in NSRL1015 (NS Infrabeheer, 1997).

$$\alpha_A = \frac{A_1}{A_1 + A_2}$$

For the maximum suspension force acting on a girder it should be incorporated that the decisive train load SW/2 does not act in the middle of the floor deck in transverse direction, rather at x = 3.4 m, as shown in Figure 35. This means that this load should be distributed to the right girder for the maximum resulting force.

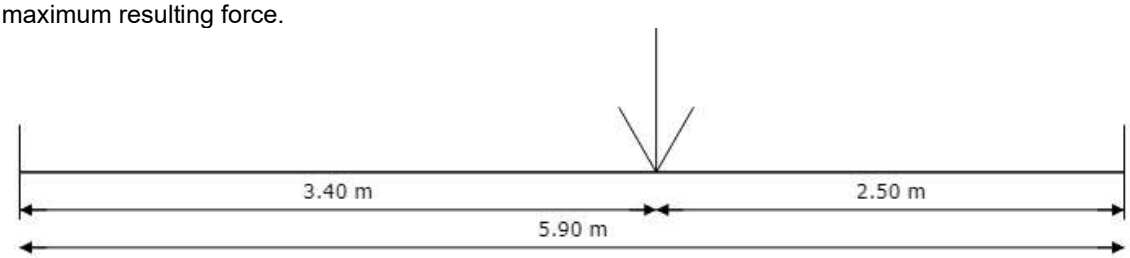

Figure 35: Position of the train load in the transverse cross-section of the bridge

Using this and the calculated self-weight of the bridge the suspension force and fixed end moment can be calculated. It should be noted that the load combination factors have to be incorporated in this calculation.

Using the calculated fixed end moment and suspension force the required reinforcement can be calculated using:

$$A_{\text{sw,F}} = \frac{\alpha_{\text{A}} F_{\text{sus}}}{f_{\text{yd}}}$$

$$A_{\text{sw,M}} = \frac{\alpha_{\text{A}} M_{\text{fix}}}{z f_{\text{yd}}}$$

$$A_{\text{sw,III,req}} = A_{\text{sw,F}} + A_{\text{sw,M}}$$

The complete calculations for the stirrups are quite time consuming. An example calculation report as the appendix C, here only the main points are summarized. Automatically recalculating these results saves the engineer a lot of time and allows for optimization of the reinforcement.

Girder cross-section check

To check the cross-section of the girder for moment resistance an algorithm is used to solve the force equilibrium, from which the steel stress, pre-stress steel stress and concrete stress can be determined using the stress-strain diagrams.

This algorithm finds the combination of maximum concrete strain and concrete compression zone height x_u that satisfies the equilibrium: $\Sigma F_h = - N_c + N_c + F_{Pw} + \Delta F_P = 0$. It uses the iterative bisection method to quickly find equilibrium. An example of the obtained stress and strain diagram is shown in Figure 36.

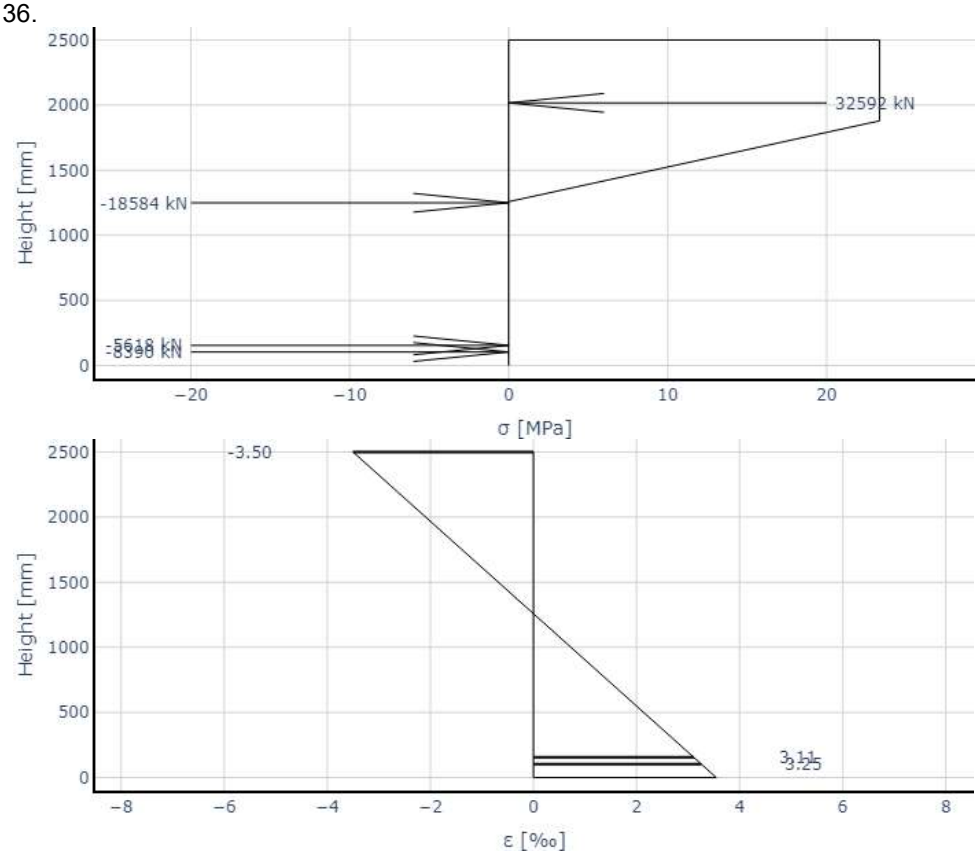

Figure 36: a) Stress diagram girder cross-section, b) Strain diagram girder cross-section

The calculated concrete steel and pre-stress forces are calculated using:

$$N_c = \alpha f_{cd} w_{gir} x_u$$

$$N_s = A_s \cdot \min(E_s \varepsilon_s; f_{yd})$$

$$\Delta F_{Pw} = \sigma_P(\varepsilon_P) A_P - F_{Pw}$$

Using the eccentricities of these forces to the middle of the cross-section the moment resistance can be calculated and compared against M_{Ed} following from the FEM model.

$$M_{Rd} = N_c e_c + e_s N_s + \Delta F_P e_P$$

The cross-section is also checked for the maximum height of the concrete compression zone according to NEN-EN 1992-1-1 NB 6.1(9), which is decisive in most cases. This article prescribes that:

$$\frac{x_u}{d} \leq \frac{500}{500 + f}$$

Where f is the weighted steel strength of the pre-stress and steel where the initial pre-stressing stress is subtracted from the pre-stress steel strength.
If this is not satisfied, the pre-stress can fictitiously be lowered to make sure this requirement is satisfied. It is important to note that M_{Ed} will increase when lowering pre-stress and M_{Rd} will decrease. In this manner the pre-stress can for example be lowered to 70 % which will result in an increase in M_{Ed} and a reduction in M_{Rd}. If in this case $M_{Ed} < M_{Rd}$ and the requirement of the height of the compression zone is fulfilled the cross-section can be accepted.

The parametric model automatically checks both requirements by reducing the pre-stress if the concrete compression zone height is not fulfilled. Through calculations using an iterative bisection method the algorithm searches for a pre-stress reduction that satisfies both conditions. If it cannot be found the pre-stress or reinforcement has to be adjusted.

Floor cross-section check
The floor is checked with the same algorithm as the girder, however the floor it can be simplified as it is not pre-stressed. It also does not have to be checked for concrete compression zone as it is not a girder, which means that NEN-EN 1992-1-1 NB 6.1(9) does not have to be fulfilled.
However it is an important distinction that the floor reinforcement should be checked both in x and y direction for MxD+ and MyD+.

Longitudinal shear

The girder floor section is checked for longitudinal shear according using the method proposed in NEN-EN 1992-1-1 6.2.4. It turns out that for most cases concrete through girder bridges do not need reinforcement for longitudinal shear and the concrete strut is sufficient to withstand the stress.
This is checked by calculating the shear stress due to longitudinal shear:

$$v_{Ed} = \frac{\Delta F_d}{h_f \Delta x}$$

The maximum value that may be assumed for Δx is half the distance between the cross-section where the moment is 0 and the cross-section where the moment is at a maximum (6.2.4 (3)). In this case this means that Δx half the length of the span of the bridge. The other parameters are summarized in Figure 37:

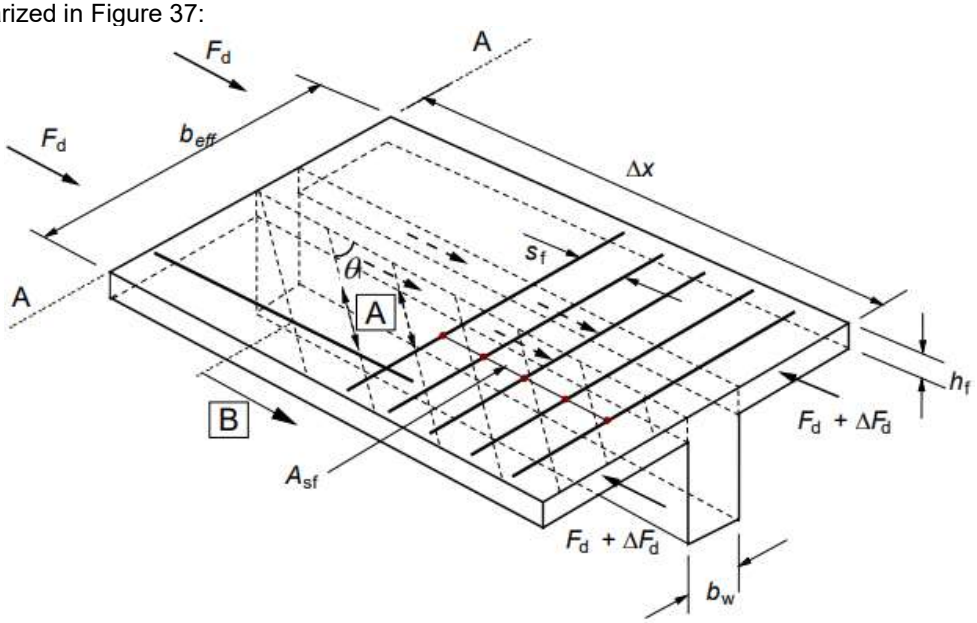

Figure 37: Longitudinal shear sketch (CEN, 2011a)

The figure shows a T-girder however for a trough girder bridge one flange can be ignored to find the equivalent of half a through girder bridge.
To obtain the maximum shear stress calculated using the above expression an automatic algorithm was used. It iterates through all different sections of the floor. This is achieved by discretizing the structure into check sections. At each check section the normal force is computed which is than pairwise compared to the normal forces at the other sections. By using a brute force algorithm the maximum shear stress is found by using a minimum resolution Δx of the grid size of the floor.

If the obtained shear stress fulfils the condition in NEN-EN 1992-1-1 6.2.4 (6):

$$v_{Ed} < k f_{ctd}$$

No longitudinal shear reinforcement is required if this condition holds true, if this is not the case the design has to be adjusted or longitudinal shear reinforcement has to be designed.

Splitting forces ends of the deck

At the ends of the deck the splitting forces need to resisted by reinforcement as these tension stresses are too high to be resisted by the concrete only. To find the forces a strut and tie model is used. For the STM it is assumed that all pre-stressing stresses are equally divided over the whole bridge cross-section at a distance of $0.5W_{gir}$ from the introduction of the pre-stress. Then, making sure equilibrium is fulfilled the force in the concrete tie can be calculated. An example of such an STM is shown in Figure 38.

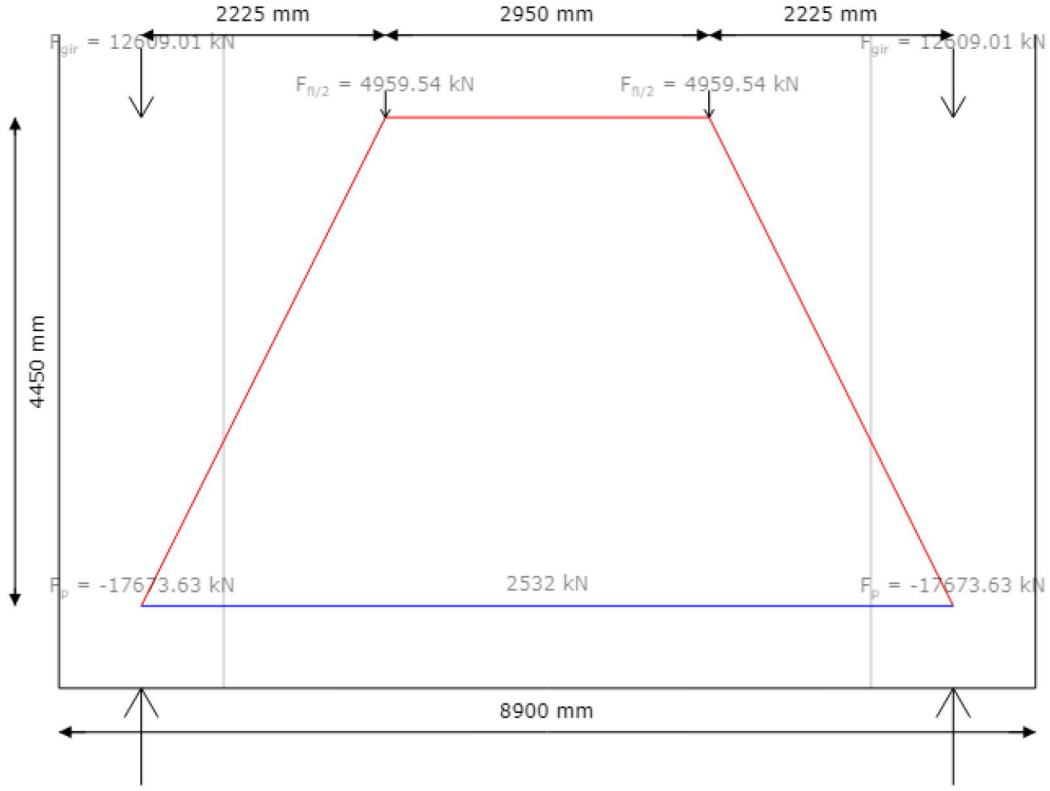

Figure 38: Strut and tie model for splitting reinforcement at the end of the decks

Using the obtained tension force in the steel tie, the steel stress in the reinforcement can be calculated which should be lower than the ultimate steel stress:

$$\sigma_{spl} = \frac{F_{spl}}{A_{spl}} < f_{yd,spl}$$

Main tension stress

As mentioned in the literature study the main tension stress in a concrete through girder bridge deserves some attention. Unlike T-girder bridges where the main tension stress occurs at the top or bottom of the cross-section, the main stress will occur just above the haunch at the inner wall of the girder and should be checked at 0.8d and 2d away from the bearing cross-sections according to NSRL015 (NS Railinfrabeheer, 1997). Because, at x < 0.8d the forces are expected to be carried to the support directly and at x = 2d the shear force is expected to change sign. Both the decisive V_z and M_x have to be checked at these locations.

This main tension stress consists of three parts: σ_{xx}, σ_{zz} and τ. The concrete should be strong enough to withstand this main stress. A complete calculation of these stresses can be found in appendix C, the main points of the calculation will be highlighted in this report.

σ_{xx} is the stress component caused normal force and moment by external loading and pre-stress. This can simply be calculated by taking the sum of the stress caused by the moment and the normal force for half the bridge cross-section:

$$\sigma_{xx,N} = \frac{N_{tot}}{A_{bridge/2}}$$
$$\sigma_{xx,M} = \frac{zM_y}{I_{bridge/2}}$$

σ_{zz} is the stress component caused by suspension forces and fixed end moments, which is calculated similarly to how these stresses were calculated for stirrup suspension reinforcement. In this manner again F_{sus} and $M_{fixed\ end}$ can be calculated, however because this is an SLS check different load combination factors apply.

The same reduction factor due to the different areas may be used again, such that the stresses can be calculated using:

$$\sigma_{zz,M} = \frac{M_{fixed\ end}\alpha_A}{\frac{1}{6}W_{gir}^2}$$
$$\sigma_{zz,N} = \frac{N_{tot}\alpha_A}{W_{gir}}$$

These stresses are calculated per meter width.

Finally, τ is the stress component caused by torsion, mobile loads and shear force caused by external loading and pre-stress. The shear force at the section just above the haunch can be calculated using:

$$\tau_V = \frac{V_{Ed}S_{A,haunch}}{IW_{gir}}$$

Where $S_{A\ haunch}$ is the sectional modulus at the section just above the haunch.

The stress due to torsion can be calculated similarly to how the torsional shear stress was calculated for the stirrups using NEN-EN 1992-1-1. Using the same t_{eff} and A_k this stress can be calculated:

$$\tau_T = \frac{M_{T,Ed}}{2A_k t_{eff}}$$

To evaluate the concrete tension stress caused by all these components the following rule may be used according to NSRL015 (NS Infrabeheer, 1997):

$$\sigma_{ct} = \frac{1}{2}(\sigma_{xx} + \sigma_{zz}) + \sqrt{\frac{1}{4}(\sigma_{xx} - \sigma_{zz})^2 + \tau^2} < 0.6f_{ctd}$$

SLS Stresses

OVS requires pre-stressed bridges to be fully pre-stressed to limit fatigue stress deviations. This means that the maximum tension stress for all SLS combinations should be checked according to these requirements. Next to that the maximum concrete compression stress at t=0 should not exceed the ultimate concrete compression stress.

The first check is required by OVS00030-6 (ProRail, 2018) as an amendment to NEN-EN 1992-1-1 (CEN, 2011a) 7.3.1, which requires that:

- In SLS-quasi: $\sigma_{ct} < 0$
- In SLS-freq: $\sigma_{ct} < 0.5\ f_{ctk,0.05}$ and $\sigma_{ct} < 0.5\ f_{ctk,0.05}$
- In SLS-char: $\sigma_{ct} < 0.5\ f_{ctk,0.05}$ and $\sigma_{ct} < 0.5\ f_{ctk,0.05}$

These stresses can be calculated using:

$$\sigma_{ct} = \frac{M_{Ed}}{W_{bot}} + \frac{N_{Ed}}{A_c}$$

M_{Ed} and N_{Ed} in all SLS limit states can be obtained from the FEM results. In this way this requirement is checked for each state.

Next to the tension stress, the compressive stress in the bridge at t=0 should not exceed the compression strength. This check is performed in SLS-quasi permanent, because that is representative of the forces acting at t=0. The maximum compressive stress can be calculated similar as before looking at both the situation with maximum compressive force and max moment to find:

$$\sigma_c = -\frac{M_{Ed}}{W_{top}} + \frac{N_{Ed}}{A_c}$$

This compressive stress should be lower than the max concrete compressive strength f_{cd}.

Deflection

Lastly the parametric model also calculates the maximum deflection and pre-scribes the required pre-camber to reach the pre-camber requirement in the OVS (ProRail, 2016) of L/1000. From the FEM results the maximum deflection can be obtained which is subtracted from the required camber to find the required pre-camber for the construction.

Crack-width floor

The floor should fulfil the OVS requirements of maximum 0.2 mm crack width. This is checked using the calculations in NEN-EN 1992-1-1 (CEN, 2011a) section 7.3.4. Therefore again the equilibrium should solved to find the steel stress. However in this case not only the force equilibrium has to be solved, the moment equilibrium in the cross-section should also be fulfilled with the representative SLS moment. Using the same bisection iterative approach the equilibrium can be solved. The stress and strain diagrams look different in de SLS situation as the concrete is not fully utilized in this situation, an example is shown in Figure 39.

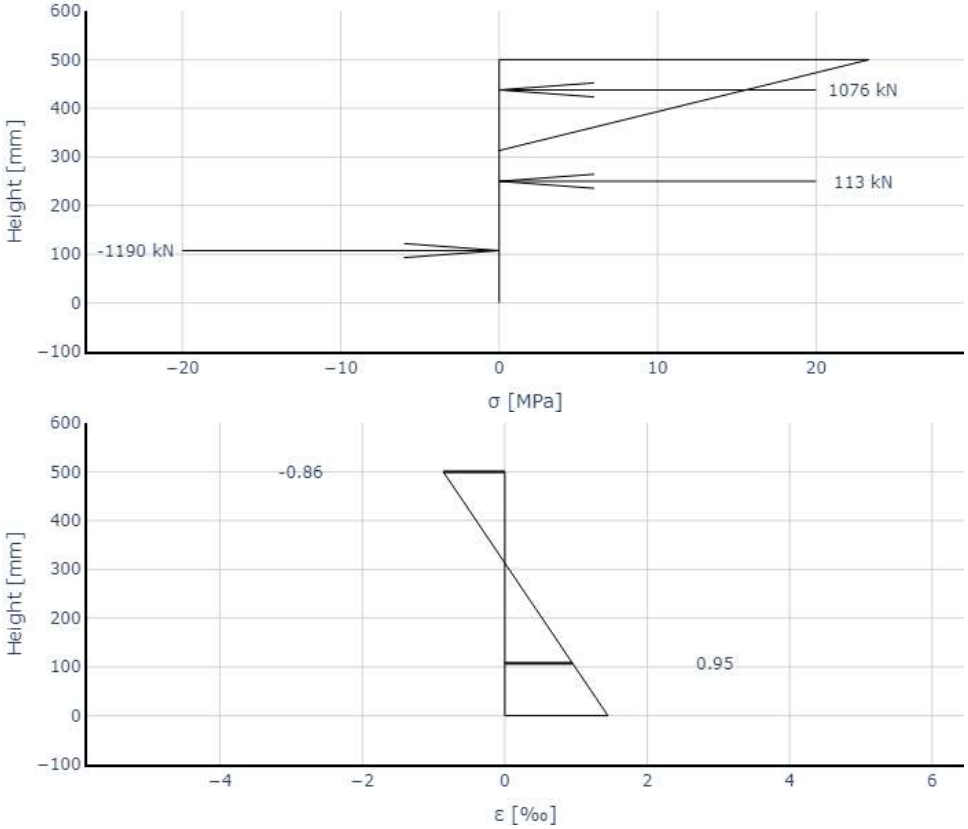

Figure 39: Stress and strain diagrams crack-width

The steel stress can be obtained from these diagrams such that ε_{sm} - ε_{cm} can be determined with NEN-EN 1992-1-1 (CEN, 2011a) formula 7.9:

$$\varepsilon_{sm} - \varepsilon_{cm} = \frac{\sigma_s - k_t \frac{f_{ct,eff}}{\rho_{p,eff}}(1 + \alpha_e \rho_{p,eff})}{E_s} \geq 0.6 \frac{\sigma_s}{E_s}$$

The maximum crack distance can be computed using NEN-EN 1992-1-1 (CEN, 2011a) formula 7.11, from which the maximum crack-width can be computed using formula 7.8.

$$s_{r,max} = k_3 c + \frac{k_1 k_2 k_4 \varnothing_{eq}}{\rho_{p,eff}}$$

$$w_k = s_{r,max}(\varepsilon_{sm} - \varepsilon_{cm})$$

For the specific calculation of each of the factors in these formula, please refer to the appendix C.

Fatigue

Fatigue is not checked as it assumed that this will not be decisive for a fully prestressed concrete through girder bridge. The stress changes caused by mobile train loads will be relatively small compared to more slender and non-prestressed bridges. This assumption is evaluated in section 5.3.

3.3 Evaluation

To compare different design alternatives made with the parametric model, there should be a way to evaluate the design. As mentioned in the literature review there is a current need to optimize structural design for both financial and environmental concerns. Therefore the parametric model tries to calculate an indication for both material costs and environmental impact shadow costs (Quist, 2024).
To achieve this the model calculates both an indication of the costs and the environmental impact based on the materials used for the design. The scope of this indication is the costs of the material itself and an indication of the additional costs for placing the materials. So for concrete this means the pouring of the concrete and for the steel this would include tying the reinforcements.
It is important to note that this is a really broad estimate as the actual costs will depend highly on specific parameters such as location and material availability. Using the cost indications given below and a bill of quantities for the materials used for the design the model is able to compute these indications.

3.3.1 Material costs

The cost indication of the materials was provided by a cost expert of Witteveen + Bos (S. Ilbrink, personal communication, February 29, 2025) for a general situation of concrete bridge construction in 2025 and can be summarized as follows:

- Concrete
  - C30/37: ± 158 EU/m^3
  - C40/50: ± 162 EU/m^3
- Reinforcement steel: ± 1.5 EU/kg
- Pre-stressing steel: ± 4 EU/kg

3.3.2 Environmental impact shadow costs

For the environmental impact the “Nationale Milieu Database” has been accessed (Stichting Nationale Milieudatabase, n.d.), which provides indications of environmental shadow costs for construction materials. The method applies a Life Cycle Assessment (LCA) approach, converting environmental impacts into monetary values per material unit. The environmental costs can be calculated by multiplying material quantities with their specific environmental cost factors.
The results are summarized below.

- Concrete
  - C30/37: 31.513 EU/m^3
  - C40/50: 26.994 EU/m^3
- Reinforcement steel: 126.026 EU/ton
- Pre-stressing steel: 213.424 EU/kg

4 Optimization

Now that the parametric model has been set-up to quickly analyse multiple bridge designs they can be optimized. The most important way an engineer can optimize designs is by iteratively improving the design such that the material usage is optimized by designing at the limit of the material strength using a trial and error approach. Next to that the design can also be optimized by looking for cross-section shapes that allow for better material usage.

4.1 Design process optimization

A problem in civil engineering is the principal of 'cost of change' (The Agile Modeling (AM) Method, 2023). In short this means that changing design parameters later on the design cycle is more expensive than doing this at the start of the design cycle.
A cost of change curve for traditional bridge design is depicted in Figure 40. Here it shows that the costs a change in design parameters for example due to a changed requirement or a design optimization will increase exponentially over time.

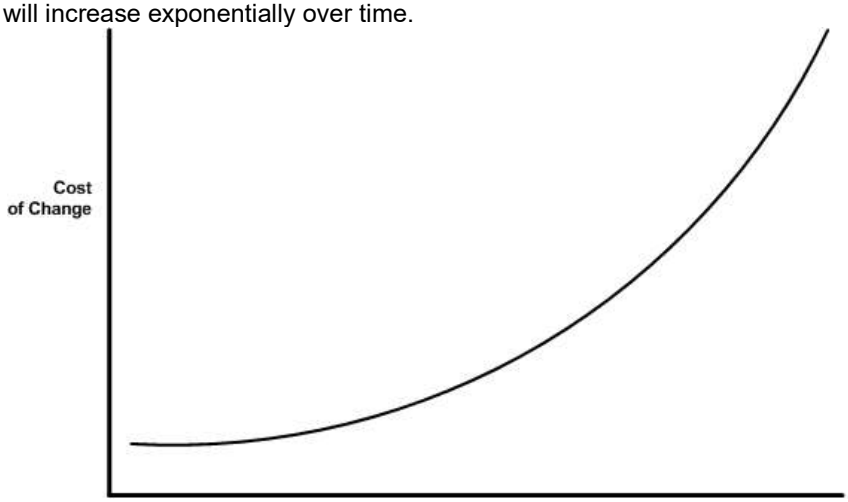

Figure 40: Traditional Cost of Change curve (The Agile Modelling (AM) Method, 2023)

In regards of the cost of change and parametric modelling the founder of the Parametric Technology Company Samuel Geisberg quoted in 1993: "*The goal is to create a system that would be flexible enough to encourage the engineer to easily consider a variety of designs. And the cost of making design changes ought to be as close to zero as possible*." (Teresko, 1993).
In contrast to traditional design, which restricts low cost changes to the design to only the early stages, parametric modelling allows to maintain a low cost of change throughout the project lifecycle (Davis, 2013).

From this, it can be concluded that the value of a parametric model is intrinsically linked to its ability to facilitate rapid design changes and evaluations throughout the project lifecycle. The power of parametric modelling is its capacity to flatten the cost of change curve, enabling an engineer to explore a wider range of design variations with minimal additional costs. This flexibility also enhances the engineer's capacity to innovate and respond to evolving project requirements.

4.1.1 Automation

When a design parameter is modified in the parametric model, all dependent results are automatically recalculated. This instant feedback allows the engineer to immediately observe the result of their change, facilitating rapid design iterations. The engineer can apply his professional judgment to evaluate if the changes yield the expected results or if further adjustments are necessary, streamlining the optimization process.
As detailed in the previous chapter, the parametric model incorporates a wide range of calculations. By adjusting the design parameters, engineers can efficiently explore various scenarios to find the optimal design solution, by taking advantage of the rapid iterations.

The parametric model can also create and adjust a FEM model to make it fit the design parameters. This integration ensures that geometry, loads, and load combinations are consistently incorporated in the FEM analysis. Furthermore, the parametric model can import FEM results for analysis, creating a cohesive design and analysis workflow.
In traditional design methods, even minor changes in design parameters often require time-consuming manual adjustments to nodes, lines, or surfaces in the model. The parametric approach eliminates this process by automatically updating the entire model based on parameter changes, significantly reducing the time required for design iterations.

Next to these automatic calculations the parametric model is also able to automatically report all the calculation results. Collecting al the parameters, calculation results and figures an extensive document is created that show the in-depth calculations made by the parametric model. This automated reporting system ensures that all documentation is instantly updated when design parameters change, maintaining consistency between the design and its documentation for current and future projects.

Also the error sensitivity is greatly reduced because the factor of human error is removed from the design calculations and the calculations are performed by the computer. This also leads to increased precision as the (intermediate) calculations are never rounded and the integration between the FEM model and the parametric model allows for great precision of data transfer. Also the computer always has the exact results and does not make approximations.

4.1.2 Broader design space

Parametric modelling expands the design space for engineers with several key advantages.
The engineer can quickly create variations of their design, exploring options that might have been too time-consuming to consider using traditional methods. This enables a more comprehensive exploration of the design space, potentially leading to innovative solutions that might otherwise have been missed.
This iterative cycle, enables engineers to progressively enhance their designs. Each iteration can incorporate new insights, leading to incremental improvements in cost and environmental effectiveness.
Moreover, the ability to quickly visualize the effects of parameter changes helps engineers develop a deeper understanding of the relationships between different design elements. This enhanced comprehension can lead to more thoughtful and well-optimized designs.

The flexibility of the parametric model also allows the engineer to respond effectively to external factors. For example if the client changes project requirements it is relatively easy to incorporate these in the design. Also changes in calculation methodology or theory can be adjusted quickly because the code for the model is easy to adjust. Once the model is adjusted it can be applied for a broader range of applications.
This is not limited to the early design stages but can also be done later on in the design reducing the cost of change.

4.1.3 Conclusion

In conclusion, parametric modelling not only accelerates the design process but also improves the quality of engineering work by enabling more thorough exploration of design alternatives and ensuring consistent, up-to-date documentation throughout the design lifecycle.

4.2 Cross-section optimization

Because the cost of changing design parameters is reduced it is much cheaper to parametrically design bridges to their material limits. This leads to cheaper designs and improved material usage. However this also opportunity to use less traditional cross-sections for the girders. This study demonstrates the possibility to design with different cross-section shapes.

The main factors influencing minimum required cross-section are:

- The cross-section at the start and end of the girder should be large enough to incorporate the pre-stress anchors for the introduction of the pre-stress.
- The pre-stress tendons follow a parabolic profile and can therefore require a certain concrete height to be contained in the cross-section.
- To withstand the internal forces the cross-section also needs certain dimensions, however these required dimensions are smaller than required by the introduction of the pre-stress.

4.2.1 Variant comparison

Three different designs for the cross-section optimization are considered. This paragraph introduces the variants and summarizes the advantages and disadvantages of the variants.

Tapered girder

The core idea is to optimize the cross-section of the girder by reducing its height where possible. The goal is to reduce the overall height of the concrete cross-section to the minimum required for structural integrity.

Closer to the supports, a larger cross-sectional area is necessary to accommodate the stress from the pre-stressing cables. This also provides space for the pre-stress anchors. Going further away from the supports toward the centre of the span, the required concrete area decreases. Therefore, the height of the cross-section can be reduced. The reduction continues until the minimum height required for ULS strength is reached. You can see this in Figure 41, where the beam tapers downwards. The green area represents the concrete area necessary to accommodate the pre-stressing forces and meet structural requirements. The red area shows the area that might potentially be reduced.

In essence, the design principle is to strategically remove concrete from areas where it's not structurally critical, resulting in a lighter, more efficient beam.

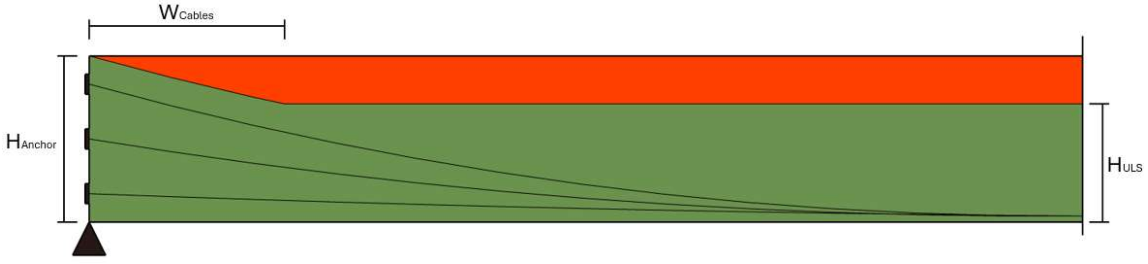

Figure 41: Length profile of half a sloping through girder

This design offers potential material savings by reducing the cross-section height where structurally permissible, however the reduced cross-section height might require heavier reinforcement. The variable geometry also introduces increased complexity in formwork and construction, and could complicate the placement and stressing of the cables. The design's efficiency hinges on a careful balance between material reduction benefits and added manufacturing costs.

I-girder

The core idea behind this variant involves strategically removing concrete from the central portion of the cross-section, creating an I-girder where the top flange accommodates compression forces and the bottom flange provides a zone for pre-stressing tendons. Also the floor can still be connected to the larger bottom side of the cross-section. For the part of the girder where the pre-stress is introduced the girder will have a larger cross-section.

The cross-section would than look like an I-girder. This cross-section shape is shown in Figure 42.

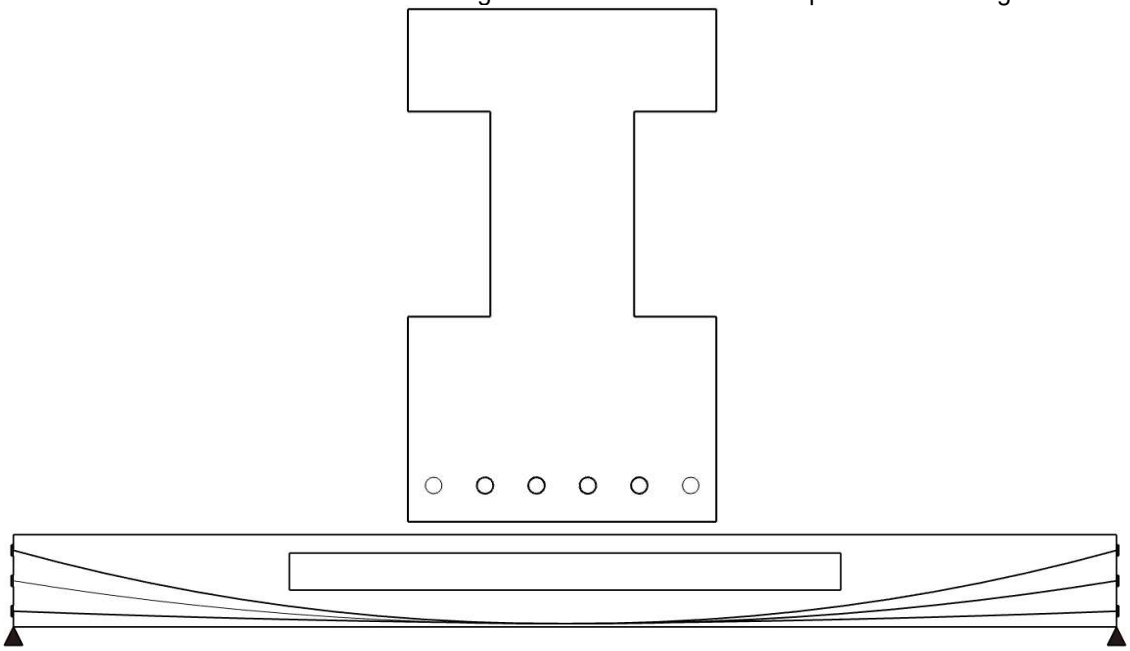

Figure 42: I-girder cross-section shape

Advantages of this design would be its bending moment resistance, because the I shape is very efficient in withstanding bending moments while also keeping space for the pre-stressing cables. This design also reduces the beam's weight where it is the most effective: at midspan.

Where the I-shape is optimal for withstanding bending moment, it is not ideal for withstanding torsional moments and shear forces that are quite important for through girder bridge design. With this design extra attention should also be paid to the reduced lateral buckling resistance.

Next to that this design can possibly feature local stress concentrations where the web joins the flanges.

This design will also pose challenges for pouring the concrete and will need more reinforcement compared to the full cross-section add midspan.

Box girder

The final variant also involves strategically removing concrete from the central portion of the cross-section, however now the concrete is removed from the centre of the cross-section creating a box girder where the top flange accommodates compression forces and the bottom flange provides a zone for pre-stressing tendons. For the part of the girder where the pre-stress is introduced the girder will have a larger cross-section. The hollow core can be filled up using EPS or other lightweight material to save self-weight.

The cross-section would than look like a box girder and is shown in Figure 43.

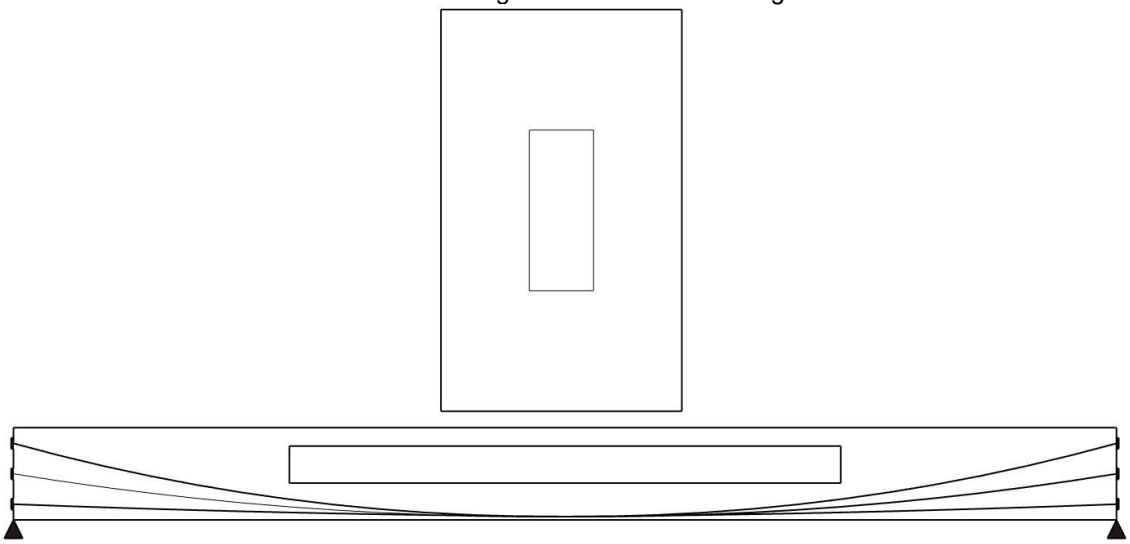

Figure 43: Box girder variant

Advantages of this design would be its torsional rigidity, because the box shape is very efficient in withstanding torsional moments while also keeping space for the pre-stressing cables. Also the loads are more evenly distributed across the whole cross-section and the bending moment resistance is not significantly reduced.

Where the Box-shape is optimal for withstanding torsion, the formwork can become very complex and can have higher construction costs. The enclosed nature of the box girder complicates internal inspections for maintenance and corrosion of reinforcement.

Lastly, he design will need more reinforcement compared to the full cross-section add midspan. Also the shear capacity and stability might be impacted.

4.2.2 Variant evaluation

To choose which cross-section will be incorporated in to the parametric model a multi-criteria analysis is performed. The designs will be judged based on their resistances and material reduction. The construction process and slenderness of the bridge for aesthetic reasons will also be judged, however they do not have as much impact as the other parameters and therefore have a lower weight.

Shear / Torsional resistance

The box girder excels in torsional resistance due to its closed shape, which efficiently resists twisting moment.

The tapered girder still has considerable shear and torsional resistance due to its solid cross-section, however due to the reduced the resistance is still lower compared to the traditional cross-section.

The I-girder, has reduced torsional capacity due to removed materials at the sides.

Moment resistance

Both the I-girder and box girder are highly efficient in resisting bending moments, with material concentrated at the top and bottom where it's most effective.

The tapered girder, due to its reduced heigh, has a lowered moment resistance. It is also less efficient as the concrete in the central portion of the cross-section is not utilized optimally.

Material reduction

The tapered girder uses the least material by reducing height as optimally as possible. Both the I-girder and box girder remove material from less critical areas which is still effective, however the full cross-section uses the most material throughout its length.

Construction process

In terms of construction process the tapered girder requires more complex formwork but is still relatively straightforward. The I-girder presents challenges in concrete pouring and formwork. The box girder is most complex, with difficulties in internal formwork and concrete placement.

Slenderness

The I-girder achieves the highest slenderness ratio due to its efficient shape. The box girder follows as close second due to its material reduction in the middle of the cross-section. The tapered girder varies in slenderness along its length. The full cross-section is the least slender due to its constant, full profile.

Table 11: MCA girder variants

	Weight	Sloped	I-girder	Box girder
Shear / Torsional resistance	3	1	-1	2
Moment resistance	3	0	1	1
Material reduction	3	2	1	1
Construction process	2	0	-1	-2
Slenderness	1	-1	2	1
Total		8	3	9

Following the MCA in Table 11 the conclusion can be drawn that the box girder design has the most potential to generate efficient designs. The options to design with such a cross-section has been added to the parametric model.

4.2.3 Integration in parametric model

To allow for through girder bridge design using the 'box-girder' design variant discussed in the chapter before the design parameters in Table 12 should be added to the parametric model:

Table 12: Input parameters for the cutout

Symbol	Unit	Description
L_{cutout}	m	Length over which the cutout is present
H_{cutout}	mm	Height of the cutout
W_{cutout}	mm	Width of the cutout

These parameters of course adapt every step of the design process from initial geometry definition to the final resistance calculation.

4.2.4 Calculations

The introduced empty section of the cross-section should be incorporated into every step of the design mentioned in chapter 3. A full calculation using a box-girder can be found in appendix D. Here the main differences for a calculation with a 'cutout' will be mentioned.

Requirements

There are certain requirements for a box-girder design. The position of the pre-stressing strands cannot overlap with the position of the removed concrete and the cover on the pre-stressing has to be large enough such no concrete spalling will occur. An example of a cutout in length direction is shown in Figure 44.

Figure 44: Example of cutout placing in length direction

Next to that the maximum width of the cutout is limited by detailing rule 9.2.2 (8) in NEN-EN 1992-1-1 (CEN, 2011a). This rule says that the centre-to-centre distance between the legs of a series of shear stirrups in the transverse direction should not be greater than 500 mm. That means that for a stirrup configuration as given in Figure 45, which is used in the parametric model, the width of the cutout is limited by the distance between the stirrups.

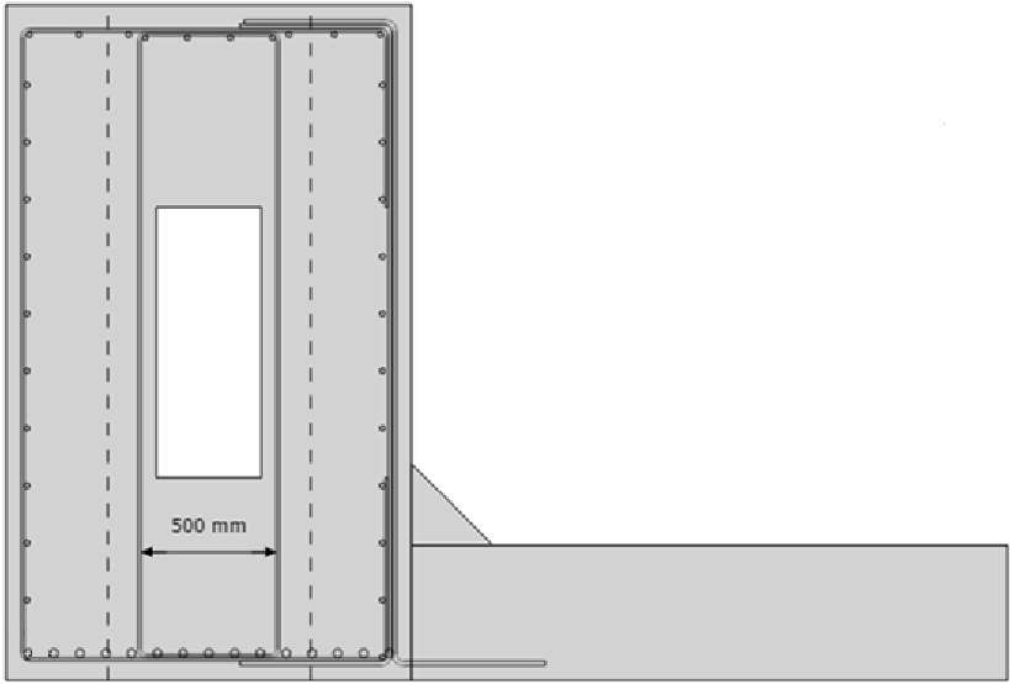

Figure 45: Box-girder cross-section

Calculations

First of all, the cross-sectional parameters have to be adjusted with the added cutout. The area moment of inertia and resistance moments of the cross-section al change due to the removed concrete. These parameters are used throughout all calculations. Also the self-weight has to be reduced according to the amount of removed concrete.

For the stirrups calculation the area reduction factor has to be adjusted to reflect the missing area due to the cutout. The area's depicted in Figure 34 change due to the added cutout in the centre of the cross-section.

For the longitudinal resistance calculation the cutout should also be accounted for. If the cutout is in the concrete compression zone, the effective width in this zone has to be reduced to account for the removed concrete area due to the cutout which can be calculated as $W_{eff} = W_{gir} - W_{cutout}$.
The concrete lever arm is also adjusted due to the removed concrete. This is done by integrating the stress diagram width the correct width for each area, from this both the correct N_c and lever arm can be calculated.
When the cutout is located inside the compression zone there is also a negative effect on the compression zone height which is often decisive for the moment calculations.

Lastly the calculation of the main tension stress should be adjusted. The main change in this calculation is the fact that the cutout increases the stress at the haunch because the area of concrete in this section reduces. This situation is sketched in Figure 46.

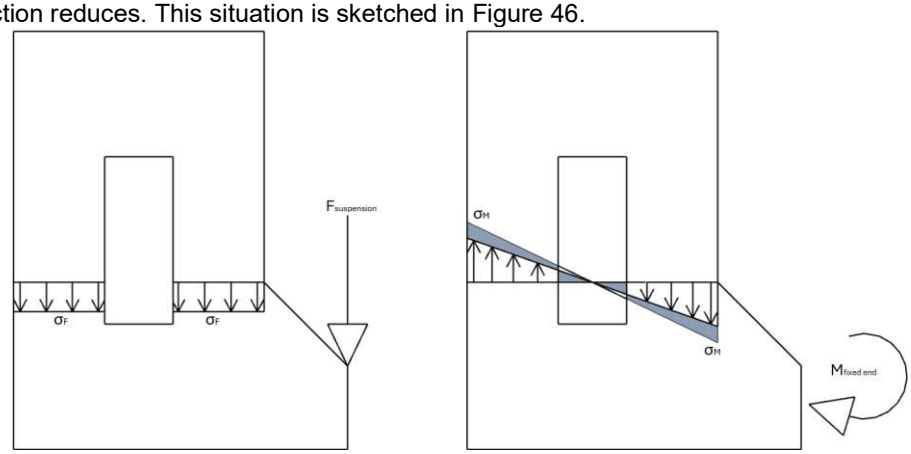

Figure 46: Adjusted stress diagrams due to cutout

To calculate the stresses at the cross-section of the haunch, the stress due to the suspension force is calculated using the reduced width W_{eff} the same as calculated above.
For the calculation for the stress due to moment, the assumption is made that the stress profile is still linear over the cross-section. The area of the stress diagram of the original cross-section without cross-section is the same as in the situation with cutout. The grey areas in Figure 46 inside and outside the cutout are the same and the slope of the line is the same over the whole stress diagram. With some geometrical calculations the stress at with cutout can be calculated from the stress in the situation without cutout:

$$\sigma_{zz,M} = \frac{W_{gir}\sigma_{zz,M,0}}{W_{gir} - W_{cutout} - \frac{W_{cutout}^2}{W_{gir}}}$$

It can be concluded that the main tension stress at the haunch is increased significantly and it is therefore crucial to check this section.

4.2.5 Integration into FEM model

The way the girder is modelled in the FEM model deserves some extra attention.
Figure 29 shows the traditional way of modelling the girder with the surface and the “result beam” to integrate the 2D forces back to 1D internal forces. However when modelling the girder with a cutout the surface is divided into three surfaces as shown in Figure 47.

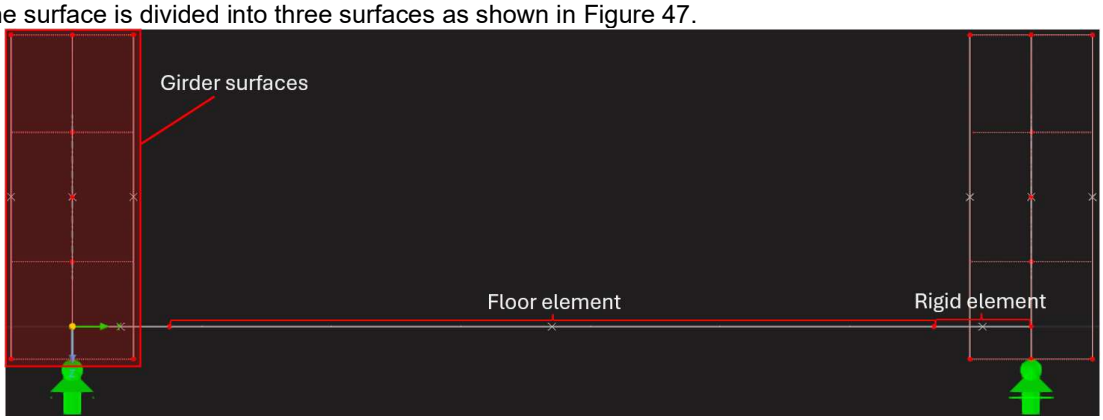

Figure 47: FEM model with cutout

The middle surface has an opening in the middle that has the same geometrical properties as the cutout. As can be seen in the 3D view of Figure 49. This way the exact geometry of the cutout is integrated in the model.
To correctly model the full force transmission between the three surfaces, contact surfaces are used that transfer forces in all directions. Contact surfaces are RFEM components that can model interaction between two surfaces. If the contact surface of full force transmission is used both shear and normal stresses are carried between the surfaces as show in Figure 48.

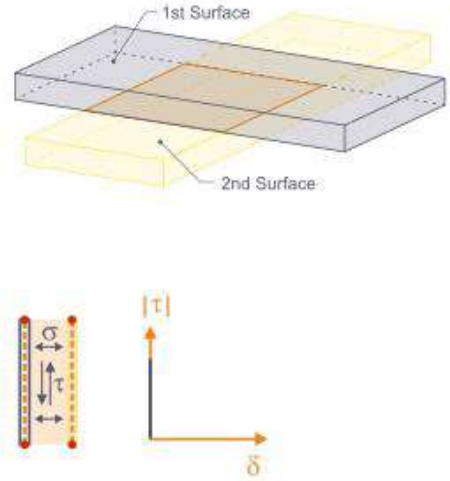

Figure 48: Contact surface in RFEM (Dlubal, n.d.)

The surfaces making up the girder are completely connected using these contact surfaces.

Also the rigid element to correctly model the connection between the floor and the girder is used again. It connects the floor rigidly to the middle girder surface.

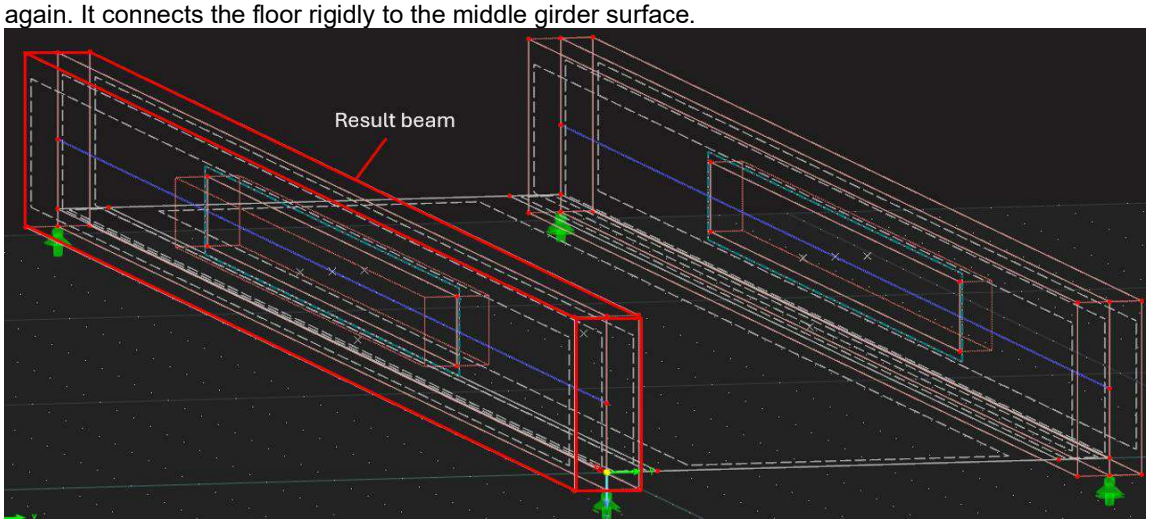

Figure 49: 3D FEM model cutout

Using the same "result beam" the 2D forces of the surfaces can be integrated back to 1D girder internal forces. The result beam can integrate forces of multiple surfaces at once.

The used elements and properties of the model are the same as in the traditional design, please refer to paragraph 3.1.5.

To verify that the FEM of the girders is working as expected, they are verified by a simple hand calculation. The properties are shown below:

- q = 100 kN/m
- l = 100 m
- h = 2500 mm
- W = 1500 mm
- E = 34000 MPa
- h_{cutout} = 1000 mm
- W_{cutout} = 410 mm

Comparing the results of the FEM calculations and the hand calculations in Table 13 shows that the differences between the results are insignificant. It is therefore assumed that the FEM model correctly models the girders.

Table 13: FEM results and hand calculation results

Calculation	FEM result	Hand calculation	Difference
Midspan moment with cutout	124947 kNm	125000 kNm	0.042 %
Midspan reflection	1997.3 mm	1994.6 mm	0.135 %

The hand calculations have used these formulas.

$$M = \frac{1}{8} q l^2$$

$$w = \frac{5}{384} \frac{q l^4}{EI}$$

$$I = I_{full\ girder} - I_{cutout}$$

5 Results

For the results of this study three designs have been made using the parametric model. These designs have been made on the basis of the reference project at station Bilthoven as described in paragraph 0. The reinforcement drawings for this design can be found in appendix B.
The reference design has been recreated in the parametric model. The principal cross-section is shown in Figure 50.

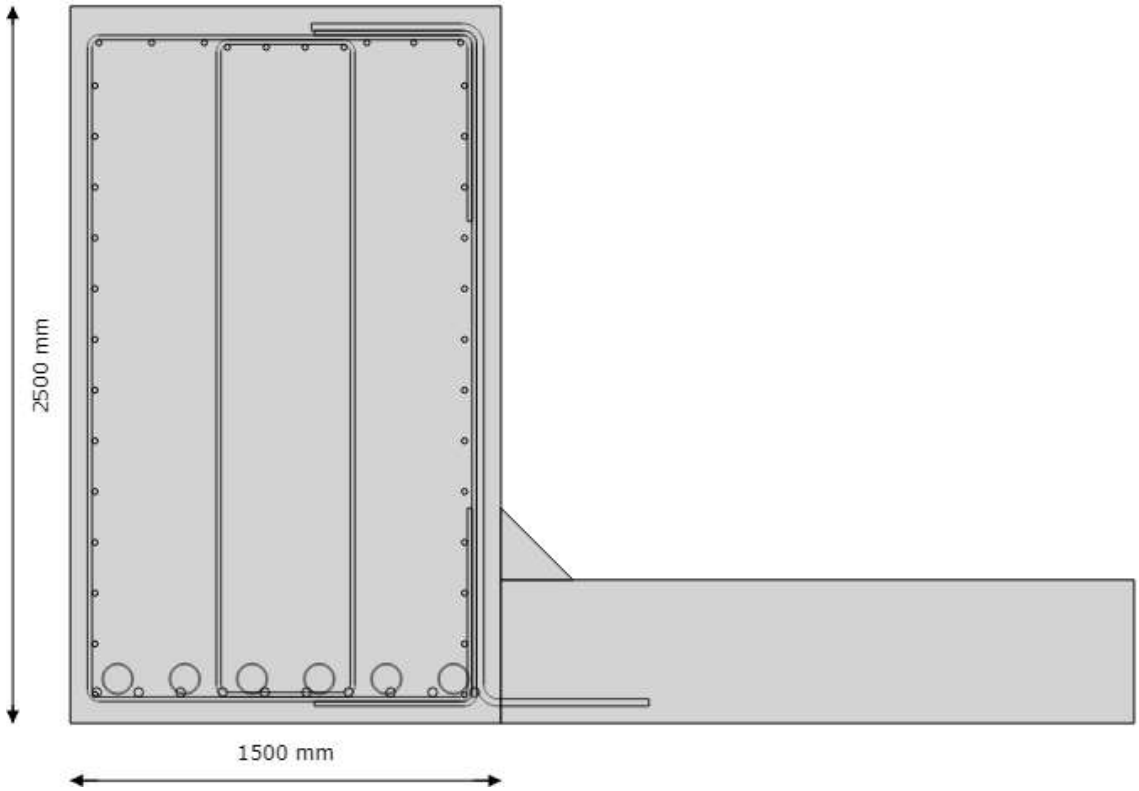

Figure 50: Principal cross-section reference design

The results for this cross-section are summarised in Table 14. Here unity checks are used to demonstrate the material usage per design check. A unity check of 1 means that the material has been used to its limit, a unity check of 0.5 means that the material is used for 50 %. A unity check of more than 1 means that the check has not been fulfilled as the material does not have enough strength to withstand the design loads.

Table 14: Calculation results reference design

	Value	Limit value	Unity Check
Longitudinal reinforcement torsion	$A_{sl,T,req}$ = 8320 mm²	$A_{sl,T}$ = 11938 mm²	0.70
Stirrup zone I reinforcement	$A_{sw,I,req}$ = 465 mm²	$A_{sw,I}$ = 670 mm²	0.69
Stirrup zone II reinforcement	$A_{sw,II,req}$ = 766 mm²	$A_{sw,II}$ = 2011 mm²	0.38
Stirrup zone III reinforcement	$A_{sw,III,req}$ = 1912 mm²	$A_{sw,III}$ = 2306 mm²	0.83
Longitudinal reinforcement moment	M_{Ed} = 18596 kNm	M_{Rd} = 40428 kNm	0.46
Main tension stress	σ_{ct} = 0.30 MPa	$0.6f_{ctd}$ = 0.88 MPa	0.34
Floor moment longitudinal	M_{Ed}=569 kNm	M_{Rd}=867 kNm	0.66
Floor moment transverse	M_{Ed}=195 kNm	M_{Rd}=220 kNm	0.89
Floor crack longitudinal	w=0.19 mm	$w_{allowed}$=0.20 mm	0.94
Floor crack transverse	w=0.05 mm	$w_{allowed}$=0.20 mm	0.23
Longitudinal shear	v_{Ed}=0.35 MPa	kf_{ctd}=0.59 MPa	0.59
Splitting reinforcement	σ_{spl}=187 MPa	f_{yd}=434 MPa	0.43

Next to that the maximum compression height check, SLS stress checks have also been calculated and these checks are fulfilled.

From these checks it can be concluded that the design fulfils the requirements as expected. However it also becomes clear that the material is not used optimally as the material usage is quite low for most checks.

5.1 Redesigns

To optimize this reference design, three different redesigns have been created that all use a different design approach. To optimize the reference design, an iterative trial and error approach has been used to try and optimize material usage, meaning the unity checks were designed to be as close to 1 as possible.

It should be noted that not all checks are independent. For example the reinforcement for crack-width and moment resistance is the same reinforcement. This means that if reinforcement is designed for the moment resistance it might be too heavy in regards of the crack-width check which leads to a low unity check for crack-width. This means that it is very hard to have a high unity check for two checks that are dependent on the same design parameters. This is why not all unity checks could be optimized to ~0.9.

5.1.1 Optimization same geometry

The first design to improving the design is by keeping the girder geometry the same as the reference design (1500 x 2500 mm) an optimizing the pre-stress and reinforcement layout. The calculation report generated by the parametric model for this design is given in appendix C.
The principal girder cross-section is shown in Figure 51.

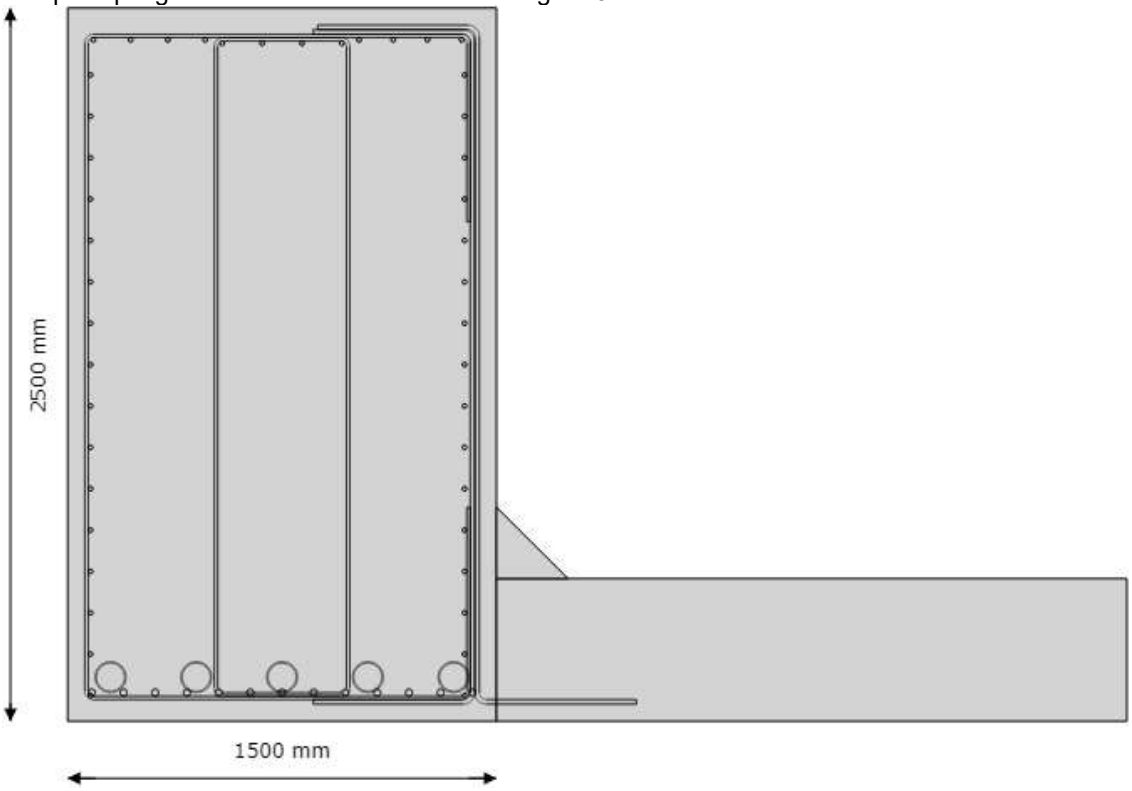

Figure 51: Redesign optimized cross-section

An important distinction in this design is that it uses 5 pre-stressing cables instead of 6 for the reference design. This is a significant save in material usage. Next to that due to the rapid iterations the unity checks for this design are designed much closer to 1. The unity checks are shown in Table 15.

Table 15: Calculations results optimized design same geometry

	Value	Limit value	Unity Check
Longitudinal reinforcement torsion	$A_{sl,T,req}$ = 8420 mm²	$A_{sl,T}$ = 9249 mm²	0.91
Stirrup zone I reinforcement	$A_{sw,I,req}$ = 511 mm²	A_{sw} = 565 mm²	0.90
Stirrup zone II reinforcement	$A_{sw,II,req}$ = 899 mm²	A_{sw} = 905 mm²	0.99
Stirrup zone III reinforcement	$A_{sw,III,req}$ = 1952 mm²	A_{sw} = 2011 mm²	0.97
Longitudinal reinforcement moment	M_{Ed} = 21743 kNm	M_{Rd} = 35709 kNm	0.61
Main tension stress	σ_{ct}=0.45 MPa	$0.6f_{ctd}$=0.88 MPa	0.51
Floor moment longitudinal	M_{Ed}=569 kNm	M_{Rd}=867 kNm	0.66
Floor moment transverse	M_{Ed}=200 kNm	M_{Rd}=220 kNm	0.91
Floor crack longitudinal	w=0.20 mm	$w_{allowed}$=0.20 mm	0.98
Floor crack transverse	w=0.05 mm	$w_{allowed}$=0.20 mm	0.25
Longitudinal shear	v_{Ed}=0.57 MPa	kf_{ctd}=0.59 MPa	0.97
Splitting reinforcement	σ_{spl}=394 MPa	f_{yd}=434 MPa	0.91

Next to that the maximum compression height check, SLS stress checks have also been calculated and these checks are fulfilled. It can be concluded that the unity checks for this design are on average much closer to 1 compared to the reference design.

5.1.2 Cross-section with cutout

The optimization as discussed in the previous chapter has also been used to make a redesign for the bridge. A cutout of 410 x 1000 mm was used for 15 meters of the bridge. The amount of pre-stressing cables had to be reduced to 4 such that the cables would not overlap with the cutout, however this means that the cables have 27 strands instead of the 22 strands for the first redesign.
The side view of the bridge is shown in Figure 52 and the principal girder cross-section is shown in Figure 53. The complete calculation report can be found in appendix D.

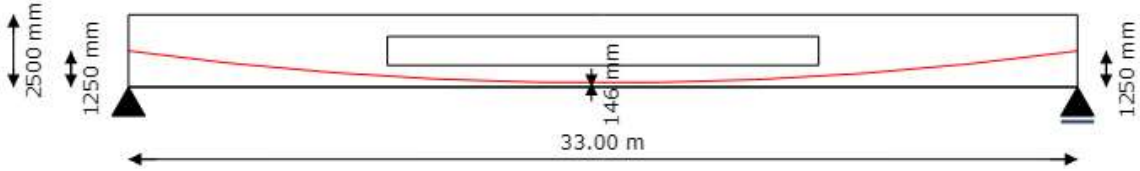

Figure 52: Side view of cutout design

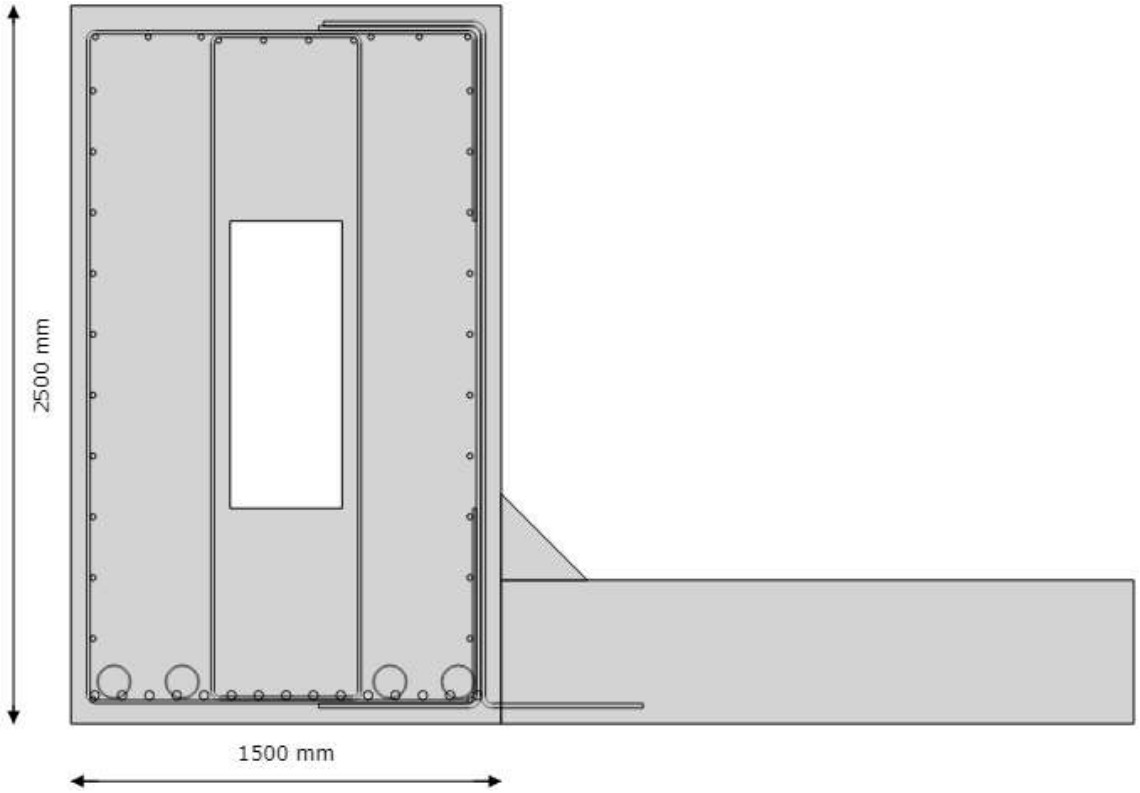

Figure 53: Redesign cross-section with cutout

The cross-section features heavier reinforcement compared to the previous optimization as the concrete compression zone is reduced due to the cutout. The calculation results are summarized in Table 16. From these results it can be concluded that this design also yields better material usage than the reference design.

Table 16: Calculations results optimized design same geometry

	Value	Limit value	Unity Check
Longitudinal reinforcement torsion	$A_{sl,T,req}$ = 9741 mm²	$A_{sl,T}$ = 10053 mm²	0.97
Stirrup zone I reinforcement	$A_{sw,I,req}$ = 535 mm²	A_{sw} = 565 mm²	0.95
Stirrup zone II reinforcement	$A_{sw,II,req}$ = 878 mm²	A_{sw} = 905 mm²	0.97
Stirrup zone III reinforcement	$A_{sw,III,req}$ = 2056 mm²	A_{sw} = 2122 mm²	0.97
Longitudinal reinforcement moment	M_{Ed} = 21027 kNm	M_{Rd} = 46206 kNm	0.46
Main tension stress	σ_{ct}=0.54 MPa	$0.6f_{ctd}$=0.88 MPa	0.62
Floor moment longitudinal	M_{Ed}=577 kNm	M_{Rd}=867 kNm	0.67
Floor moment transverse	M_{Ed}=204 kNm	M_{Rd}=220 kNm	0.93
Floor crack longitudinal	w=0.20 mm	$w_{allowed}$=0.20 mm	0.98
Floor crack transverse	w=0.05 mm	$w_{allowed}$=0.20 mm	0.24
Longitudinal shear	v_{Ed}=0.46 MPa	kf_{ctd}=0.59 MPa	0.78
Splitting reinforcement	σ_{spl}=371 MPa	f_{yd}=434 MPa	0.85

5.1.3 Cross-section with reduced width

The last redesign is characterized by a thinner cross-section. The width of the cross-section is reduced to 1200 mm. This does in result in relatively dense reinforcement, especially at the bottom of the cross-section, however the reduction in self-weight is significant as the self-weight of the girders is reduced by ~20%.

The principal girder cross-section is shown in Figure 54. The complete calculation report can be found in appendix E.

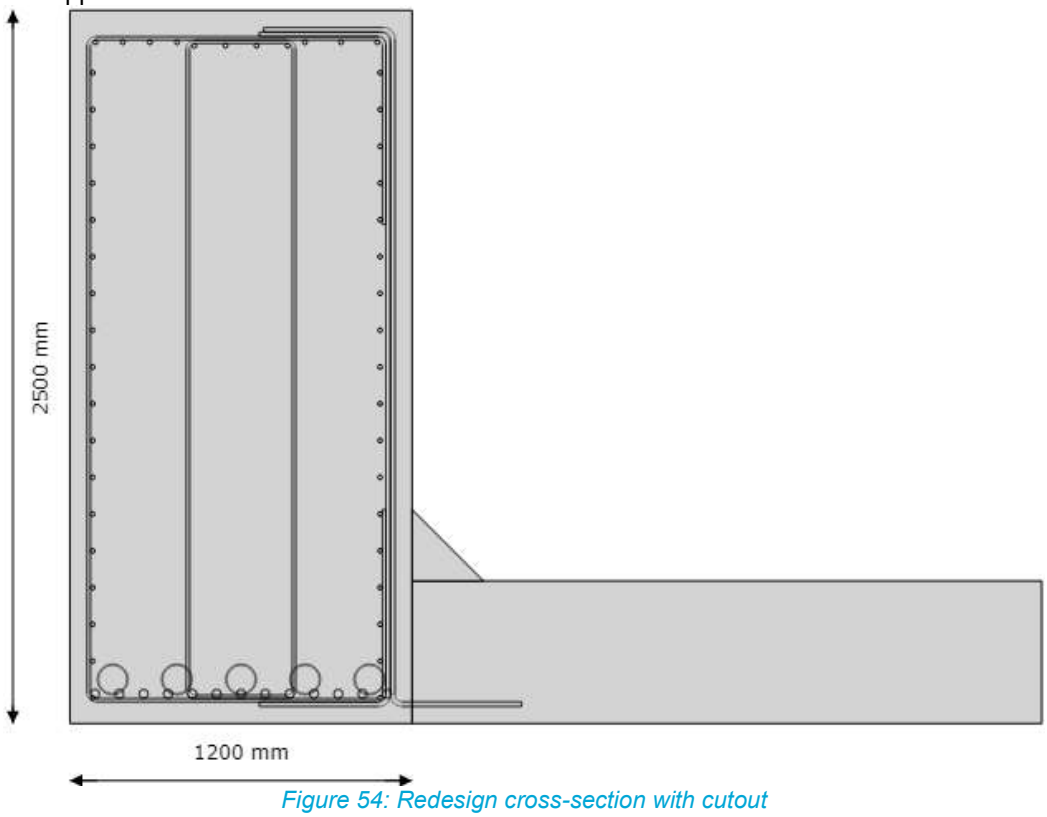

Figure 54: Redesign cross-section with cutout

This design also fulfils all design requirements. The results are summarized in Table 17.

Table 17: Calculation results reduced cross-section

	Value	Limit value	Unity Check
Longitudinal reinforcement torsion	$A_{sl,T,req}$ = 9218 mm²	$A_{sl,T}$ = 10455 mm²	0.88
Stirrup zone I reinforcement	$A_{sw,I,req}$ = 503 mm²	A_{sw} = 565 mm²	0.89
Stirrup zone II reinforcement	$A_{sw,II,req}$ = 761 mm²	A_{sw} = 905 mm²	0.84
Stirrup zone III reinforcement	$A_{sw,III,req}$ = 2166 mm²	A_{sw} = 2234 mm²	0.97
Longitudinal reinforcement moment	M_{Ed} = 19577 kNm	M_{Rd} = 36590 kNm	0.54
Main tension stress	σ_{ct}=0.80 MPa	0.6f_{ctd}=0.88 MPa	0.91
Floor moment longitudinal	M_{Ed}=549 kNm	M_{Rd}=867 kNm	0.63
Floor moment transverse	M_{Ed}=206 kNm	M_{Rd}=220 kNm	0.94
Floor crack longitudinal	w=0.18 mm	$w_{allowed}$=0.20 mm	0.92
Floor crack transverse	w=0.05 mm	$w_{allowed}$=0.20 mm	0.24
Longitudinal shear	v_{Ed}=0.56 MPa	kf_{ctd}=0.59 MPa	0.95
Splitting reinforcement	σ_{spl}=401 MPa	f_{yd}=434 MPa	0.92

This table also shows that this design has unity checks closer to 1 than the reference design.

5.2 Quantification

To compare the redesigns and the reference design on the basis of construction costs and environmental impact a bill of quantities can be used. This bill of quantities is automatically calculated by the parametric model and offers an insight into the amounts of materials used for the design.

The comparison between the designs only considers the designs parameters that are considered in the parametric model. So for example as splitting reinforcement for the introduction of pre-stress is not calculated in the parametric model, it is omitted from this comparison. The same goes for practical reinforcement.
To compare the designs a scatter plot will be made with two optimization parameters: costs and environmental impact. The results are summarized in Figure 55.

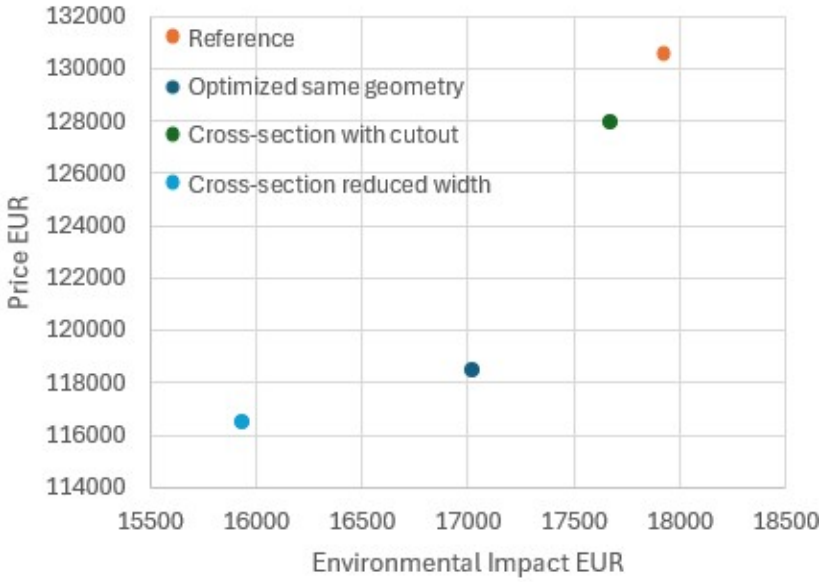

Figure 55: Results of the designs

This scatter plot is an ideal representation for multi-objective optimization, because it shows the trade-offs between designs for the two objectives. It can clearly show which designs are most efficient and which designs might have room for further improvement.

To get an understanding of the difference between the redesigns and the reference project the relative differences are summarized in Table 18.

Table 18: Relative differences costs designs

	Environmental impact shadow cost [EUR]	Material costs [EUR]	Relative difference EI [%]	Relative difference price [%]
Reference	17923	130547		
Optimized same geometry	17025	118463	-5.01	-9.26
Cross-section with cutout	17673	127956	-1.39	-1.98
Cross-section with reduced width	15939	116475	-11.07	-10.78

5.3 Fatigue considerations

Earlier in this report the assumption was made that fatigue would not be decisive because through girder bridges are very heavy and fully-prestressed, because the stress deviations due to cyclic loading will be relatively small compared to the total stress in the structure. However, this assumption needs to be checked as the pre-stress and self-weight is reduced with the redesigns which causes a higher ratio of cyclic load to the total load.

5.3.1 Assumption

The three most important considerations are the self-weight, pre-stress loads and the train loads. Assuming the reference design fulfils the fatigue requirements the redesigns can be compared to the reference design. The ratio of total cyclic load in the reference design can be calculated and compared to the redesign such that it can be concluded whether the assumption that fatigue will not be decisive holds.

The redesign with the lowest self-weight is the redesign with the reduced cross-section width. It is compared against the reference design, the results are summarized in Table 19.

Table 19: Comparison ratio cyclic loads

	Reference design	Reduced width design	Difference
Midspan moment self-weight	18672 kNm	17587 kNm	5.8 %
Midspan moment pre-stress	-20011 kNm	-18132 kNm	9.3 %
Compression due to pre-stress	17825 kN	16208 kN	9.1 %
Midspan moment due to cyclic load	10949 kNm	10611 kNm	3.09 %
Maximum stress	0.54 MPa	2.82 MPa	
Minimum stress	-6.06 MPa	-6.10 MPa	
Stress deviation	6.60 MPa	8.92 MPa	35.1 %

The forces and stresses are calculated by the FEM model. The difference in stress deviation is quite large, thus a more detailed calculation is required.

5.3.2 Calculation

FEM results

Using the load combinations in SLS-frequent given in NEN-EN 1992-1-1 (CEN, 2011a) 6.8.3 it can be determined that for the situation where the cyclic load is not present:

M_{Ed} = 1856 kNm

N_{Ed} = - 15564 kN

The whole cross-section is under compression in this case meaning that the stress in the steel is 0 and the minimum concrete compression at midspan stress is $\sigma_{c,min}$ = 5.29 MPa.

For the situation with cyclic load the FEM results are:

M_{Ed} = 11202 kNm

N_{Ed} = - 17374 kN

Using the calculation engine from the parametric model to solve the stress and strain diagrams by solving the horizontal force and the moment equilibrium to find:

$\sigma_{c,max}$ = 13.86 MPa

$\sigma_{s,max}$ = 36.19 MPa

$\Delta\sigma_{P,max}$ = 28.60 MPa

Steel check

The effect of the difference in bond of steel and pre-stressing steel is captured with formula 6.64 from NEN-EN 1992-1-1 (CEN, 2011a):

$$\eta = \frac{A_S + A_P}{A_S + A_P\sqrt{\xi\ (\varphi_S/\varphi_P)}} = \frac{20910 + 16500}{20910 + 16500\sqrt{0.7\ (32/27.475)}} = 1.045$$

Where:

ξ = 0.7 (Table 6.2)

φ_P = 1.75φ_{wire} = 1.75 · 15.7 = 27.475 mm

To check the fatigue resistance formula 6.71 is used:

$$\gamma_{F,fat}\Delta\sigma_{S,equ}(N^*) \leq \frac{\Delta\sigma_{rsk}(N^*)}{\gamma_{S,fat}};\ 37.82\ MPa \leq 94.43\ MPa$$

Where:

$\gamma_{F,fat}$ = 1 (NB. 2.4.2.3 (1))

$\Delta\sigma_{S,equ}(N^*)$ = η · $\sigma_{s,max}$ - 0 = 37.82 MPa

$\gamma_{S,fat}$ = 1.15 (NB. 2.4.2.4 (1))

And from S-N curve NB. table 6.3N, assuming 10^7 load cycles:

$\Delta\sigma_{rsk}(N^*)$ = 108.6 MPa

So it can be concluded that fatigue will not be a problem for the reinforcement.

Pre-stress check
The fatigue check for the pre-stress steel is similar to the reinforcement steel check, however and uses the same formula:

$$\gamma_{F,fat}\Delta\sigma_{P,equ}(N^*) \leq \frac{\Delta\sigma_{\mathrm{rsk}}(N^*)}{\gamma_{P,fat}}; 28.60 \leq 78.51$$

Where:
$\gamma_{F,fat}$ = 1 (NB. 2.4.2.3 (1))
$\Delta\sigma_{P,equ}(N^*)$ = $\sigma_{\mathrm{P,max}}$ - 0 = 28.60 MPa
$\gamma_{P,fat}$ = 1.1 (NB. 2.4.2.4 (1))
And using S-N curve table 6.4N and assuming 10^7 load cycles:
$\Delta\sigma_{\mathrm{rsk}}(N^*)$ = 86.36 MPa (assuming)

Concrete check
The fatigue strength of concrete can be calculated using NEN-EN 1992-2 (CEN, 2011d) NB. formula 6.76:

$$f_{cd,fat} = k_1\beta_{cc}(t_0)f_{cd}\left(1-\frac{f_{ck}}{400}\right) = \frac{35}{1.5}\left(1-\frac{35}{400}\right) = 21.29\ MPa$$

Where:
k_1 = 1 (6.8.7 (101) (e))

The factor for the concrete strength can be calculated using formula 3.2 from NEN-EN 1992-1-1 (CEN, 2011a):

$$\beta_{cc}(t_0) = \exp\left(s\left[1-\sqrt{\frac{28}{t}}\right]\right) = \exp\left(0.25\left[1-\sqrt{\frac{28}{28}}\right]\right) = 1$$

Where:
s = 0.25 (Cement class N)
t = 28 (assuming no trains will run within 28 days of pouring the concrete

The concrete fatigue check can be calculated using formula 6.72-6.75:

$$\frac{\sigma_{c,max}}{f_{cd,fat}} + 0.43\sqrt{1-\frac{\sigma_{c,min}}{\sigma_{c,min}}} = 0.99 \leq 1$$

From this it can be concluded that the concrete does fulfil the fatigue requirements, however it is dimensioned right on the limit. Saving anymore material would likely lead to a failed fatigue check.

5.4 Initial costs versus total costs

It is important to get an indication for the value of the parametric model. For the a parametric model an indication of the value can be calculated by the possible cost reduction it can deliver. In the case of the concrete through girder bridge design, an approximation can be made for both initial costs and potential cost savings by using the parametric model. For these calculations it is assumed that the bridge that is designed is similar to that of the reference study such that a good approximation can be obtained for potential cost saving on the materials.
The value of the new methodology and developed software when creating a parametric model are not considered in this analysis as it is complex to get an accurate estimate for these values.

Concluding from 5.2 the material costs of bridge design without the parametric model can be approximated as 130 547 EUR and with the parametric model as 116 475 EUR.
Engineering firm Witteveen + Bos approximates that an experienced engineer would develop a concrete through girder bridge design in ~7 weeks, meaning the costs would be ~55 000 EUR (B. Jongstra, personal communication, February 13, 2025).
However, the development of the parametric model took ~18 weeks, the costs for development of this model would be ~140 000 EUR.
The parametric model allows for faster designs. An experienced engineer with access to the parametric model would be able to design a concrete through girder bridge in one week for ~8000 EUR.

Following this logic the cost effectiveness of the parametric model can be plotted such as in Figure 56.

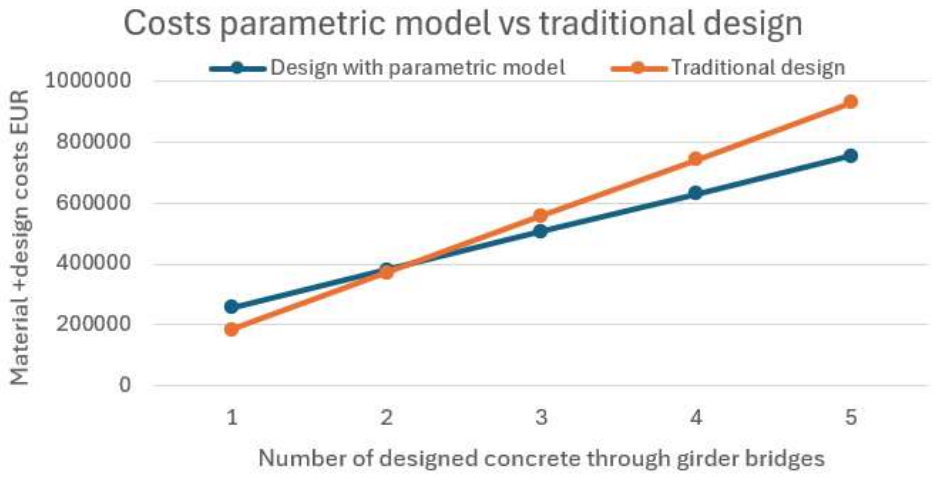

Figure 56: Break even line for the parametric model

From this break-even line it can be shown that the parametric model has a positive value when it's used for the design of 3 bridges or more. From this it can be concluded that if it is expected that more than 2 concrete through girder bridges will be designed, the investment in the parametric model will be worthwhile.

6 Discussion

The developed model demonstrates its ability to generate optimized designs, as evidenced by the three redesigns produced. Each redesign showed improvements in both environmental impact and cost compared to the reference design. This initial success validates the model's potential as a valuable tool for structural engineers in the preliminary design phase. However, a critical distinction must be maintained: the reference design represented a definitive, fully-developed design, while the parametric model currently produces only a preliminary design. This difference in design phase limits the applicability of comparing absolute performance metrics.

Next to that the model also has some scope limitations as the research was solely focused on single span single track bridges, that way the model may not be directly applicable to different scenarios. Future development should prioritize expanding the model's capabilities to accommodate multi-span bridges, varying track arrangements, and potentially even different bridge types.

This research also demonstrates the complexity of structural design as many design choices come with their trade-offs. For instance, the thin model produces a very material efficient model that might be present challenges in terms of constructability. This design might require innovative construction techniques and it might potentially increase labour costs due to the dense reinforcement and limited free space.

The study explored various optimization strategies, including geometry refinement, material reduction through cutouts. Each approach offers benefits and disadvantages, suggesting that a combination of these strategies might yield even more optimized designs in future iterations of the model. Introducing innovative construction together with advanced optimization algorithms, could be key improvements to allow the parametric model to optimize bridge design further.
The current trial-and-error approach, while yielding improvements, may not fully exploit the model's potential for design optimization. This method relies heavily on engineering judgement and manual adjustments, which could potentially overlook optimal solutions in the greater design space.
A more sophisticated approach would involve implementing automated optimization algorithms capable of exploring a wider range of design possibilities. These could include genetic algorithms or particle swarm optimization that can efficiently navigate complex design spaces. Such methods could potentially uncover design solutions that the engineer might not consider.

Furthermore, the current optimization criteria are focused on environmental impact and cost. While these are crucial factors, practical design questions often involve a multitude of additional considerations. Future iterations of the model could incorporate a more comprehensive set of optimization criteria, such as:

- Durability and maintenance requirements
- Aesthetic considerations and visual impact
- Construction time and logistical constraints

The use of environmental impact as a key metric is a very important insight, aligning with growing industry focus on sustainable infrastructure. However, the environmental impact calculation could be expanded to include a more comprehensive life cycle assessment in future research.
This is not only limited to the environmental impact assessment as the cost indications suffers from the same shortcomings as well. However, calculating a good cost indication for the bridge was not the main focus of this research.
Next to that it will always be complex to estimate environmental and costs purely based on a general parametric design. Other metrics could be introduced as design parameters such that the estimations could be improved. For example, the location of the bridge or the exact price of the materials.

Lastly it can be concluded that the model shows promise in an academic context, however its practical implementation in real-world bridge design projects may face challenges. These could include: resistance to novel design approaches, the lack of opportunities for use of the model or the need for extensive validation.
Bridging this gap between academic promise and practical adoption will require collaboration between industry and university, beginning with smaller-scale pilot projects to demonstrate the model's reliability and effectiveness.

7 Conclusion

This study developed a parametric model for optimizing concrete through girder bridges, targeting more sustainable and cost-effective designs. The model focuses on single-span, single-track railway bridges within a 25-45 meter span range not located on high-speed lines, adhering to Dutch and ProRail standards. This scope limitation allows for a focused approach to preliminary design optimization.
This was achieved through a systematic process of a comprehensive literature review, the creation of an automated parametric model linked to external FEM software RFEM (Dlubal, n.d.).

The developed parametric model has demonstrated its capability to generate and optimize designs for concrete through girder bridges efficiently. By incorporating relevant the relevant standards and specific requirements for train bridges, the model produces viable design alternatives that meet all necessary criteria for a preliminary design.
Through a combination of factors including optimized material usage, which directly translates to reduced environmental impact and cost savings the viability of the redesigns is demonstrated. The model ensures that while minimizing material, the designs still satisfy all structural requirements for load-bearing capacity and stability, making them a promising foundation for further detailed design and analysis.

This research introduced three potential cross-section optimizations. The three variants were compared against a traditional full cross-section based on their shear/torsional resistance, moment resistance, material reduction potential, construction process complexity, and slenderness. The variants can be summarized as:

- Tapered girders optimize material use by reducing cross-section height away from supports, where pre-stress demands are lower.
- I-girders remove concrete from the centre of the cross-section, concentrating material in the flanges to resist bending moments while providing space for pre-stressing tendons
- Box-girder with a ‘cutout’ in the cross-section that tries to keep a high torsional resistance while also having a high moment resistance

A multi-criteria analysis (MCA) revealed the box girder design as the most promising, offering a superior balance between torsional rigidity, material efficiency, and constructability. Consequently, the option to design with a box girder cross-section was incorporated into the developed parametric model.

To evaluate the effectiveness of the parametric model, three redesigns were generated, each showing improvements over the reference design:

- An optimized design with the same geometry reduced environmental impact by 5.01% and material cost by 9.26%
- A design featuring a cutout achieved modest improvements of 1.39% in environmental impact and 1.98% in material cost
- A thin cross-section design with reduced cross-section width resulted in the most significant reductions: 11.07% in environmental impact and 10.78% in material cost

An interesting conclusion to draw from this is that the cutout model is the least efficient redesign in terms of costs and environmental impact. This is mainly due to the fact that the cross-section required much heavier longitudinal reinforcement due to the reduced concrete compression zone width and highlights the trade-offs between and complexity between different design choices.
This underscores the importance of considering the complete impact of design modifications, rather than focusing solely on reducing concrete volume. It demonstrates that a more nuanced approach, balancing concrete and steel usage, is essential for achieving optimized concrete through girder bridge designs.

To ensure long-term structural integrity, fatigue considerations were incorporated into the research. While a comprehensive fatigue analysis was beyond the scope of this preliminary design model, a simplified approach based on Eurocode 2 was implemented. This analysis showed that decreasing the self-weight of the bridge, while leading to lower design moments might cause problems with cyclic loading, as the ratio of cyclic loading to permanent loads strongly increases. However, within the scope of the redesigns presented in this paper, the designs where at the limit of the fatigue resistance.

The study established a design method that, through an effective, iterative process, produces designs that utilize materials with near-optimal efficiency. This approach led to tangible improvements, such as reducing the number of pre-stressing cables from 6 to 5 in the redesigns and generally improving steel and concrete usage.
The parametric approach allowed for rapid iteration and evaluation of multiple design options, proving to be a valuable tool for exploring the design space of concrete through girder bridges and generating innovative solutions that might not be viable through traditional design methods. This not only accelerates the design process but also empowers engineers to investigate a wider range of possibilities, potentially uncovering more efficient and sustainable solutions.
As an indication for the investment costs in a parametric model it can be concluded that if the parametric model is to be used for more than 2 concrete through girder bridge designs, the cost savings will outweigh the high initial costs of developing the parametric model.

In conclusion, the developed parametric model addresses the main research question by providing a flexible, efficient, and objective method for optimizing concrete through girder bridges. It enables the engineer to effectively balance sustainability and cost considerations while meeting the specific requirements for train bridges in the Netherlands. This approach not only facilitates the design process but also contributes to more sustainable and cost-effective infrastructure solutions, potentially paving the way for broader adoption of parametric design in bridge engineering and a more circular approach to bridge construction in the Netherlands.

7.1 Recommendations

Based on the findings of this research, several recommendations can be made for future development and expansion of the parametric model:

Structural analysis
- Incorporate fatigue calculations for future applications of the model
- Implement multi-span / multi-track design options
- Expand the evaluation to include multiple critical sections along the bridge length, not just the midspan

The current model does not explicitly account for fatigue damage, which is a critical factor in the long-term performance of railway bridges. Future development should prioritize integrating a fatigue analysis. Also incorporating multiple spans or tracks would allow the model to be used in much more cases than is possible right now.
Also, the current model only evaluates stresses and resistances at the midspan. A more comprehensive assessment of different sections of the bridge would allow for more detailed design and possibly material reductions.

Model robustness
- Developing a more detailed reinforcement layout for specific local checks that have not been considered in this research
- Add more practical considerations to the model
- Extend the model to allow for different concrete bridge types such as box girder or slab bridges

The current model relies on simplified reinforcement layouts. Future work should focus on developing more detailed reinforcement layouts that account for specific local checks not currently considered and practical reinforcement considerations. In this manner the preliminary design could be expanded to a definitive design.
This parametric model could also prove to be a good basis for general parametric modelling of concrete bridges as this basis can be expanded to fit multiple bridge types.

Other considerations
- Adding more material options to allow for more environmental-friendly designs
- Include end-of-life considerations to the (environmental) cost calculation

The current model is limited to a small selection of commonly used concrete and steel grades. Expanding the material options to include innovative materials could prove to be a good next step into more environmental friendly bridge design. Incorporating the end-of-life value of the designs can also prove to be a good insight for environmental impact concerns.

Bibliography

BDP. (n.d.). *Bilthoven, Centrum en Stationsgebied*. https://www.bdp.com/nl/projects/projects/a-g/Bilthoven-Inrichtingsplan-Stationsgebied/

Biswas, P. (2025, January 20). Genetic Algorithm – an optimization approach. Towards Data Science. https://towardsdatascience.com/genetic-algorithm-an-optimization-approach-dd60e23261e6/

Canestro, E., Strauss, A., & Sousa, H. (2021). Multiscale modelling of the long-term performance of prestressed concrete structures – Case studies on T-Girder beams. *Engineering Structures/Engineering Structures (Online)*, *231*, 111761. https://doi.org/10.1016/j.engstruct.2020.111761

Cement. (2013). Omlegging Zuid-Willemsvaart. *Cement*, *6*, 48–53. https://issuu.com/aeneas/docs/cement_6_2013

CEN. (2011a). *NEN-EN 1992-1-1+C2: Eurocode 2: Ontwerp en berekening van betonconstructies - Deel 1-1: Algemene regels en regels voor gebouwen*.

CEN. (2011b). *NEN-EN 1991-1-4+A1+C2: Eurocode 1: Belastingen op constructies - Deel 1-4: Algemene belastingen - Windbelasting*.

CEN. (2011c). *NEN-EN 1991-1-5+C1: Eurocode 1: Belastingen op constructies - Deel 1-5: Algemene belastingen - Thermische belasting*.

CEN. (2011d). *NEN-EN 1992-2+C1: Eurocode 2: Ontwerp en berekening van betonconstructies - Betonnen bruggen - Regels voor ontwerp, berekening en detaillering*.

CEN. (2015a). *NEN-EN 1991-1-7+C1+A1: Eurocode 1: Belastingen op constructies - Deel 1-7: Algemene belastingen - Buitengewone belastingen: stootbelastingen en ontploffingen*.

CEN. (2015b). NEN-EN 1991-2+C1. In *Eurocode 1: Belastingen Op Constructies – Deel 2: Verkeersbelasting Op Bruggen*.

CEN. (2019a). *NEN-EN 1990+A1+A1/C2: Eurocode: Grondslagen voor het constructief ontwerp*.

CEN. (2019b). *NEN-EN 1991-1-1+C1+C11: Eurocode 1: Belastingen op constructies – Deel 1-1: Algemene belastingen – Volumieke gewichten, eigen gewicht en gebruiksbelastingen voor gebouwen*.

Chalouhi, E. K. (2019). Optimal design solutions of concrete bridges considering environmental impact and investment cost (Licentiate Thesis TRITA-ABE-DLT-194, KTH School of ABE). https://www.diva-portal.org/smash/get/diva2:1293043/FULLTEXT01.pdf

Davis, D. (2013, September 20). Chapter 2 – The Challenges of Parametric Modelling. Daniel Davis. https://www.danieldavis.com/thesis-ch2/

De Bekker, P. (2016, November 10). *Aannemer draait op voor te lage spoorbrug over Máximakanaal Den Bosch*. Omroep Brabant. https://www.omroepbrabant.nl/nieuws/2385815/aannemer-draait-op-voor-te-lage-spoorbrug-over-maximakanaal-den-bosch

Dlubal. (n.d.). *RFEM* (6.07) [Software].

Dlubal Software. (2024, October 25). Finite Elements from Topological Point of View. https://www.dlubal.com/en/downloads-and-information/documents/online-manuals/software-validation/004013

Fu, C. C., & Wang, S. (2014). Computational analysis and design of bridge structures. In *Google Books*. CRC Press. https://books.google.nl/books?hl=en&lr=&id=3SLcBQAAQBAJ&oi=fnd&pg=PP1&ots=cFUUPi5Lur&sig=XHH8U4JiSmMqf5vHa1dqX_5vsms&redir_esc=y#v=onepage&q&f=false

García-Segura, T., Penadés-Plà, V., & Yepes, V. (2018). Sustainable bridge design by metamodel-assisted multi-objective optimization and decision-making under uncertainty. *Journal of Cleaner Production*, *202*, 904–915. https://doi.org/10.1016/j.jclepro.2018.08.177

Jongstra, E. (2015). Partially prestressed railway bridge [Master thesis, TU Delft]. In *TU Delft repository*. http://resolver.tudelft.nl/uuid:d5c33e2e-b6d7-4694-a9b4-7a7fe7129ec9

Kompeer, J., & Schellevis, J. (2021, August 23). *"Babyboomerbruggen" toe aan groot onderhoud, files en kosten verwacht*. NOS. Retrieved November 20, 2024, from https://nos.nl/artikel/2394865-babyboomerbruggen-toe-aan-groot-onderhoud-files-en-kosten-verwacht

Lantsoght, O. L., De Boer, A., Van Der Veen, C., & Hordijk, A. (2019). Optimizing Finite Element Models for Concrete Bridge Assessment With Proof Load Testing. *Frontiers in Built Environment*, *5*. https://www.frontiersin.org/journals/built-environment/articles/10.3389/fbuil.2019.00099/full

Ministerie van Infrastructuur en Waterstaat. (2024, September 20). *Circulaire economie*. https://www.rijkswaterstaat.nl/leefomgeving/duurzaam-werken/circulaire-economie

NS Infrabeheer. (1997). *Richtlijn 1015 Versie 1.3 Uitgangspunten voor het ontwerp van trogbruggen*.

Ossendrijver, M. J. (n.d.). *Hangtrogbrug Terneuzen toont: beton en staal gaan goed samen*. Nederlandse Bruggenstichting. Retrieved November 20, 2024, from https://bruggenstichting.nl/76-bruggen/bruggen-2004/bruggen-maart-2004/489-hangtrogbrug-terneuzen-toont-beton-en-staal-gaan-goed-samen

ProRail. (2016). OVS00030-1-V004 Kunstwerken voor spoorverkeer. In *ProRail*.

ProRail. (2018). OVS00030-6-V005 Aanvullingen en wijzigingen op NEN-EN normen. In *ProRail*.

Refactoring.Guru. (n.d.). *Behavioral design patterns*. https://refactoring.guru/design-patterns/behavioral-patterns

Quist, A. Z. (2024, January 22). Wat zijn schaduwkosten? - Ecochain - LCA software company. Ecochain - NL. https://ecochain.com/nl/blog/wat-zijn-schaduwkosten/

Rijkswaterstaat. (2021). *RTD 1001 Richtlijnen Ontwerp Kunstwerken*. https://standaarden.rws.nl/index.html

Ruslanova, D. (2024, March). *What is a single source of truth?* Mad Devs. https://maddevs.io/glossary/single-source-of-truth/

Salamak, M. (2024). Optimization of geometric parameters of arch bridges using visual programming FEM components and genetic algorithm. Polsl. https://www.academia.edu/96195450/Optimization_of_geometric_parameters_of_arch_bridges_using_visual_programming_FEM_components_and_genetic_algorithm?auto=download

Sharma, P. (2023, December 15). How Parametric Modelling Helps in Bridge Design? *NOVATR*. https://www.novatr.com/blog/all-about-parametric-bridge-design

Stichting Nationale Milieudatabase. (n.d.). Viewer | Overzicht van milieuverklaringen in de Nationale Milieudatabase. NMD. https://milieudatabase.nl/nl/viewer/

Teresko, J. (1993). Parametric Technology Corp.: Changing the way Products are Designed. Industry Week, 28.

The Agile Modeling (AM) Method. (2023, November 25). Examining the agile cost of change curve. The Agile Modeling (AM) Method - Effective Strategies for Modeling and Documentation. https://agilemodeling.com/essays/costofchange.htm

TU Delft. (2023, March 13). *Dutch bridges are stronger than assumed*. Retrieved November 25, 2024, from https://www.tudelft.nl/en/2023/citg/dutch-bridges-are-stronger-than-assumed

Van der Horst, C. S. (n.d.). *Trogbruggen, Specifieke ontwerpaspecten*. Nederlandse Bruggenstichting. Retrieved November 20, 2024, from https://bruggenstichting.nl/76-bruggen/bruggen-2004/bruggen-maart-2004/488-trogbruggen-specifieke-ontwerpaspecten

Wouterlood, R. J. (2018). Shear and torsion in a prestressed through railway bridge [Master Thesis, TU Delft]. In *TU Delft Repository*. https://repository.tudelft.nl/record/uuid:cdd3a972-900a-4b12-8138-5a128d8dd1a8

Zaheer, Q., Yonggang, T., & Qamar, F. (2022). Literature review of bridge structure's optimization and it's development over time. *International Journal for Simulation and Multidisciplinary Design Optimization*, *13*, 5. https://doi.org/10.1051/smdo/2021039

Appendix A: Walkthrough of application

1. Start page

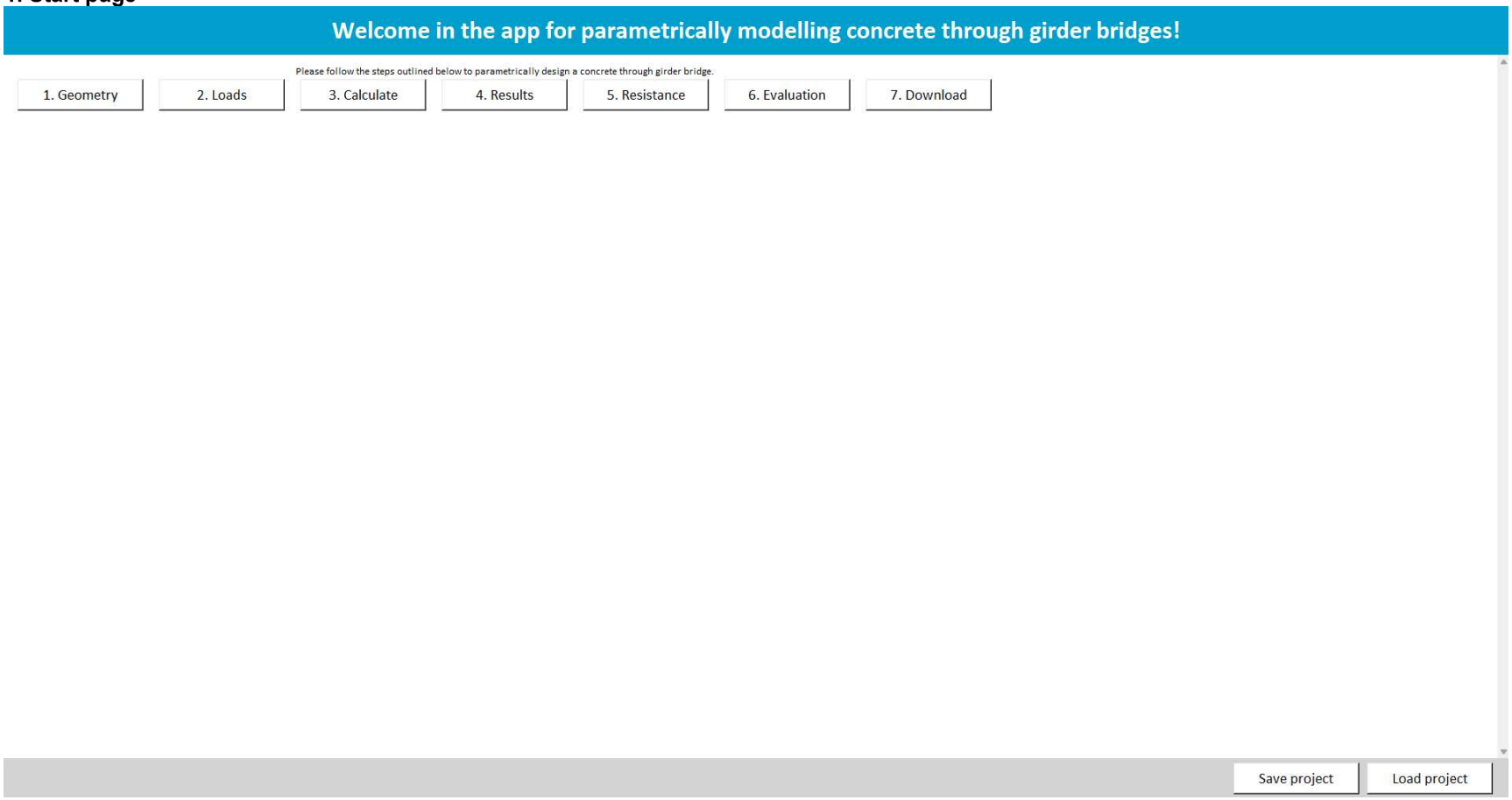

2. Geometry definition

Input for the geometrical properties of the bridge

Geometry input

l	Bridge length	33.0	[m]
h_{gir}	Girder heigth	2500.0	[mm]
w_{gir}	Girder width	1500.0	[mm]
h_{fl}	Floor heigth	500.0	[mm]
w_{fl}	Floor width	5.9	[m]
a_{vou}	Haunch size	500.0	[mm]
	Add cutout to girder	No	[-]

Sectional properties

A	Area	10.700	[m²]
I_{zz}	Moment of intertia	6.143	[m⁴]
W_{top}	Section modulus top	3.991	[m³]
W_{bot}	Section modulus bottom	6.394	[m³]
Z	Neutral line from bottom	0.961	[m]

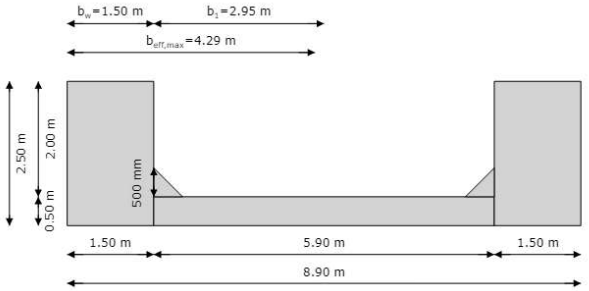

Effective width in span direction (NEN-EN 1992-2)

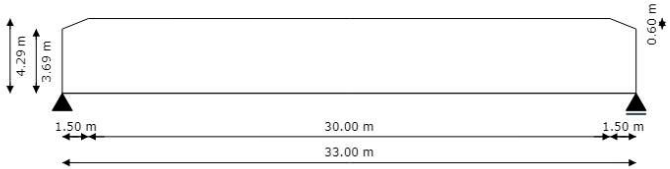

NEN-EN 1992-2 fig. NB-5.105

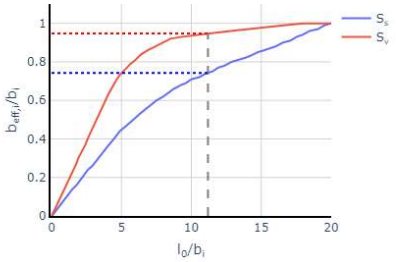

Next step

3. Pre-stress definition

Input for the loads acting on the bridge

Show loadcase: LC2 Prestressing

Prestress parameters

c_{app}	Applied cover	60.0	[mm]
f_{pk}	Characteristic tensile strength pre-stress steel	1860.0	[MPa]
n_{cable}	Numbber of pre-stressing cables	5.0	[-]
$n_{strands}$	Number of pre-stressing strands	22.0	[-]
$\varnothing_{strands}$	Nominal diameter of pre-stressing strands	15.7	[mm]
y_{low}	Lowest point pre-stress	140.0	[mm]
$y_{top,left}$	Highest point pre-stress left side	1250.0	[mm]
$y_{top,right}$	Highest point pre-stress right side	1250.0	[mm]

Pre-stress output

R	Radius pre-stress	124.28	[m]
A_p	Area pre-stress	16500	[mm²]
	Pre-stress duct	STB-100x109x0.40	[-]
$c_{min,P}$	Min. cover pre-stress	70	mm
$c_{min,P,app}$	Applied cover pre-stress	100	mm
$\sigma_{pi,max}$	Maximum allowed stress during tensioning	1440	[MPa]
$\sigma_{pi,max,d}$	Occuring maximum stress during tensioning	1427	[MPa]
$\sigma_{pm0,max}$	Maximum allowed stress after tensioning	1360	[MPa]
$\sigma_{PM0,max,SLS}$	Maximum allowed stress in SLS after tensioning	3055	[MPa]
$\sigma_{pm0,max,d}$	Occruing maximum stress after tensioning	1360	[MPa]
ϕ_l	Angle of inclination left	-0.135	[rad]
ϕ_r	Angle of inclination right	0.135	[rad]
Δz	Vertical displacement strands	14.73	[mm]

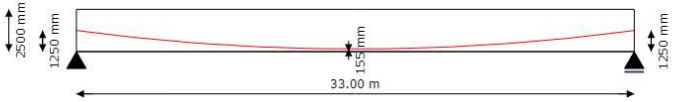

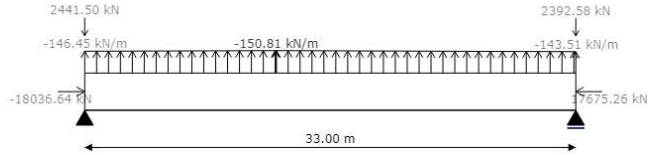

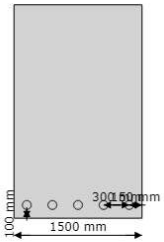

Calculate losses

Next step

4. Pre-stress loss

Input for the pre-stress loss

Input Paremeters

ΔL_w	Wedge set	7.0	[mm]
	Type of pre-stressing duct	Steel strip sheath	
t	The age of the concrete	36500.0	[days]
t_0	The age of the concrete at the start of loading	10.0	[days]
RH	Relative humidity	65.0	[%]
ρ_{1000}	Relaxation loss	2.5	[%]

Pre-stress loss factors

k	Unintended skew	0.005	[rad/m]
μ	Friction coefficient	0.18	[rad^{-1}]
σ_c	Assumed concrete compressive stress	5.9	[MPa]
$\phi(t, t_0)$	Creep coefficient at t	1.91483	[-]
$\varepsilon_{cc}(\infty, t_0)$	Creep strain	0.351	[‰]
$\varepsilon_{cd,\infty}$	Drying shrinkage strain	0.423	[‰]
$\varepsilon_{ca}(\infty)$	Autogenous shrinkage strain	0.062	[‰]
ε_{total}	Total creep and shrinkage strain	0.836	[‰]
$\Delta\sigma_{p,cr,sh}$	Creep and shrinkage loss	163.1	[MPa]
$\Delta\sigma_{p,r}$	Max relaxation loss	60.9	[MPa]

Pre-stresses loss plot

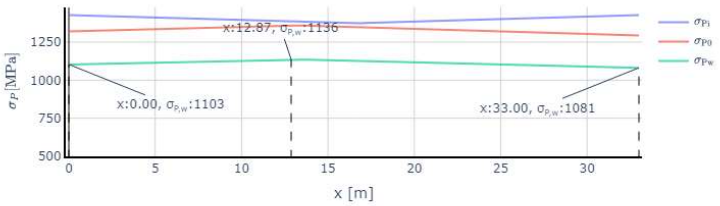

Loads page

5. Wind loads

Input for the loads acting on the bridge

Show loadcase: LC7.1 Wind loads

Wind paremeters

h_{gl}	Height between bridge and ground level	6.0	[m]
	Wind area (NEN-EN 1991-1-4 NB fig. 1)	I	[-]
	Terrain category (NEN-EN 1991-1-4 NB)	0	[-]

Wind-load output

h_{tot}	Total height	5.19	[m]
z_e	Reference height	7.25	[m]
v_b	Base windspeed	30.6	[m/s]
v_m	Base windspeed	36.1	[m/s]
$q_p(z)$	Extreme hydrostatic pressure	1.59	[kN/m²]
$c_e(z)$	Exposure factor	2.72	[kN/m²]

Wind-load forces

$q_{wk,x}$	Distributed Load in x-direction	16.73	[kN/m]
$p_{wk,z}$	Distributed load z-direction	1.44	[kN/m²]
$q''_{wk,x}$	Reduced distributed Load in x-direction	12.01	[kN/m]
$p''_{wk,z}$	Reduced distributed load z-direction	1.03	[kN/m²]

Next step

6. Train loads

Input for the loads acting on the bridge

Show loadcase: LC9.3.1 Train loads model SW/2 M

General paremeters

t_{bal}	Thickness ballast layer	300.0	[mm]
	Type of concrete	C35/45	

Influence line max M

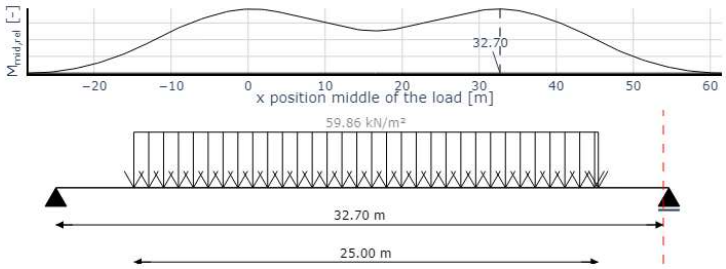

Influence line max V

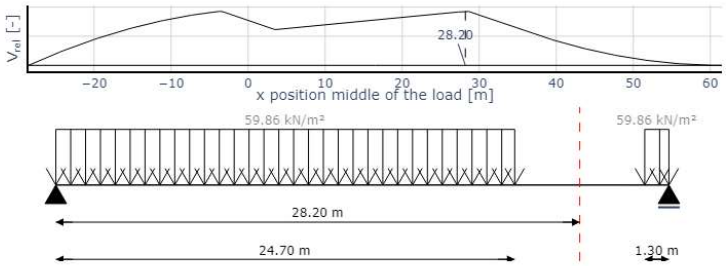

Next step

7. Results

Results of the FEM calculation

Normal force diagram girder

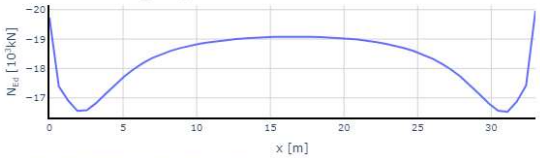

Bending moment diagram girder

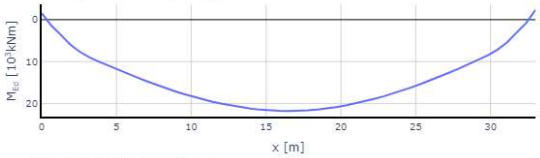

Shear force diagram girder

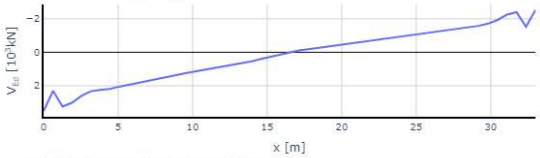

Torsional moment diagram girder

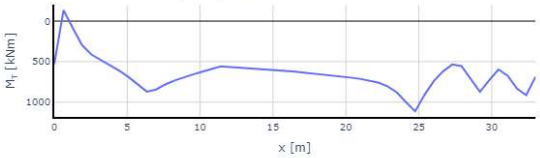

Next step

8. Resistance page

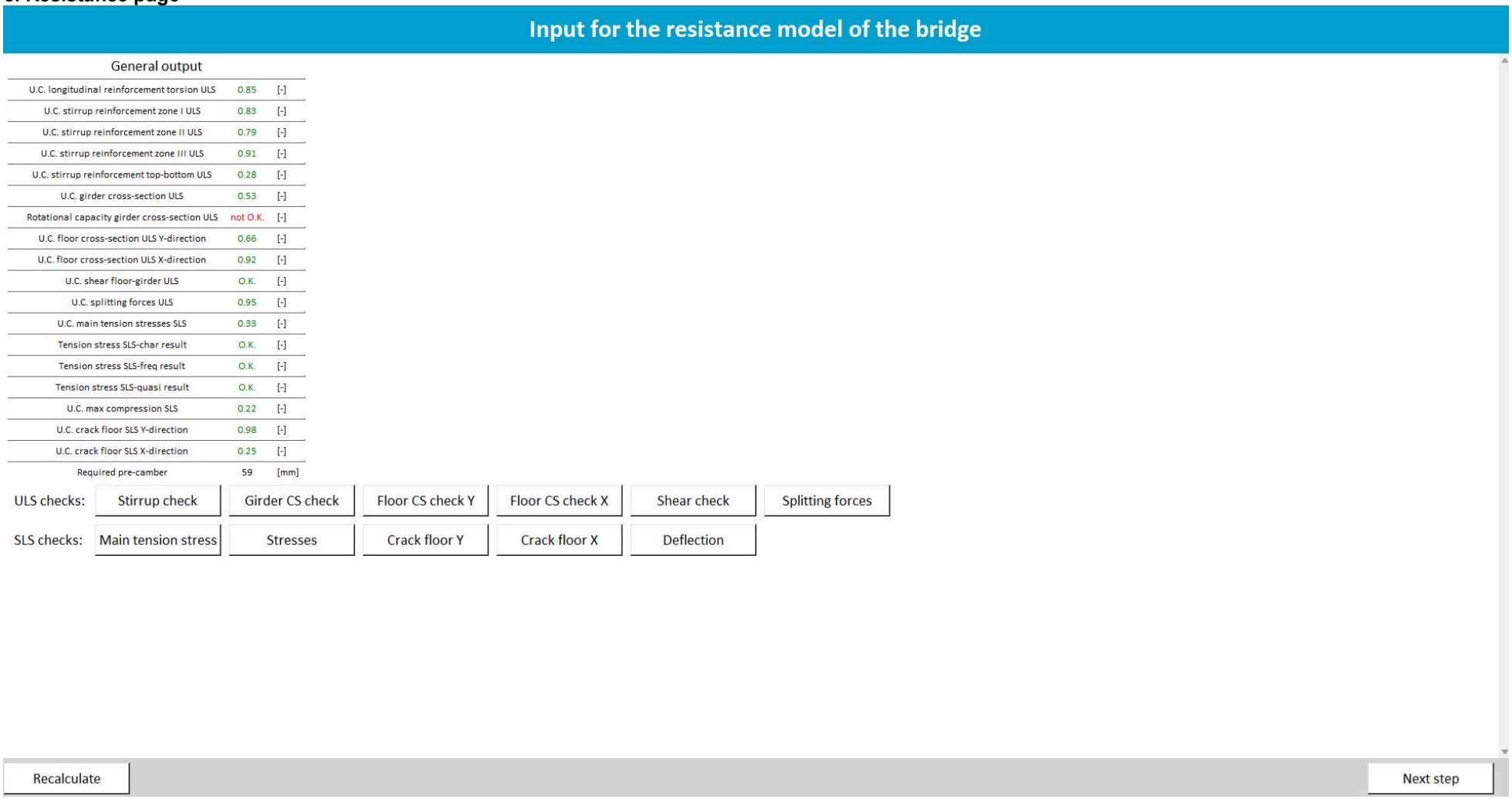

9. Stirrup calculations

ULS stirrup check

Input Parameters

	Steel material	FeB500	[-]
θ	Angle of concrete strut	21.8	[°]
$\varnothing_{long,stir}$	Diameter longitudinal reinforcement for stirrups	16.0	[mm]
$s_{long,stir}$	Spacing longitudinal reinforcement for stirrups	170.0	[mm]
$\varnothing_{stirrup,left}$	Diameter main stirrup left (1)	12.0	[mm]
$s_{stirrup,left}$	Spacing main stirrups left (1)	200.0	[mm]
$\varnothing_{stirrup,middle}$	Diameter middle stirrup (2)	12.0	[mm]
$s_{stirrup,middle}$	Spacing middle stirrups (2)	200.0	[mm]
$\varnothing_{stirrup,C}$	Diameter inverted C stirrup (3)	16.0	[mm]
$s_{stirrup,C}$	Spacing inverted C stirrups (3)	200.0	[mm]
$\varnothing_{stirrup,Z}$	Diameter Z stirrup (4)	16.0	[mm]
$s_{stirrup,Z}$	Spacing Z stirrups (4)	250.0	[mm]

Stirrup results

θ	Computed ideal angle concrete strut	21.8	[°]
$A_{l,s,req}$	Required area longitudinal reinforcement shear	6874	[mm²]
$A_{l,s}$	Total area longitudinal reinforcement shear	8042	[mm²]
	U.C. longitudinal reinforcement shear	0.85	[-]
$A_{s,req,I}$	Required stirrup area zone I	470	[mm²]
$A_{s,I}$	Total stirrup area zone I	565	[mm²/m]
	U.C. zone I	0.83	[-]
$A_{s,req,II}$	Required stirrup area zone II	892	[mm²]
$A_{s,II}$	Total stirrup area zone II	1131	[mm²/m]
	U.C. zone II	0.79	[-]
$A_{s,req,III}$	Required stirrup area zone III	1639	[mm²]
$A_{s,III}$	Total stirrup area zone III	1810	[mm²/m]
	U.C. zone III	0.91	[-]
$A_{s,req,TB}$	Required stirrup area top/bottom	160	[mm²]
$A_{s,TB}$	Total stirrup area top/bottom	565	[mm²/m]
	U.C. top/bottom	0.28	[-]

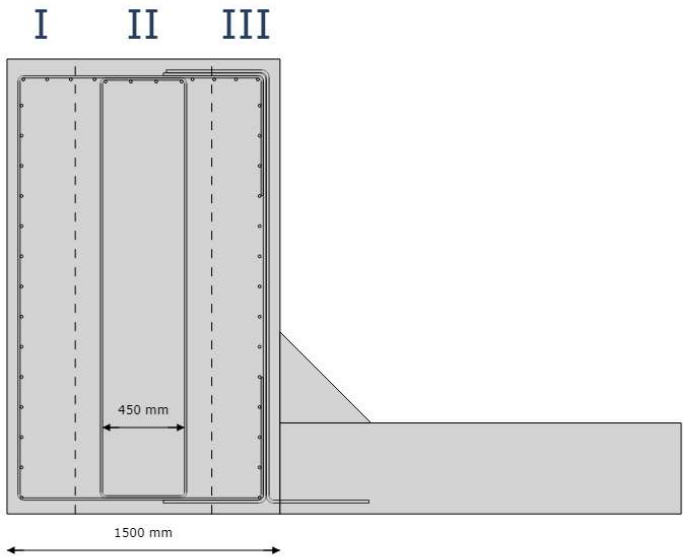

Resistance page

10. Girder cross-section check

ULS cross-section check

Input Parameters

	Steel material	FeB500	[-]
$\varnothing_1$	Diameter long. reinforcement	32.0	[mm]
$n_{bars,1}$	Number of long. reinforcement bars	13.0	[-]
c_{app}	Applied cover	60.0	[mm]

Calculation parameters

$A_{sl,torsion}$	Additional reinforcement due to torsion	1289	[mm²]
f_{pw}	Pre-stress force	18586	[kN]
d_s	Distance reinforcement	2396	[mm]
A_s	Available area reinforcement	19622	[mm²]
$\epsilon_{c,max}$	Max concrete strain	3.50	[‰]
X_u	Compressive zone height	1246	[mm]
σ_{su}	Steel stress	434	[MPa]
σ_{pu}	Pre-stress steel stress	1467	[MPa]
M_{Ed}	Moment	21806	[kNm]
M_{Rd}	Resistance moment	40945	[kNm]
	Unity check rotational capacity	1.58	[-]
	Unity Check	0.53	[-]

Reinforcement output

$c_{min,girder}$	Minimum cover girder	55	[mm]
S_{min}	Minimum spacing reinforcement	37	[mm]
S_{act}	Realised spacing reinforcement	78	[mm]

Calculation reduced pre-stress

	Factor for pre-stress for rotational capacity	0.59	[-]
M_{Ed}	Moment	28709	[kNm]
M_{Rd}	Resistance moment	34626	[kNm]
$x_{u,alt}/d$	Allowed compression zone height rotational capacity	0.37	[-]
x_u/d	Realised compression zone height	0.37	[-]
	Unity check rotational capacity	1.00	[-]
	Unity check moment	0.83	[-]

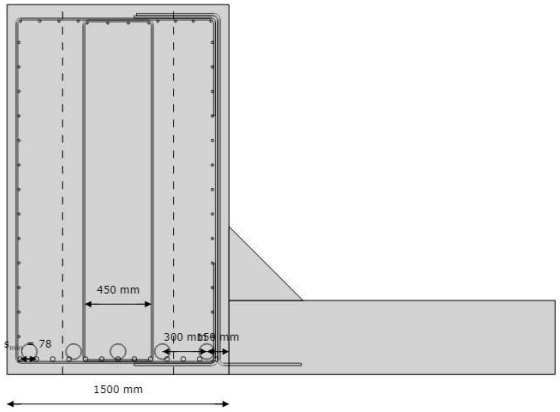

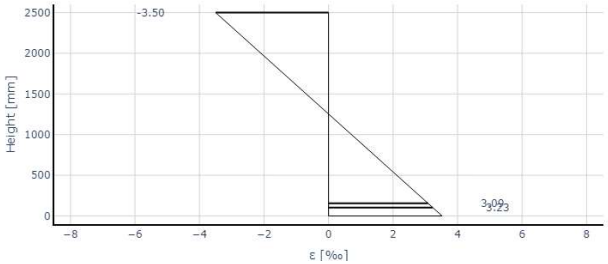

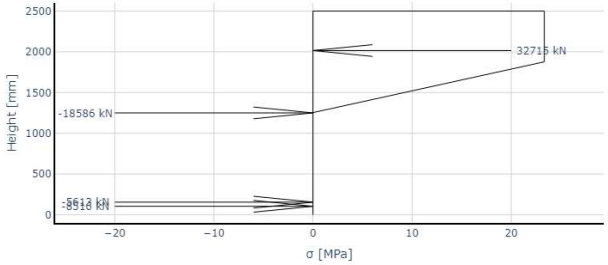

Recalculate

Resistance page

11. Floor cross-section check

ULS cross-section check floor Y-direction

Input Parameters

$\varnothing_{main,y}$	Diameter main long. reinforcement floor y	25.0	[mm]
$n_{bars,main,y}$	Number of main long. reinforcement bars floor y	8.0	[-]
$s_{layers,y}$	Spacing reinforcement layers floor y	37.0	[-]
$\varnothing_{add,y}$	Diameter additional long. reinforcement floor y	12.0	[mm]
$n_{bars,add,y}$	Number of additional long. reinforcement bars floor y	18.0	[-]
$c_{app,y}$	Applied cover floor y	55.0	[mm]

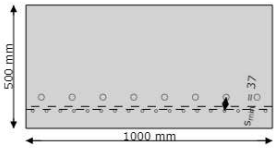

Reinforcement output

$c_{min,floor}$	Minimum cover floor	55	[mm]
s_{min}	Minimum spacing reinforcement	37	[mm]
s_{act}	Realised spacing reinforcement	37	[mm]

Calculation parameters

d_s	Distance reinforcement	392	[mm]
A_s	Area reinforcement	5963	[mm²]
$\varepsilon_{c,max}$	Max concrete strain	3.50	[‰]
x_u	Compressive zone height	148	[mm]
σ_{su}	Steel stress	434	[MPa]
z	Internal lever arm	335	[mm]
M_{Ed}	Moment	570	[kNm]
M_{Rd}	Resistance moment	867	[kNm]
	Unity check rotational capacity	0.70	[-]
	Unity Check	0.66	[-]

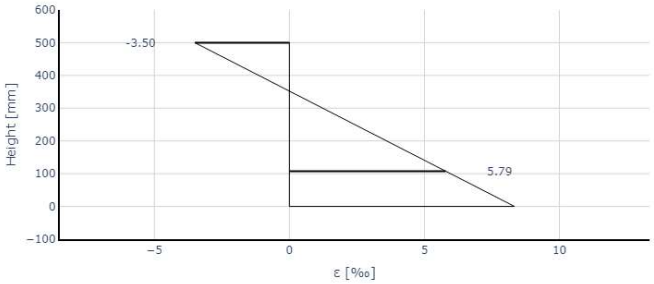

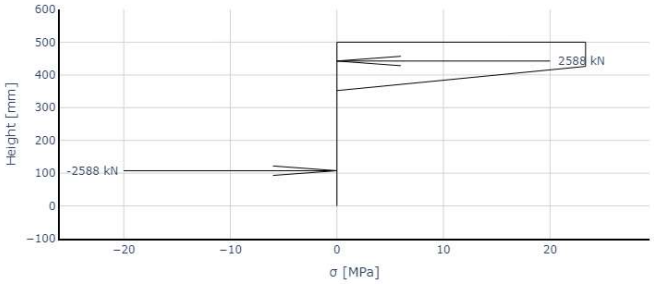

Recalculate

Resistance page

12. Shear check

ULS shear floor girder check

Shear results			
	Check section 1	6.50	[m]
	Check section 2	6.75	[m]
Δx	Considered distance max stress	0.25	[m]
ΔF_d	Change in force	72.51	[kN]
v_{Ed}	Shear stress	0.58	[MPa]
kf_{ctd}	Limit stress	0.59	[MPa]
$v_{Ed} \leq kf_{ctd}$	Check result	O.K.	[-]

Resistance page

13. Splitting reinforcement check

ULS splitting forces check

Input Parameters

$\varnothing_{spl}$	Diameter splitting reinforcement	32.0	[mm]
n_{spl}	Number of splitting reinforcement bars	8.0	[-]

Calculation results

σ_{spl}	Steel stress	411	[MPa]
f_{yd}	Max steel stress	434	[MPa]
	u.c.	0.95	[-]

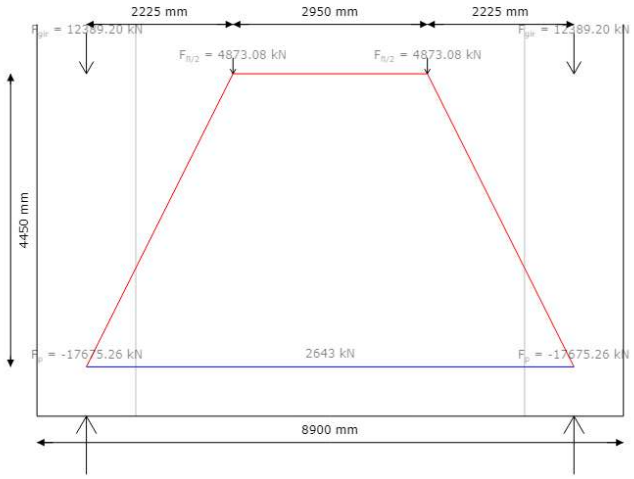

Resistance page

14. Main tension check

SLS Main tension stresses check

Calculation results

X_{check}	Check section	31.101	[m]
$\sigma_{xx,N}$	Stresses length direction due to normal force	-3.126	[MPa]
$\sigma_{xx,M}$	Stresses length direction due to moment	-0.000	[MPa]
σ_{xx}	Total stresses in length direction	-3.126	[MPa]
$\sigma_{zz,N}$	Stresses in transverse direction due to normal force	0.070	[MPa]
$\sigma_{zz,M}$	Stresses in transverse direction due to moment	0.857	[MPa]
σ_{zz}	Total stresses in transverse direction	0.927	[MPa]
τ_V	Shear stresses due to shear	0.375	[MPa]
τ_{Mt}	Shear stresses due to torsional moment	0.474	[MPa]
τ	Total shear stresses	0.849	[MPa]
σ_c	Total tension stress	0.290	[MPa]
$0.6f_{ctd}$	Allowed tension stress	0.880	[MPa]
	u.c.	0.33	[-]

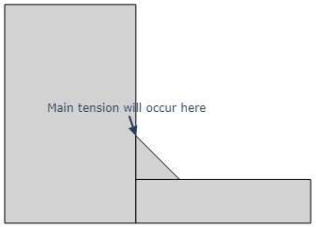

Resistance page

15. SLS Stresses check

SLS stresses checks

Decompression requirement OVS			
M	SLS char	13334	[kNm]
N	SLS char	-18935	[kN]
σ	SLS char	0.63	[MPa]
$\sigma_{allowed}$	SLS char	1.10	[MPa]
	SLS char result	O.K.	[-]
M	SLS freq	10963	[kNm]
N	SLS freq	-18640	[kN]
σ	SLS freq	-0.05	[MPa]
$\sigma_{allowed}$	SLS freq	1.10	[MPa]
	SLS freq result	O.K.	[-]
M	SLS quasi	2667	[kNm]
N	SLS quasi	-15821	[kN]
σ	SLS quasi	-2.12	[MPa]
$\sigma_{allowed}$	SLS quasi	0.00	[MPa]
	SLS quasi result	O.K.	[-]

Compression requirement t=0			
M	Max M, t=0	-671	[kNm]
N	Max M, t=0	-18804	[kN]
M	Max N, t=0	-1824	[kNm]
N	Max N, t=0	-22880	[kN]
σ	Max t=0	3.85	[MPa]
$\sigma_{allowed}$		23	[MPa]
	Unity check	0.22	[-]

Resistance page

16. Crack width floor

SLS crack-width check floor Y-direction

Input Parameters

$\varnothing_{main,y}$	Diameter main long. reinforcement floor y	25.0	[mm]
$n_{bars,main,y}$	Number of main long. reinforcement bars floor y	8.0	[-]
$s_{layers,y}$	Spacing reinforcement layers floor y	37.0	[-]
$\varnothing_{add,y}$	Diameter additional long. reinforcement floor y	12.0	[mm]
$n_{bars,add,y}$	Number of additional long. reinforcement bars floor y	18.0	[-]
$c_{app,y}$	Applied cover floor y	55.0	[mm]

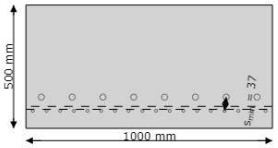

Reinforcement output

$c_{min,floor}$	Minimum cover floor	55	[mm]
s_{min}	Minimum spacing reinforcement	37	[mm]
s_{act}	Realised spacing reinforcement	37	[mm]

Equibilibrium calculation

d_s	Distance reinforcement	392	[mm]
A_s	Area reinforcement	5963	[mm²]
$\varepsilon_{c,max}$	Max concrete strain	0.87	[‰]
x	Compressive zone height	187	[mm]
σ_s	Steel stress	200	[MPa]
z	Internal lever arm	330	[mm]
M_{Ed}	Design Moment SLS	372	[kNm]
N_{Ed}	Design normal force SLS	116	[kN]

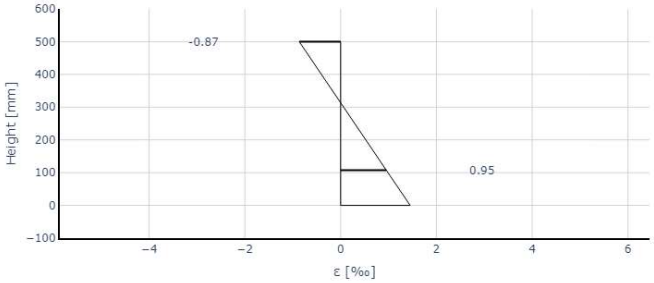

Crack-width calculation

$A_{c,eff}$	Effective concrete area	104419	[mm²]
$\rho_{p,eff}$	Effective reinforcement ratio	0.057	[-]
$\varepsilon_{sm} - \varepsilon_{cm}$	Difference reinforcement and crack strains	0.82	[‰]
$\varnothing_{eq}$	Equivalent diameter	18	[mm]
k_2	Factor incorporating excentricity	0.50	[-]
$s_{r,max}$	Max crack distance	241.33	[mm]
w	Crack-width	0.20	[mm]
$w_{allowed}$	Allowed crack-width	0.2	[mm]
	Unity Check	0.98	[-]

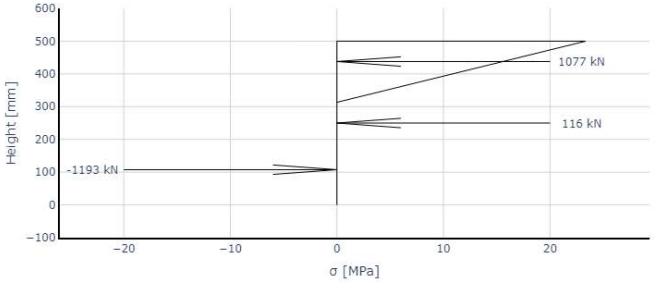

Recalculate

Resistance page

17. Evaluation

Evaluation of design

Material usage

$V_{c,tot}$	Total volume of concrete	353	[m³]
$m_{s,tot}$	Total mass of steel	31	[tonne]
$\rho_{p,eff,gir}$	Reinforcement percentage girder	5.36	[%]
$\rho_{p,eff,fl,x}$	Reinforcement percentage floor x-direction	1.49	[%]
$\rho_{p,eff,fl,y}$	Reinforcement percentage floor y-direction	7.16	[%]
	ECI of concrete	12391	[€]
	ECI of steel	6622	[€]
	Total ECI	19013	[€]
	Price steel	42445	[€]
	Price pre-stress steel	127334	[€]
	Price concrete	57555	[€]
	Total price	227334	[€]

Next step

Appendix B: Reinforcement reference project

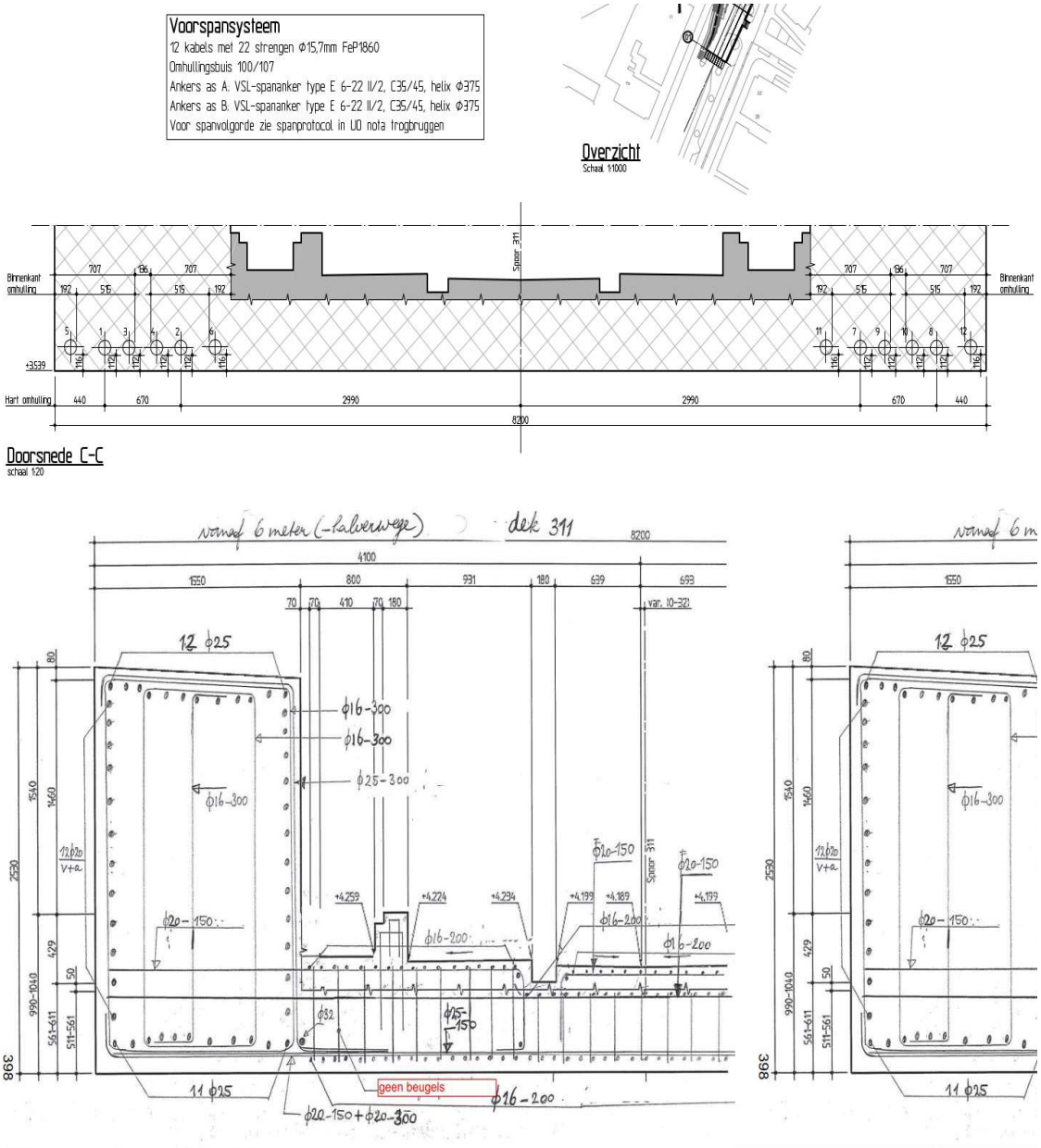

Appendix C: Calculation report optimization

Calculation report super structure concrete through girder bridge

Table of contents

1. Introduction

1.1 Cross-section

The cross-section of the bridge is given in figure 1.

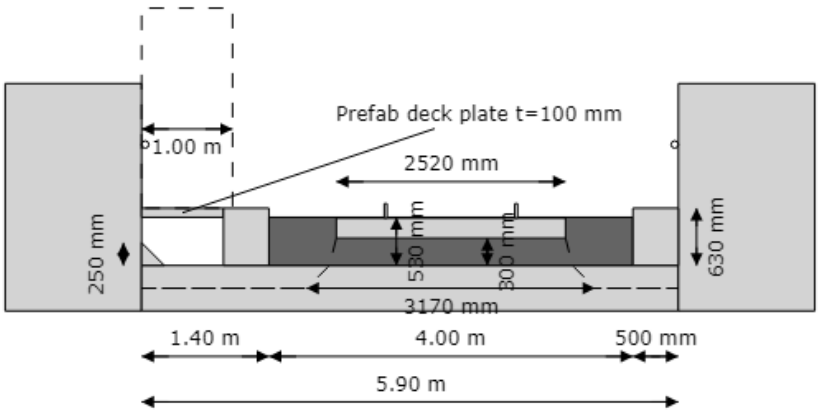

Figure 1: Cross-section of the through girder bridge

1.2 Length profile

The length profile of the bridge is given in figure 2.

Figure 2: Length profile of the through girder bridge

1.3 Aim of the report

The aim of this report is to calculate and optimize the reinforcement and pre-stressing of the super structure of a concrete through girder bridge in preliminary design phase. For this report a parametric design tool has been used to optimize the design and to make use of the automatic calculations.

2. Boundary conditions

2.1 Norms and guidelines

The most important norms and guidelines are listed below, however the applied norms are not limited to those listed.

- NEN-EN 1990-1-1:2019: Basis of structural design + NB
- NEN-EN 1991-1-4:2011: Actions on structures - General actions - Wind actions + NB
- NEN-EN 1991-2:2015: Actions on structures - Traffic loads on bridges + NB
- NEN-EN 1992-1-1:2011: Design of concrete structures - General rules and rules for buildings + NB
- NEN-EN 1992-2:2011: Design of concrete structures - Concrete bridges - Design and detailing rules + NB
- OVS00030-6-V005: Ontwerpvoorschrift kunstwerken - deel 6 - Aanvullingen en wijzigingen op NEN-EN normen
- OVS00030-1-V004: Ontwerpvoorschrift kunstwerken - deel 1 - Kunstwerken voor spoorverkeer
- RTD 1001 Richtlijnen Ontwerp Kunstwerken (ROK) 2.0
- NS Richtlijn 1015 1.3 Uitgangspunten van het ontwerp van trogbruggen

2.2 References

The references and techincal information used in this report is listed below.

- European Tehcnincal Assessment ETA-06/0147 (BBR VT CONA CMI)
- Table technical data pre-stressing strands Netherlands voorspanstaal.nl
- Product specification sheaths Tension Technology Martin

2.3 Calculation software

The following software is used for the creation of this report.

- Dlubal RFEM 6.07
- Python 3.10.8

2.4 Materials

This chapter will provide an overview of the used materials for the design.

2.4.1 Concrete

Concrete of strenght class C35/45 with the following parameters, according to NEN-EN 1992-1-1 table 3.1, are used for the design:

- f_{ck}: 35 MPa
- f_{ctm}: 3.2 MPa
- E_{cm}: 34 GPa (uncracked)
- γ_M: 1.5
- v: 0.2 (uncracked)

2.4.2 Steel

Reinforcement steel of strenght class FeB500 with the following parameters is used for the design:

- f_{yk}: 500 MPa
- f_{yd}: 434 MPa
- E_s: 210 GPa

2.4.3 Pre-stress steel

Pre-stressing steel of strenght class FeP1860 with the following parameters is used for the design:

- f_{pk}: 1860 MPa
- $f_{p,0.1,k}$: 1600 MPa
- E_p: 195 GPa

2.4.3 Pre-stress system

The design makes use of a BBR VT CONA CMI prestressing system internal post-tensioning system with cables and a duct of:

- $n_{strands}$: 22
- $\varnothing_{strands}$: 15.7 mm

The pre-stress ducts used are of type: STB-100x109x0.40 as described in the product specification of TTM

The filling degree of the pre-stress duct thus becomes: 0.54.

2.5 Environmental classes

In table 1 the environmental classes and crack width requirements have been summarized. The design life of all train bridges is 100 years and the crack width

requirement and the environmental classes have been decided by OVS-00030-6 and NEN-EN 1992-1-1.

Structural element	Environmental class	$c_{nom,reinf}$ mm	c_{app} mm	$c_{nom,p}$ mm	w_{max} mm
Girder	XC4, XD3, XF4, XA2	55.0	60.0	70.0	0
Top of deck	XC4, XD3, XF4, XA2	55.0			0.2
Bottom of deck	XC4, XD3, XF4, XA2	55.0			0.2

Table 1: Durability factors

2.6 Loads

The loads working on the super structure of the bridge will be summarized here. For the complete calculation of the loads please refer to annex B. Also the load combinations considered are summarized in annex C.

2.6.1 Permanent loads

LC1.1 Self-Weight

The self-weight of the structure is calculated automatically calculated by RFEM.

LC1.2 Permanent loads train

Other permanent loads that are considered are due to the infrastructure on the bridge for the trains. The loads are visualised in figure 3.

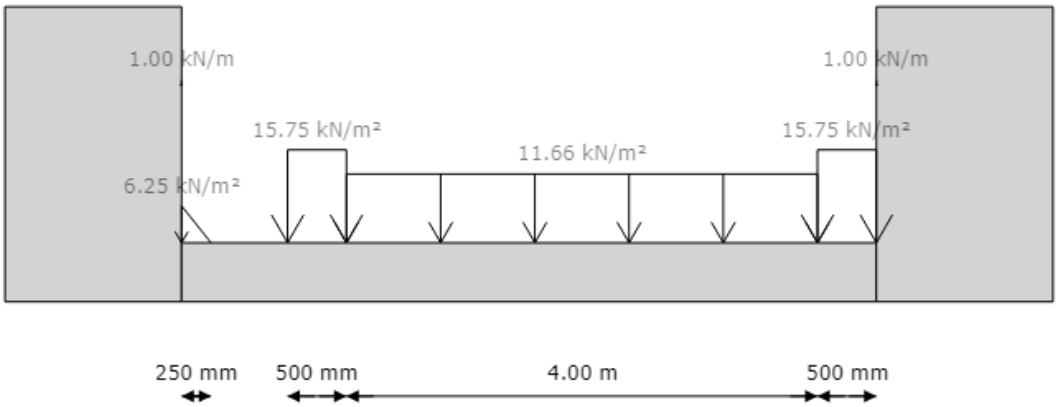

Figure 3: Permanent loads

LC2 Prestressing

For the calculation of the pre-stress forces and losses please refer to annex B. Figure 4 shows the pre-stress profile and figure 5 shows the resulting forces.

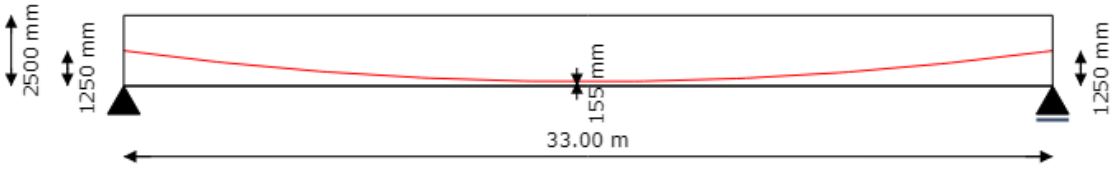

Figure 4: Pre-stress profile

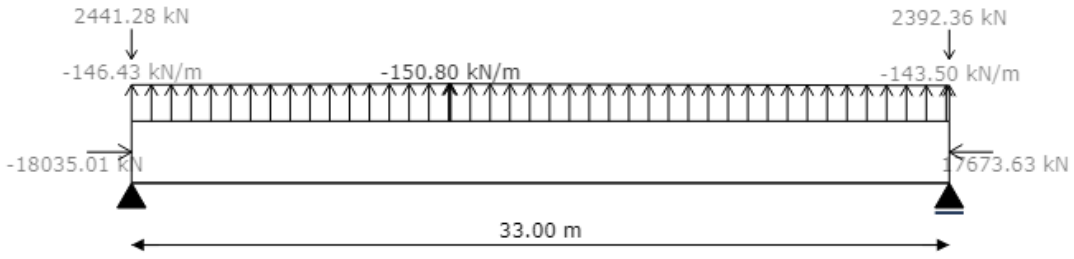

Figure 5: Pre-stress loads

LC3 Setting
Because a single span statically determined bridge is considered, settings will not cause loads.

2.6.2 Variable loads

LC4 Other variable loads
Variable loads on the passing path are considered as per NEN-EN 1991-2.

- $Q_{passing\ path}$: 5 kN/m^2

Snow loads are not considered because these will be inisgnificant compared to the train loads.

LC5 Braking loads and LC6 Accelerating loads
Brake and accelerating forces are not considered for the super structure as these will be mostly important for the substructure.

LC7 Wind loads
Windloads are calculated using NEN-EN 1991-1-4, for the complete calculation please refer to Annex B.

The decisive loads F_{wk} and the reduced F_{wk}^{**} that are considered are given below. The loads in x-direction are modelled as line loads acting on the wall of the structure, while the loads in z direction are considered as distributed loads over the whole area of the bridge.

- $q_{wk,x}$: 16.73 kN/m
- $q_{wk,x}^{**}$: 12.01 kN/m
- $p_{wk,z}$: 1.44 kN/m^2
- $p_{wk,z}^{**}$: 1.03 kN/m^2

LC8 Temperature loads
Temperature loads have not yet been incorporated in the design.

LC9.1.1 Train loads model LM71 M

The position of the train load model LM71 from NEN-EN 1991-2 is automatically calculated using influence lines. Also the effective width over which the load may be spread is calculated:

$$W_{\text{load}} = l_{\text{sleeper}} + 2 \cdot (\frac{t_{\text{bal}}}{4} + \frac{h_{\text{fl}}}{2}) = 2520 + 2 \cdot (75.0 + 250.0) = 3170 \text{ mm}$$

It is assumed that the point loads in the middle of this load model can be evenly distributed over the whole area. The loads resulting in the highest moment from LM71 are shown in figure 6:

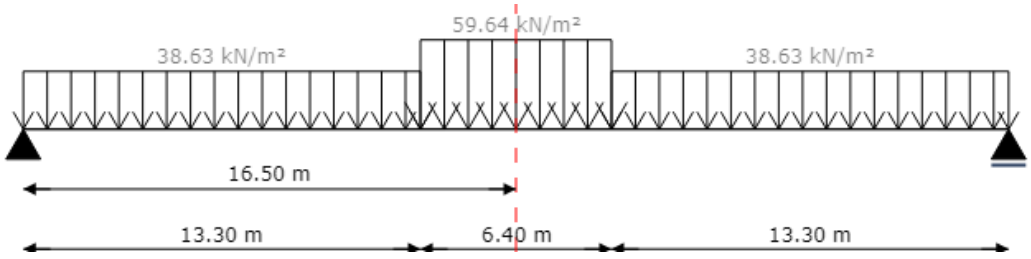

Figure 6: Load model LM71, max moment

LC9.1.2 Train loads model LM71 V

The loads resulting in the highest shear force from LM71 are shown in figure 7:

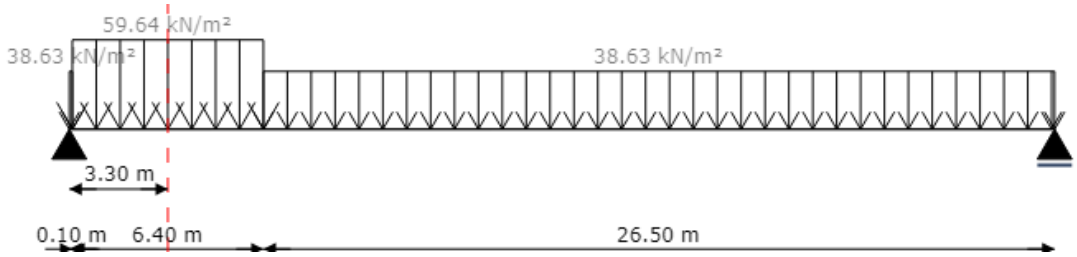

Figure 7: Load model LM71, max shear force

LC9.2.1 Train loads model SW/0 M

Because a single span bridge is designed load model SW/0 is not considered.

LC9.3.1 Train loads model SW/2 M

The position of the train load model SW/2 from NEN-EN 1991-2 is automatically calculated using influence lines. The effective width is the same as before. The loads resulting in the highest moment from SW/2 are shown in figure 8:

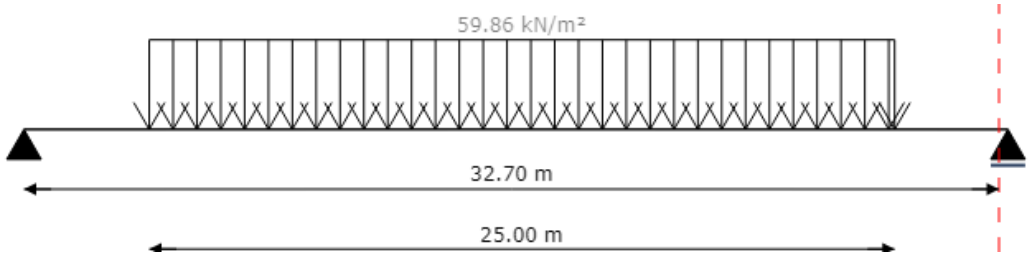

Figure 8: Load model LM71, max moment

LC9.3.2 Train loads model SW/2 V

The loads resulting in the highest shear force from SW/2 are shown in figure 9:

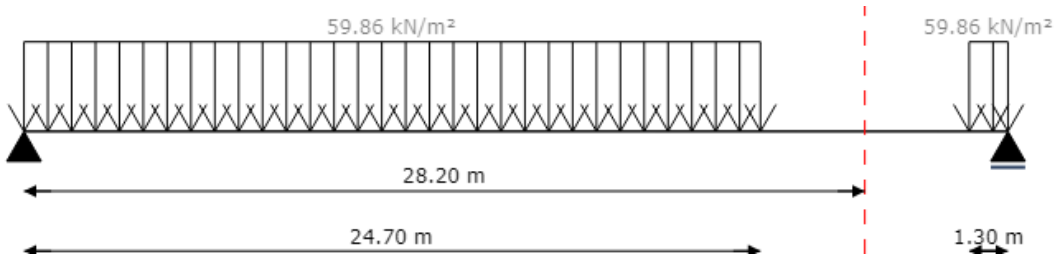

Figure 9: Load model LM71, max shear force

2.6.3 Special loads

LC10.1 Train loads tilting and LC10.2 Rerailing loads

These load cases have not been implemented yet. Also centrifugal force is not considered because the bridge is straight.

3. Calculations

For the pre-stress and reinforcement layouts of the design please refer to annex B.

3.1 Modelling and loadtransfer

As mentioned before the FEM model is build in RFEM. The principal cross-section in RFEM is shown in figure 10. In the following paragraphs the most important elements of the model will be explained.

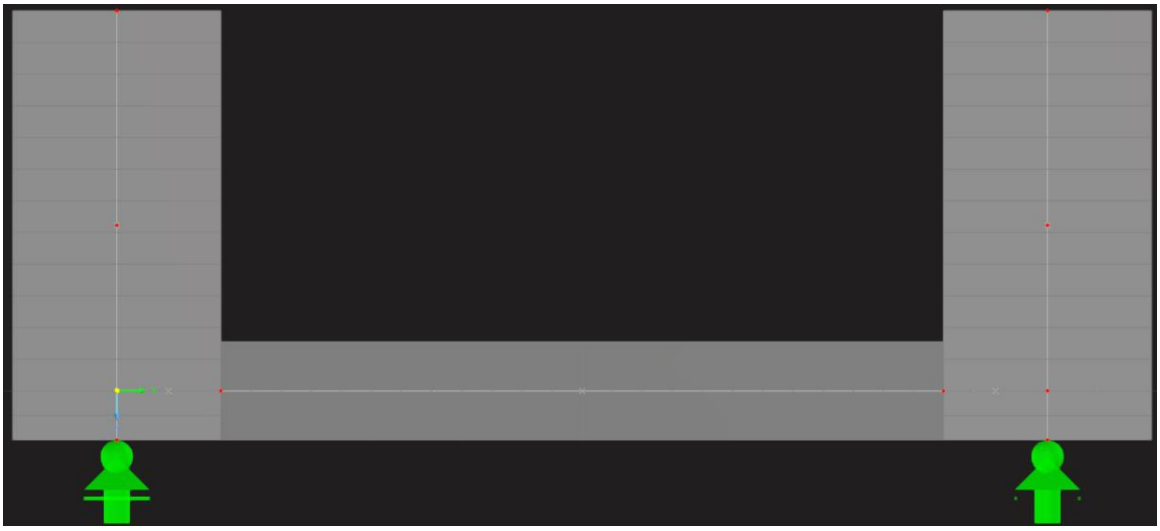

Figure 10: Principal cross-section in RFEM

3.2.1 Girders

The girders are modelled as vertical planar 2D plate elements with a uniform thickness that transfer moments and membrane forces. This way the homogenous en isotropic behaviour of the girder is correctly modelled. The target mesh size for the elements is 0.25 m.

3.2.2 Floor

The floor is modelled simillarly as the girders. For the floor again a vertical planar 2D plate element with a uniform thickness that transfer moments and membrane forces is used. For the floor also a mesh size of 0.25 m is used.

3.2.3 Connection floor-girder

The floor and girders are connected via a rigid planar surface with zero mass density such that the self-weight is not doubled in this area. By making sure this surface connects the floor and the girder the connection correctly models the bahaviour of load transfer between these elements. Figure 11 shows how the elements are modelled by side view.

Figure 11: Side view of the surface elements in RFEM

3.2.4 Supports

The model has 4 supports all of them restricting movement in z-direction and none of them restricting rotation. Figure 12 shows how the supports of the model are ordered and in which direction they allow for translation.

Figure 12: Top view of the support directions

3.2.5 Result beams

To transfer the loads of the 2D elements of the girders into 1D internal forces to be used for evaluation result beams are used. These beams cover the surface elements and integrate the internal forces to 1D internal forces.

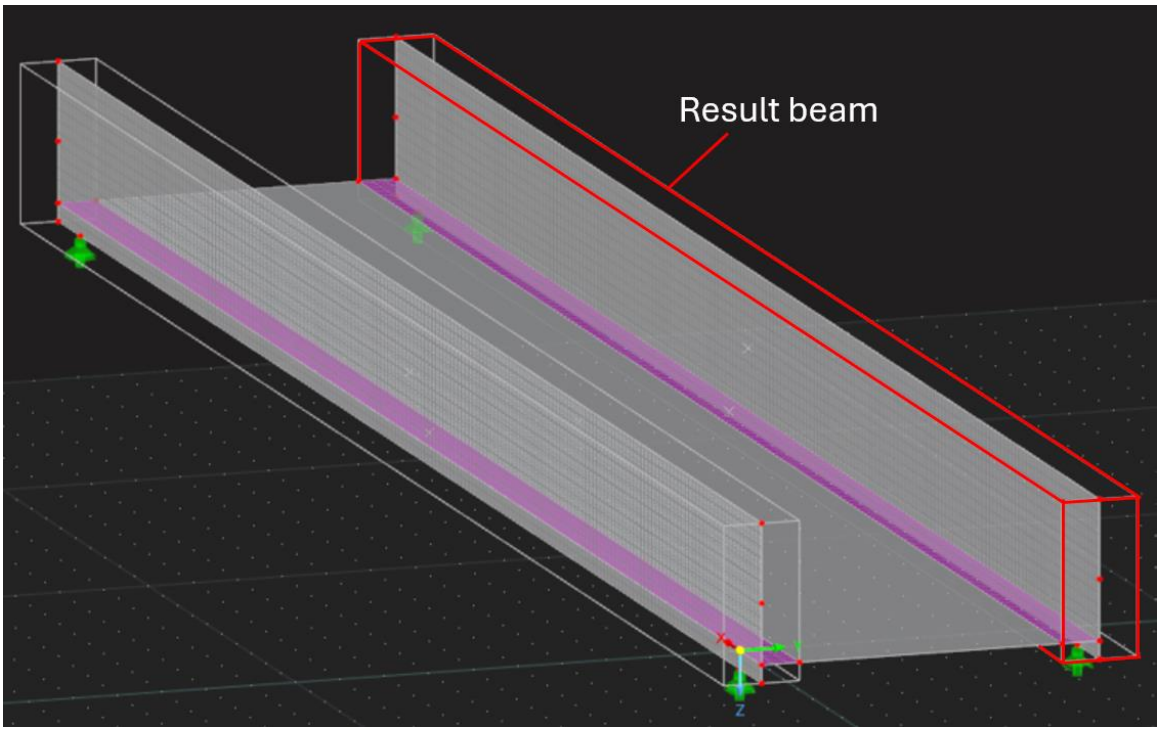

Figure 13: Result beam in model

3.2 Calculations girder

This paragraph outlines the results of the calculations made for the girder. The reinforcement and pre-stress layout can be found in annex B.

3.2.1 Ultimate limit state

These calculations can be found in Annex E and F. The longitudinal and stirrups reinforcement has been checked according to NEN-EN 1992-1-1. The stirrups have been divided into three regions, each having a different purpose for the type of load they carry. Next to that the longitudinal reinforcement is tested both for capacity and for max compression zone height according to NEN-EN 1992-1-1 6.1 (9). To achieve this the pre-stress has been ficticiously reduced to 62 % such that only the part of the pre-stress that is needed to carry the load remains. With this case the compression zone height is checked.

The results are summarized in table 2.

	Symbol	Value	Limit value	Result
Longitudinal reinforcement torsion	$u.c_{sl,T}$	$A_{sl,T,req}$ = 8420 mm^2	$A_{sl,T}$ = 9249 mm^2	0.91
Stirrup horizontal reinforcement	$u.c_{sw,T,hor}$	$A_{sw,T,hor,req}$ = 196 mm^2	$A_{sw,T}$ = 565 mm^2	0.35
Stirrup zone I reinforcement	$u.c_{sw,I}$	$A_{sw,I,req}$ = 511 mm^2	A_{sw} = 565 mm^2	0.90

Stirrup zone II reinforcement	$u.c_{sw,II}$	$A_{sw,II,req}$ = 899 mm^2	A_{sw} = 905 mm^2	0.99
Stirrup zone III reinforcement	$u.c_{sw,III}$	$A_{sw,III,req}$ = 1952 mm^2	A_{sw} = 2011 mm^2	0.97
Moment reinforcement	$u.c_{M,gir}$	M_{Ed} = 21743 kNm	M_{Rd} = 35709 kNm	0.61
Increased moment reinforcement	$u.c_{M,rot}$	$M_{Ed,rot}$ = 28137 kNm	$M_{Rd,rot}$ = 29064 kNm	0.97
Compression zone height	$u.c_{x,rot}$	x_u = 773 mm	$x_{u,allowed}$ = 773 mm	1.00

Table 2: Calculation results girder ULS

3.2.2 Serviceability limit state

This section covers the SLS calculations for the girder. Both the compressive and tension stresses in the concrete have been checked in annex J. The tension stresses have been checked according to the requirements of the OVS and the compressive stress has been checked at t=0. Next to that the main tension stress just above the haunch at the inner wall of the girder has also been checked in accordance with NSRL1015. This stress is built up out of three stres components σ_{xx}, σ_{zz} and τ and they are calculated in annex K.

The results are summarized in table 3.

	Symbol	Value	Limit value	Result
Tension stress SLS-quas		$\sigma_{ct,quas}$=-2.17 MPa	$\sigma_{ct,quas,allowed}$=0.00 MPa	O.K.
Tension stress SLS-freq		$\sigma_{ct,freq}$=-0.11 MPa	$\sigma_{ct,freq,allowed}$=1.10 MPa	O.K.
Tension stress SLS-char		$\sigma_{ct,char}$=0.59 MPa	$\sigma_{ct,char,allowed}$=1.10 MPa	O.K.
Compressive stress	$u.c_{compr}$	σ_c=5.27 MPa	f_{cd}=23 MPa	0.23
Main tension stress	$u.c_{main\ tension}$	σ_{ct}=0.45 MPa	$0.6f_{ctd}$=0.88 MPa	0.51

Table 3: Calculation results floor SLS

3.3 Calculations floor

This paragraph outlines the results of the calculations made for the floor.

3.3.1 Ultimate limit state

The ULS calculations for the floor are conducted using NEN-EN 1992-1-1. Reinforcement in both x and y direction is applied en checked in annex G.

The results are summarized in table 4.

	Symbol	Value	Limit value	Result
Longitudinal reinforcement	$u.c_{M,floor,y}$	M_{Ed}=569 kNm	M_{Rd}=867 kNm	0.66
Transverse reinforcement	$u.c_{M,floor,x}$	M_{Ed}=200 kNm	M_{Rd}=220 kNm	0.91

Table 4: Calculation results floor ULS

3.3.2 Servicability limit state

The SLS calculations for the floor are conducted using NEN-EN 1992-1-1. Annex L outlines how the crack-width has been calculated.

The results are summarized in table 5.

	Symbol	Value	Limit value	Result
Crack-width longitudinal	$u.c_{cw,y}$	w=0.20 mm	$w_{allowed}$=0.20 mm	0.98
Crack-width transverse	$u.c_{cw,x}$	w=0.05 mm	$w_{allowed}$=0.20 mm	0.25

Table 5: Calculation results floor ULS

3.4 Other calculations

This paragraph outlines the results of the other calculations.

3.3.1 Ultimate limit state

Longitudinal shear between the girder and the floor has ben checked in annex H according to NEN-EN 1992-1-1 6.2.4.Next to that splitting reinforcement at the ends of the deck has also been calculated in annex I using a strut and tie model
The results of these calculations have been summarized in table 6.

	Symbol	Value	Limit value	Result
Longitudinal shear	$u.c_{l,s}$	v_{Ed}=0.57 MPa	kf_{ctd}=0.59 MPa	0.97
Splitting reinforcement	$u.c_{spl}$	σ_{spl}=394 MPa	f_{yd}=434 MPa	0.91

Table 6: Calculation results other calculations ULS

3.3.2 Servicability limit state

The maximum displacement is calculated with the FEM model is 26.3 mm. The by OVS required camber is 33.0 mm, this means that the pre-camber of the bridge should be 59.3 mm

4. Results

Based on the internal forces from the 3D FEM model of the design model, the reinforcement and prestressing of the superstructure of the trough bridge have been determined. The structure has been checked for strength and durability in a preliminary design stage. The geometry and reinforcement is summarized in appendix A and B.

4.1 Points of attention

- This report is made for a preliminary design, further detailling is needed to complete the design.
- Temperature loads are not considered in this report.
- This bridge has not been tested in FAT.
- Splitting reinforcement for the introduction of the pre-stressing has not been designed.
- No calculations for detailing around the supports have been made.
- It is essential for the design that the bridge is correctly protected from stray currents by isolation of the clearway in accordance with OVS.

Annex A: Geometry and effective width

Cross-sectional properties

The calculation of certain cross-sectional parameters is displayed below.

$$A = 2 \cdot h_{\text{gir}} \cdot W_{\text{gir}} + h_{\text{fl}} \cdot W_{\text{fl}} + a_{\text{vou}}^2 = 10.51\ \text{m}^2$$

$$z_{\text{neutral,axis}} = \frac{2 \cdot A_{\text{gir}} \cdot z_{\text{gir}} + A_{\text{fl}} \cdot z_{\text{fl}} + 2 \cdot A_{\text{vou}} \cdot z_{\text{vou}}}{A} = 0.965\ \text{m}$$

$$I = 2 \cdot (I_{\text{girder}} + A_{\text{girder}} \cdot a_{\text{girder}}^2) + I_{\text{fl}} + A_{\text{fl}} \cdot a_{\text{fl}}^2 + 2 \cdot (I_{\text{vou}} + A_{\text{vou}} \cdot a_{\text{vou}}^2) = 6.096\ \text{m}^4$$

The cross-section for including the max effective width is shown in figure 14.

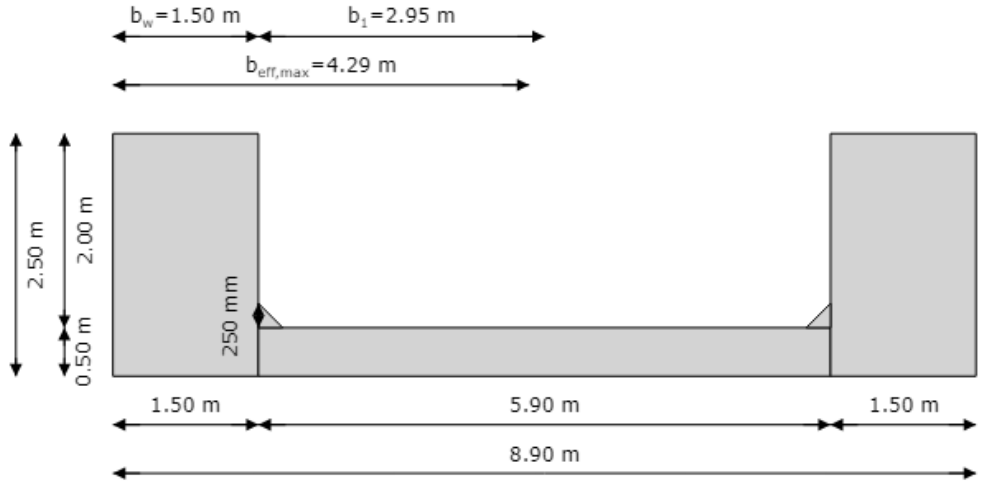

Figure 14: Cross-section including maximum effective width

The effective width over the length of the bridge is shown in figure 15

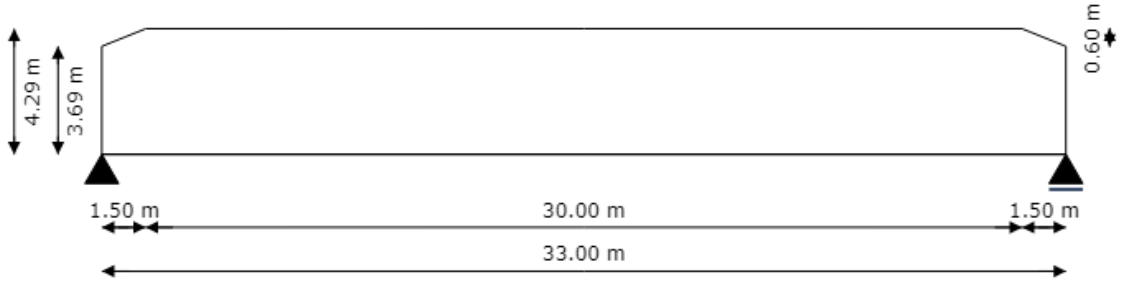

Figure 15: Length profile with effective width of the through girder bridge

The effective width is calculated via NEN-EN 1992-2. First the l_0/b_i ratio can be calculated as: 33/2.95=11.19.
Referencing this ratio in figure 16, it is found that the ratio b_{eff}/b_i for S_s should be: 0.74 and for S_v: 0.95. The effective width can be calculated accordingly.

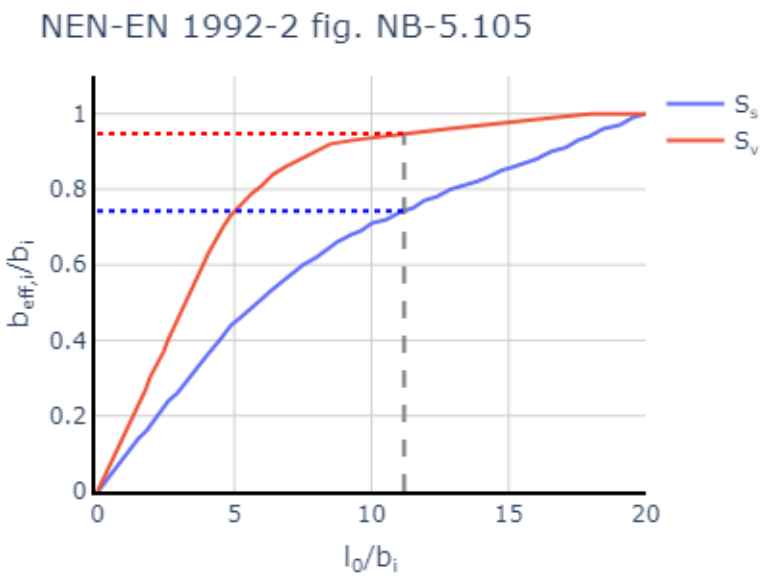

Figure 16: NEN-EN 1992-2 fig. NB.5-105 and the effective width ratio's

Train infrastructure

The geometry of the train infrastructure in the cross-section should also be determined in accordance with OVS00030-6-V005 and OVS00030-1-V004.
Sleepers are 2520x260x121 mm based on OVS6 article 6.3.6.2 and on the fact that a UIC-54 rail has a height of 159 mm, they have a spacing of 600 mm according to NEN-EN 1991-2 fig. 6.5.
The thickness of the ballast layer is 300.0 mm and the thickness of the deck plate for the passing path is 100 mm. The width of this passing path is 1 m according to OVS1 article 3.3.3 and it should be atleast 2.4 m out of the center of the rails knowing no high-speed trains will cross this bridge.
The derailment guards should be placed at least 2 m out of the center of the rails according to OVS1 article 4.1.4.1 and the width of the derailment guard is 500 mm to accomodate the reinforcement needed for big impacts. The height of these guards should at least be 100 mm above the top of the rail.
For design purposes the height of the ballast bed should be from the top of the deck to the top of the rails - 150 mm with a volumetric of 22 kN/m^3 according to OVS-6 article 5.2.3.
Using these rules the cross-section with train infrastructure in the report is designed.

Annex B: Pre-stress and reinforcement

Pre-stress

The pre-stress layout at midspan is shown in 17. This system uses 5 cables per girder.

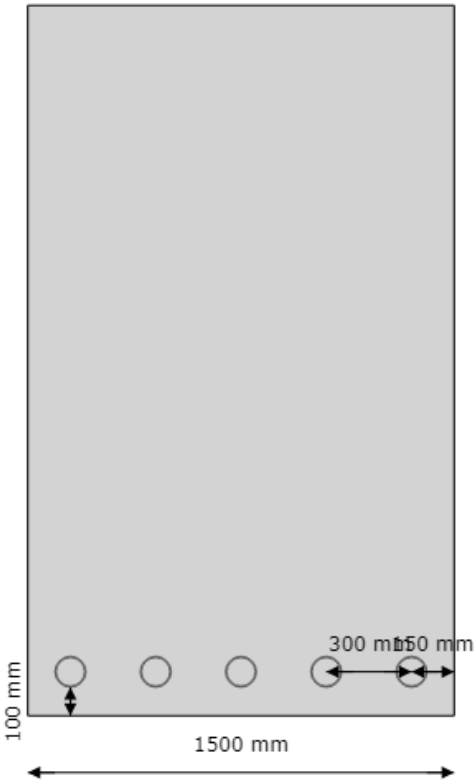

Figure 17: Pre-stress layout

- R: 124 m
- A_P: 16500 mm^2
- $d_{P,mid}$: 2345 mm
- $\sigma_{Pi,max}$: 1427 MPa
- $\sigma_{Pw,max}$: 1136 MPa
- $c_{P,min}$: 70 mm
- $c_{P,app}$: 100 mm

Girder reinforcement

The reinforcement layout of the girder is shown in 18.

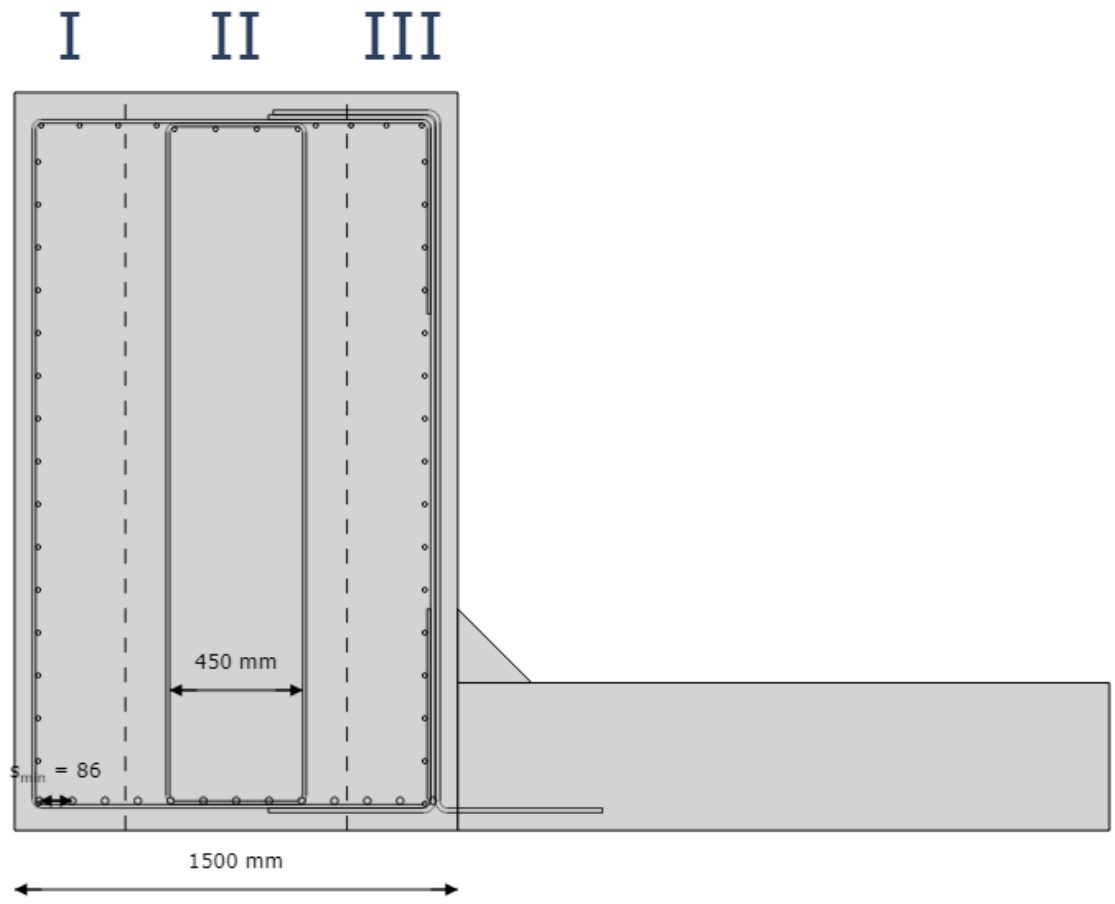

Figure 18: Girder reinforcement layout

Main longitudinal reinforcement:

- $\varnothing_{sl}$: 25 mm
- A_{sl}: 12763 mm^2
- d_{sl}: 2400 mm

Longitudinal reinforcement for torsional resistance:

- $\varnothing_{sl,T}$: 16 mm
- $s_{sl,T}$: 150 mm
- $A_{sl,T}$: 9249 mm^2

Stirrups:

- $\varnothing_{sw,C}$: 12 mm
- $s_{sw,C}$: 200 mm
- $\varnothing_{sw,mid}$: 12 mm
- $s_{sw,mid}$: 250 mm
- $\varnothing_{sw,inverted\ C}$: 16 mm
- $s_{sw,inverted\ C}$: 200 mm
- $\varnothing_{sw,Z}$: 16 mm
- $s_{sw,Z}$: 200 mm
- $A_{sw,I}$: 565 mm^2
- $A_{sw,II}$: 905 mm^2
- $A_{sw,III}$: 2011 mm^2

Cover:

- c_{min}: 55 mm
- c_{app}: 60 mm

The stirrup reinforcement is divided in three different areas. Area I serves as torsional and shear forces reinforcement, area II serves for shear reinforcement and area III serves for both shear and torsional reinforcement and also carries the loads from the suspension forces from the floor.
Due to the limitation is NEN-EN 1992-1-1, the maximum spacing of the stirrups in the girder is 500 mm. This requirement is fulfilled

Floor reinforcement

The reinforcement layout of the floor in y-direction is shown in 19. The reinforcement in x-direction is shown in the transverse direction.

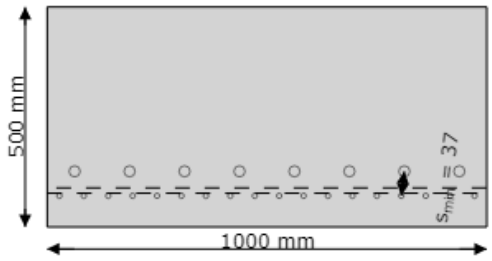

Figure 19: Floor reinforcement layout

Longitudinal reinforcement y-direction:

- $\varnothing_{1,y}$: 12 mm
- $s_{1,y}$: 56 mm
- $\varnothing_{2,y}$: 25 mm
- $s_{2,y}$: 125 mm
- $A_{sl,y}$: 5963 mm^2
- $d_{sl,y}$: 392 mm

Longitudinal reinforcement x-direction:

- $\varnothing_{1,x}$: 12 mm
- $s_{1,x}$: 91 mm
- $A_{sl,x}$: 1244 mm^2
- $d_{sl,x}$: 417 mm

Cover:

- c_{min}: 55 mm
- c_{app}: 55 mm

Splitting reinforcement

The splitting reinforcement at the ends of the span has also been calculated. The layout for both ends of the bridge is:

- $\varnothing_{spl}$: 32 mm
- n_{spl}: 8
- A_{spl}: 6434 mm^2

Annex C: Loads

LC1.2 Permanent loads train

This section will feature the calculation of the additional permanent loads

- Weight haunches

The additional load of the haunches which are not modelled in SCIA as structural elements is calculated with:

$$Q_{\text{haunch}} = h_{\text{haunch}} \cdot \gamma_{\text{concrete}} = h_{\text{haunch}} \cdot 25$$

Because the haunchs have a slope of 1:1 and the max height of 250.0 mm, this leads to the loads represented in the report.

- Weight derailment guard

The additional load of the derailment guards is calculated as:

$$Q_{\text{derailment guard}} = h_{\text{derailment guard}} \cdot \gamma_{\text{concrete}} = 630.0 \cdot 25 = 15.75 \text{ kN/m}^2$$

- Weight ballastbed

The additional load of the ballast bed is calculated as:

$$Q_{\text{ballast bed}} = h_{\text{ballast bed}} \cdot \gamma_{\text{concrete}} = 530.0 \cdot 25 = 11.66 \text{ kN/m}^2$$

With these calculations the loads shown in the report have been calculated.

LC2 Prestressing

The tendon profile of the prestress is given in figure 20.

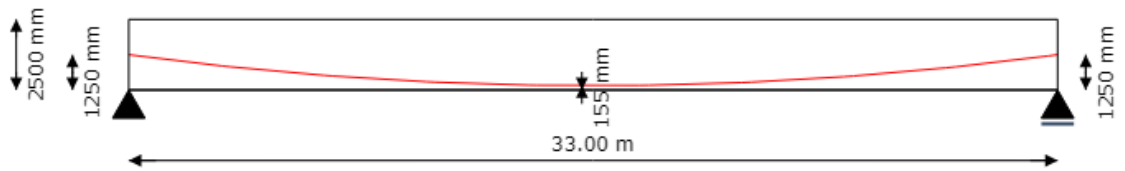

Figure 20: Prestress tendon profile

The tendon profile is given by:

$$y = 4.08 \cdot 10^{-6}x^2 + -0.13x + 1250;\ R = 124\ \text{m}$$

In addition to this the vertical displacement of the cable Δz due to the stressing of the cable is calculated with a maximum of 18 mm due as prescribed by ROK

First the maximum force should be determined. From a simple calculation it follows that the maximum pre-stressing force is limited by the material properties rather than by the maximum pre-stressing force that will yield a positive moment at t=0 when only the self-weight and the prestressing force will be acting on the bridge:

$$\frac{N_\text{P}}{A} - \frac{M_\text{P}}{W_\text{top}} + \frac{M_\text{sw}}{W_\text{top}} > 0;\ N_\text{P} = \sigma_\text{P} A_\text{P}$$

Using:

$$M_\text{P} = \frac{1}{2} \cdot N_\text{P}(e_1 + e_2) + \frac{N_\text{P} l^2}{8R}$$

$$M_\text{sw} = \frac{1}{8} \cdot A\gamma_\text{conc} l^2$$

$$A_\text{P} = A_\text{strand} n_\text{strands} n_\text{cable} = 150 \cdot 22 \cdot 5 = 16500\ \text{mm}^2$$

It can be concluded that $\sigma_{\text{PM0,max}}$=3022 MPa, which is much higher than the limit given by:

$$\sigma_{\text{PM0,max}} = \min(0.75 \cdot f_\text{pk}, 0.85 \cdot f_{\text{p0.1k}}) = \min(0.75 \cdot 1860, 0.85 \cdot 1600) = 1360\ \text{MPa}$$

The maximum stress during tensioning is:

$$\sigma_{\text{PMi,max}} = \min(0.8 \cdot f_\text{pk}, 0.9 \cdot f_{\text{p0.1k}}) = \min(0.8 \cdot 1860, 0.9 \cdot 1600) = 1440\ \text{MPa}$$

These two stresses are the basis for the pre-stress loss calculations. For these calculations the following losses are considered:

- Friction losses

The prestressing system makes use of a Steel strip sheath with: k=0.005 rad/m and μ=0.18 rad^{-1} following from European Technical Assessment ETA-06/0147. The friction losses over the length profile can be calculated using:

$$F = F_0 e^{-\mu(\theta + k \cdot x)}$$

Where θ is the sum of the angular displacements over the distance x, irrespective of direction or sign. The pre-stressing steel is stressed first from the left side and than from the right side. Now σ_{PMi} can be calculated.

- Wedge set

The wedge set for the pre-stressing system is assumed to be 7 mm because of the ROK. How this loss is spread over the length of the bridge is calculated by discretizing the length of the bridge into many small dx's. For the each dx and $\Delta\sigma_{slip}$ the total Δl is calculated using:

$$\Delta l = \frac{\Delta\sigma_{\text{slip}}}{E_{\text{P}}} \cdot \Delta x$$

Using a smart optimization algorithm the actual stress losses can be calcualted by finding the $\Delta\sigma_{slip}$ values such that ΣΔl=7 mm using the follwing rule.

$$\Delta\sigma_{\text{slip},x=i+1} = \max(\Delta\sigma_{\text{slip},x=i} - \max(2(\sigma_{\text{PMi},x=i} - \sigma_{\text{PMi},x=i+1}),0),0)$$

- Creep loss

The creep loss can be calculated assuming: t=36500 days, t_0=10 days and RH=65 %. The calculation from Annex B of NEN-EN 1992-1-1 can be used to calculate the creep coefficient:

$$\alpha_1 = \left(\frac{35}{f_{\text{cm}}}\right)^{0.7} = 0.87;\ \alpha_2 = \left(\frac{35}{f_{\text{cm}}}\right)^{0.2} = 0.96;\ \alpha_3 = \left(\frac{35}{f_{\text{cm}}}\right)^{0.5} = 0.90$$

$$h_0 = \frac{2A_{\text{c}}}{u} = \frac{2 \cdot 10512500}{26800} = 785 \text{ mm}$$

Where u is the perimeter of the cross-section of the bridge.

$$\begin{aligned}\beta_{\text{H}} &= \min(1.5(1 + (0.012\text{RH})^{18})h_0 + 250\alpha_3, 1500\alpha_3) \\ &= \min(1.5(1 + (0.012 \cdot 65)^{18})785 + 226, 1353) = 1353\end{aligned}$$

$$\beta_{\text{c}}(t, t_0) = \left(\frac{t - t_0}{\beta_{\text{H}} + t - t_0}\right)^{0.3} = \left(\frac{36500 - 10}{1353 + 36500 - 10}\right)^{0.3} = 0.99$$

$$\beta(t_0) = \frac{1}{0.1 + t_0^{0.20}} = \frac{1}{0.1 + 10^{0.20}} = 0.59$$

$$\beta(f_{\text{cm}}) = \frac{16.8}{\sqrt{f_{\text{cm}}}} = \frac{16.8}{\sqrt{43}} = 2.56$$

$$\phi_{\text{RH}} = \alpha_2(1 + \alpha_1 \cdot \frac{1 - \text{RH}/100}{0.1h_0^{\frac{1}{3}}}) = 0.96(1 + 0.87 \cdot \frac{1 - 0.65}{0.19}) = 1.27$$

$$\phi_0 = \phi_{\text{RH}}\beta(f_{\text{cm}})\beta(t_0) = 1.27 \cdot 2.56 \cdot 0.59 = 1.94$$

Using these parameters the creep coefficient can be calculated. Using the creep coefficient and the aforementioned first estimate of steel stress the creep strain can be calculated:

$$\phi(t, t_0) = \phi_0\beta_{\text{c}}(t, t_0) = 1.94 \cdot 0.99 = 1.92$$

$$E_{\text{c}} = 1.05E_{\text{cm}};\ \sigma_{\text{c}} = \sigma_{\text{P}} \cdot \frac{A_{\text{P}}}{A_{\text{c}}}$$

$$\varepsilon_{\text{cc}}(\infty, t_0) = \phi(\infty, t_0) \cdot \frac{\sigma_{\text{c}}}{E_{\text{c}}} = 1.92 \cdot \frac{6}{35700} = 0.351\ ‰$$

- Drying shrinkage loss

Drying shrinkage ε_{cd} strain can also be calculated via NEN-EN 1992-1-1. Cement of class N is used or this design giving α_{ds1}=4 and α_{ds2}=0.12, also f_{cmo}=10 MPa and RH_0=100 %. Now $\varepsilon_{cd,0}$ can be calculated:

$$\beta_{\text{RH}} = 1.55(1 - (\frac{RH}{RH_0})^3) = 1.55(1 - (\frac{65}{100})^3) = 1.12$$

$$\varepsilon_{\text{cd,0}} = 0.85((220 + 110\alpha_{\text{ds1}}) \cdot \exp(-\alpha_{\text{ds2}} \cdot \frac{f_{\text{cm}}}{f_{\text{cmo}}})) \cdot 10^{-6} \cdot \beta_{\text{RH}}$$
$$= 0.85((220 + 110 \cdot 4) \cdot \exp(-0.12 \cdot \frac{43}{10})) \cdot 10^{-6} \cdot 1.12 = 376.50 \cdot 10^{-6}$$

The value of k_h can be found in table 3.3 and is 0.70. Now the final drying shrinkage can be calculated:

$$\varepsilon_{\text{cd},\infty} = k_{\text{h}} \cdot \varepsilon_{cd,0} = 0.423\ ‰$$

- Autognenous shrinkage loss

This loss can be also be calculated using NEN-EN 1992-1-1 and follows quite straightforwardly from:

$$\varepsilon_{\text{ca}}(\infty) = 2.5(f_{\text{ck}} - 10) \cdot 10^{-6} = 2.5(35 - 10) \cdot 10^{-6} = 0.062\ ‰$$

- Relaxation loss

The final considered pre-stress loss is relaxation loss. With ρ_{1000}=2.5 % this can be calculated, again using NEN-EN 1992-1-1 formula 3.29 and using pre-stress strands of class 2 as presribed by ROK. For this calculation the length of the bridge is again discretized such that for all dx:

$$\Delta\sigma_{PR} = 0.66\sigma_{Pi}\rho_{1000}e^{9.1\mu}\left(\frac{t}{1000}\right)^{0.75(1-\mu)} \cdot 10^{-5}$$

Using:

$$\mu = \frac{\sigma_{Pi}}{f_{pk}}$$

The maximum relaxation loss $\Delta\sigma_{PR,max}$ ilustratively is computed as 60.9 MPa, assuming t=500000 h using 3.3.2 (8).

Incorporating all these losses in the internal stress of the pre-stress tendon over the length of the bridge, figure 21 can be plotted finalizing the prestress losses.

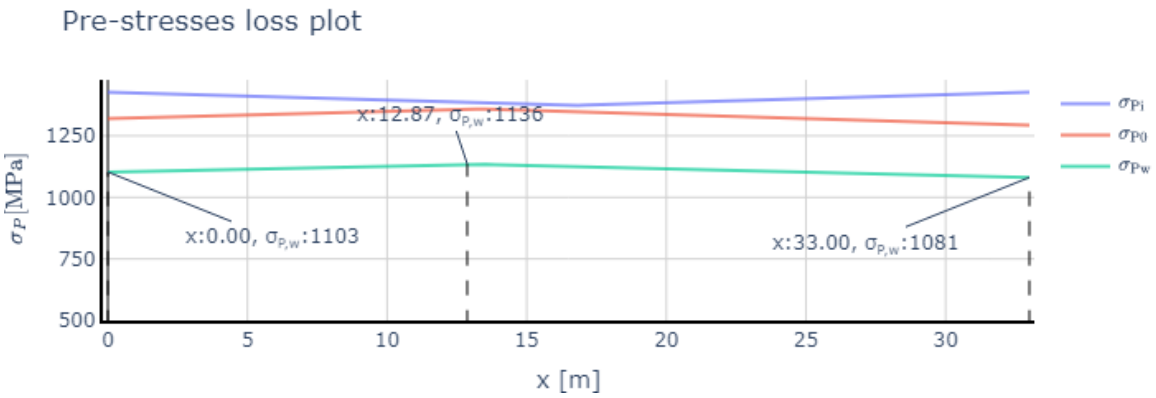

Figure 21: The prestress stresses over the length profile of the bridge.

Combining this loss plot and the pre-stress profile from figure 21 the loads shown in the report will be found

LC7.1 Wind loads

This section covers the calculations made for the windloads on the bridge in accordance with NEN-EN 1991-1-4.

The bridge is located in windarea I, and has terrain category 0. Next to that it is important to note that the free height of the bridge to ground level is 6 m.
Refering to NEN-EN 1991-1-4 some values for the variables can already be determined:

- The height of the traffic band $h_{traffic}$=4 m
- Wind direction factor c_{dir}=1.00 (NB. 4.2 (2))
- Seasonal factor c_{season}=1.00 (NB. 4.2 (2))
- Annual exceedance probability p=0.01 (NB. 4.2 (2))
- Orographic factor c_0=1 (4.3.1 (1), assumption)
- Maximum height for these calculations z_{max}=200 m (NB. 4.3.2 (1))
- Turbulence factor k_l=1 (NB. 4.4 (1))
- Volumetric weight of air ρ=1.25 kg/m^3 (NB. 4.5 (1))
- Reduced fundamental base wind speed $v^{**}_{b,0}$=25 m/s (NB. 8.1 (5))
- Building factor $c_s c_d$=1 (8.2 (1))
- Force coefficient z-direction $c_{f,z}$=1 (NB. 8.3.3 (1))

Now the steps outlined in NEN-EN 1991-1-4 + NB can be followed to calculate the windloads on the bridge.
The total height of the bridge can be calculated according to 8.3.1 (1):

$$d_{\text{tot}} = \max(h_{\text{girder}}, h_{\text{floor}} + t_{\text{ballast}} + h_{\text{sleeper}} + h_{\text{rail}} + h_{\text{traffic}}) \\ = \max(2.50, 0.50 + 1.01 + 0.22 + 0.16 + 4.00) = 5.19 \text{ m}$$

$c_{b,0}$=29.5 m/s can be found in table NB.1 and the values for K=0.200 and n=0.5 can be found in table NB.2. After that c_{prob} can be calculated:

$$c_{\text{prob}} = \left(\frac{1 - K \cdot \ln(-\ln(1-p))}{1 - K \cdot \ln(-\ln(0.98))}\right)^n = \left(\frac{1 - 0.200 \cdot \ln(-\ln(1-0.01))}{1 - 0.200 \cdot \ln(-\ln(0.98))}\right)^{0.5} = 1.04$$

Base wind speed v_b=30.64 m/s can now be calculated via 4.1 and 4.2:

$$v_{\text{b}} = c_{\text{dir}} \cdot c_{\text{season}} \cdot v_{\text{b,0}} \cdot c_{\text{prob}}$$

For the calculation of the reduced windspeed F^{**}_w, $v^{**}_{b,0}$=25.00 m/s should be used for calculating the windspeed and the resulting forces.
z_{min}=1.000 m and z_0=0.005 m can now be gathered from NB.3 - 4.1, such that k_r can be calculated with NB form 4.5:

$$k_{\text{r}} = 0.19 \cdot \left(\frac{z_0}{0.05}\right)^{0.07} = 0.19 \cdot \left(\frac{0.005}{0.05}\right)^{0.07} = 0.16$$

The reference height for the wind forces is taken as z = h_{ground}+0.5h_{girder}=6.00+0.5*2.50 = 7.25 m.

The roughness factor and additionally the average windspeed can now be calculated using formula 4.4.

$$c_{\mathrm{r}}(z) = k_{\mathrm{r}} \cdot \ln(\frac{z}{z_0}) = 0.16 \cdot \ln(\frac{7.25}{0.01}) = 1.18$$

$$v_{\mathrm{m}}(z) = c_{\mathrm{r}}(z) c_0(z) v_{\mathrm{b}} = 1.18 \cdot 1.00 \cdot 30.64 = 36.06\ \mathrm{m/s}$$

In similar fashion the turbulence intensity factor $\mathrm{l_v}$ can be calculated based on form. 4.7.

$$l_{\mathrm{v}}(z) = \frac{k_{\mathrm{l}}}{c_0(z) \cdot \ln(\frac{z}{z_0})} = \frac{1.00}{1.00 \cdot \ln(\frac{7.25}{0.01})} = 0.14$$

The base hydrostatic pressure $\mathrm{q_b}$ can be calculated using formula 4.10 and the following extreme hydrostatic pressure $\mathrm{q_p}$ from 4.8.

$$q_{\mathrm{b}} = \frac{1}{2} \cdot \rho v_{\mathrm{b}}^2 = \frac{1}{2} \cdot 1.25 \cdot 30.64^2 = 0.59\ \mathrm{kN/m^2}$$

$$q_{\mathrm{p}} = (1 + 7 l_{\mathrm{v}}(z)) \frac{1}{2} \cdot \rho v_{\mathrm{m}}(z)^2 = (1 + 7 \cdot 0.14) \cdot \frac{1}{2} \cdot 1.25 \cdot 36.06^2 = 1.59\ \mathrm{kN/m^2}$$

The wind load factor in x direction $\mathrm{c_{f,x}}$ can now be determined to be 2.02 following from fig. 8.3. $\mathrm{A_{ref,x}}$, $\mathrm{A_{ref,z}}$ can be determined by fig. 8.3 and fig. 8.6 respectively.

$$A_{\mathrm{ref,x}} = d_{\mathrm{total}} \cdot l_{\mathrm{bridge}}$$

$$A_{\mathrm{ref,x}} = b_{\mathrm{total}} \cdot l_{\mathrm{bridge}}$$

Finally the wind forces can be calculated using formula 5.3. The loads calculated from this formula are presented in the report. The loads denoted with ** represent reduced loads calculated with $\mathrm{v^{**}_{b,0}}$.

$$F_{\mathrm{w},i} = c_{\mathrm{s}} c_{\mathrm{d}} \cdot c_{\mathrm{f},i} \cdot q_{\mathrm{p}}(z_{\mathrm{e}}) A_{\mathrm{ref},i}$$

LC9.1.1 Train loads model LM71 M

This section covers the calculations made for the train load model LM71 in accordance with NEN-EN 1992-1. The load model as given in the eurocode is shown in figure 22.

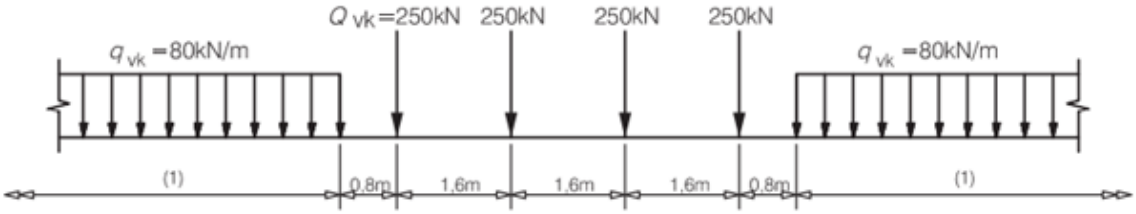

Figure 22: Load model LM71 as given in NEN-EN 1992-1

These loads need to be multiplied with α which is 1.21 according to the national annex and dynamic factor Φ_2 for carefully maintained rail. This factor can be calculated via formula 6.4 from NEN-EN 1991-2 where L_Φ can be calculated as twice the span of the deck from table 6.2 4.3.

$$\Phi_2 = \min(\max(\frac{1.44}{\sqrt{L_\Phi} - 0.2} + 0.82; 1); 1.67) = 1.27$$

The loads may be divided by the effective with over which they are spread, which is calculated in the main report. Next to that the point loads in the middle are assumed to be evenly destributed for middle part of the load.

The position of the load on the bridge has been choossen by running an influence line analysis which shows the position of the load which gives the highest possible moment at mid-span given in figure 23. Next to that also an excentricity e calculated with NEN-EN 1991-2 figure 6.3 is introduced for the LM71 loads. However the effect of this excentricity is not significant.

$$e = \frac{r}{18} = \frac{1435}{18} = 79.7 \text{ mm}$$

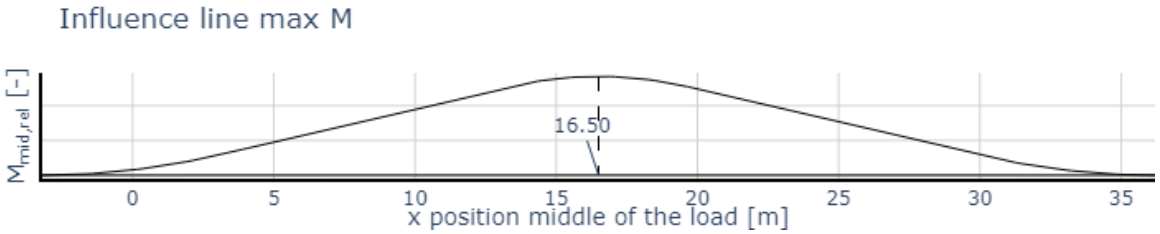

Figure 23: Influence line LM71 load model for the bridge, maximum moment

LC9.1.2 Train loads model LM71 V

The load resulting in the highest shear force is calculated in the same manner and results in the following influence line 24.

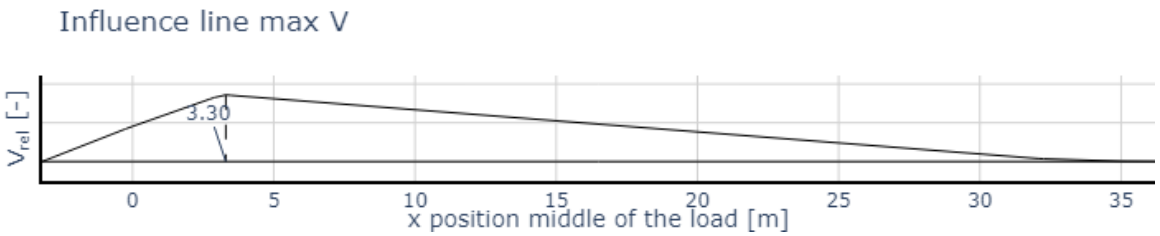

Figure 24: Influence line LM71 load model for the bridge, maximum shear force

LC9.3.1 Train loads model SW/2 M

This section covers the calculations made for the train load model SW/2 in accordance with NEN-EN 1992-1. The load model as given in the eurocode is shown in figure 25.

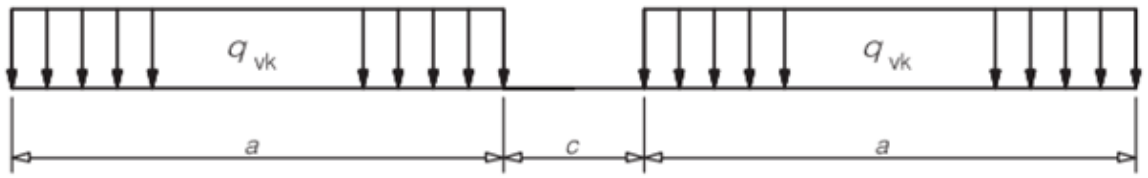

Figure 25: Load model SW as given in NEN-EN 1992-1

The values of a, c and q_{vk} are given as 25 m, 7 m, 150 kN/m respectively. Loads for SW/2 should not be multiplied with factor α and dynamic factor Φ_2.
Just like before these loads are spread over the effective width and the position has once again been choossen using influence lines. Figure 26 shows the influence line for max mid-span moment for this load model.

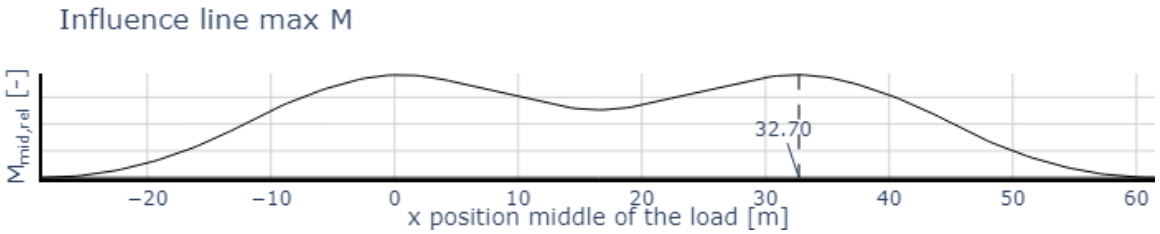

Figure 26: Influence line SW/2 load model for the bridge, maximum moment

LC9.3.2 Train loads model SW/2 V

In the same manner the influence line for the maximum shear force is displayed in figure 27.

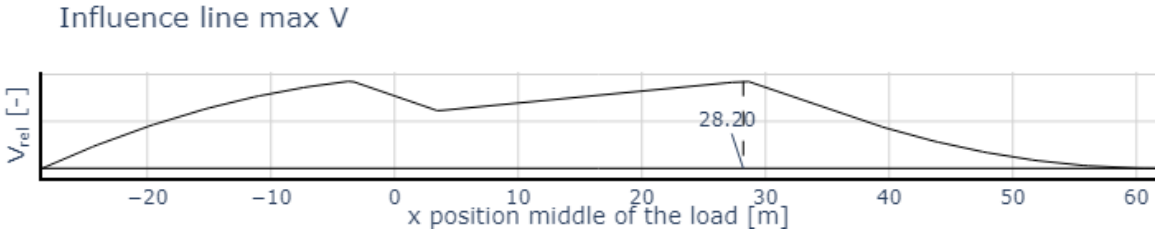

Figure 27: Influence line SW/2 load model for the bridge, maximum shear force

Annex D: Load combinations

The limit states ULS, SLS-Characteristic, SLS-Frequent, SLS-Quasi Permanent are considered in the FEM model.
The decisive load combination for ULS is the least favourable of NEN-EN 1990 form. 6.10a, 6.10b:

$$\sum_{j\geq 1} \gamma_{G,j} G_{k,j} + \gamma_P P + \gamma_{Q,1} \Psi_{0,1} Q_{k,1} + \sum_{i>1} \gamma_{Q,i} \Psi_{0,i} Q_{k,i}$$

$$\sum_{j\geq 1} \xi_j \gamma_{G,j} G_{k,j} + \gamma_P P + \gamma_{Q,1} Q_{k,1} + \sum_{i>1} \gamma_{Q,i} \Psi_{0,i} Q_{k,i}$$

For SLS-Characteristic the desicive load combination is governed by 6.14b:

$$\sum_{j\geq 1} G_{k,j} + P + Q_{k,1} + \sum_{i>1} \Psi_{0,i} Q_{k,i}$$

And for SLS-Frequent the desicive load combination is governed by 6.15b:

$$\sum_{j\geq 1} G_{k,j} + P + \Psi_{1,1} Q_{k,1} + \sum_{i>1} \Psi_{2,i} Q_{k,i}$$

Finally for SLS-Quasi Permanent the desicive load combination is governed by 6.16b:

$$\sum_{j\geq 1} G_{k,j} + P + \sum_{i\geq 1} \Psi_{2,i} Q_{k,i}$$

For the load combinations it is important to note that the bridge is CC3 and it only features one rail, the gamma factors are shown in table 7

$\gamma_{G,j,sup}$ 6.10a	1.40
$\gamma_{G,j,sup}$ 6.10b	1.25
$\gamma_{G,j,inf}$	0.90
$\gamma_{G,i}$ Train load gr16, gr17, gr26, gr27	1.25
$\gamma_{G,i}$ Train load other groups	1.50
$\gamma_{G,i}$ Wind load	1.65
$\gamma_{G,i}$ Other variable loads	1.65

Table 7: γ factors from NEN-EN 1990 Table NB.17

The Ψ factors from NEN-EN 1990 table A2.3 can be translated to the different limit states as shown in tables 8 - 11:

	LM71				SW/2	
Load combination	gr11	gr12	gr13	gr14	gr16	gr17
LC1 Permanent loads	1.00					
LC4 Other variable loads	0.80					
LC7.1 Wind loads	0.75			0.75		
LC7.2 Reduced wind loads	1.00			1.00		
LC9.1.1 Train loads model LM71 M	0.80		0.40			
LC9.3.1 Train loads model SW/2 M					0.80	

Table 8: Ψ factors for form. 6.10a

	LM71				SW/2		Wind			
Load combination	gr11	gr12	gr13	gr14	gr16	gr17	gr11	gr12	gr14	gr15
LC1 Permanent loads	1.00									
LC4 Other variable loads	0.80									
LC7.1 Wind loads	0.75			0.75			1.00			
LC7.2 Reduced wind loads	1.00			1.00			1.00			
LC9.1.1 Train loads model LM71 M	1.00		0.50				0.80		0.40	
LC9.3.1 Train loads model SW/2 M					1.00					

Table 9: Ψ factors for form. 6.10b and 6.14b

	LM71				SW/2		Wind	Wind deflection			
Load combination	gr11	gr12	gr13	gr14	gr16	gr17	force	gr11	gr12	gr14	gr15
LC1 Permanent loads	1.00										
LC4 Other variable loads											
LC7.1 Wind loads							0.50				
LC7.2 Reduced wind loads											
LC9.1.1 Train loads model LM71 M	0.80		0.40					1.00		0.50	
LC9.3.1 Train loads model SW/2 M					0.80						

Table 10: Ψ factors for form. 6.15b

Load combination	Quasi-permanent
LC1 Permanent loads	1.00
LC4 Other variable loads	
LC7.1 Wind loads	
LC7.2 Reduced wind loads	
LC9.1.1 Train loads model LM71 M	
LC9.3.1 Train loads model SW/2 M	

Table 11: Ψ factors for form. 6.16b

From these factors the decisive load combinations can be summarized as shown in tables 12 - 16. The wind and train loads are exclusive load cases, meaning that e.g. both wind loads can not be present at the same time.

Load combination	gr11 LM71	gr16 SW/2	gr17 SW/2
LC1 Permanent loads	1.40		
LC4 Other variable loads	1.32		
LC7.1 Wind loads	1.24		
LC7.2 Reduced wind loads	1.65		
LC9.1.1 Train loads model LM71 M	1.20		
LC9.3.1 Train loads model SW/2 M		1.00	

Table 12: ULS 6.10a

Load combination	gr11 LM71	gr16 SW/2	gr17 SW/2	gr11 Wind
LC1 Permanent loads	1.25			
LC4 Other variable loads	1.32			
LC7.1 Wind loads	1.24			1.65
LC7.2 Reduced wind loads	1.65			1.65
LC9.1.1 Train loads model LM71 M	1.50			1.20
LC9.3.1 Train loads model SW/2 M		1.25		

Table 13: ULS 6.10b

Load combination	gr11 LM71	gr16 SW/2	gr17 SW/2	gr11 Wind
LC1 Permanent loads	1.00			
LC4 Other variable loads	0.80			
LC7.1 Wind loads	0.75			1.00
LC7.2 Reduced wind loads	1.00			1.00
LC9.1.1 Train loads model LM71 M	1.00			0.80
LC9.3.1 Train loads model SW/2 M		1.00		

Table 14: SLS 6.14b

Load combination	gr11 LM71	gr16 SW/2	gr17 SW/2
LC1 Permanent loads	1.00		
LC4 Other variable loads			
LC7.1 Wind loads			
LC7.2 Reduced wind loads			
LC9.1.1 Train loads model LM71 M	0.80		
LC9.3.1 Train loads model SW/2 M		0.80	

Table 15: SLS 6.15b

Load combination	Quasi-permanent
LC1 Permanent loads	1.00
LC4 Other variable loads	
LC7.1 Wind loads	
LC7.2 Reduced wind loads	
LC9.1.1 Train loads model LM71 M	
LC9.3.1 Train loads model SW/2 M	

Table 16: SLS 6.16b

Annex E: ULS Girder stirrup calculations

This section will feature the calculation of the stirrups of the girder in ULS. The angle of θ is 21.8°.

Torsion

The decisive torsional moment T_{Ed} in the beam follows from the FEM results and is: 1364 kNm.
For determining the shear stresses the effective width t_{eff} should first be calculated according to NEN-EN 1992-1-1 figure 6.11:

$$t_{\text{eff}} = \min(W_{\text{gir}} \cdot 0.5; \frac{A_{\text{gir}}}{u_{\text{gir}}}) = 140 \text{ mm}$$

Where u_{gir}=8000 mm, is the perimeter of the girder.

With the effective effective width A_k as described in NEN-EN 1992-1-1 figure 6.11 can be calculated.

$$A_{\text{k}} = (h_{\text{gir}} - t_{\text{eff}}) \cdot (W_{\text{gir}} - t_{\text{eff}}) = 3209878 \text{ mm}^2$$

The required area of longitudinal reinforcement required for this torsion $A_{sl,T,req}$ can be calculated with formula 6.28.

$$A_{\text{sl,T,req}} = \frac{u_{\text{k}} T_{\text{Ed}} \cot(\theta)}{2 A_{\text{k}} f_{\text{yd}}} = 8420 \text{ mm}^2$$

Using u_k = 6881 mm, the perimeter of A_k.
The shear stress τ_T due to torsion can be calculated using formula 6.26.

$$\tau_{\text{T}} = \frac{T_{\text{Ed}}}{2 A_{\text{k}} t_{\text{eff}}} = 1.52 \text{ MPa}$$

Using these results and formula 6.27 an equivalent shear force $V_{Ed,T}$ on the vertical ribs can be calculated.

$$V_{\text{Ed,T}} = \tau_{\text{T}} t_{\text{eff}} z_{\text{y}} = 501 \text{ kN}$$

Using z_y=h_{gir}-t_{eff}=2360 mm.
Finally the required shear reinforcement for torsion in the vertical ($A_{sw,T}$) and horizontal ($A_{sw,T,hor}$) stirrups parts can be calculated using 6.8.

$$A_{\text{sw,T,req}} = \frac{V_{\text{Ed,T}}}{z f_{\text{yd}} \cot(\theta)} = 212 \text{ mm}^2$$

$$A_{\text{sw,T,hor,req}} = \frac{T_{\text{Ed}}}{2 A_{\text{k}} f_{\text{yd}} \cot(\theta)} = 196 \text{ mm}^2$$

Shear

The decisive shear force V_{Ed} in the beam follows from the FEM results and is: 3547 kN. Continuing from the torsion results, the maxium shear force in a wall with thickness t_{eff} in the cross-section can be calculated. It is assumed that 60% of the shear force will be transfered by the middle stirrup and the other 40% will be distributed to the outside walls, where the shear is also present:

$$V_{\text{Ed,max}} = V_{\text{Ed}} \cdot 0.2 + V_{\text{Ed,T}} = 1210708 \text{ kN}$$

To check if calculated stirrups are needed the check $V_{Ed,max} < V_{Rd,c}$ using formula 6.4:

$$V_{\text{Rd,c}} = \frac{Ib_{\text{w}}}{S}\sqrt{f_{\text{ctd}}^2 + \alpha_{\text{l}}\sigma_{\text{cp}}f_{\text{ctd}}} = 536811 \text{ kN}$$

Where α_l=1 and σ_P is calculated as:

$$\sigma_{\text{cp}} = \frac{\sigma_{\text{Pw}}A_{\text{P}}}{A_{\text{gir}}} = 4.96 \text{ MPa}$$

From this we can conclude that $V_{Ed,max} > V_{Rd,c}$ and the assumption that stirrups are needed is justified. The required stirrup area per zone can be calculated, again using 6.8:

$$A_{\text{sw,I,req}} = \frac{0.2V_{\text{Ed}}}{zf_{\text{yd}}\cot(\theta)} = 300 \text{ mm}^2$$

$$A_{\text{sw,II,req}} = \frac{0.6V_{\text{Ed}}}{zf_{\text{yd}}\cot(\theta)} = 899 \text{ mm}^2$$

$$A_{\text{sw,III,req}} = \frac{0.2V_{\text{Ed}}}{zf_{\text{yd}}\cot(\theta)} = 300 \text{ mm}^2$$

Suspension force and fixed end moment

For the calculation of the hanging moment and suspension forces NSRL1015 is used as guideline. The suspension force and fixed end moment of the floor acting on the girder cause tension stresses in the cross-section as shown in figure 28.

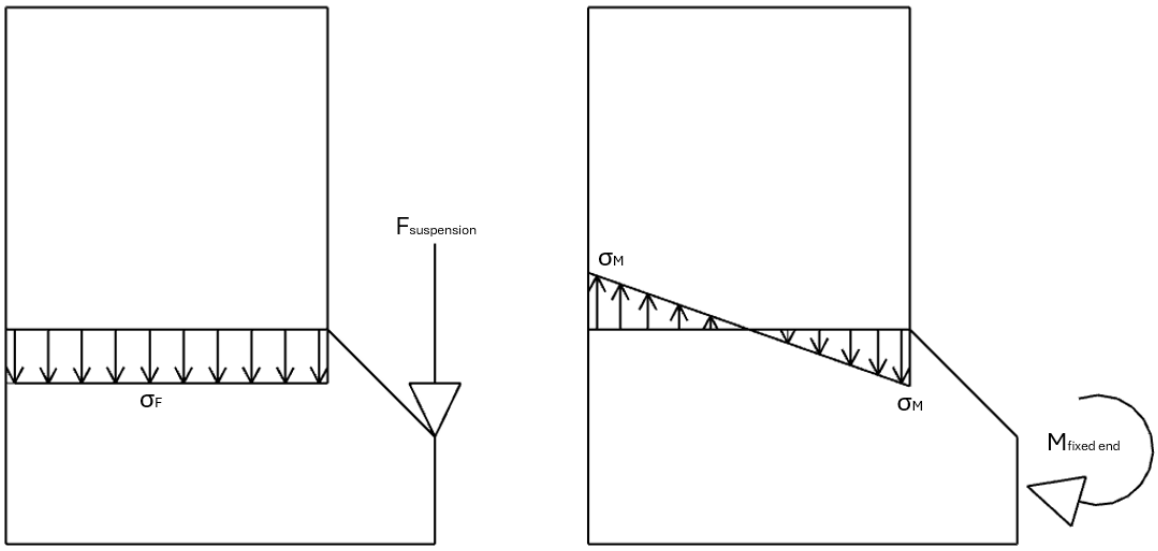

Figure 28: Stress distribution in cross-section

These stresses need to resisted by stirrups in the girder. Because the critical line for the connection of the girder and the floor is along the top of the haunch. This way only the load that needs to be carried by the top part of the girder needs to be accounted for because this needs to be carried to the top part of the cross-section. This is translated to a reduction factor based on the area of the cross-section, as described in NSRL1015.

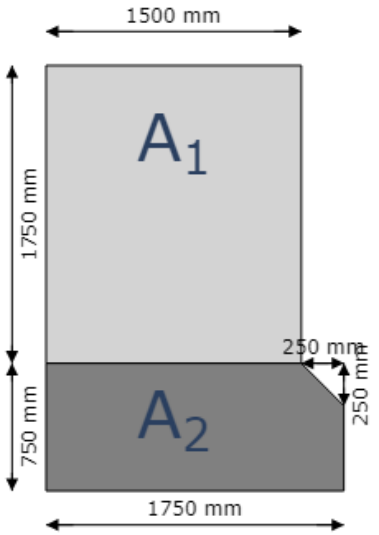

Figure 29: Area's used for reduction factor

$$\alpha_A = \frac{A_1}{A_1 + A_2} = \frac{2625000}{3906250} = 0.67$$

For the maximum suspension force acting on a girder it should be incorporated that the decisive train load SW/2 does not act in the middle of the floor, rather at x = 3.4 m, as shown in figure 30. This means that this load should be distributed to the right girder for the maximum resulting force.

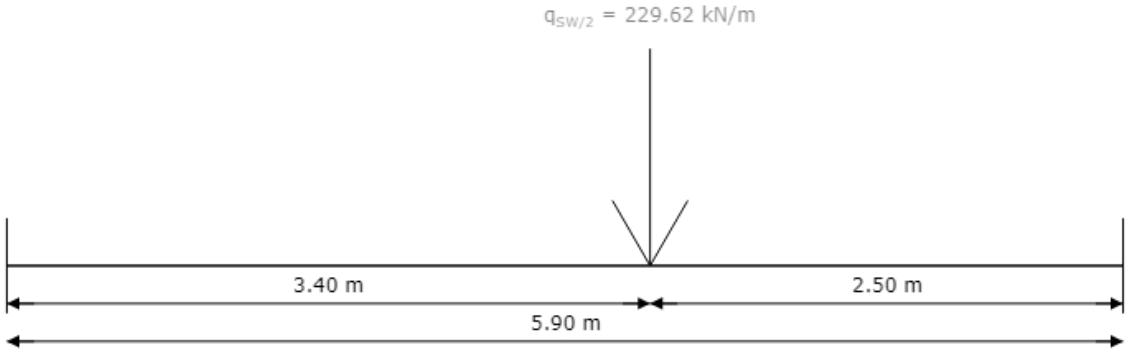

Figure 30: Position of the train load as seen on the cross-section of the floor

$$q_{\text{SW/2}} = 150\alpha\phi_2 = 150 \cdot 1.21 \cdot 1.27 = 230 \text{ kN/m}$$

$$F_{\text{SW/2}} = \frac{q_{\text{SW/2}}a}{a + 2 \cdot \frac{1}{2} \cdot 2.50}\frac{3.40}{5.90} = 120 \text{ kN/m}$$

Using the length of the load model SW/2 a = 25 m. The self-weight of the bridge and dead loads of the train infrastructure can be divided by 2 to find F_G = 73 kN/m. Incorporating the load factors to find the suspension force:

$$F_{\text{sus}} = \max(1 \cdot F_{\text{SW/2}} + 1.4 \cdot F_{\text{G}}; 1.25 \cdot F_{\text{SW/2}} + 1.25 \cdot F_{\text{G}}) = 241 \text{ kN/m}$$

The fixed end moment can be calculated using the structural model in figure 30, conservatively assuming fully clamped boundary conditions.

$$M_{\text{SW/2}} = \frac{q_{\text{SW/2}} \cdot 3.4^2 \cdot 2.5}{5.9} = 396 \text{ kNm/m}$$

Next to that the suspension force also causes a moment:

$$M_{\text{sus}} = F_{\text{G}} \cdot \frac{1}{2} W_{\text{girder}} = 79 \text{ kNm/m}$$

The maximum fixed end moment can now be calculated as:

$$M_{\text{fix}} = \max(1 \cdot M_{\text{SW/2}} + 1.4 \cdot M_{\text{sus}}; 1.25 \cdot M_{\text{SW/2}} + 1.25 \cdot M_{\text{sus}}) = 241 \text{ kNm/m}$$

The required area of the reinforcement can now be calculated according to the stresses shown in figure 28.

$$A_{\text{sw,F}} = \frac{\alpha_{\text{A}} F_{\text{sus}}}{f_{\text{yd}}} = 374 \text{ mm}^2$$

$$A_{\text{sw,M}} = \frac{\alpha_{\text{A}} M_{\text{fix}}}{z f_{\text{yd}}} = 1067 \text{ mm}^2$$

Using z = 0.9W_{gir} the total additional required area of stirrups in zone III can be calculated.

$$A_{\text{sw,III,req}} = A_{\text{sw,F}} + A_{\text{sw,M}} = 1440 \text{ mm}^2$$

Evaluation

The unity checks per zone of stirrups can now be calculated.

$$u.c_{sl,T} = \frac{A_{sl,T,req}}{A_{sl,T}} = \frac{8420}{9249} = 0.91$$

$$u.c_{sw,T,hor} = \frac{A_{sl,T,hor,req}}{A_{sl,T,hor}} = \frac{196}{565} = 0.35$$

$$u.c_{sw,I} = \frac{A_{sl,I,req}}{A_{sl,I}} = \frac{511}{565} = 0.90$$

$$u.c_{sw,II} = \frac{A_{sl,II,req}}{A_{sl,II}} = \frac{899}{905} = 0.99$$

$$u.c_{sw,III} = \frac{A_{sl,III,req}}{A_{sl,III}} = \frac{1952}{2011} = 0.97$$

Please note that the required longitudinal reinforcement for torsion at the bottom of the cross-section is added to the longitudinal reinforcement for moment and normal force.

Annex F: ULS Girder cross-section calculations

This section will feature the calculation for the girder in ULS. The decisive moment for the girder M_{Ed} = 21743 kNm.

Cross-sectional analysis

To calculate the moment resistance the stress and strain diagrams of the cross-section need to be determined. This is done with an automatic algorithm that solves the force equilibrium ΣF_h = - N_c + N_c + F_{Pw} + ΔF_P = 0 to find figures 31 and 32.

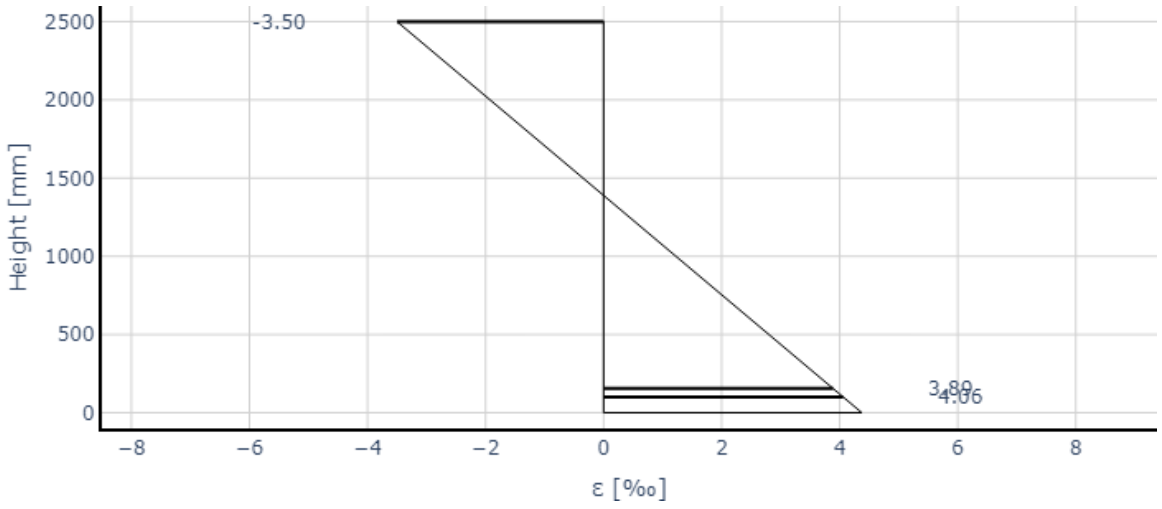

Figure 31: Strain diagram

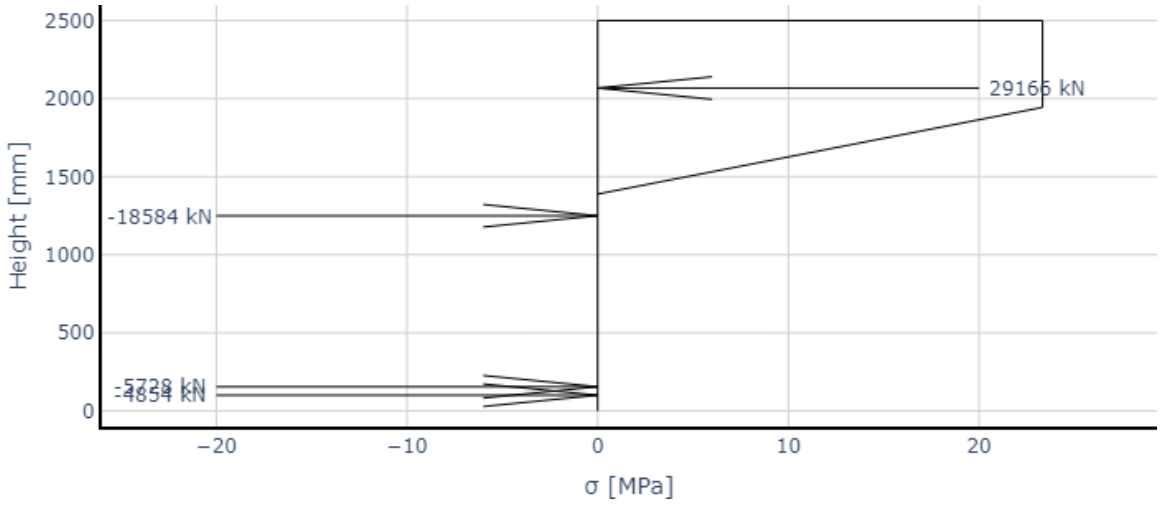

Figure 32: Stress diagram

To justify these diagrams the following calculations are made.

$$N_c = \alpha f_{cd} w_{gir} x_u = 29166 \text{ kN}$$

Here α = 0.75 and x_u = 1111 mm.
The force in the steel can be calculated using:

$$N_s = A_s \cdot \min(E_s \varepsilon_s; f_{yd}) = 4854 \text{ kN}$$

Where the area of longitudinal reinforcement required for torsion $A_{sl,T,req}$ = 1578.729608298077 mm^2 is subtracted from A_s and:

$$\varepsilon_s = \varepsilon_{cu} \frac{d_s - x_u}{x_u} = 4.06 \text{ ‰}$$

Using ε_{cu} = 3.50‰.
For the prestress force both the pre-stress force F_{Pw} and the force induced by the strain in the pre-stress ΔF_P are important. First F_{Pw} is calculated:

$$F_{Pw} = \sigma_{Pw} A_P = 18584 \text{ kN}$$

Now ΔF_P can be calculated:

$$\Delta\varepsilon_P = \varepsilon_{cu} \frac{d_P - x_u}{x_u} = 3.89 \text{ ‰}$$

$$\varepsilon_{P,tot} = \frac{F_{Pw}}{A_P E_P} + \Delta\varepsilon_P = 9.66 \text{ ‰}$$

$$\Delta F_{Pw} = \sigma_P(\varepsilon_P) A_P - F_{Pw} = 5728 \text{ kN}$$

Where σ_P is dependent on the strain of the pre-stress steel via the bilinear relationship\nIt can now be verfied that ΣF_h = 0. The moment resistance can now be calculated using:

$$e_{\mathrm{P}} = d_{\mathrm{P}} - \frac{1}{2}h_{\mathrm{gir}};\ e_{\mathrm{s}} = d_{\mathrm{s}} - \frac{1}{2}h_{\mathrm{gir}}$$

$$e_{\mathrm{c}} = \frac{1}{2}h_{\mathrm{gir}} - \beta x_{\mathrm{u}}$$

$$M_{\mathrm{Rd}} = N_{\mathrm{c}}e_{\mathrm{c}} + e_{\mathrm{s}}N_{\mathrm{s}} + \Delta F_{\mathrm{P}}e_{\mathrm{P}} = 35709\ \mathrm{kNm}$$

Finally the unity check can be calculated:

$$\mathrm{u.c}_{\mathrm{M,gir}} = \frac{M_{\mathrm{Ed}}}{M_{\mathrm{Rd}}} = \frac{21743}{35709} = 0.61$$

Compression zone height

NEN-EN 1992-1-1 NB 6.1 (9) describes the maximum height of the concrete compression zone of concrete girders:

$$\frac{x_u}{d} \leq \frac{500}{500 + f} = 0.30$$

Where f=1182 MPa is the weighted steel strength of the pre-stress and steel where the σ_{Pw} is subtracted from the pre-stress steel strength.
This is not satisfied as $x_u/d=0.47$.However the pre-stress can fictitiously be lowered to make sure this requirement is satisfied. It is important to note that M_{Ed} will increase when lowering pre-stress and M_{Rd} will decrease. When the pre-stress is lowered to 62 %, M_{Ed} becomes 28137 kNm. When also lowering A_P with this factor, the new distriubutions can be found:

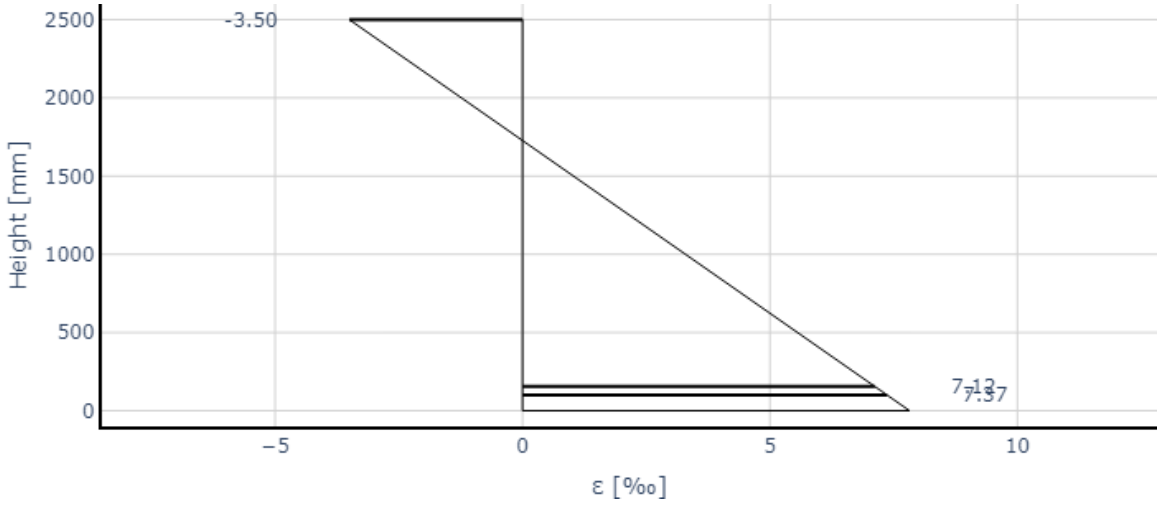

Figure 33: Strain diagram

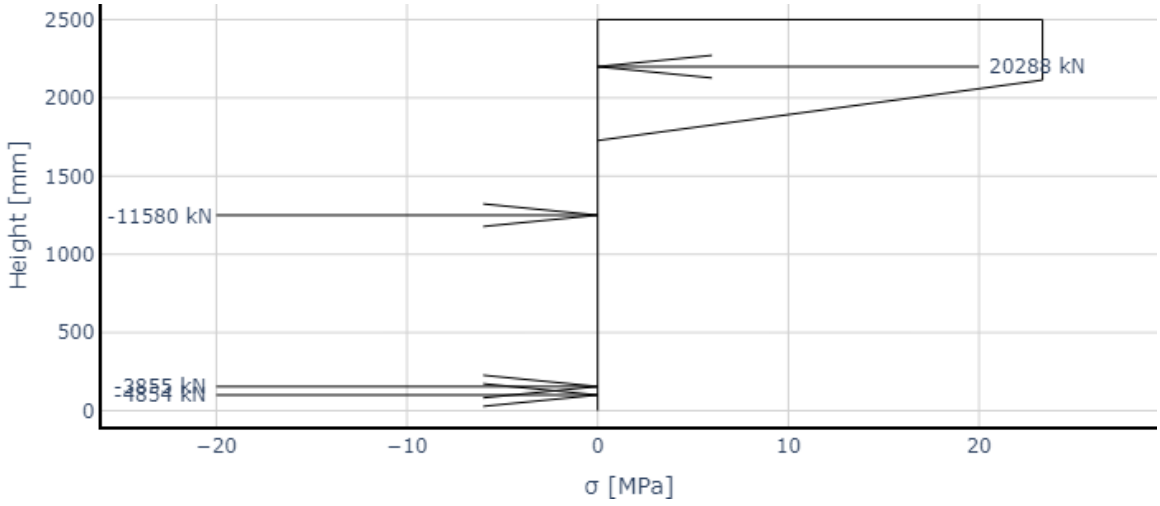

Figure 34: Stress diagram

Using the same equations as before it is obtained that:

$$M_{\text{Rd}} = N_{\text{c}} e_{\text{c}} + e_{\text{s}} N_{\text{s}} + \Delta F_{\text{P}} e_{\text{P}} = 29064 \text{ kNm}$$

Resulting in:

$$\text{u.c}_{\text{M,rot}} = \frac{M_{\text{Ed}}}{M_{\text{Rd}}} = \frac{28137}{29064} = 0.97$$

Also the maximum height of the compression zone is now sufficient:

$$\frac{x_{\text{u}}}{d} \leq \frac{500}{500 + f} = 0.33$$

$$0.33 \leq 0.33$$

Annex G: ULS Floor cross-section calculations

In this chapter the ULS calculations for the floor will be displayed.

y-direction

The decisive moment in the floor is at midspan: $M_yD+ = 569$ kNm/m. Again the stress-strain distribution can be determined given in figure 35 and 36, making sure that $\Sigma F_h = 0$.

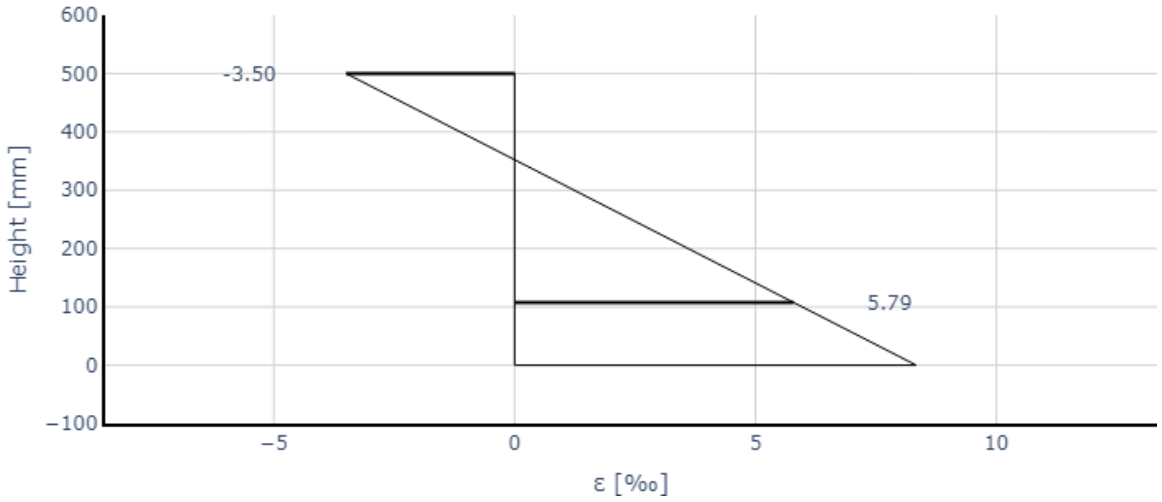

Figure 35: Strain diagram

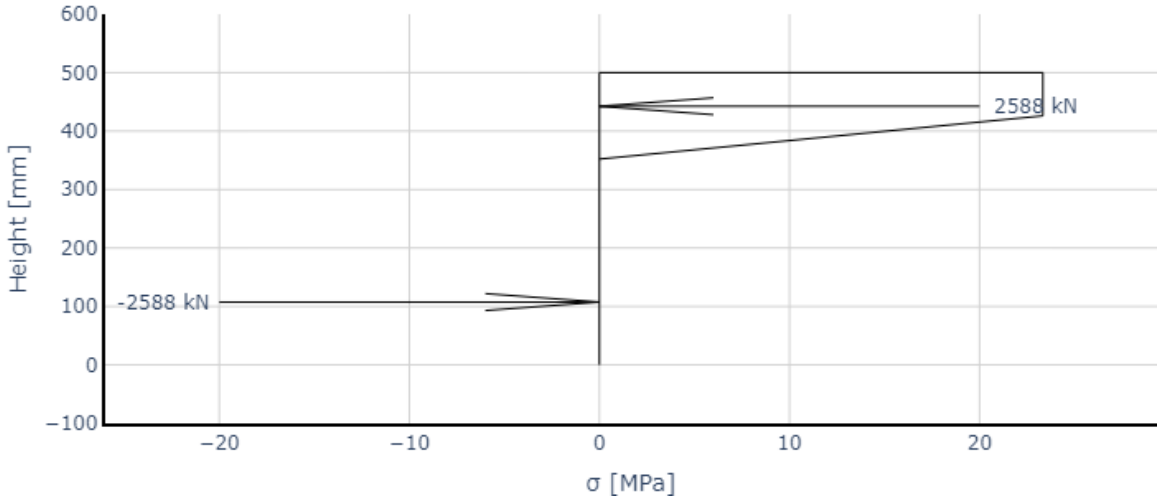

Figure 36: Stress diagram

The calculations for these diagrams are given below.

$$N_c = \alpha f_{cd} w_{gir} x_u = 2588 \text{ kN}$$

Here $\alpha = 0.75$ and $x_u = 148$ mm.
The force in the steel can be calculated using:

$$N_s = A_s \cdot \min(E_s \varepsilon_s; f_{yd}) = 2588 \text{ kN}$$

Where:

$$\varepsilon_s = \varepsilon_{cu} \frac{d_s - x_u}{x_u} = 5.79\ ‰$$

Using ε_{cu} = 3.50‰.
The moment capacity can be calculated using:

$$M_{Rd} = N_s z = 867\ \text{kNm}$$

Using $z = d_s - \beta x_u$.
Finally the unity check can be calculated:

$$\text{u.c}_{M,floor,y} = \frac{M_{Ed}}{M_{Rd}} = \frac{569}{867} = 0.66$$

x-direction

This whole calculation can be repeated for the reinforcement in longitudinal directon: M_xD+ = 200 kNm/m. be determined given in figure 37 and 38, making sure that ΣF_h.

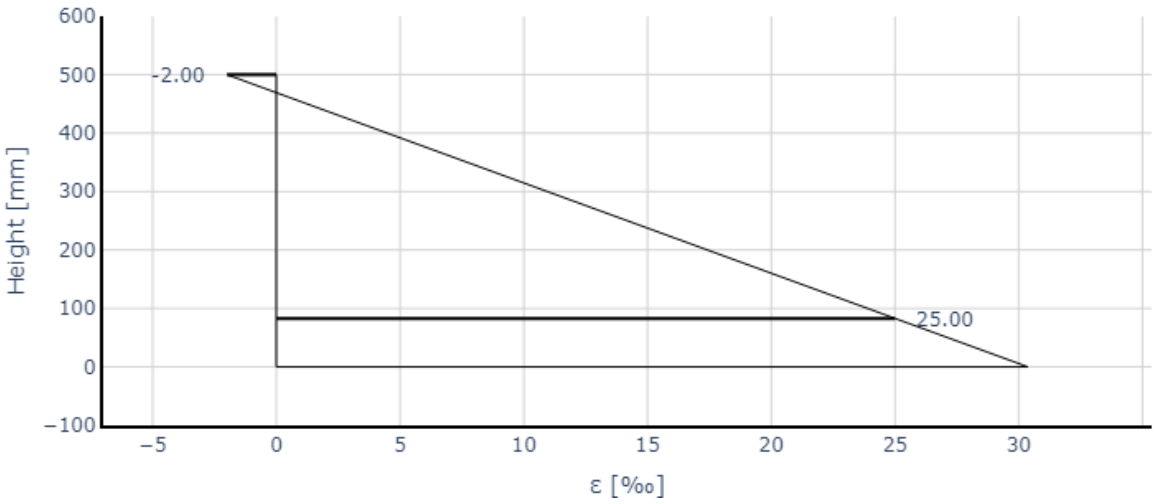

Figure 37: Strain diagram

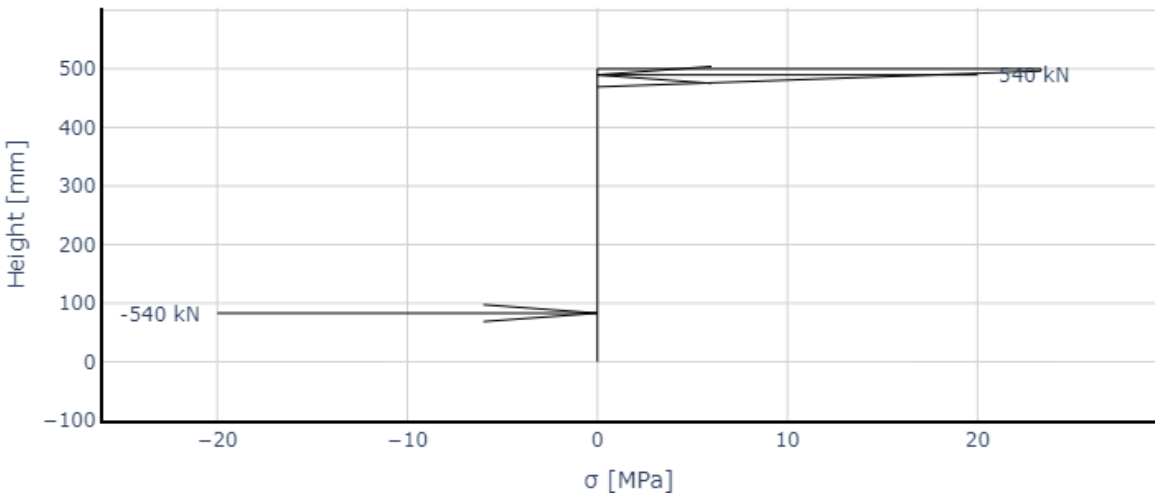

Figure 38: Stress diagram

The calculations for these diagrams are given below.

$$N_c = \alpha f_{cd} w_{gir} x_u = 540 \text{ kN}$$

Here α = 0.75 and x_u = 31 mm.
The force in the steel can be calculated using:

$$N_s = A_s \cdot \min(E_s \varepsilon_s; f_{yd}) = 540 \text{ kN}$$

Where:

$$\varepsilon_s = \varepsilon_{cu} \frac{d_s - x_u}{x_u} = 25.00 \text{ ‰}$$

Using ε_{cu} = 2.00‰.
The moment capacity can be calculated using:

$$M_{Rd} = N_s z = 220 \text{ kNm}$$

Using $z = d_s - \beta x_u$
Finally the unity check can be calculated:

$$\text{u.c}_{M,floor,y} = \frac{M_{Ed}}{M_{Rd}} = \frac{200}{220} = 0.91$$

Annex H: ULS Longitudinal shear calculations

In this chapter the ULS calculations for the longitudinal shear between the floor and the girder will be described according to the calculation method of NEN-EN 1992-1-1 6.2.4. This method calculates the longitudinal shear as:

$$v_{Ed} = \frac{\Delta F_d}{h_f \Delta x} = 0.57 \text{ MPa}$$

The maximum value that may be assumed for Δx is half the distance between the cross-section where the moment is 0 and the cross-section where the moment is at a maximum (6.2.4 (3)). In this case this means that Δx half the length of the span of the bridge. The other parameters are summarized in figure 39:

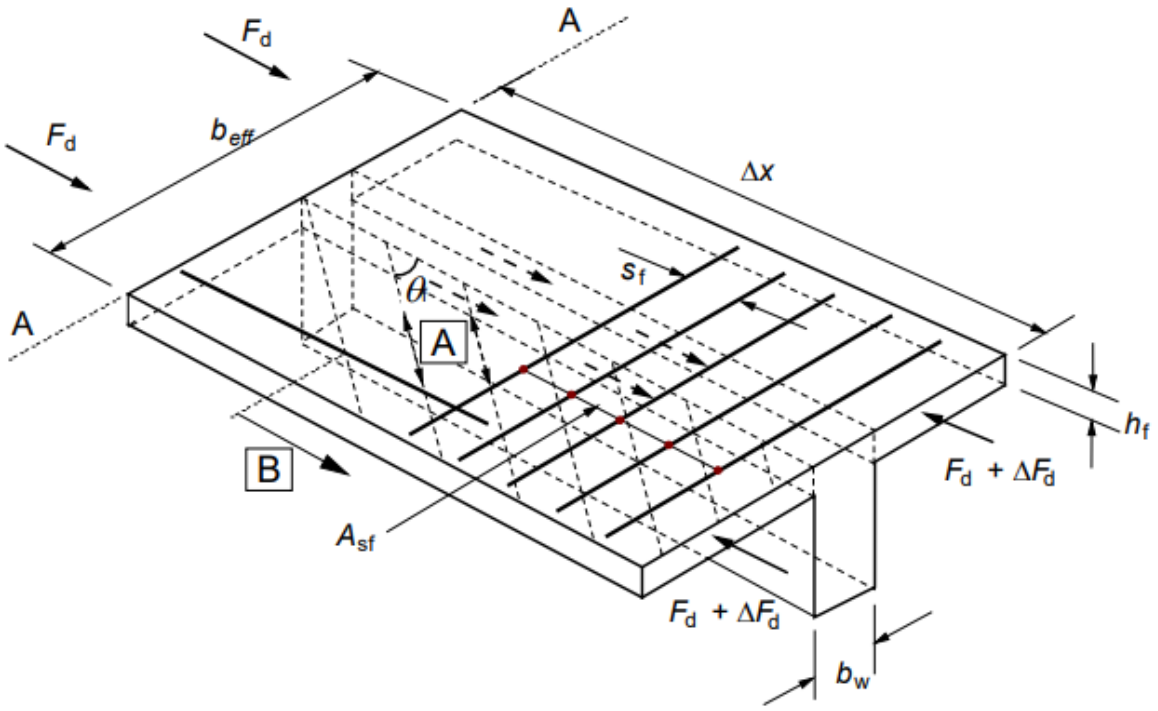

Figure 39: NEN-EN 1992-1-1 figure 6.7

The figure shows a T-girder however for a trough girder bridge one flange can be ignored. To obtain the maximum shear stress calculated above an automatic algorithm was used to find Δx = 0.25 m and ΔF_d = 71 kN, between the sections at x = 6.50 m and x = 6.75 m. The forces are obtained by integrated the 2D forces of the floor over the effective width of the floor on one side. To check if reinforcement is required the following check is performded:

$$v_{Ed} < k f_{ctd}; 0.57 < 0.59$$

This check is O.K. so no reinforcement is needed.

Annex I: ULS Splitting forces ends of deck

In this chapter the ULS calculations for the splitting reinforcement at the ends of the deck will be performed. A tension force in the ends of the deck is introduced due to the introduction of the prestress as shown in figure 40:

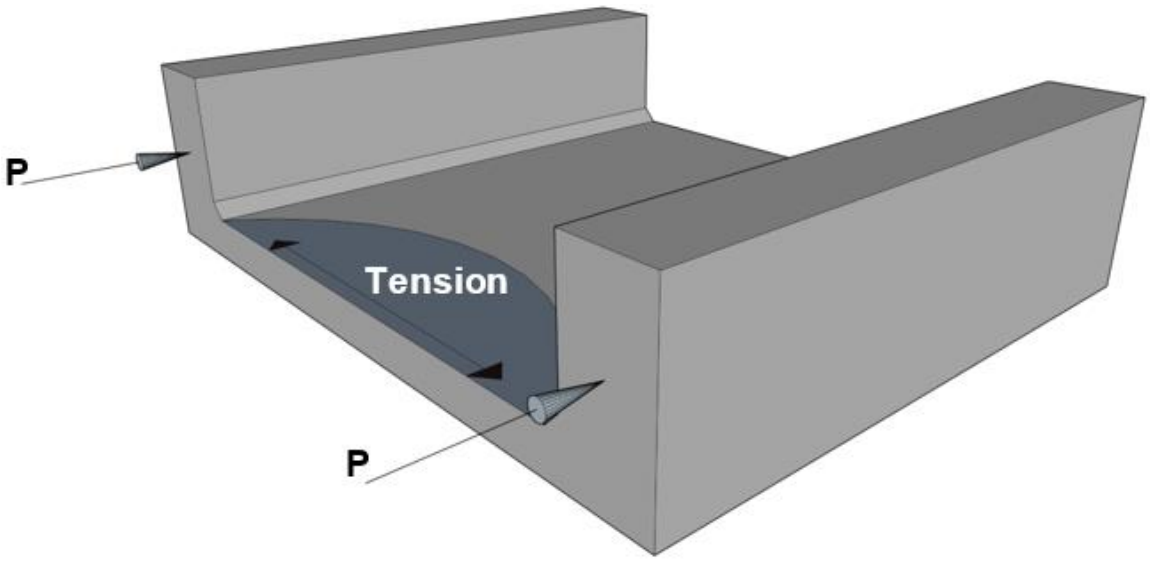

Figure 40: Splitting forces at the ends of the deck

To reinforce the bridge against these tension stresses, extra reinforcement is needed. The required reinforcement is calculated using a strut and tie model. First the equivalent stress in the whole bridge in the bernouilli zone at x = 4450 mm due to pre-stress is calculated.

$$\sigma_{\text{eq}} = \frac{2F_P}{A_{\text{P}}} = 3.36 \text{ MPa}$$

Using this stress the force in the girders and beam can be calculated:

$$F_{\text{floor/}} = \frac{1}{2}\sigma_{\text{eq}} A_{\text{floor}} = 4960 \text{ kN}$$

$$F_{\text{girder}} = \sigma_{\text{eq}} A_{\text{girder}} = 12609 \text{ kN}$$

With these values the STM shown in figure 41 can be obtained:

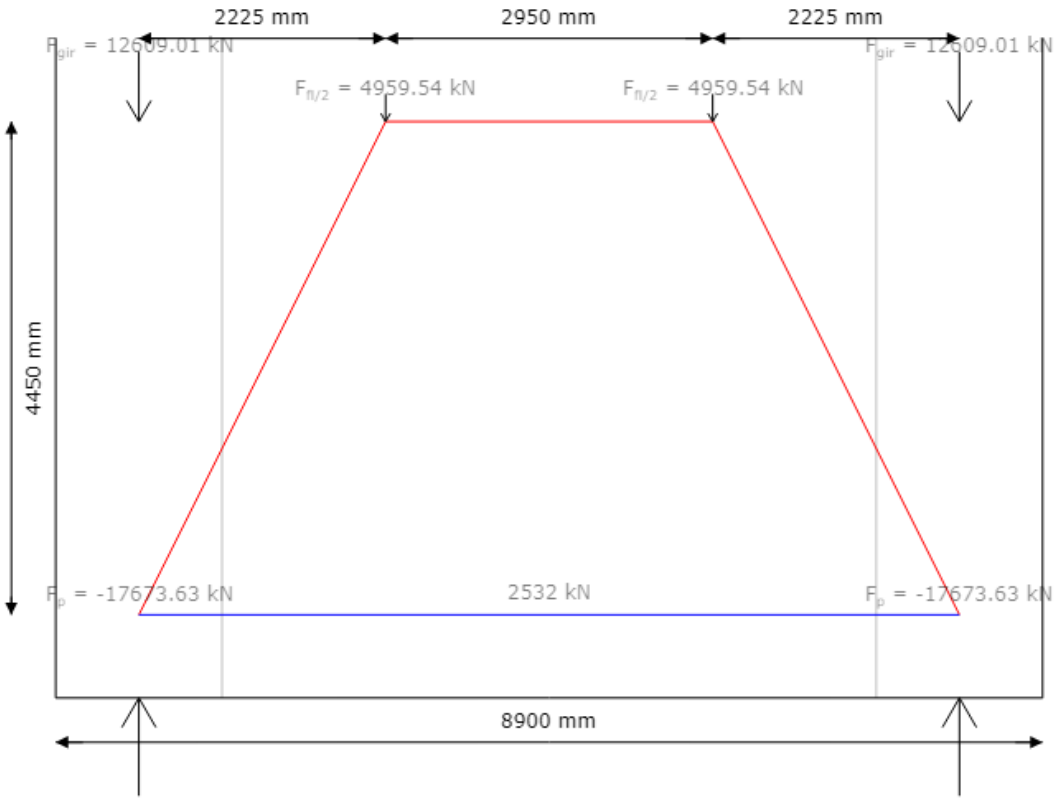

Figure 41: Strut and tie model splitting reinforcement

With the calculated force the stress in the splitting reinforcement can be calculated knowing that the designed splitting reinforcement is 8⌀32:

$$\sigma_{\text{spl}} = \frac{F_{\text{spl}}}{A_{\text{spl}}} = \frac{2532309}{6434} = 394 \text{ MPa}$$

Now the unity check can be calculated:

$$\text{u.c}_{\text{spl}} = \frac{\sigma_{\text{spl}}}{f_{\text{yd}}} = \frac{394}{434} = 0.91$$

Annex J: SLS Girder stress checks

This annex will show two SLS stresses checks for the girder.

Tension checks

The first check is an extra check required by OVS00030-6 as an amendment to NEN-EN 1992-1-1 7.3.1, which requires that:

1. In SLS-quasi: $\sigma_{ct} < 0$
2. In SLS-freq: $\sigma_{ct} < 0.5\, f_{ctk,0.05}$ and $\sigma_{ct} < 0.5\, f_{ctk,0.05}$
3. In SLS-char: $\sigma_{ct} < 0.5\, f_{ctk,0.05}$ and $\sigma_{ct} < 0.5\, f_{ctk,0.05}$

These stresses can be calculated using:

$$\sigma_{ct} = \frac{M_{Ed}}{W_{bot}} + \frac{N_{Ed}}{A_c}$$

Due to the pre-stress the axial force is always compressive. Now for each limit state the highest stress can be computed:

$$\sigma_{ct,quas} = \frac{M_{Ed,quas}}{W_{bot}} + \frac{N_{Ed,quas}}{A_c} = \frac{2641}{W_{bot}} + \frac{-15823}{A_t} = -2.17 \text{ MPa}$$

$$\sigma_{ct,quas} < 0.00$$

So ,the SLS-quas check is O.K.

$$\sigma_{ct,freq} = \frac{M_{Ed,freq}}{W_{bot}} + \frac{N_{Ed,freq}}{A_c} = \frac{10862}{W_{bot}} + \frac{-18649}{A_t} = -0.11 \text{ MPa}$$

$$\sigma_{ct,freq} < 1.10$$

So, the SLS-freq check is O.K.

$$\sigma_{ct,char} = \frac{M_{Ed,char}}{W_{bot}} + \frac{N_{Ed,char}}{A_c} = \frac{13232}{W_{bot}} + \frac{-18944}{A_t} = 0.59 \text{ MPa}$$

$$\sigma_{ct,char} < 1.10$$

So, the SLS-char check is O.K.

Compression checks

Next to the tension stress, the compressive stress in the bridge at t=0 should not exceed the compression strength. This check is performed in SLS-quasi permanent, because that is representative of the forces acting at t=0. The maximum compressive stress can be calculated similar like before looking at both the situation with maximum compressive force and max moment to find:

$$\sigma_c = -\frac{M_{Ed}}{W_{top}} + \frac{N_{Ed}}{A_c} = 5.27 \text{ MPa}$$

Concluding with the unity check:

$$\text{u.c}_{compr} = \frac{\sigma_c}{f_{cd}} = \frac{5.27}{23} = 0.23$$

Annex K: SLS Girder main tension stress

In this chapter the main tension stress in the girder will be calculated in accordance with NSRL1015, to limit crack formation at the haunch. The main stress will ocur just above the haunch at the inner wall of the girder and should be checked at 0.8d and 2d away from the bearing cross-sections. At x < 0.8d the forces are expected to be carried to the support directly and at x = 2d the shear force is expected to change sign. The location of the main tension stress is shown in figure 42.

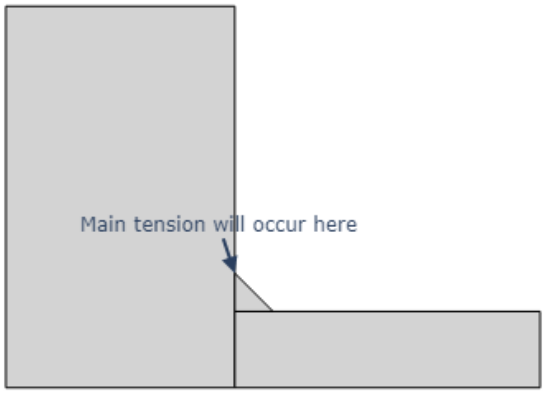

Figure 42: Location of main tension stress

The load combinations with both max V_z and max M_x and at both locations have been checked. The decisive combination is shown here at x = 31.10 m and with load combination: CO73 and effective width b_{eff} = 3704 mm. The main tension stress consists of thee components.

- σ_{xx} is the stress component caused normal force and moment by external loading and pre-stress
- σ_{zz} is the stress component caused by suspension forces and fixed end moments simillarly to how it was calculated for the stirrups
- τ is the stress component caused by torsion and mobile loads and shear force caused by external loading and pre-stress

These stresses are combined to find the main concrete tension stress.

σxx

First the stress the normal force and moment in the girder are obtained. The normal force in the girder is the normal force in the floor integrated over half the width of the floor plus the normal force in the girder. The moment M_{Ed} = 3727 kNm is obtained directly from the girder as the moment from the floor is already integrated.

$$N_{\text{tot}} = N_{\text{gir}} + N_{\text{x,floor}} = -15901 - 398 = -16299 \text{ kN}$$

The stresses due to normal force and moment can now be computed, with those stresses the stress at the haunch can be calculated. For this calculation the cross-sectional properties of half the cross-section of the whole bridge have been used to compute the stress for one girder.

$$\sigma_{\text{xx,N}} = \frac{N_{\text{tot}}}{A_{\text{bridge/2}}} = -3.10 \text{ MPa}$$

$$\sigma_{\text{xx,M}} = \frac{zM_{\text{y}}}{I_{\text{bridge/2}}} = -0.00 \text{ MPa}$$

Where z = -270 mm is the distance between the neutral line of the cross-section and the top of the haunch, such that:

$$\sigma_{\text{xx}} = \sigma_{\text{xx,N}} + \sigma_{\text{xx,M}} = -3.10 \text{ MPa}$$

σzz

σ_{zz} is caclculated similar to how the suspension and hanging forces were determined for the ULS girder calculations. From there it is obtained that N_{tot} = 193 kN. The moment is also calculated in the same way. However for the main tension stress only mobile loads should be considered as the other loads are present over the whole bridge length and will not cause the main tension stresses. In this way $M_{fixed\ end}$ = 589 kNm. The stress diagrams are shown in figure 43. Also the same reduction factor as for the stirrup calculation may be used.

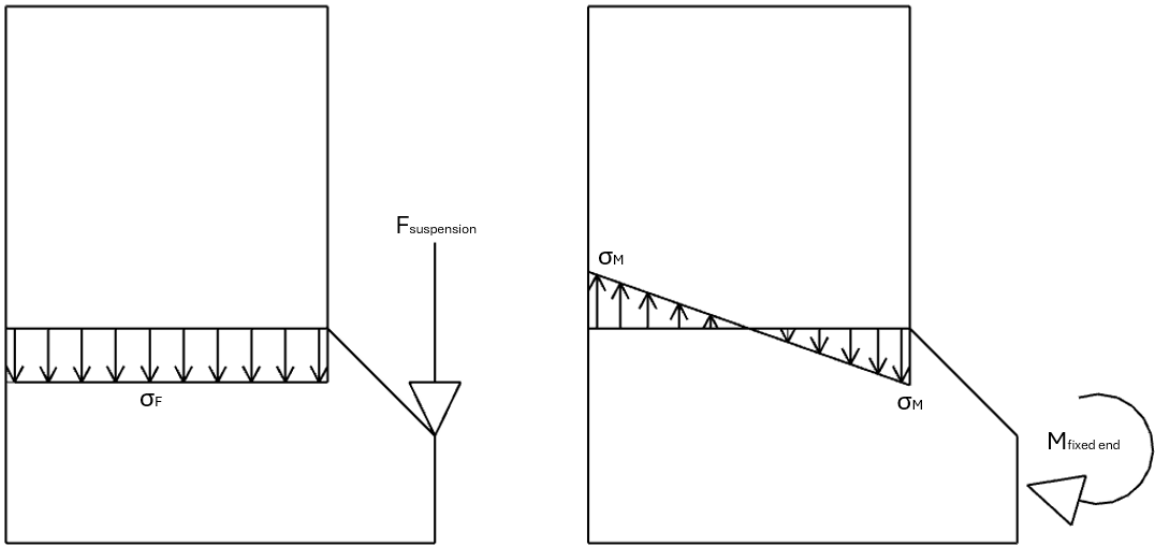

Figure 43: Stress distribution in cross-section

The stress distribution can now be calculated:

$$\sigma_{zz,M} = \frac{M_{\text{fixed end}}\alpha_A}{\frac{1}{6}W_{gir}^2} = 1.06\ \text{MPa}$$

$$\sigma_{zz,N} = \frac{N_{tot}\alpha_A}{W_{gir}} = 0.09\ \text{MPa}$$

With these results the total σ_{zz} = 1.14 MPa can be determined.

τ

τ consists of two parts, one is the shear force that causes a stress at the haunch and the other is the torsion in the girder. First the stress due to shear is calculated, using the FEM result V_{Ed} = -1672 kN.To get the shear stress at the haunch section the sectional modulus $S_{A,haunch}$ is calculated.

With this sectional modulus the stress can be calculated using:

$$\tau_V = \frac{V_{Ed} S_{A,haunch}}{I W_{gir}} = 0.44 \text{ MPa}$$

The stress due to torsion can be calculated simillarly to how the torsional shear stress was calculated for the stirrups using NEN-EN 1992-1-1 using the same t_{eff} and A_k and the FEM result T_{Ed} = 537 kNm, such that:

$$\tau_T = \frac{M_{Ed}}{2 A_k t_{eff}} = 0.60 \text{ MPa}$$

Now the total tau is computed as τ = 0.60 MPa

Evaluation

From all the calculated stress components the total tension stress at the haunch can be calculated.

$$\sigma_{ct} = \frac{1}{2}(\sigma_{xx} + \sigma_{zz}) + \sqrt{\frac{1}{4}(\sigma_{xx} - \sigma_{zz})^2 + \tau^2} = 0.45 \text{ MPa}$$

This stress should be lower than $0.6f_{ctd}$.

$$\text{u.c}_{\text{main tension}} = \frac{\sigma_{ct}}{0.6f_{ctd}} = \frac{0.45}{0.88} = 0.51$$

Annex L: SLS Crack width floor

This section covers the calculation of crack width in the floor both in longitudinal and transverse direction. The calculation method of NEN-EN 1992-1-1 formulas 7.8-7.9 has been used to find the maximum crack-width. According to OVS crack-width should be checked in SLS-freq.

Longitudinal

First the stress in the steel should be determined that occurs at M_{rep} = 371 kNm and N_{rep} = 113 kN. The steel stress can be determined when satisfying both ΣM = 0 and ΣN = 0. The result is calculated using an automatic algorithm and shown in figure 44 and 44.

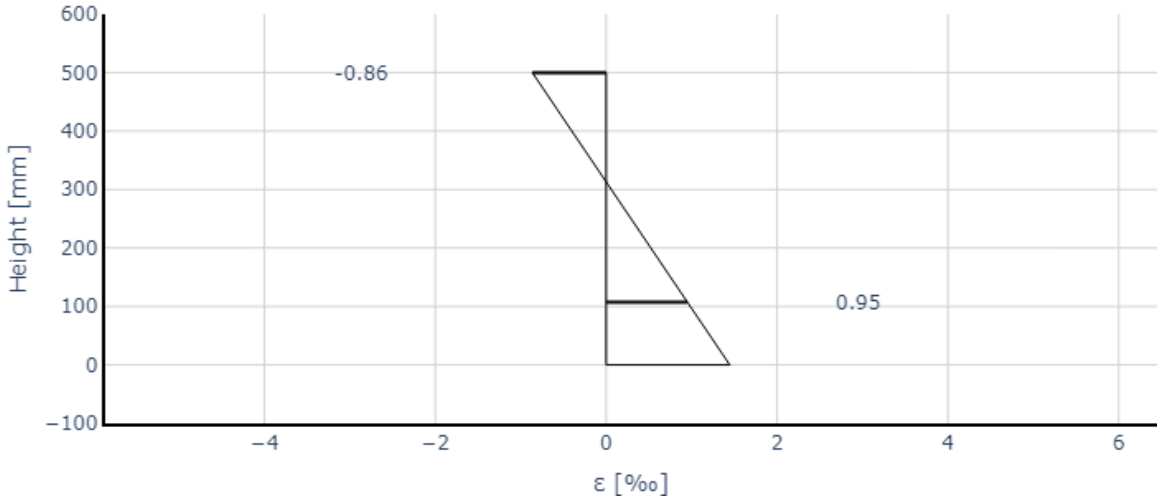

Figure 44: Strain diagram

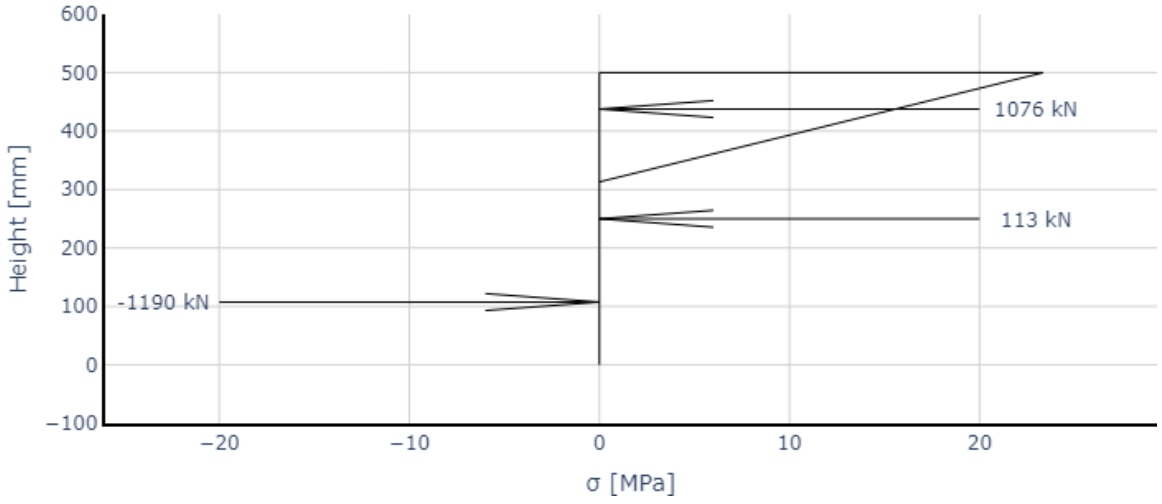

Figure 45: Stress diagram

To support these diagrams the following calculations have been made.

$$N_c = \alpha\sigma_s(\varepsilon)w_{gir}x = 1076 \text{ kN}$$

Here α = 0.50, x = 187 mm and. σ_c = 11.52 MPa at ε_c = 0.86 ‰.
The force in the steel can be calculated using:

$$N_s = A_s \cdot \sigma_s = 1190 \text{ kN}$$

Where σ_s = 199 MPa. This way both the moment and force equilibirum are statisfied knowing z = d_s - βx = 330 mm.

Now that the steel stress is known ε_{sm} - ε_{cm} can be determined with 7.9:

$$\varepsilon_{sm} - \varepsilon_{cm} = \frac{\sigma_s - k_t \frac{f_{ct,eff}}{\rho_{p,eff}}(1 + \alpha_e \rho_{p,eff})}{E_s} \geq 0.6 \frac{\sigma_s}{E_s} = 0.81 \text{ ‰}$$

Where α_e = 5 (OVS), k_t = 0.4 (long term loading) and:

$$\rho_{p,eff} = \frac{A_s}{A_{c,eff}} = 0.06$$

Where $A_{c,eff}$ = 104364 mm^2.

Also $s_{r,max}$ needs to be calculated with formula 7.11 to find the maximum crack-width.

$$s_{r,max} = k_3 c + \frac{k_1 k_2 k_4 \varnothing_{eq}}{\rho_{p,eff}} = 241 \text{ mm}$$

Where: k_1 = 0.8 assuming good bond conditions, k_3 = 3.4, k_4 = 0.425. Also:

$$\varnothing_{eq} = \frac{n_1 \varnothing_1^2 + n_2 \varnothing_2^2}{n_1 \varnothing_1 + n_2 \varnothing_2} = 18 \text{ mm}$$

And:

$$k_2 = \frac{\varepsilon_1 + \varepsilon_2}{2\varepsilon_1} = 0.50$$

Now finally w_k can be calcualted with formula 7.8:

$$w_k = s_{r,max}(\varepsilon_{sm} - \varepsilon_{cm}) = 0.20 \text{ mm}$$

To conclude with the unity check for crack-width using k_x = c / c_{nom} = 1.00:

$$\text{u.c}_{cw,y} = \frac{w_k}{k_x w_{allowed}} = \frac{0.20}{0.20} = 0.98$$

Transverse

For the transverse direction the same calculations can be made: M_{rep} = 124 kNm and N_{rep} = 106 kN. The stress and strain diagrams are shown in figure 46 and 46.

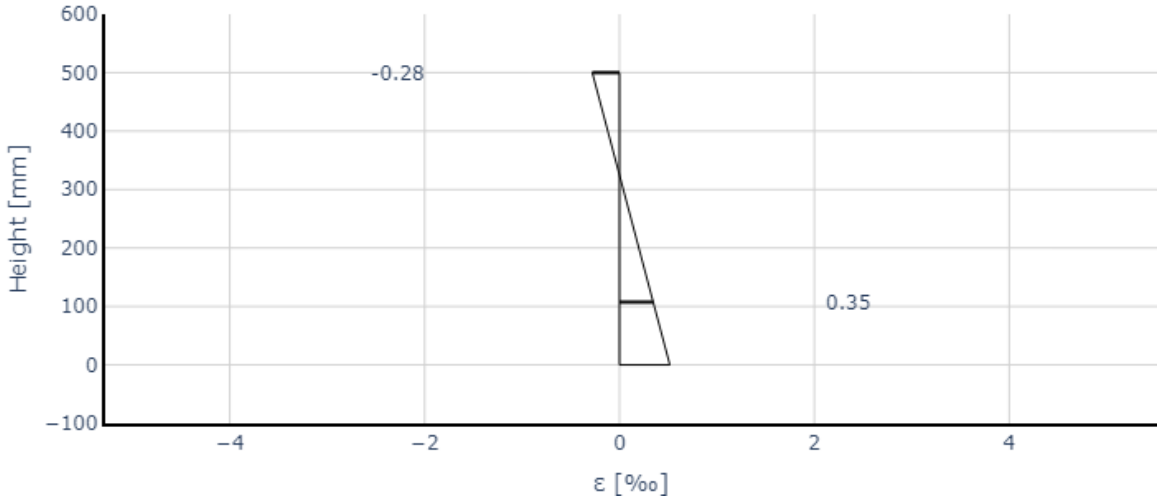

Figure 46: Strain diagram

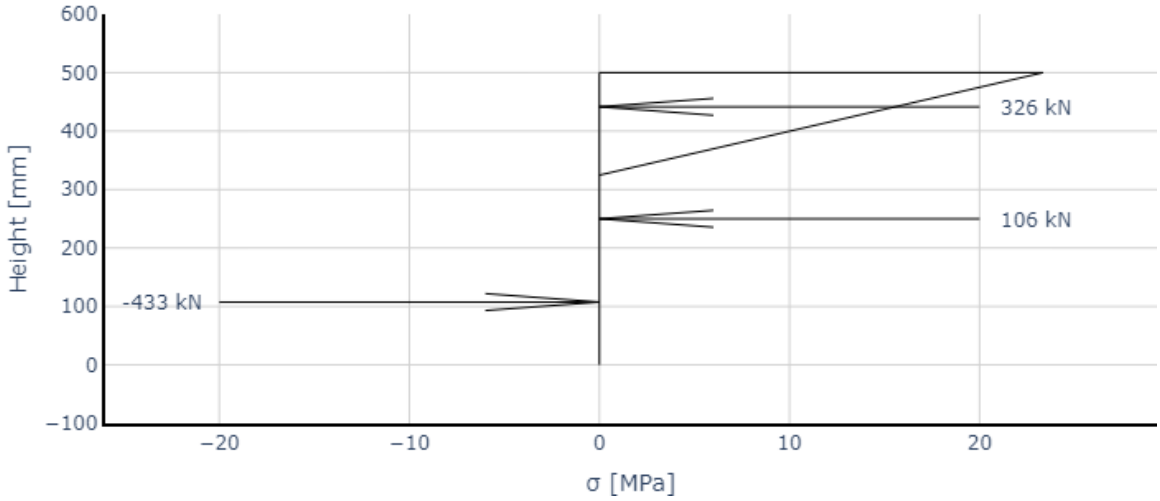

Figure 47: Stress diagram

$$N_c = \alpha \sigma_s(\varepsilon) w_{gir} x = 326 \text{ kN}$$

Here α = 0.50, x = 175 mm and. σ_c = 3.72 MPa at ε_c = 0.28 ‰.

$$N_s = A_s \cdot \sigma_s = 433 \text{ kN}$$

Where σ_s = 73 MPa. This way both the moment and force equilibirum are statisfied knowing z = d_s - βx = 334 mm.

$$\varepsilon_{sm} - \varepsilon_{cm} = \frac{\sigma_s - k_t \frac{f_{ct,eff}}{\rho_{p,eff}}(1 + \alpha_e \rho_{p,eff})}{E_s} \geq 0.6 \frac{\sigma_s}{E_s} = 0.21 \text{ ‰}$$

Where α_e = 5 (OVS), k_t = 0.4 (long term loading) and:

$$\rho_{\text{p,eff}} = \frac{A_{\text{s}}}{A_{\text{c,eff}}} = 0.06$$

Where $A_{c,eff}$ = 108218 mm^2.

And:

$$s_{\text{r,max}} = k_3 c + \frac{k_1 k_2 k_4 \varnothing_{\text{eq}}}{\rho_{\text{p,eff}}} = 243 \text{ mm}$$

Where: k_1 = 0.8 assuming good bond conditions, k_3 = 3.4, k_4 = 0.425. Also:

$$\varnothing_{\text{eq}} = \frac{n_1 \varnothing_1^2 + n_2 \varnothing_2^2}{n_1 \varnothing_1 + n_2 \varnothing_2} = 18 \text{ mm}$$

And:

$$k_2 = \frac{\varepsilon_1 + \varepsilon_2}{2\varepsilon_1} = 0.50$$

To find w_k:

$$w_{\text{k}} = s_{\text{r,max}}(\varepsilon_{\text{sm}} - \varepsilon_{\text{cm}}) = 0.05 \text{ mm}$$

To conclude with the unity check for crack-width in transverse direction using k_x = c / c_{nom} = 1.00:

$$\text{u.c}_{\text{cw,x}} = \frac{w_{\text{k}}}{k_{\text{x}} w_{\text{allowed}}} = \frac{0.05}{0.20} = 0.25$$

Appendix D: Calculation report box-girder

Calculation report super structure concrete through girder bridge

Table of contents

1. Introduction

1.1 Cross-section

The cross-section of the bridge is given in figure 1.

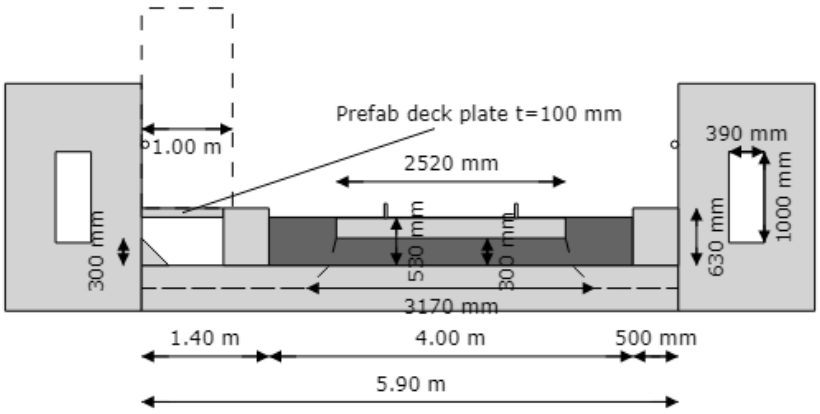

Figure 1: Cross-section of the through girder bridge

1.2 Length profile

The length profile of the bridge is given in figure 2.

Figure 2: Length profile of the through girder bridge

1.3 Aim of the report

The aim of this report is to calculate and optimize the reinforcement and pre-stressing of the super structure of a concrete through girder bridge in preliminary design phase. For this report a parametric design tool has been used to optimize the design and to make use of the automatic calculations.

2. Boundary conditions

2.1 Norms and guidelines

The most important norms and guidelines are listed below, however the applied norms are not limited to those listed.

- NEN-EN 1990-1-1:2019: Basis of structural design + NB
- NEN-EN 1991-1-4:2011: Actions on structures - General actions - Wind actions + NB
- NEN-EN 1991-2:2015: Actions on structures - Traffic loads on bridges + NB
- NEN-EN 1992-1-1:2011: Design of concrete structures - General rules and rules for buildings + NB
- NEN-EN 1992-2:2011: Design of concrete structures - Concrete bridges - Design and detailing rules + NB
- OVS00030-6-V005: Ontwerpvoorschrift kunstwerken - deel 6 - Aanvullingen en wijzigingen op NEN-EN normen
- OVS00030-1-V004: Ontwerpvoorschrift kunstwerken - deel 1 - Kunstwerken voor spoorverkeer
- RTD 1001 Richtlijnen Ontwerp Kunstwerken (ROK) 2.0
- NS Richtlijn 1015 1.3 Uitgangspunten van het ontwerp van trogbruggen

2.2 References

The references and techincal information used in this report is listed below.

- European Tehcnincal Assessment ETA-06/0147 (BBR VT CONA CMI)
- Table technical data pre-stressing strands Netherlands voorspanstaal.nl
- Product specification sheaths Tension Technology Martin

2.3 Calculation software

The following software is used for the creation of this report.

- Dlubal RFEM 6.07
- Python 3.10.8

2.4 Materials

This chapter will provide an overview of the used materials for the design.

2.4.1 Concrete

Concrete of strenght class C35/45 with the following parameters, according to NEN-EN 1992-1-1 table 3.1, are used for the design:

- f_{ck}: 35 MPa
- f_{ctm}: 3.2 MPa
- E_{cm}: 34 GPa (uncracked)
- γ_M: 1.5
- v: 0.2 (uncracked)

2.4.2 Steel

Reinforcement steel of strenght class FeB500 with the following parameters is used for the design:

- f_{yk}: 500 MPa
- f_{yd}: 434 MPa
- E_s: 210 GPa

2.4.3 Pre-stress steel

Pre-stressing steel of strenght class FeP1860 with the following parameters is used for the design:

- f_{pk}: 1860 MPa
- $f_{p,0.1,k}$: 1600 MPa
- E_p: 195 GPa

2.4.3 Pre-stress system

The design makes use of a BBR VT CONA CMI prestressing system internal post-tensioning system with cables and a duct of:

- $n_{strands}$: 27
- $\varnothing_{strands}$: 15.7 mm

The pre-stress ducts used are of type: STB-110x119x0.40 as described in the product specification of TTM

The filling degree of the pre-stress duct thus becomes: 0.55.

2.5 Environmental classes

In table 1 the environmental classes and crack width requirements have been summarized. The design life of all train bridges is 100 years and the crack width

requirement and the environmental classes have been decided by OVS-00030-6 and NEN-EN 1992-1-1.

Structural element	Environmental class	$c_{nom,reinf}$ mm	c_{app} mm	$c_{nom,p}$ mm	w_{max} mm
Girder	XC4, XD3, XF4, XA2	55.0		80.0	0
Top of deck	XC4, XD3, XF4, XA2	55.0			0.2
Bottom of deck	XC4, XD3, XF4, XA2	55.0			0.2

Table 1: Durability factors

2.6 Loads

The loads working on the super structure of the bridge will be summarized here. For the complete calculation of the loads please refer to annex B. Also the load combinations considered are summarized in annex C.

2.6.1 Permanent loads

LC1.1 Self-Weight

The self-weight of the structure is calculated automatically calculated by RFEM.

LC1.2 Permanent loads train

Other permanent loads that are considered are due to the infrastructure on the bridge for the trains. The loads are visualised in figure 3.

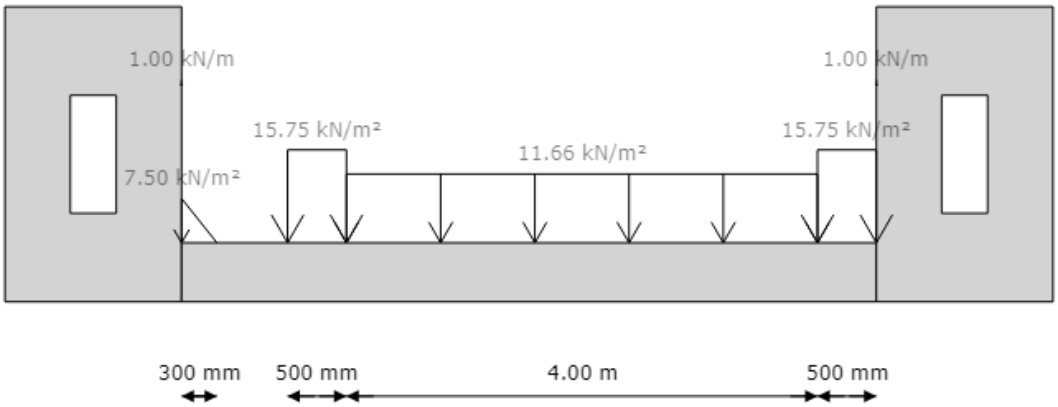

Figure 3: Permanent loads

LC2 Prestressing

For the calculation of the pre-stress forces and losses please refer to annex B. Figure 4 shows the pre-stress profile and figure 5 shows the resulting forces.

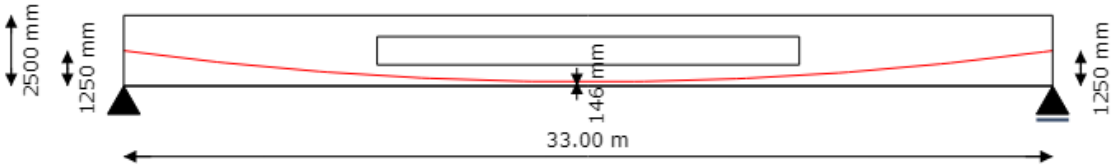

Figure 4: Pre-stress profile

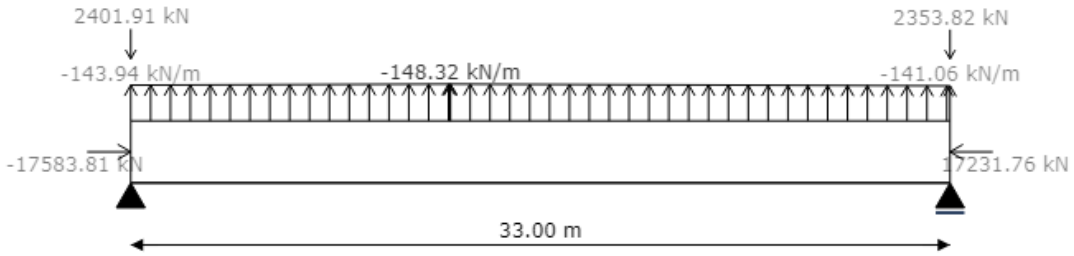

Figure 5: Pre-stress loads

LC3 Setting
Because a single span statically determined bridge is considered, settings will not cause loads.

2.6.2 Variable loads

LC4 Other variable loads
Variable loads on the passing path are considered as per NEN-EN 1991-2.

- $Q_{passing\ path}$: 5 kN/m^2

Snow loads are not considered because these will be inisgnificant compared to the train loads.

LC5 Braking loads and LC6 Accelerating loads
Brake and accelerating forces are not considered for the super structure as these will be mostly important for the substructure.

LC7 Wind loads
Windloads are calculated using NEN-EN 1991-1-4, for the complete calculation please refer to Annex B.

The decisive loads F_{wk} and the reduced F_{wk}^{**} that are considered are given below. The loads in x-direction are modelled as line loads acting on the wall of the structure, while the loads in z direction are considered as distributed loads over the whole area of the bridge.

- $q_{wk,x}$: 16.73 kN/m
- $q_{wk,x}^{**}$: 12.01 kN/m
- $p_{wk,z}$: 1.44 kN/m^2
- $p_{wk,z}^{**}$: 1.03 kN/m^2

LC8 Temperature loads
Temperature loads have not yet been incorporated in the design.

LC9.1.1 Train loads model LM71 M

The position of the train load model LM71 from NEN-EN 1991-2 is automatically calculated using influence lines. Also the effective width over which the load may be spread is calculated:

$$W_{\text{load}} = l_{\text{sleeper}} + 2 \cdot (\frac{t_{\text{bal}}}{4} + \frac{h_{\text{fl}}}{2}) = 2520 + 2 \cdot (75.0 + 250.0) = 3170 \text{ mm}$$

It is assumed that the point loads in the middle of this load model can be evenly distributed over the whole area. The loads resulting in the highest moment from LM71 are shown in figure 6:

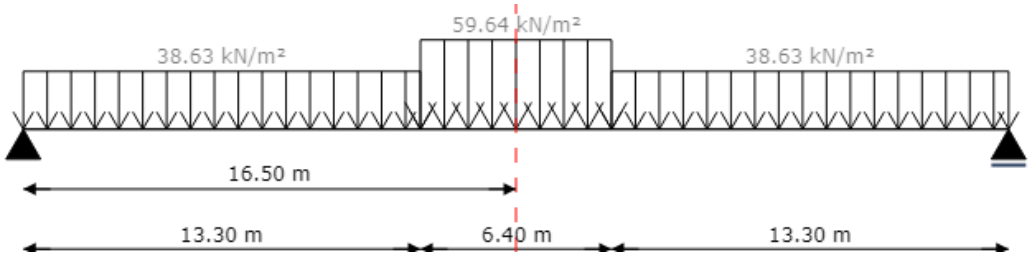

Figure 6: Load model LM71, max moment

LC9.1.2 Train loads model LM71 V

The loads resulting in the highest shear force from LM71 are shown in figure 7:

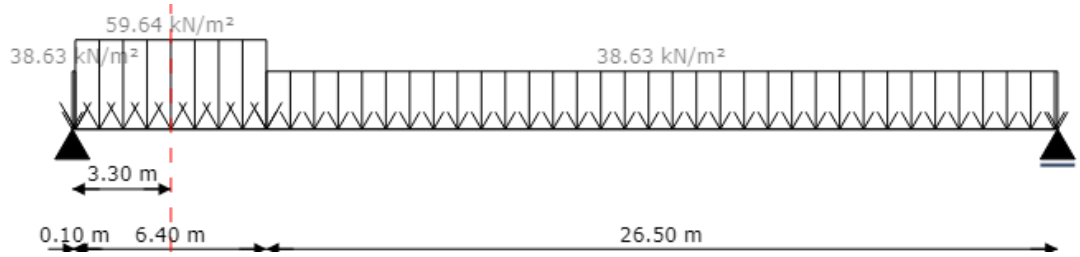

Figure 7: Load model LM71, max shear force

LC9.2.1 Train loads model SW/0 M

Because a single span bridge is designed load model SW/0 is not considered.

LC9.3.1 Train loads model SW/2 M

The position of the train load model SW/2 from NEN-EN 1991-2 is automatically calculated using influence lines. The effective width is the same as before. The loads resulting in the highest moment from SW/2 are shown in figure 8:

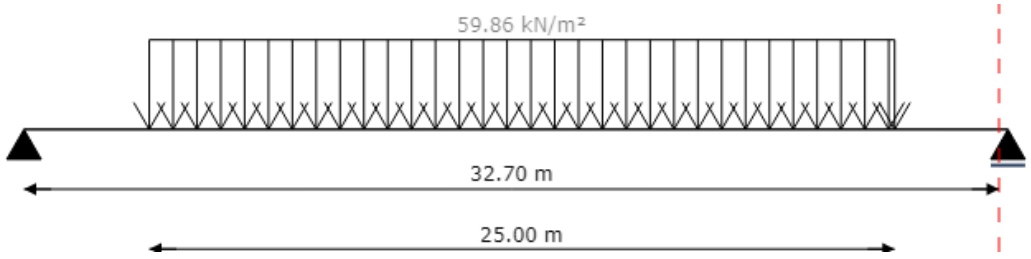

Figure 8: Load model LM71, max moment

LC9.3.2 Train loads model SW/2 V

The loads resulting in the highest shear force from SW/2 are shown in figure 9:

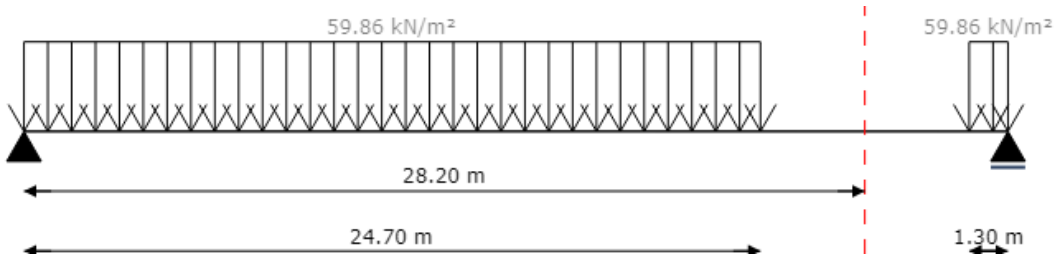

Figure 9: Load model LM71, max shear force

2.6.3 Special loads

LC10.1 Train loads tilting and LC10.2 Rerailing loads

These load cases have not been implemented yet. Also centrifugal force is not considered because the bridge is straight.

3. Calculations

For the pre-stress and reinforcement layouts of the design please refer to annex B.

3.1 Modelling and loadtransfer

As mentioned before the FEM model is build in RFEM. The principal cross-section in RFEM is shown in figure 10. In the following paragraphs the most important elements of the model will be explained.

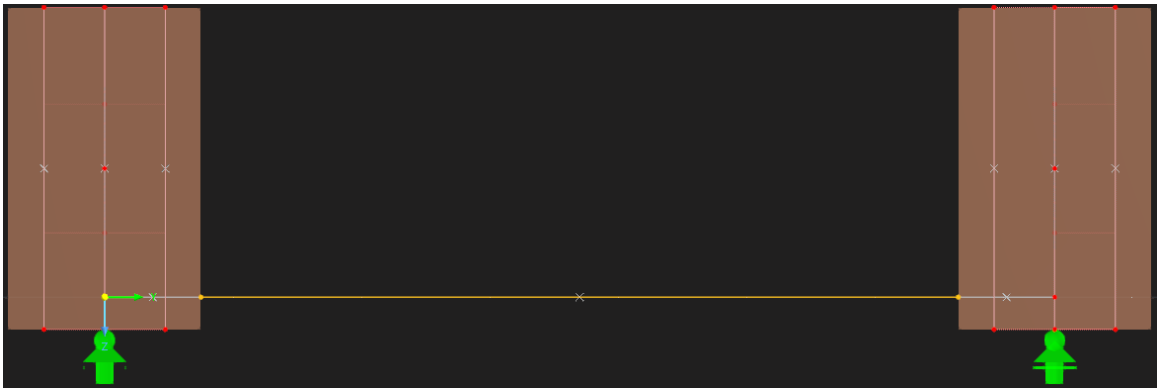

Figure 10: Principal cross-section in RFEM

3.2.1 Girders

The girders are modelled as vertical planar 2D plate elements with a uniform thickness that transfer moments and membrane forces. This way the homogenous en isotropic behaviour of the girder is correctly modelled. The target mesh size for the elements is 0.25 m.

To correctly model the girder, the girder is divided in three surfaces that are connected with surface contacts that transfer loads in all directions. The middle surface of this girder has an opening such that the opening is enclosed by the other surfaces. This situation is shown in figure 13.

3.2.2 Floor

The floor is modelled simillarly as the girders. For the floor again a vertical planar 2D plate element with a uniform thickness that transfer moments and membrane forces is used. For the floor also a mesh size of 0.25 m is used.

3.2.3 Connection floor-girder

The floor and girders are connected via a rigid planar surface with zero mass density such that the self-weight is not doubled in this area. By making sure this surface connects the floor and the girder the connection correctly models the bahaviour of load transfer between these elements. Figure 11 shows how the elements are modelled by side view.

Figure 11: Side view of the surface elements in RFEM

3.2.4 Supports

The model has 4 supports all of them restricting movement in z-direction and none of them restricting rotation. Figure 12 shows how the supports of the model are ordered and in which direction they allow for translation.

Figure 12: Top view of the support directions

3.2.5 Result beams

To transfer the loads of the 2D elements of the girders into 1D internal forces to be used for evaluation result beams are used. These beams cover the surface elements and integrate the internal forces to 1D internal forces.

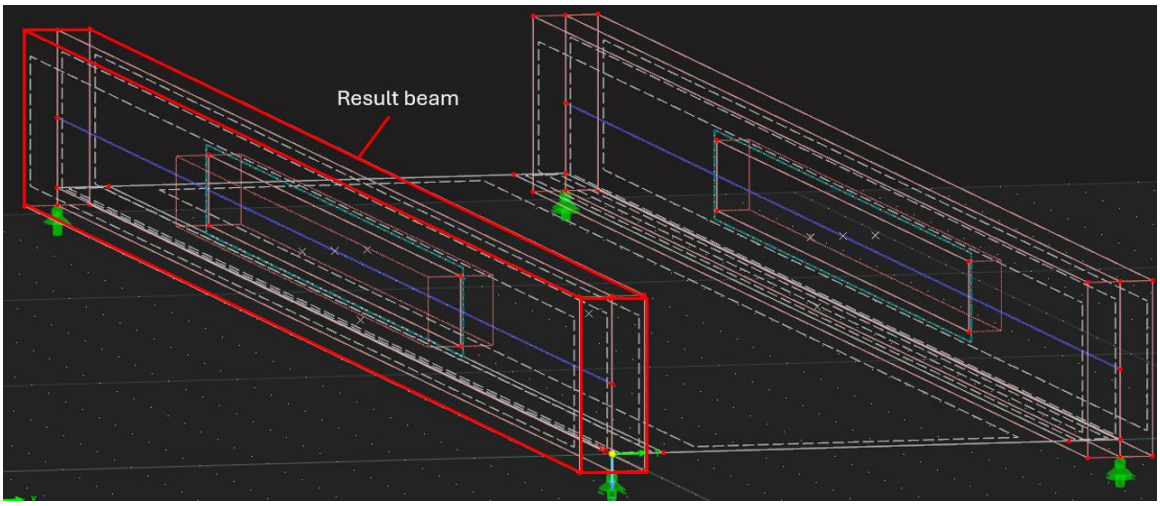

Figure 13: Result beam in model

3.2 Calculations girder

This paragraph outlines the results of the calculations made for the girder. The reinforcement and pre-stress layout can be found in annex B.

3.2.1 Ultimate limit state

These calculations can be found in Annex E and F. The longitudinal and stirrups reinforcement has been checked according to NEN-EN 1992-1-1. The stirrups have been divided into three regions, each having a different purpose for the type of load they carry. Next to that the longitudinal reinforcement is tested both for capacity and for max compression zone height according to NEN-EN 1992-1-1 6.1 (9). To achieve this the pre-stress has been ficticiously reduced to 57 % such that only the part of the pre-stress that is needed to carry the load remains. With this case the compression zone height is checked.

The results are summarized in table 2.

	Symbol	Value	Limit value	Result
Longitudinal reinforcement torsion	$u.c_{sl,T}$	$A_{sl,T,req}$ = 9741 mm^2	$A_{sl,T}$ = 10053 mm^2	0.97
Stirrup horizontal reinforcement	$u.c_{sw,T,hor}$	$A_{sw,T,hor,req}$ = 223 mm^2	$A_{sw,T}$ = 565 mm^2	0.39
Stirrup zone I reinforcement	$u.c_{sw,I}$	$A_{sw,I,req}$ = 535 mm^2	A_{sw} = 565 mm^2	0.95
Stirrup zone II reinforcement	$u.c_{sw,II}$	$A_{sw,II,req}$ = 878 mm^2	A_{sw} = 905 mm^2	0.97
Stirrup zone III reinforcement	$u.c_{sw,III}$	$A_{sw,III,req}$ = 2056 mm^2	A_{sw} = 2122 mm^2	0.97
Moment reinforcement	$u.c_{M,gir}$	M_{Ed} = 21027 kNm	M_{Rd} = 46206 kNm	0.46
Increased moment reinforcement	$u.c_{M,rot}$	$M_{Ed,rot}$ = 27514 kNm	$M_{Rd,rot}$ = 27924 kNm	0.99
Compression zone height	$u.c_{x,rot}$	x_u = 917 mm	$x_{u,allowed}$ = 917 mm	1.00

Table 2: Calculation results girder ULS

3.2.2 Serviceability limit state

This section covers the SLS calculations for the girder. Both the compressive and tension stresses in the concrete have been checked in annex J. The tension stresses have been checked according to the requirements of the OVS and the compressive stress has been checked at t=0. Next to that the main tension stress just above the haunch at the inner wall of the girder has also been checked in accordance with NSRL1015. This stress is built up out of three stres components σ_{xx}, σ_{zz} and τ and they are calculated in annex K.

The results are summarized in table 3.

	Symbol	Value	Limit value	Result
Tension stress SLS-quas		$\sigma_{ct,quas}$=-2.41 MPa	$\sigma_{ct,quas,allowed}$=0.00 MPa	O.K.
Tension stress SLS-freq		$\sigma_{ct,freq}$=-0.35 MPa	$\sigma_{ct,freq,allowed}$=1.10 MPa	O.K.
Tension stress SLS-char		$\sigma_{ct,char}$=0.34 MPa	$\sigma_{ct,char,allowed}$=1.10 MPa	O.K.
Compressive stress	$u.c_{compr}$	σ_c=5.68 MPa	f_{cd}=23 MPa	0.24
Main tension stress	$u.c_{main\ tension}$	σ_{ct}=0.54 MPa	$0.6f_{ctd}$=0.88 MPa	0.62

Table 3: Calculation results floor SLS

3.3 Calculations floor

This paragraph outlines the results of the calculations made for the floor.

3.3.1 Ultimate limit state

The ULS calculations for the floor are conducted using NEN-EN 1992-1-1. Reinforcement in both x and y direction is applied en checked in annex G.

The results are summarized in table 4.

	Symbol	Value	Limit value	Result
Longitudinal reinforcement	$u.c_{M,floor,y}$	M_{Ed}=577 kNm	M_{Rd}=867 kNm	0.67
Transverse reinforcement	$u.c_{M,floor,x}$	M_{Ed}=204 kNm	M_{Rd}=220 kNm	0.93

Table 4: Calculation results floor ULS

3.3.2 Servicability limit state

The SLS calculations for the floor are conducted using NEN-EN 1992-1-1. Annex L outlines how the crack-width has been calculated.

The results are summarized in table 5.

	Symbol	Value	Limit value	Result
Crack-width longitudinal	$u.c_{cw,y}$	w=0.20 mm	$w_{allowed}$=0.20 mm	0.98
Crack-width transverse	$u.c_{cw,x}$	w=0.05 mm	$w_{allowed}$=0.20 mm	0.24

Table 5: Calculation results floor ULS

3.4 Other calculations

This paragraph outlines the results of the other calculations.

3.3.1 Ultimate limit state

Longitudinal shear between the girder and the floor has ben checked in annex H according to NEN-EN 1992-1-1 6.2.4.Next to that splitting reinforcement at the ends of the deck has also been calculated in annex I using a strut and tie model
The results of these calculations have been summarized in table 6.

	Symbol	Value	Limit value	Result
Longitudinal shear	$u.c_{l,s}$	v_{Ed}=0.46 MPa	kf_{ctd}=0.59 MPa	0.78
Splitting reinforcement	$u.c_{spl}$	σ_{spl}=371 MPa	f_{yd}=434 MPa	0.85

Table 6: Calculation results other calculations ULS

3.3.2 Servicability limit state

The maximum displacement is calculated with the FEM model is 27.2 mm. The by OVS required camber is 33.0 mm, this means that the pre-camber of the bridge should be 60.2 mm

4. Results

Based on the internal forces from the 3D FEM model of the design model, the reinforcement and prestressing of the superstructure of the trough bridge have been determined. The structure has been checked for strength and durability in a preliminary design stage. The geometry and reinforcement is summarized in appendix A and B.

4.1 Points of attention

- This report is made for a preliminary design, further detailling is needed to complete the design.
- Temperature loads are not considered in this report.
- This bridge has not been tested in FAT.
- Splitting reinforcement for the introduction of the pre-stressing has not been designed.
- No calculations for detailing around the supports have been made.
- It is essential for the design that the bridge is correctly protected from stray currents by isolation of the clearway in accordance with OVS.

Annex A: Geometry and effective width

Cross-sectional properties

The calculation of certain cross-sectional parameters is displayed below.

$$A = 2 \cdot h_{\text{gir}} \cdot W_{\text{gir}} + h_{\text{fl}} \cdot W_{\text{fl}} + a_{\text{vou}}^2 - 2 \cdot W_{\text{cutout}} \cdot h_{\text{cutout}} = 9.76\ \text{m}^2$$

$$z_{\text{neutral,axis}} = \frac{2 \cdot A_{\text{gir}} \cdot z_{\text{gir}} + A_{\text{fl}} \cdot z_{\text{fl}} + 2 \cdot A_{\text{vou}} \cdot z_{\text{vou}}}{A} = 0.942\ \text{m}$$

$$I = 2 \cdot (I_{\text{girder}} + A_{\text{girder}} \cdot a_{\text{girder}}^2) + I_{\text{fl}} + A_{\text{fl}} \cdot a_{\text{fl}}^2 + 2 \cdot (I_{\text{vou}} + A_{\text{vou}} \cdot a_{\text{vou}}^2) = 5.969\ \text{m}^4$$

Where the area of the cutout is subtracted from the area of the girder.

The cross-section for including the max effective width is shown in figure 14.

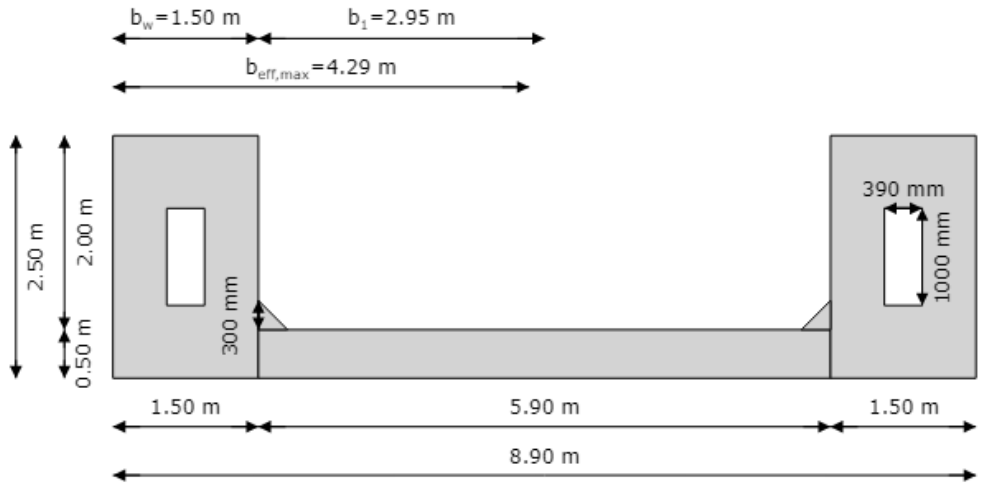

Figure 14: Cross-section including maximum effective width

The effective width over the length of the bridge is shown in figure 15

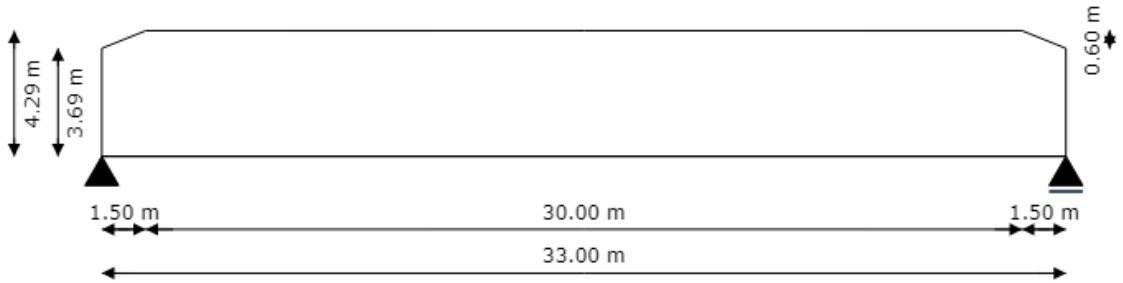

Figure 15: Length profile with effective width of the through girder bridge

The effective width is calculated via NEN-EN 1992-2. First the l_0/b_i ratio can be calculated as: 33/2.95=11.19.
Referencing this ratio in figure 16, it is found that the ratio b_{eff}/b_i for S_s should be: 0.74 and for S_v: 0.95. The effective width can be calculated accordingly.

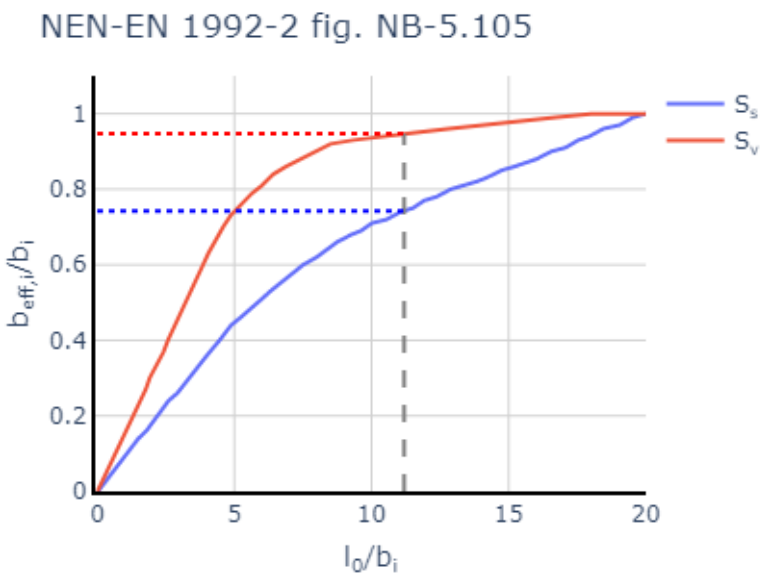

Figure 16: NEN-EN 1992-2 fig. NB.5-105 and the effective width ratio's

Train infrastructure

The geometry of the train infrastructure in the cross-section should also be determined in accordance with OVS00030-6-V005 and OVS00030-1-V004.
Sleepers are 2520x260x121 mm based on OVS6 article 6.3.6.2 and on the fact that a UIC-54 rail has a height of 159 mm, they have a spacing of 600 mm according to NEN-EN 1991-2 fig. 6.5.
The thickness of the ballast layer is 300.0 mm and the thickness of the deck plate for the passing path is 100 mm. The width of this passing path is 1 m according to OVS1 article 3.3.3 and it should be atleast 2.4 m out of the center of the rails knowing no high-speed trains will cross this bridge.
The derailment guards should be placed at least 2 m out of the center of the rails according to OVS1 article 4.1.4.1 and the width of the derailment guard is 500 mm to accomodate the reinforcement needed for big impacts. The height of these guards should at least be 100 mm above the top of the rail.
For design purposes the height of the ballast bed should be from the top of the deck to the top of the rails - 150 mm with a volumetric of 22 kN/m^3 according to OVS-6 article 5.2.3.
Using these rules the cross-section with train infrastructure in the report is designed.

Annex B: Pre-stress and reinforcement

Pre-stress

The pre-stress layout at midspan is shown in 17. This system uses 4 cables per girder.

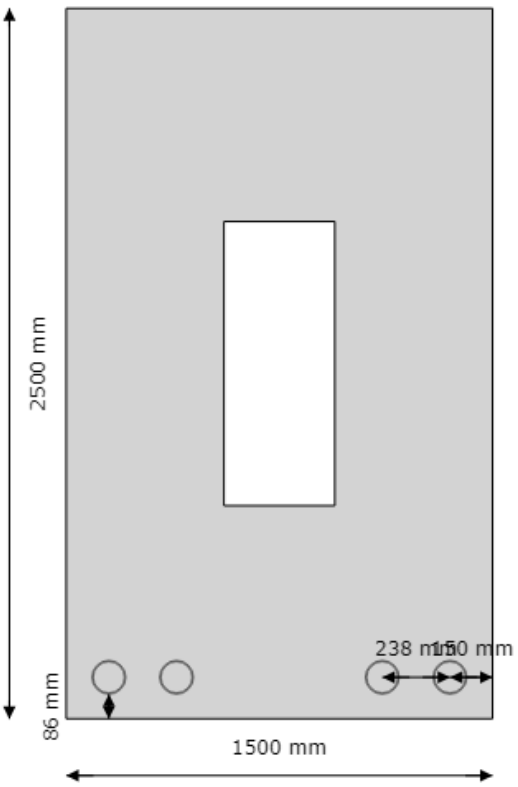

Figure 17: Pre-stress layout

- R: 123 m
- A_P: 16200 mm^2
- $d_{P,mid}$: 2354 mm
- $\sigma_{Pi,max}$: 1427 MPa
- $\sigma_{Pw,max}$: 1129 MPa
- $c_{P,min}$: 80 mm
- $c_{P,app}$: 86 mm

Girder reinforcement

The reinforcement layout of the girder is shown in 18.

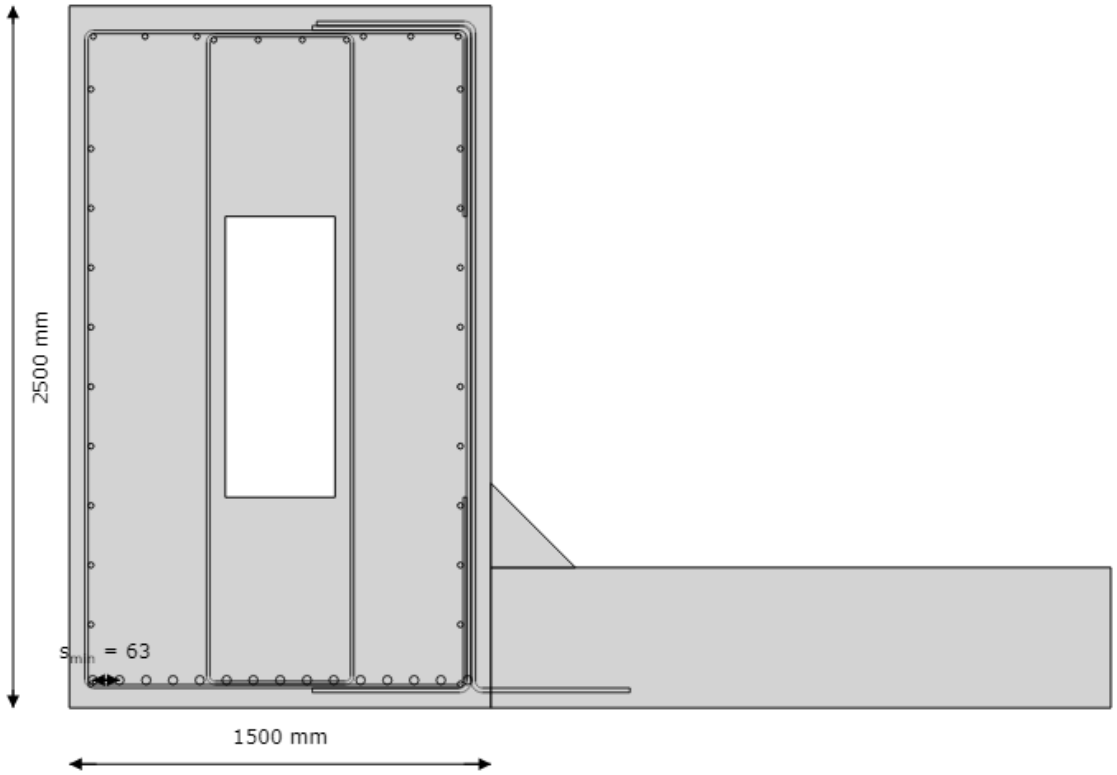

Figure 18: Girder reinforcement layout

Main longitudinal reinforcement:

- $\varnothing_{sl}$: 32 mm
- A_{sl}: 24127 mm^2
- d_{sl}: 2401 mm

Longitudinal reinforcement for torsional resistance:

- $\varnothing_{sl,T}$: 20 mm
- $s_{sl,T}$: 220 mm
- $A_{sl,T}$: 10053 mm^2

Stirrups:

- $\varnothing_{sw,C}$: 12 mm
- $s_{sw,C}$: 200 mm
- $\varnothing_{sw,mid}$: 12 mm
- $s_{sw,mid}$: 250 mm
- $\varnothing_{sw,inverted\ C}$: 16 mm
- $s_{sw,inverted\ C}$: 180 mm
- $\varnothing_{sw,Z}$: 16 mm
- $s_{sw,Z}$: 200 mm
- $A_{sw,I}$: 565 mm^2
- $A_{sw,II}$: 905 mm^2
- $A_{sw,III}$: 2122 mm^2

Cover:

- c_{min}: 55 mm
- c_{app}: 55 mm

The stirrup reinforcement is divided in three different areas. Area I serves as torsional and shear forces reinforcement, area II serves for shear reinforcement and area III serves for both shear and torsional reinforcement and also carries the loads from the suspension forces from the floor.
Due to the limitation is NEN-EN 1992-1-1, the maximum spacing of the stirrups in the girder is 500 mm. This requirement is fulfilled

Floor reinforcement

The reinforcement layout of the floor in y-direction is shown in 19. The reinforcement in x-direction is shown in the transverse direction.

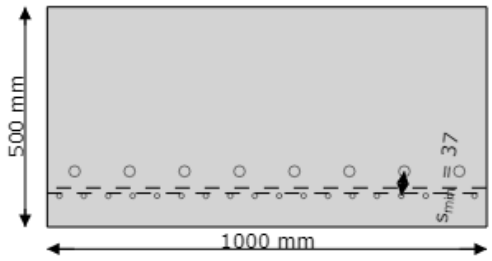

Figure 19: Floor reinforcement layout

Longitudinal reinforcement y-direction:

- $\varnothing_{1,y}$: 12 mm
- $s_{1,y}$: 56 mm
- $\varnothing_{2,y}$: 25 mm
- $s_{2,y}$: 125 mm
- $A_{sl,y}$: 5963 mm^2
- $d_{sl,y}$: 392 mm

Longitudinal reinforcement x-direction:

- $\varnothing_{1,x}$: 12 mm
- $s_{1,x}$: 91 mm
- $A_{sl,x}$: 1244 mm^2
- $d_{sl,x}$: 417 mm

Cover:

- c_{min}: 55 mm
- c_{app}: 55 mm

Splitting reinforcement

The splitting reinforcement at the ends of the span has also been calculated. The layout for both ends of the bridge is:

- $\varnothing_{spl}$: 32 mm
- n_{spl}: 9
- A_{spl}: 7238 mm^2

Annex C: Loads

LC1.2 Permanent loads train

This section will feature the calculation of the additional permanent loads

- Weight haunches

The additional load of the haunches which are not modelled in SCIA as structural elements is calculated with:

$$Q_{\text{haunch}} = h_{\text{haunch}} \cdot \gamma_{\text{concrete}} = h_{\text{haunch}} \cdot 25$$

Because the haunchs have a slope of 1:1 and the max height of 300.0 mm, this leads to the loads represented in the report.

- Weight derailment guard

The additional load of the derailment guards is calculated as:

$$Q_{\text{derailment guard}} = h_{\text{derailment guard}} \cdot \gamma_{\text{concrete}} = 630.0 \cdot 25 = 15.75 \text{ kN/m}^2$$

- Weight ballastbed

The additional load of the ballast bed is calculated as:

$$Q_{\text{ballast bed}} = h_{\text{ballast bed}} \cdot \gamma_{\text{concrete}} = 530.0 \cdot 25 = 11.66 \text{ kN/m}^2$$

With these calculations the loads shown in the report have been calculated.

LC2 Prestressing

The tendon profile of the prestress is given in figure 20.

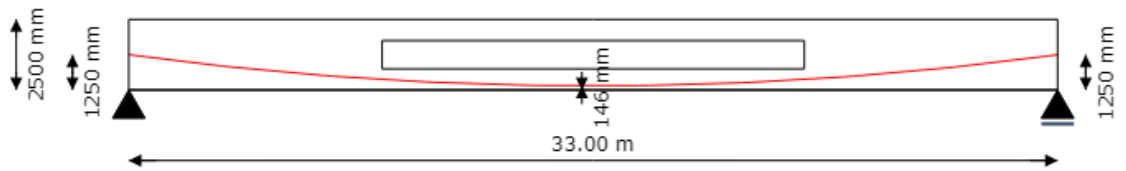

Figure 20: Prestress tendon profile

The tendon profile is given by:

$$y = 4.11 \cdot 10^{-6}x^2 + -0.14x + 1250;\ R = 123\ \text{m}$$

In addition to this the vertical displacement of the cable Δz due to the stressing of the cable is calculated with a maximum of 18 mm due as prescribed by ROK

First the maximum force should be determined. From a simple calculation it follows that the maximum pre-stressing force is limited by the material properties rather than by the maximum pre-stressing force that will yield a positive moment at t=0 when only the self-weight and the prestressing force will be acting on the bridge:

$$\frac{N_\text{P}}{A} - \frac{M_\text{P}}{W_\text{top}} + \frac{M_\text{sw}}{W_\text{top}} > 0;\ N_\text{P} = \sigma_\text{P} A_\text{P}$$

Using:

$$M_\text{P} = \frac{1}{2} \cdot N_\text{P}(e_1 + e_2) + \frac{N_\text{P} l^2}{8R}$$

$$M_\text{sw} = \frac{1}{8} \cdot A\gamma_\text{conc} l^2$$

$$A_\text{P} = A_\text{strand} n_\text{strands} n_\text{cable} = 150 \cdot 27 \cdot 4 = 16200\ \text{mm}^2$$

It can be concluded that $\sigma_{\text{PM0,max}}$=2881 MPa, which is much higher than the limit given by:

$$\sigma_{\text{PM0,max}} = \min(0.75 \cdot f_\text{pk}, 0.85 \cdot f_{\text{p0.1k}}) = \min(0.75 \cdot 1860, 0.85 \cdot 1600) = 1360\ \text{MPa}$$

The maximum stress during tensioning is:

$$\sigma_{\text{PMi,max}} = \min(0.8 \cdot f_\text{pk}, 0.9 \cdot f_{\text{p0.1k}}) = \min(0.8 \cdot 1860, 0.9 \cdot 1600) = 1440\ \text{MPa}$$

These two stresses are the basis for the pre-stress loss calculations. For these calculations the following losses are considered:

- Friction losses

The prestressing system makes use of a Steel strip sheath with: k=0.005 rad/m and μ=0.18 rad^{-1} following from European Technical Assessment ETA-06/0147. The friction losses over the length profile can be calculated using:

$$F = F_0 e^{-\mu(\theta + k \cdot x)}$$

Where θ is the sum of the angular displacements over the distance x, irrespective of direction or sign. The pre-stressing steel is stressed first from the left side and than from the right side. Now σ_{PMi} can be calculated.

- Wedge set

The wedge set for the pre-stressing system is assumed to be 7 mm because of the ROK. How this loss is spread over the length of the bridge is calculated by discretizing the length of the bridge into many small dx's. For the each dx and $\Delta\sigma_{slip}$ the total Δl is calculated using:

$$\Delta l = \frac{\Delta\sigma_{\text{slip}}}{E_{\text{P}}} \cdot \Delta x$$

Using a smart optimization algorithm the actual stress losses can be calcualted by finding the $\Delta\sigma_{slip}$ values such that ΣΔl=7 mm using the follwing rule.

$$\Delta\sigma_{\text{slip},x=i+1} = \max(\Delta\sigma_{\text{slip},x=i} - \max(2(\sigma_{\text{PMi},x=i} - \sigma_{\text{PMi},x=i+1}),0),0)$$

- Creep loss

The creep loss can be calculated assuming: t=36500 days, t_0=10 days and RH=65 %. The calculation from Annex B of NEN-EN 1992-1-1 can be used to calculate the creep coefficient:

$$\alpha_1 = \left(\frac{35}{f_{\text{cm}}}\right)^{0.7} = 0.87;\ \alpha_2 = \left(\frac{35}{f_{\text{cm}}}\right)^{0.2} = 0.96;\ \alpha_3 = \left(\frac{35}{f_{\text{cm}}}\right)^{0.5} = 0.90$$

$$h_0 = \frac{2A_{\text{c}}}{u} = \frac{2 \cdot 9760000}{26800} = 728\ \text{mm}$$

Where u is the perimeter of the cross-section of the bridge.

$$\begin{aligned}\beta_{\text{H}} &= \min(1.5(1 + (0.012\text{RH})^{18})h_0 + 250\alpha_3, 1500\alpha_3) \\ &= \min(1.5(1 + (0.012 \cdot 65)^{18})728 + 226, 1353) = 1331\end{aligned}$$

$$\beta_{\text{c}}(t, t_0) = \left(\frac{t - t_0}{\beta_{\text{H}} + t - t_0}\right)^{0.3} = \left(\frac{36500 - 10}{1331 + 36500 - 10}\right)^{0.3} = 0.99$$

$$\beta(t_0) = \frac{1}{0.1 + t_0^{0.20}} = \frac{1}{0.1 + 10^{0.20}} = 0.59$$

$$\beta(f_{\text{cm}}) = \frac{16.8}{\sqrt{f_{\text{cm}}}} = \frac{16.8}{\sqrt{43}} = 2.56$$

$$\phi_{\text{RH}} = \alpha_2(1 + \alpha_1 \cdot \frac{1 - \text{RH}/100}{0.1h_0^{\frac{1}{3}}}) = 0.96(1 + 0.87 \cdot \frac{1 - 0.65}{0.19}) = 1.28$$

$$\phi_0 = \phi_{\text{RH}}\beta(f_{\text{cm}})\beta(t_0) = 1.28 \cdot 2.56 \cdot 0.59 = 1.95$$

Using these parameters the creep coefficient can be calculated. Using the creep coefficient and the aforementioned first estimate of steel stress the creep strain can be calculated:

$$\phi(t, t_0) = \phi_0\beta_{\text{c}}(t, t_0) = 1.95 \cdot 0.99 = 1.93$$

$$E_{\text{c}} = 1.05E_{\text{cm}};\ \sigma_{\text{c}} = \sigma_{\text{P}} \cdot \frac{A_{\text{P}}}{A_{\text{c}}}$$

$$\varepsilon_{\text{cc}}(\infty, t_0) = \phi(\infty, t_0) \cdot \frac{\sigma_{\text{c}}}{E_{\text{c}}} = 1.93 \cdot \frac{6}{35700} = 0.387\ ‰$$

- Drying shrinkage loss

Drying shrinkage ε_{cd} strain can also be calculated via NEN-EN 1992-1-1. Cement of class N is used or this design giving α_{ds1}=4 and α_{ds2}=0.12, also f_{cmo}=10 MPa and RH_0=100 %. Now $\varepsilon_{cd,0}$ can be calculated:

$$\beta_{\text{RH}} = 1.55(1 - (\frac{RH}{RH_0})^3) = 1.55(1 - (\frac{65}{100})^3) = 1.12$$

$$\varepsilon_{\text{cd,0}} = 0.85((220 + 110\alpha_{\text{ds1}}) \cdot \exp(-\alpha_{\text{ds2}} \cdot \frac{f_{\text{cm}}}{f_{\text{cmo}}})) \cdot 10^{-6} \cdot \beta_{\text{RH}}$$
$$= 0.85((220 + 110 \cdot 4) \cdot \exp(-0.12 \cdot \frac{43}{10})) \cdot 10^{-6} \cdot 1.12 = 376.50 \cdot 10^{-6}$$

The value of k_h can be found in table 3.3 and is 0.70. Now the final drying shrinkage can be calculated:

$$\varepsilon_{\text{cd},\infty} = k_{\text{h}} \cdot \varepsilon_{cd,0} = 0.423\ ‰$$

- Autognenous shrinkage loss

This loss can be also be calculated using NEN-EN 1992-1-1 and follows quite straightforwardly from:

$$\varepsilon_{\text{ca}}(\infty) = 2.5(f_{\text{ck}} - 10) \cdot 10^{-6} = 2.5(35 - 10) \cdot 10^{-6} = 0.062\ ‰$$

- Relaxation loss

The final considered pre-stress loss is relaxation loss. With ρ_{1000}=2.5 % this can be calculated, again using NEN-EN 1992-1-1 formula 3.29 and using pre-stress strands of class 2 as presribed by ROK. For this calculation the length of the bridge is again discretized such that for all dx:

$$\Delta\sigma_{PR} = 0.66\sigma_{Pi}\rho_{1000}e^{9.1\mu}\left(\frac{t}{1000}\right)^{0.75(1-\mu)} \cdot 10^{-5}$$

Using:

$$\mu = \frac{\sigma_{Pi}}{f_{pk}}$$

The maximum relaxation loss $\Delta\sigma_{PR,max}$ ilustratively is computed as 60.9 MPa, assuming t=500000 h using 3.3.2 (8).

Incorporating all these losses in the internal stress of the pre-stress tendon over the length of the bridge, figure 21 can be plotted finalizing the prestress losses.

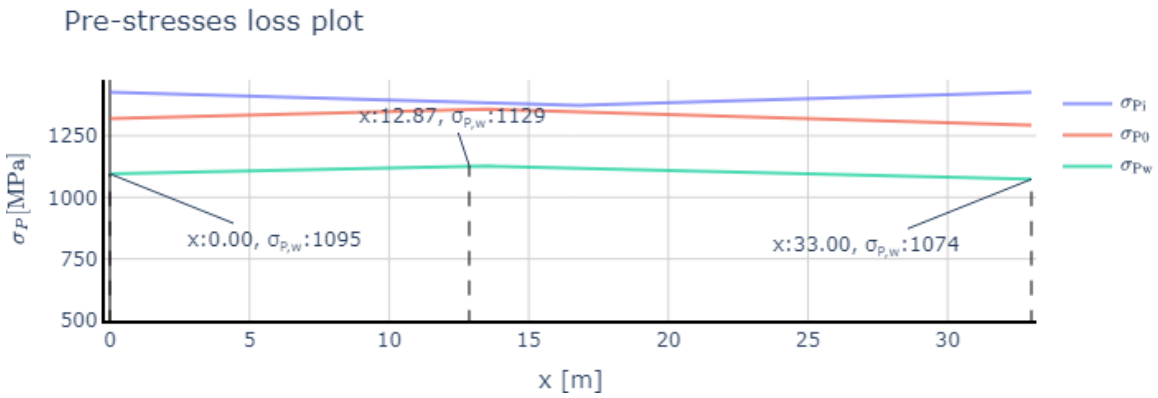

Figure 21: The prestress stresses over the length profile of the bridge.

Combining this loss plot and the pre-stress profile from figure 21 the loads shown in the report will be found

LC7.1 Wind loads

This section covers the calculations made for the windloads on the bridge in accordance with NEN-EN 1991-1-4.

The bridge is located in windarea I, and has terrain category 0. Next to that it is important to note that the free height of the bridge to ground level is 6 m.
Refering to NEN-EN 1991-1-4 some values for the variables can already be determined:

- The height of the traffic band $h_{traffic}$=4 m
- Wind direction factor c_{dir}=1.00 (NB. 4.2 (2))
- Seasonal factor c_{season}=1.00 (NB. 4.2 (2))
- Annual exceedance probability p=0.01 (NB. 4.2 (2))
- Orographic factor c_0=1 (4.3.1 (1), assumption)
- Maximum height for these calculations z_{max}=200 m (NB. 4.3.2 (1))
- Turbulence factor k_l=1 (NB. 4.4 (1))
- Volumetric weight of air ρ=1.25 kg/m^3 (NB. 4.5 (1))
- Reduced fundamental base wind speed $v^{**}_{b,0}$=25 m/s (NB. 8.1 (5))
- Building factor $c_s c_d$=1 (8.2 (1))
- Force coefficient z-direction $c_{f,z}$=1 (NB. 8.3.3 (1))

Now the steps outlined in NEN-EN 1991-1-4 + NB can be followed to calculate the windloads on the bridge.
The total height of the bridge can be calculated according to 8.3.1 (1):

$$d_{\text{tot}} = \max(h_{\text{girder}}, h_{\text{floor}} + t_{\text{ballast}} + h_{\text{sleeper}} + h_{\text{rail}} + h_{\text{traffic}}) \\ = \max(2.50, 0.50 + 1.01 + 0.22 + 0.16 + 4.00) = 5.19 \text{ m}$$

$c_{b,0}$=29.5 m/s can be found in table NB.1 and the values for K=0.200 and n=0.5 can be found in table NB.2. After that c_{prob} can be calculated:

$$c_{\text{prob}} = \left(\frac{1 - K \cdot \ln(-\ln(1-p))}{1 - K \cdot \ln(-\ln(0.98))}\right)^n = \left(\frac{1 - 0.200 \cdot \ln(-\ln(1-0.01))}{1 - 0.200 \cdot \ln(-\ln(0.98))}\right)^{0.5} = 1.04$$

Base wind speed v_b=30.64 m/s can now be calculated via 4.1 and 4.2:

$$v_{\text{b}} = c_{\text{dir}} \cdot c_{\text{season}} \cdot v_{\text{b,0}} \cdot c_{\text{prob}}$$

For the calculation of the reduced windspeed F^{**}_w, $v^{**}_{b,0}$=25.00 m/s should be used for calculating the windspeed and the resulting forces.
z_{min}=1.000 m and z_0=0.005 m can now be gathered from NB.3 - 4.1, such that k_r can be calculated with NB form 4.5:

$$k_{\text{r}} = 0.19 \cdot \left(\frac{z_0}{0.05}\right)^{0.07} = 0.19 \cdot \left(\frac{0.005}{0.05}\right)^{0.07} = 0.16$$

The reference height for the wind forces is taken as z = h_{ground}+0.5h_{girder}=6.00+0.5*2.50 = 7.25 m.

The roughness factor and additionally the average windspeed can now be calculated using formula 4.4.

$$c_{\mathrm{r}}(z) = k_{\mathrm{r}} \cdot \ln(\frac{z}{z_0}) = 0.16 \cdot \ln(\frac{7.25}{0.01}) = 1.18$$

$$v_{\mathrm{m}}(z) = c_{\mathrm{r}}(z) c_0(z) v_{\mathrm{b}} = 1.18 \cdot 1.00 \cdot 30.64 = 36.06\ \mathrm{m/s}$$

In similar fashion the turbulence intensity factor $\mathrm{l_v}$ can be calculated based on form. 4.7.

$$l_{\mathrm{v}}(z) = \frac{k_{\mathrm{l}}}{c_0(z) \cdot \ln(\frac{z}{z_0})} = \frac{1.00}{1.00 \cdot \ln(\frac{7.25}{0.01})} = 0.14$$

The base hydrostatic pressure $\mathrm{q_b}$ can be calculated using formula 4.10 and the following extreme hydrostatic pressure $\mathrm{q_p}$ from 4.8.

$$q_{\mathrm{b}} = \frac{1}{2} \cdot \rho v_{\mathrm{b}}^2 = \frac{1}{2} \cdot 1.25 \cdot 30.64^2 = 0.59\ \mathrm{kN/m^2}$$

$$q_{\mathrm{p}} = (1 + 7 l_{\mathrm{v}}(z)) \frac{1}{2} \cdot \rho v_{\mathrm{m}}(z)^2 = (1 + 7 \cdot 0.14) \cdot \frac{1}{2} \cdot 1.25 \cdot 36.06^2 = 1.59\ \mathrm{kN/m^2}$$

The wind load factor in x direction $\mathrm{c_{f,x}}$ can now be determined to be 2.02 following from fig. 8.3. $\mathrm{A_{ref,x}}$, $\mathrm{A_{ref,z}}$ can be determined by fig. 8.3 and fig. 8.6 respectively.

$$A_{\mathrm{ref,x}} = d_{\mathrm{total}} \cdot l_{\mathrm{bridge}}$$

$$A_{\mathrm{ref,x}} = b_{\mathrm{total}} \cdot l_{\mathrm{bridge}}$$

Finally the wind forces can be calculated using formula 5.3. The loads calculated from this formula are presented in the report. The loads denoted with ** represent reduced loads calculated with $\mathrm{v^{**}_{b,0}}$.

$$F_{\mathrm{w},i} = c_{\mathrm{s}} c_{\mathrm{d}} \cdot c_{\mathrm{f},i} \cdot q_{\mathrm{p}}(z_{\mathrm{e}}) A_{\mathrm{ref},i}$$

LC9.1.1 Train loads model LM71 M

This section covers the calculations made for the train load model LM71 in accordance with NEN-EN 1992-1. The load model as given in the eurocode is shown in figure 22.

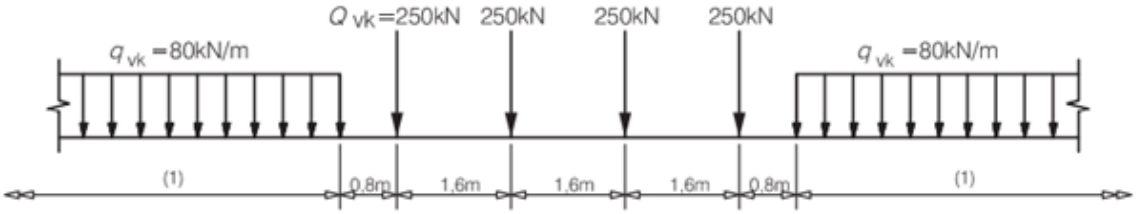

Figure 22: Load model LM71 as given in NEN-EN 1992-1

These loads need to be multiplied with α which is 1.21 according to the national annex and dynamic factor Φ_2 for carefully maintained rail. This factor can be calculated via formula 6.4 from NEN-EN 1991-2 where L_Φ can be calculated as twice the span of the deck from table 6.2 4.3.

$$\Phi_2 = \min(\max(\frac{1.44}{\sqrt{L_\Phi} - 0.2} + 0.82; 1); 1.67) = 1.27$$

The loads may be divided by the effective with over which they are spread, which is calculated in the main report. Next to that the point loads in the middle are assumed to be evenly destributed for middle part of the load.

The position of the load on the bridge has been choossen by running an influence line analysis which shows the position of the load which gives the highest possible moment at mid-span given in figure 23. Next to that also an excentricity e calculated with NEN-EN 1991-2 figure 6.3 is introduced for the LM71 loads. However the effect of this excentricity is not significant.

$$e = \frac{r}{18} = \frac{1435}{18} = 79.7 \text{ mm}$$

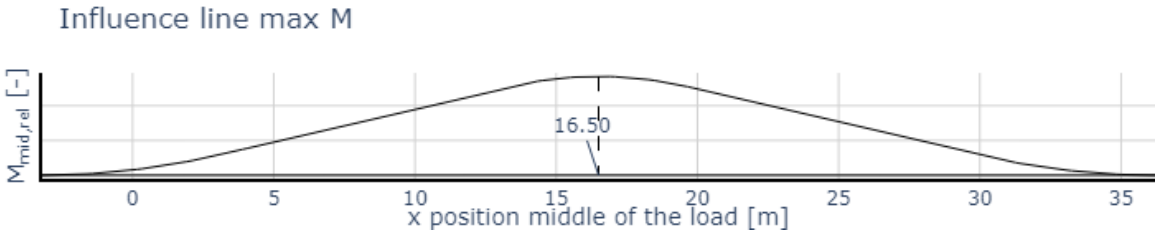

Figure 23: Influence line LM71 load model for the bridge, maximum moment

LC9.1.2 Train loads model LM71 V

The load resulting in the highest shear force is calculated in the same manner and results in the following influence line 24.

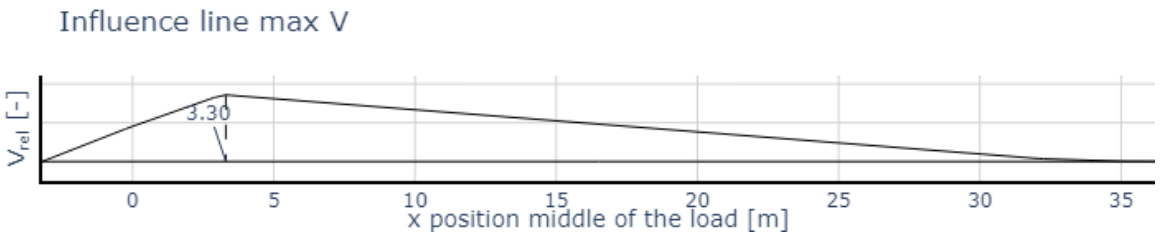

Figure 24: Influence line LM71 load model for the bridge, maximum shear force

LC9.3.1 Train loads model SW/2 M

This section covers the calculations made for the train load model SW/2 in accordance with NEN-EN 1992-1. The load model as given in the eurocode is shown in figure 25.

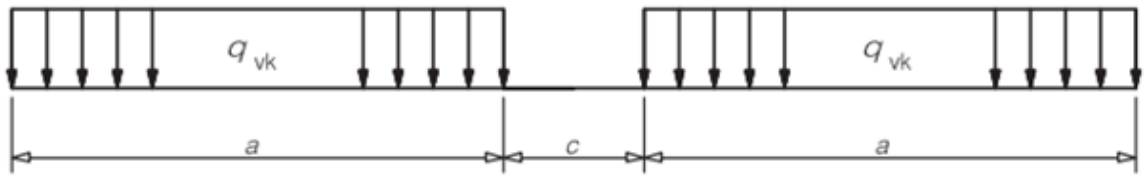

Figure 25: Load model SW as given in NEN-EN 1992-1

The values of a, c and q_{vk} are given as 25 m, 7 m, 150 kN/m respectively. Loads for SW/2 should not be multiplied with factor α and dynamic factor Φ_2.
Just like before these loads are spread over the effective width and the position has once again been choossen using influence lines. Figure 26 shows the influence line for max mid-span moment for this load model.

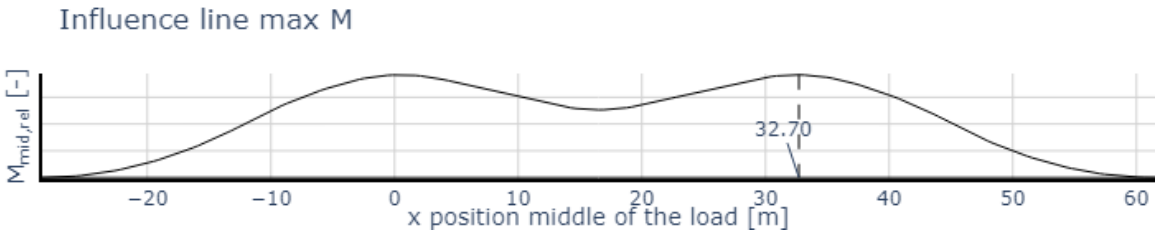

Figure 26: Influence line SW/2 load model for the bridge, maximum moment

LC9.3.2 Train loads model SW/2 V

In the same manner the influence line for the maximum shear force is displayed in figure 27.

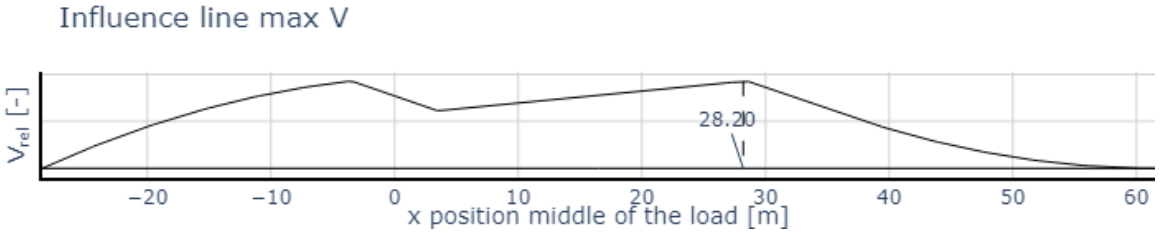

Figure 27: Influence line SW/2 load model for the bridge, maximum shear force

Annex D: Load combinations

The limit states ULS, SLS-Characteristic, SLS-Frequent, SLS-Quasi Permanent are considered in the FEM model.
The decisive load combination for ULS is the least favourable of NEN-EN 1990 form. 6.10a, 6.10b:

$$\sum_{j\geq 1} \gamma_{G,j} G_{k,j} + \gamma_P P + \gamma_{Q,1} \Psi_{0,1} Q_{k,1} + \sum_{i>1} \gamma_{Q,i} \Psi_{0,i} Q_{k,i}$$

$$\sum_{j\geq 1} \xi_j \gamma_{G,j} G_{k,j} + \gamma_P P + \gamma_{Q,1} Q_{k,1} + \sum_{i>1} \gamma_{Q,i} \Psi_{0,i} Q_{k,i}$$

For SLS-Characteristic the desicive load combination is governed by 6.14b:

$$\sum_{j\geq 1} G_{k,j} + P + Q_{k,1} + \sum_{i>1} \Psi_{0,i} Q_{k,i}$$

And for SLS-Frequent the desicive load combination is governed by 6.15b:

$$\sum_{j\geq 1} G_{k,j} + P + \Psi_{1,1} Q_{k,1} + \sum_{i>1} \Psi_{2,i} Q_{k,i}$$

Finally for SLS-Quasi Permanent the desicive load combination is governed by 6.16b:

$$\sum_{j\geq 1} G_{k,j} + P + \sum_{i\geq 1} \Psi_{2,i} Q_{k,i}$$

For the load combinations it is important to note that the bridge is CC3 and it only features one rail, the gamma factors are shown in table 7

$\gamma_{G,j,sup}$ 6.10a	1.40
$\gamma_{G,j,sup}$ 6.10b	1.25
$\gamma_{G,j,inf}$	0.90
$\gamma_{G,i}$ Train load gr16, gr17, gr26, gr27	1.25
$\gamma_{G,i}$ Train load other groups	1.50
$\gamma_{G,i}$ Wind load	1.65
$\gamma_{G,i}$ Other variable loads	1.65

Table 7: γ factors from NEN-EN 1990 Table NB.17

The Ψ factors from NEN-EN 1990 table A2.3 can be translated to the different limit states as shown in tables 8 - 11:

	LM71				SW/2	
Load combination	gr11	gr12	gr13	gr14	gr16	gr17
LC1 Permanent loads	1.00					
LC4 Other variable loads	0.80					
LC7.1 Wind loads	0.75			0.75		
LC7.2 Reduced wind loads	1.00			1.00		
LC9.1.1 Train loads model LM71 M	0.80		0.40			
LC9.3.1 Train loads model SW/2 M					0.80	

Table 8: Ψ factors for form. 6.10a

	LM71				SW/2		Wind			
Load combination	gr11	gr12	gr13	gr14	gr16	gr17	gr11	gr12	gr14	gr15
LC1 Permanent loads	1.00									
LC4 Other variable loads	0.80									
LC7.1 Wind loads	0.75			0.75			1.00			
LC7.2 Reduced wind loads	1.00			1.00			1.00			
LC9.1.1 Train loads model LM71 M	1.00		0.50				0.80		0.40	
LC9.3.1 Train loads model SW/2 M					1.00					

Table 9: Ψ factors for form. 6.10b and 6.14b

	LM71				SW/2		Wind	Wind deflection			
Load combination	gr11	gr12	gr13	gr14	gr16	gr17	force	gr11	gr12	gr14	gr15
LC1 Permanent loads	1.00										
LC4 Other variable loads											
LC7.1 Wind loads							0.50				
LC7.2 Reduced wind loads											
LC9.1.1 Train loads model LM71 M	0.80		0.40					1.00		0.50	
LC9.3.1 Train loads model SW/2 M					0.80						

Table 10: Ψ factors for form. 6.15b

Load combination	Quasi-permanent
LC1 Permanent loads	1.00
LC4 Other variable loads	
LC7.1 Wind loads	
LC7.2 Reduced wind loads	
LC9.1.1 Train loads model LM71 M	
LC9.3.1 Train loads model SW/2 M	

Table 11: Ψ factors for form. 6.16b

From these factors the decisive load combinations can be summarized as shown in tables 12 - 16. The wind and train loads are exclusive load cases, meaning that e.g. both wind loads can not be present at the same time.

Load combination	gr11 LM71	gr16 SW/2	gr17 SW/2
LC1 Permanent loads	1.40		
LC4 Other variable loads	1.32		
LC7.1 Wind loads	1.24		
LC7.2 Reduced wind loads	1.65		
LC9.1.1 Train loads model LM71 M	1.20		
LC9.3.1 Train loads model SW/2 M		1.00	

Table 12: ULS 6.10a

Load combination	gr11 LM71	gr16 SW/2	gr17 SW/2	gr11 Wind
LC1 Permanent loads	1.25			
LC4 Other variable loads	1.32			
LC7.1 Wind loads	1.24			1.65
LC7.2 Reduced wind loads	1.65			1.65
LC9.1.1 Train loads model LM71 M	1.50			1.20
LC9.3.1 Train loads model SW/2 M		1.25		

Table 13: ULS 6.10b

Load combination	gr11 LM71	gr16 SW/2	gr17 SW/2	gr11 Wind
LC1 Permanent loads	1.00			
LC4 Other variable loads	0.80			
LC7.1 Wind loads	0.75			1.00
LC7.2 Reduced wind loads	1.00			1.00
LC9.1.1 Train loads model LM71 M	1.00			0.80
LC9.3.1 Train loads model SW/2 M		1.00		

Table 14: SLS 6.14b

Load combination	gr11 LM71	gr16 SW/2	gr17 SW/2
LC1 Permanent loads	1.00		
LC4 Other variable loads			
LC7.1 Wind loads			
LC7.2 Reduced wind loads			
LC9.1.1 Train loads model LM71 M	0.80		
LC9.3.1 Train loads model SW/2 M		0.80	

Table 15: SLS 6.15b

Load combination	Quasi-permanent
LC1 Permanent loads	1.00
LC4 Other variable loads	
LC7.1 Wind loads	
LC7.2 Reduced wind loads	
LC9.1.1 Train loads model LM71 M	
LC9.3.1 Train loads model SW/2 M	

Table 16: SLS 6.16b

Annex E: ULS Girder stirrup calculations

This section will feature the calculation of the stirrups of the girder in ULS. The angle of θ is 21.8°.

Torsion

The decisive torsional moment T_{Ed} in the beam follows from the FEM results and is: 1578 kNm.
For determining the shear stresses the effective width t_{eff} should first be calculated according to NEN-EN 1992-1-1 figure 6.11:

$$t_{\text{eff}} = \min((W_{\text{gir}} - W_{\text{cu}}) \cdot 0.5; \frac{A_{\text{gir}}}{u_{\text{gir}}}) = 125 \text{ mm}$$

Where u_{gir}=8000 mm, is the perimeter of the girder.

With the effective effective width A_k as described in NEN-EN 1992-1-1 figure 6.11 can be calculated.

$$A_{\text{k}} = (h_{\text{gir}} - t_{\text{eff}}) \cdot (W_{\text{gir}} - t_{\text{eff}}) = 3264226 \text{ mm}^2$$

The required area of longitudinal reinforcement required for this torsion $A_{sl,T,req}$ can be calculated with formula 6.28.

$$A_{\text{sl,T,req}} = \frac{u_{\text{k}} T_{\text{Ed}} \cot(\theta)}{2 A_{\text{k}} f_{\text{yd}}} = 9741 \text{ mm}^2$$

Using u_k = 6997 mm, the perimeter of A_k.
The shear stress τ_T due to torsion can be calculated using formula 6.26.

$$\tau_{\text{T}} = \frac{T_{\text{Ed}}}{2 A_{\text{k}} t_{\text{eff}}} = 1.93 \text{ MPa}$$

Using these results and formula 6.27 an equivalent shear force $V_{Ed,T}$ on the vertical ribs can be calculated.

$$V_{\text{Ed,T}} = \tau_{\text{T}} t_{\text{eff}} z_{\text{y}} = 574 \text{ kN}$$

Using z_y=h_{gir}-t_{eff}=2375 mm.
Finally the required shear reinforcement for torsion in the vertical ($A_{sw,T}$) and horizontal ($A_{sw,T,hor}$) stirrups parts can be calculated using 6.8.

$$A_{\text{sw,T,req}} = \frac{V_{\text{Ed,T}}}{z f_{\text{yd}} \cot(\theta)} = 242 \text{ mm}^2$$

$$A_{\text{sw,T,hor,req}} = \frac{T_{\text{Ed}}}{2 A_{\text{k}} f_{\text{yd}} \cot(\theta)} = 223 \text{ mm}^2$$

Shear

The decisive shear force V_{Ed} in the beam follows from the FEM results and is: 3470 kN. Continuing from the torsion results, the maxium shear force in a wall with thickness t_{eff} in the cross-section can be calculated. It is assumed that 60% of the shear force will be transfered by the middle stirrup and the other 40% will be distributed to the outside walls, where the shear is also present:

$$V_{\text{Ed,max}} = V_{\text{Ed}} \cdot 0.2 + V_{\text{Ed,T}} = 1267892 \text{ kN}$$

To check if calculated stirrups are needed the check $V_{Ed,max} < V_{Rd,c}$ using formula 6.4:

$$V_{\text{Rd,c}} = \frac{Ib_{\text{w}}}{S}\sqrt{f_{\text{ctd}}^2 + \alpha_{\text{l}}\sigma_{\text{cp}}f_{\text{ctd}}} = 510154 \text{ kN}$$

Where α_l=1 and σ_P is calculated as:

$$\sigma_{\text{cp}} = \frac{\sigma_{\text{Pw}}A_{\text{P}}}{A_{\text{gir}}} = 5.40 \text{ MPa}$$

From this we can conclude that $V_{Ed,max} > V_{Rd,c}$ and the assumption that stirrups are needed is justified. The required stirrup area per zone can be calculated, again using 6.8:

$$A_{\text{sw,I,req}} = \frac{0.2V_{\text{Ed}}}{zf_{\text{yd}}\cot(\theta)} = 293 \text{ mm}^2$$

$$A_{\text{sw,II,req}} = \frac{0.6V_{\text{Ed}}}{zf_{\text{yd}}\cot(\theta)} = 878 \text{ mm}^2$$

$$A_{\text{sw,III,req}} = \frac{0.2V_{\text{Ed}}}{zf_{\text{yd}}\cot(\theta)} = 293 \text{ mm}^2$$

Suspension force and fixed end moment

For the calculation of the hanging moment and suspension forces NSRL1015 is used as guideline. The suspension force and fixed end moment of the floor acting on the girder cause tension stresses in the cross-section as shown in figure 28.

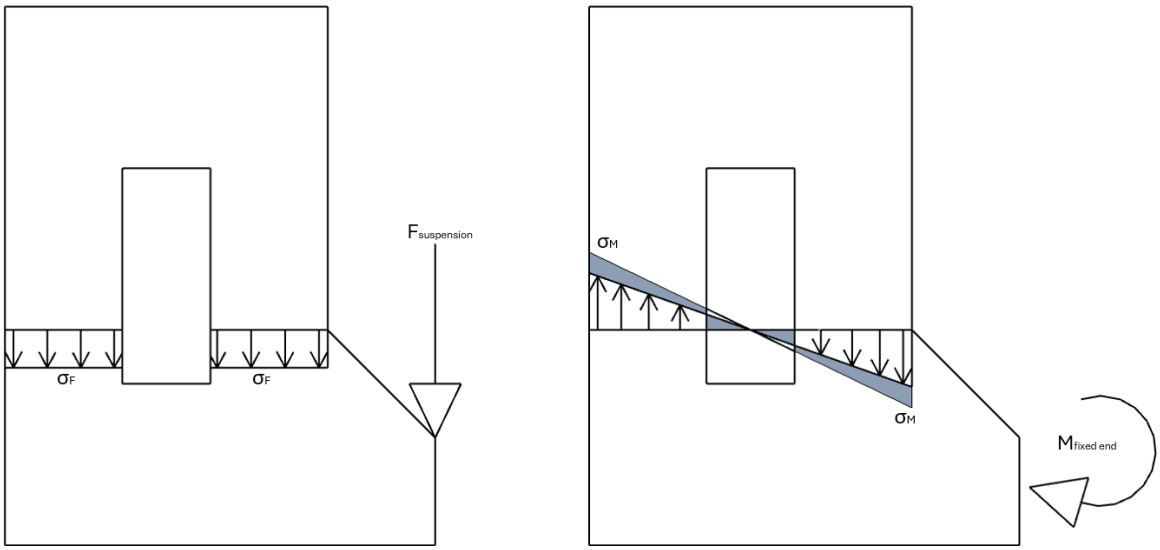

Figure 28: Stress distribution in cross-section

These stresses need to resisted by stirrups in the girder. Because the critical line for the connection of the girder and the floor is along the top of the haunch. This way only the load that needs to be carried by the top part of the girder needs to be accounted for because this needs to be carried to the top part of the cross-section. This is translated to a reduction factor based on the area of the cross-section, as described in NSRL1015.

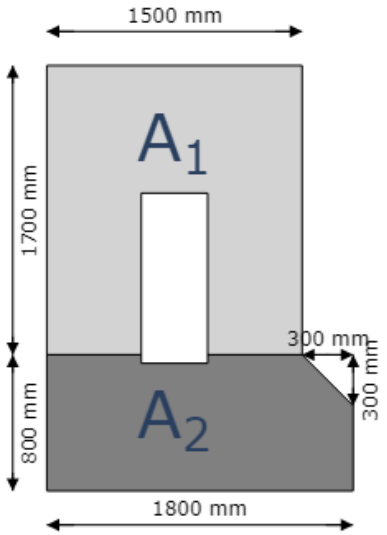

Figure 29: Area's used for reduction factor

$$\alpha_A = \frac{A_1}{A_1 + A_2} = \frac{2530500}{3555000} = 0.71$$

For the maximum suspension force acting on a girder it should be incorporated that the decisive train load SW/2 does not act in the middle of the floor, rather at x = 3.4 m, as shown in figure 30. This means that this load should be distributed to the right girder for the maximum resulting force.

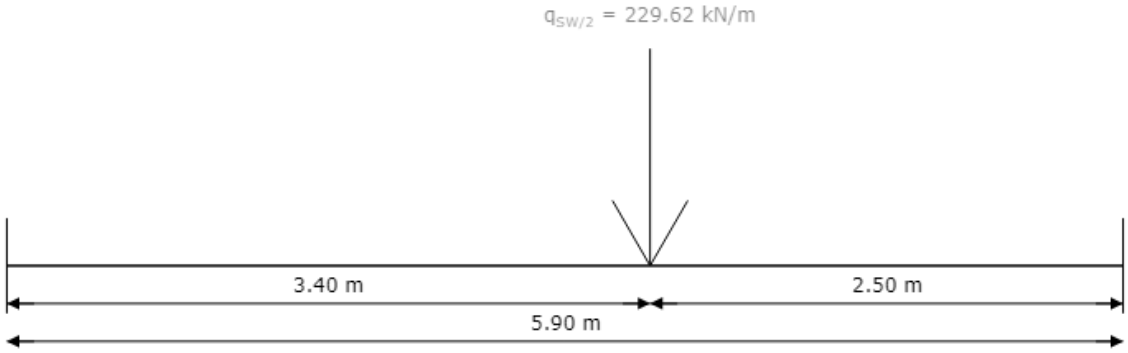

Figure 30: Position of the train load as seen on the cross-section of the floor

$$q_{\text{SW/2}} = 150\alpha\phi_2 = 150 \cdot 1.21 \cdot 1.27 = 230 \text{ kN/m}$$

$$F_{\text{SW/2}} = \frac{q_{\text{SW/2}}a}{a + 2 \cdot \frac{1}{2} \cdot 2.50}\frac{3.40}{5.90} = 120 \text{ kN/m}$$

Using the length of the load model SW/2 a = 25 m. The self-weight of the bridge and dead loads of the train infrastructure can be divided by 2 to find F_G = 73 kN/m. Incorporating the load factors to find the suspension force:

$$F_{\text{sus}} = \max(1 \cdot F_{\text{SW/2}} + 1.4 \cdot F_{\text{G}}; 1.25 \cdot F_{\text{SW/2}} + 1.25 \cdot F_{\text{G}}) = 241 \text{ kN/m}$$

The fixed end moment can be calculated using the structural model in figure 30, conservatively assuming fully clamped boundary conditions.

$$M_{\text{SW/2}} = \frac{q_{\text{SW/2}} \cdot 3.4^2 \cdot 2.5}{5.9} = 419 \text{ kNm/m}$$

Next to that the suspension force also causes a moment:

$$M_{\text{sus}} = F_{\text{G}} \cdot \frac{1}{2} W_{\text{girder}} = 83 \text{ kNm/m}$$

The maximum fixed end moment can now be calculated as:

$$M_{\text{fix}} = \max(1 \cdot M_{\text{SW/2}} + 1.4 \cdot M_{\text{sus}}; 1.25 \cdot M_{\text{SW/2}} + 1.25 \cdot M_{\text{sus}}) = 241 \text{ kNm/m}$$

The required area of the reinforcement can now be calculated according to the stresses shown in figure 28.

Please note that the stress distribution changes compared to the cross-section without a cutout, however the resulting force that needs reinforcement is still the same as the

area under the stress diagram is the same. The grey area that is 'in the cutout' is the same as the grey area for which the distribution is increased.

$$A_{sw,F} = \frac{\alpha_A F_{sus}}{f_{yd}} = 396 \text{ mm}^2$$

$$A_{sw,M} = \frac{\alpha_A M_{fix}}{z f_{yd}} = 1126 \text{ mm}^2$$

Using $z = 0.9W_{gir}$ the total additional required area of stirrups in zone III can be calculated.

$$A_{sw,III,req} = A_{sw,F} + A_{sw,M} = 1522 \text{ mm}^2$$

Evaluation

The unity checks per zone of stirrups can now be calculated.

$$u.c_{sl,T} = \frac{A_{sl,T,req}}{A_{sl,T}} = \frac{9741}{10053} = 0.97$$

$$u.c_{sw,T,hor} = \frac{A_{sl,T,hor,req}}{A_{sl,T,hor}} = \frac{223}{565} = 0.39$$

$$u.c_{sw,I} = \frac{A_{sl,I,req}}{A_{sl,I}} = \frac{535}{565} = 0.95$$

$$u.c_{sw,II} = \frac{A_{sl,II,req}}{A_{sl,II}} = \frac{878}{905} = 0.97$$

$$u.c_{sw,III} = \frac{A_{sl,III,req}}{A_{sl,III}} = \frac{2056}{2122} = 0.97$$

Please note that the required longitudinal reinforcement for torsion at the bottom of the cross-section is added to the longitudinal reinforcement for moment and normal force.

Annex F: ULS Girder cross-section calculations

This section will feature the calculation for the girder in ULS. The decisive moment for the girder M_{Ed} = 21027 kNm.

Cross-sectional analysis

To calculate the moment resistance the stress and strain diagrams of the cross-section need to be determined. This is done with an automatic algorithm that solves the force equilibrium $\Sigma F_h = - N_c + N_c + F_{Pw} + \Delta F_P = 0$ to find figures 31 and 32.

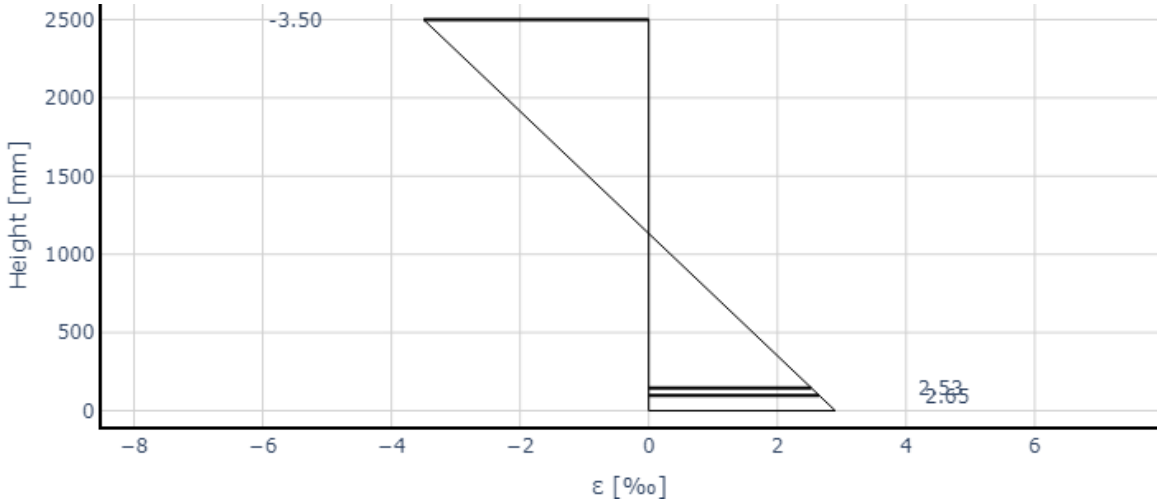

Figure 31: Strain diagram

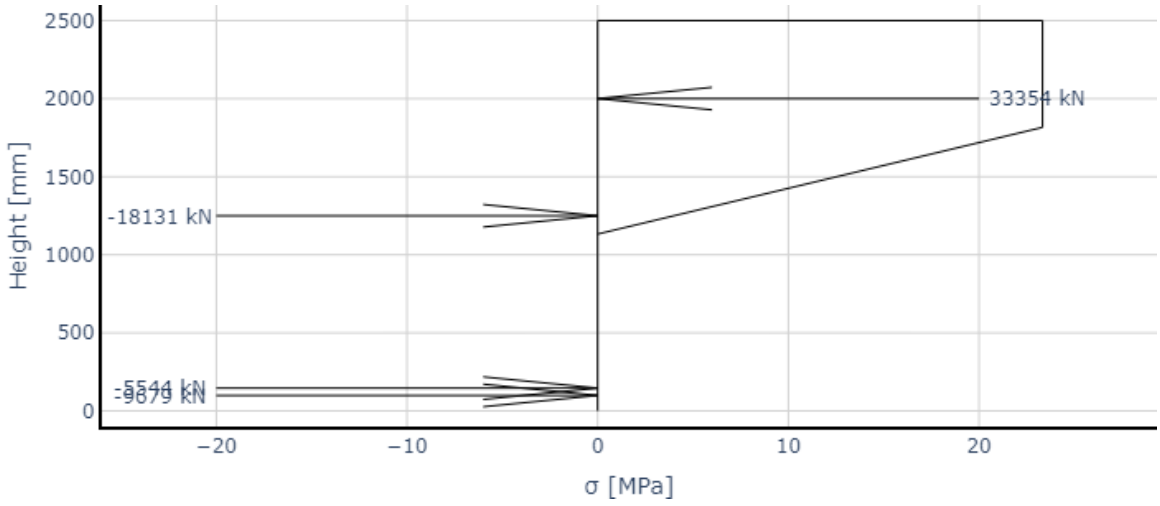

Figure 32: Stress diagram

To justify these diagrams the following calculations are made.

$$N_c = \alpha f_{cd} w_{gir} x_u = 33354 \text{ kN}$$

Here α = 0.75 and x_u = 1367 mm. Due to the cutout in the girder the effective width of the bottom 617 mm of the compression zone is reduced to W=1110 mm. This leads to a

lower N_c.
The force in the steel can be calculated using:

$$N_s = A_s \cdot \min(E_s \varepsilon_s; f_{yd}) = 9679 \text{ kN}$$

Where the area of longitudinal reinforcement required for torsion $A_{sl,T,req}$ = 1826.4389332035398 mm^2 is subtracted from A_s and:

$$\varepsilon_s = \varepsilon_{cu} \frac{d_s - x_u}{x_u} = 2.65 \text{ ‰}$$

Using ε_{cu} = 3.50‰.
For the prestress force both the pre-stress force F_{Pw} and the force induced by the strain in the pre-stress ΔF_P are important. First F_{Pw} is calculated:

$$F_{Pw} = \sigma_{Pw} A_P = 18131 \text{ kN}$$

Now ΔF_P can be calculated:

$$\Delta\varepsilon_P = \varepsilon_{cu} \frac{d_P - x_u}{x_u} = 2.53 \text{ ‰}$$

$$\varepsilon_{P,tot} = \frac{F_{Pw}}{A_P E_P} + \Delta\varepsilon_P = 8.27 \text{ ‰}$$

$$\Delta F_{Pw} = \sigma_P(\varepsilon_P) A_P - F_{Pw} = 5544 \text{ kN}$$

Where σ_P is dependent on the strain of the pre-stress steel via the bilinear relationship\nIt can now be verfied that $\Sigma F_h = 0$. The moment resistance can now be calculated using:

$$e_P = d_P - \frac{1}{2} h_{gir};\ e_s = d_s - \frac{1}{2} h_{gir}$$

The lever arm for concrete for concrete needs to be calculated by finding the position of the resultant force of the compression zone: 2001 mm

$$M_{Rd} = N_c e_c + e_s N_s + \Delta F_P e_P = 46206 \text{ kNm}$$

Finally the unity check can be calculated:

$$\text{u.c}_{M,gir} = \frac{M_{Ed}}{M_{Rd}} = \frac{21027}{46206} = 0.46$$

Compression zone height

NEN-EN 1992-1-1 NB 6.1 (9) describes the maximum height of the concrete compression zone of concrete girders:

$$\frac{x_u}{d} \leq \frac{500}{500 + f} = 0.34$$

Where f=962 MPa is the weighted steel strength of the pre-stress and steel where the σ_{Pw} is subtracted from the pre-stress steel strength.
This is not satisfied as $x_u/d=0.57$.However the pre-stress can fictitiously be lowered to make sure this requirement is satisfied. It is important to note that M_{Ed} will increase when lowering pre-stress and M_{Rd} will decrease. When the pre-stress is lowered to 57 %, M_{Ed} becomes 28145 kNm. When also lowering A_P with this factor, the new distriubutions can be found:

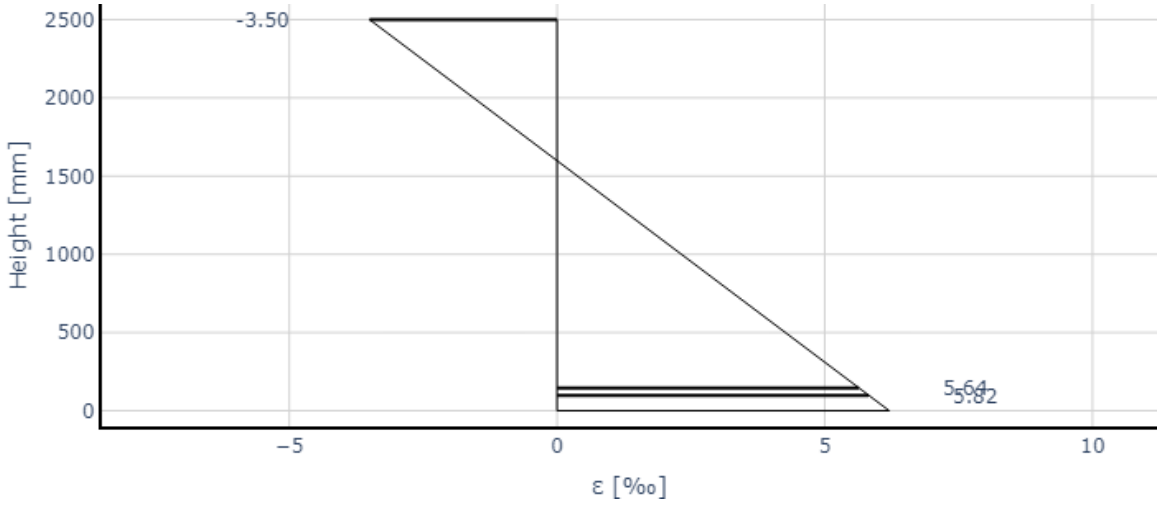

Figure 33: Strain diagram

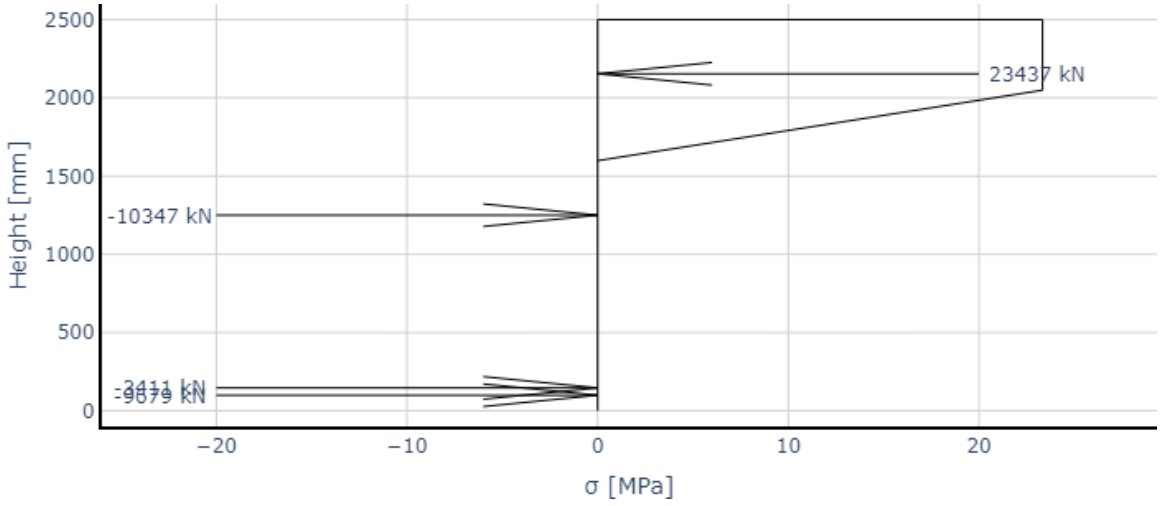

Figure 34: Stress diagram

Using the same equations as before it is obtained that:

$$M_{\text{Rd}} = N_{\text{c}} e_{\text{c}} + e_{\text{s}} N_{\text{s}} + \Delta F_{\text{P}} e_{\text{P}} = 27924 \text{ kNm}$$

Resulting in:

$$\text{u.c}_{\text{M,rot}} = \frac{M_{\text{Ed}}}{M_{\text{Rd}}} = \frac{28145}{27924} = 1.01$$

Also the maximum height of the compression zone is now sufficient:

$$\frac{x_{\text{u}}}{d} \leq \frac{500}{500 + f} = 0.38$$

$$0.38 \leq 0.38$$

Annex G: ULS Floor cross-section calculations

In this chapter the ULS calculations for the floor will be displayed.

y-direction

The decisive moment in the floor is at midspan: $M_yD+ = 577$ kNm/m. Again the stress-strain distribution can be determined given in figure 35 and 36, making sure that $\Sigma F_h = 0$.

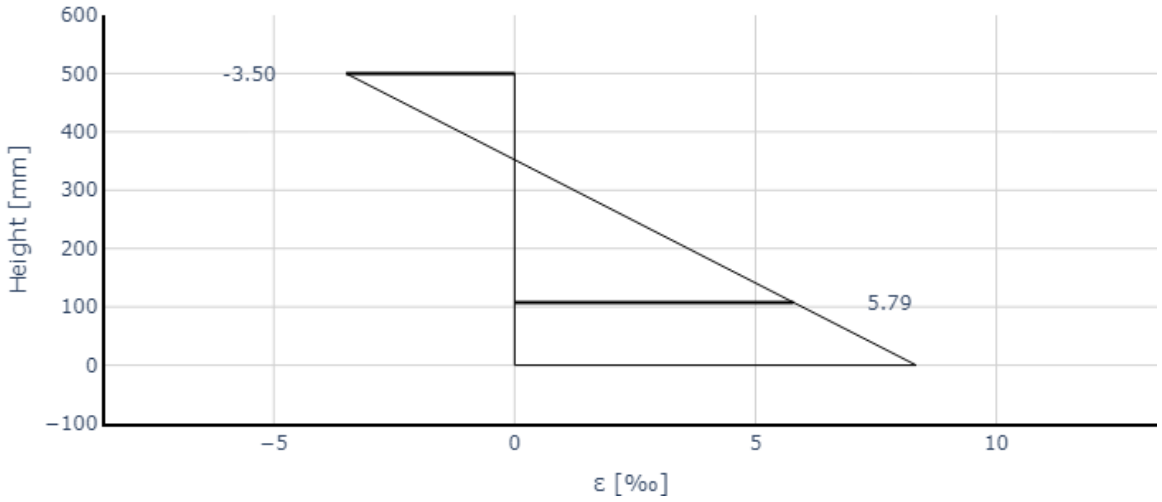

Figure 35: Strain diagram

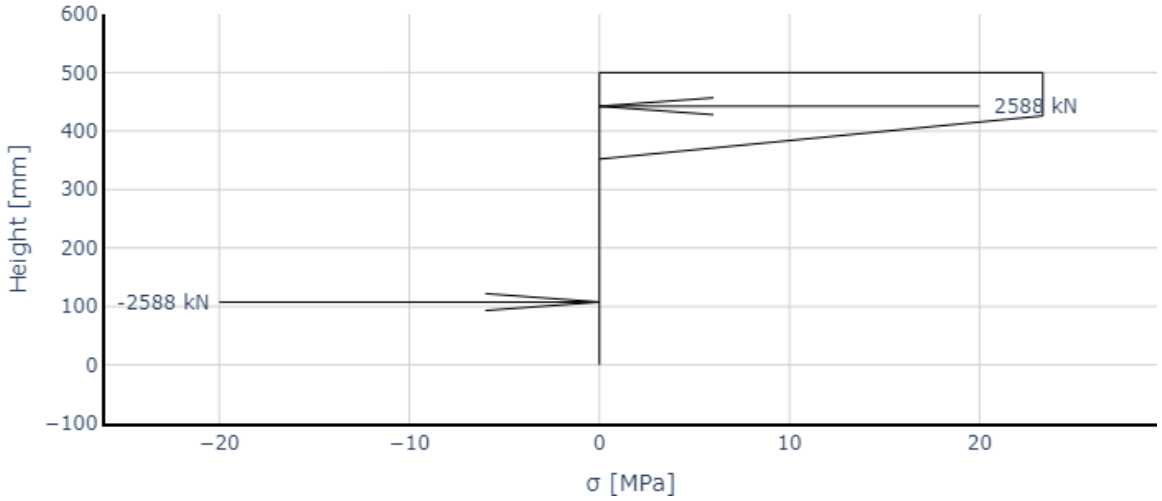

Figure 36: Stress diagram

The calculations for these diagrams are given below.

$$N_c = \alpha f_{cd} w_{gir} x_u = 2588 \text{ kN}$$

Here α = 0.75 and x_u = 148 mm.
The force in the steel can be calculated using:

$$N_s = A_s \cdot \min(E_s \varepsilon_s; f_{yd}) = 2588 \text{ kN}$$

Where:

$$\varepsilon_s = \varepsilon_{cu} \frac{d_s - x_u}{x_u} = 5.79\ ‰$$

Using ε_{cu} = 3.50‰.
The moment capacity can be calculated using:

$$M_{Rd} = N_s z = 867\ \text{kNm}$$

Using $z = d_s - \beta x_u$.
Finally the unity check can be calculated:

$$\text{u.c}_{M,floor,y} = \frac{M_{Ed}}{M_{Rd}} = \frac{577}{867} = 0.67$$

x-direction

This whole calculation can be repeated for the reinforcement in longitudinal directon: M_xD+ = 204 kNm/m. be determined given in figure 37 and 38, making sure that ΣF_h.

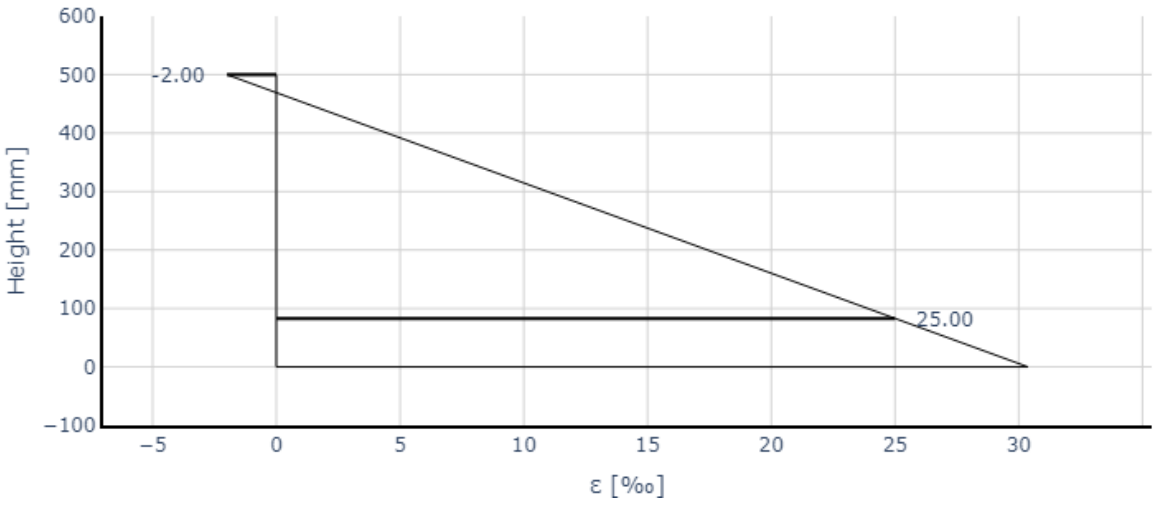

Figure 37: Strain diagram

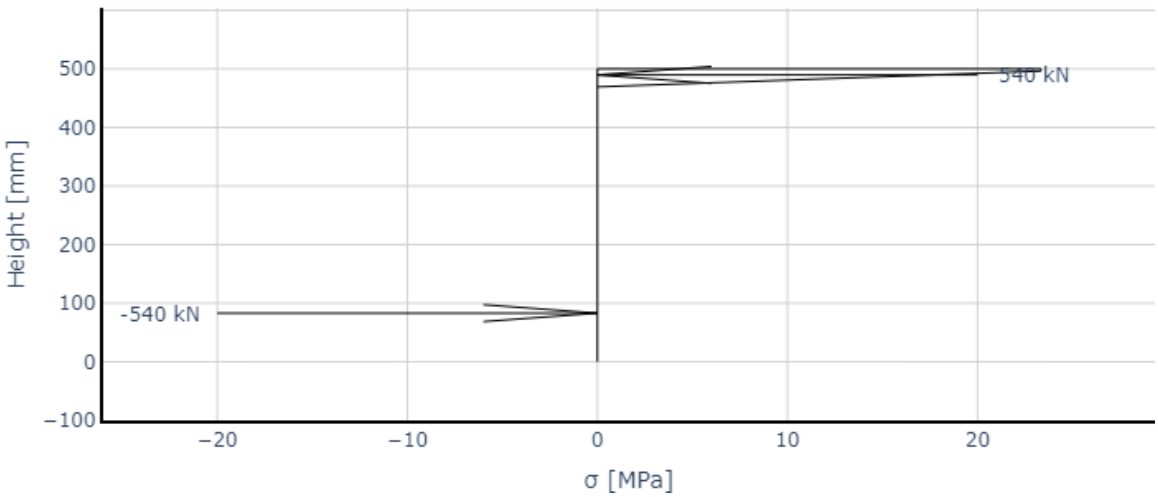

Figure 38: Stress diagram

The calculations for these diagrams are given below.

$$N_c = \alpha f_{cd} w_{gir} x_u = 540 \text{ kN}$$

Here α = 0.75 and x_u = 31 mm.
The force in the steel can be calculated using:

$$N_s = A_s \cdot \min(E_s \varepsilon_s; f_{yd}) = 540 \text{ kN}$$

Where:

$$\varepsilon_s = \varepsilon_{cu} \frac{d_s - x_u}{x_u} = 25.00 \text{ ‰}$$

Using ε_{cu} = 2.00‰.
The moment capacity can be calculated using:

$$M_{Rd} = N_s z = 220 \text{ kNm}$$

Using $z = d_s - \beta x_u$
Finally the unity check can be calculated:

$$\text{u.c}_{M,floor,y} = \frac{M_{Ed}}{M_{Rd}} = \frac{204}{220} = 0.93$$

Annex H: ULS Longitudinal shear calculations

In this chapter the ULS calculations for the longitudinal shear between the floor and the girder will be described according to the calculation method of NEN-EN 1992-1-1 6.2.4. This method calculates the longitudinal shear as:

$$v_{\text{Ed}} = \frac{\Delta F_{\text{d}}}{h_{\text{f}} \Delta x} = 0.46 \text{ MPa}$$

The maximum value that may be assumed for Δx is half the distance between the cross-section where the moment is 0 and the cross-section where the moment is at a maximum (6.2.4 (3)). In this case this means that Δx half the length of the span of the bridge. The other parameters are summarized in figure 39:

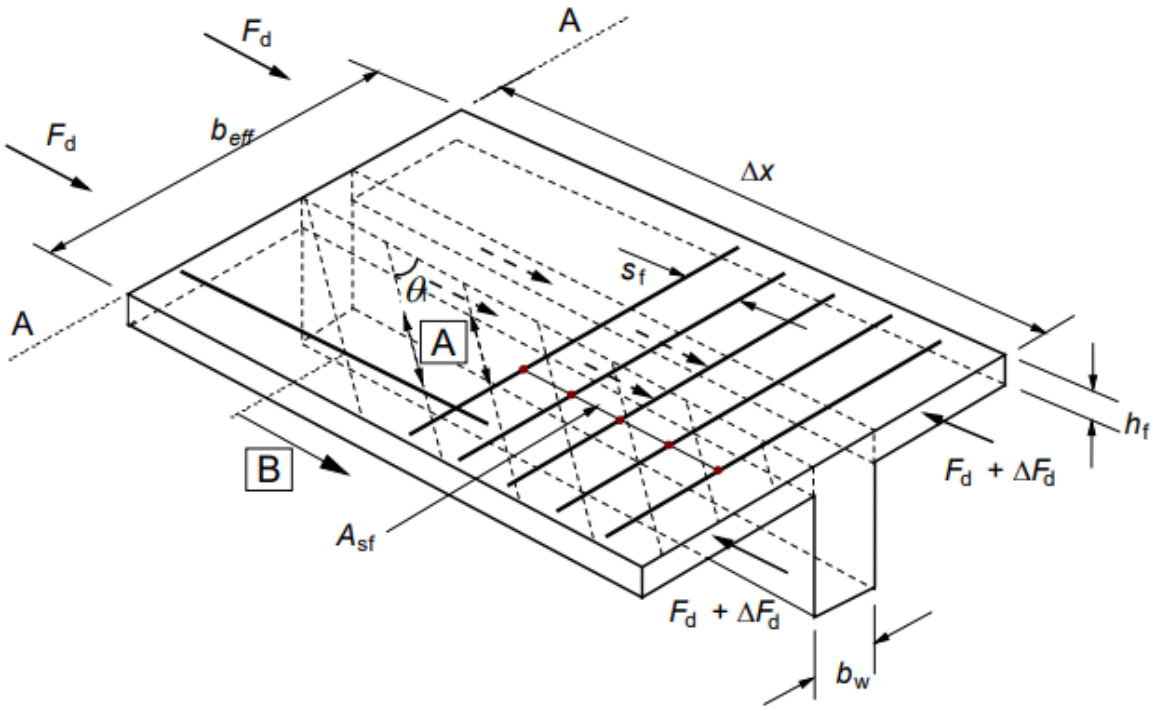

Figure 39: NEN-EN 1992-1-1 figure 6.7

The figure shows a T-girder however for a trough girder bridge one flange can be ignored. To obtain the maximum shear stress calculated above an automatic algorithm was used to find Δx = 0.25 m and ΔF_d = 57 kN, between the sections at x = 7.00 m and x = 7.25 m. The forces are obtained by integrated the 2D forces of the floor over the effective width of the floor on one side. To check if reinforcement is required the following check is performded:

$$v_{\text{Ed}} < k f_{\text{ctd}}; 0.46 < 0.59$$

This check is O.K. so no reinforcement is needed.

Annex I: ULS Splitting forces ends of deck

In this chapter the ULS calculations for the splitting reinforcement at the ends of the deck will be performed. A tension force in the ends of the deck is introduced due to the introduction of the prestress as shown in figure 40:

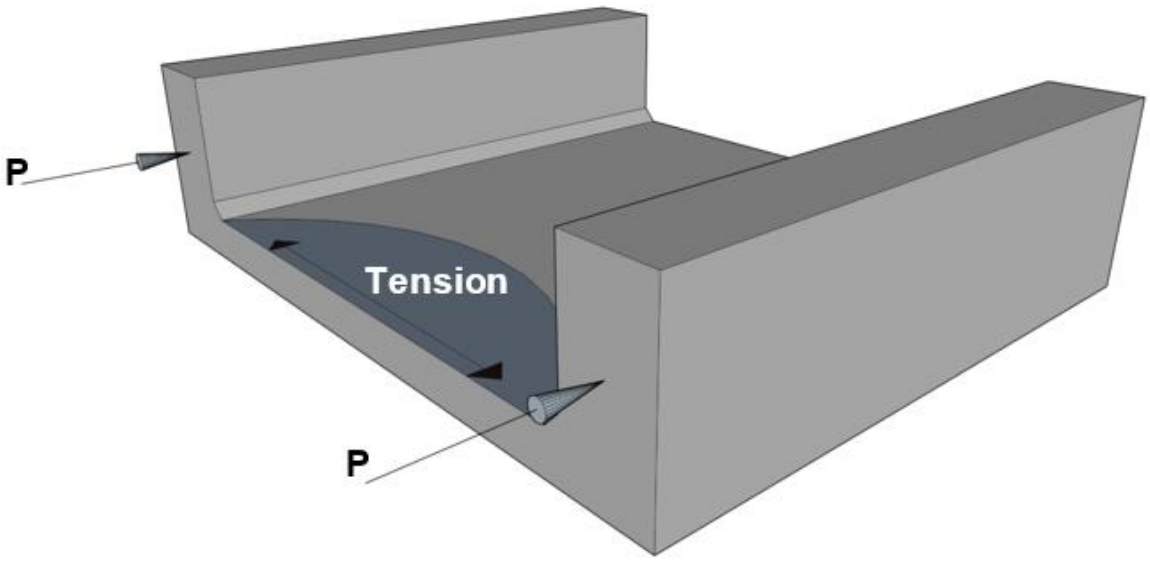

Figure 40: Splitting forces at the ends of the deck

To reinforce the bridge against these tension stresses, extra reinforcement is needed. The required reinforcement is calculated using a strut and tie model. First the equivalent stress in the whole bridge in the bernouilli zone at x = 4450 mm due to pre-stress is calculated.

$$\sigma_{\text{eq}} = \frac{2F_P}{A_{\text{P}}} = 3.53 \text{ MPa}$$

Using this stress the force in the girders and beam can be calculated:

$$F_{\text{floor/}} = \frac{1}{2}\sigma_{\text{eq}} A_{\text{floor}} = 5208 \text{ kN}$$

$$F_{\text{girder}} = \sigma_{\text{eq}} A_{\text{girder}} = 11864 \text{ kN}$$

With these values the STM shown in figure 41 can be obtained:

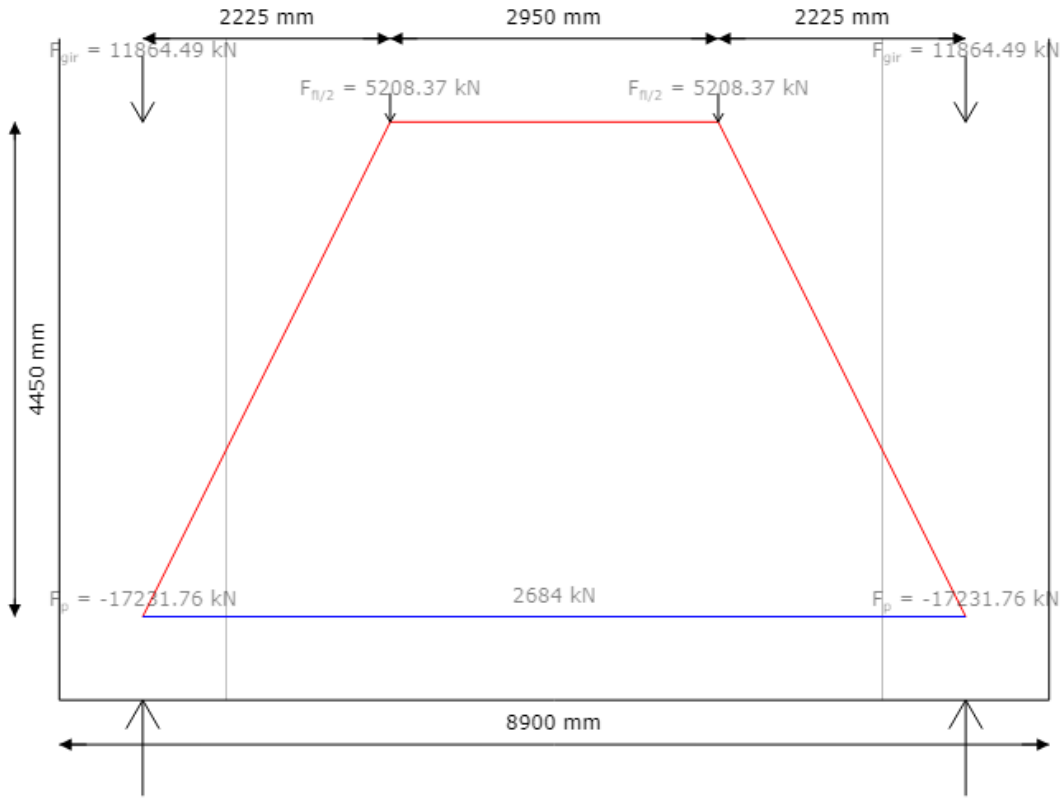

Figure 41: Strut and tie model splitting reinforcement

With the calculated force the stress in the splitting reinforcement can be calculated knowing that the designed splitting reinforcement is 9⌀32:

$$\sigma_{\text{spl}} = \frac{F_{\text{spl}}}{A_{\text{spl}}} = \frac{2683635}{7238} = 371 \text{ MPa}$$

Now the unity check can be calculated:

$$\text{u.c}_{\text{spl}} = \frac{\sigma_{\text{spl}}}{f_{\text{yd}}} = \frac{371}{434} = 0.85$$

Annex J: SLS Girder stress checks

This annex will show two SLS stresses checks for the girder.

Tension checks

The first check is an extra check required by OVS00030-6 as an amendment to NEN-EN 1992-1-1 7.3.1, which requires that:

1. In SLS-quasi: $\sigma_{ct} < 0$
2. In SLS-freq: $\sigma_{ct} < 0.5\, f_{ctk,0.05}$ and $\sigma_{ct} < 0.5\, f_{ctk,0.05}$
3. In SLS-char: $\sigma_{ct} < 0.5\, f_{ctk,0.05}$ and $\sigma_{ct} < 0.5\, f_{ctk,0.05}$

These stresses can be calculated using:

$$\sigma_{ct} = \frac{M_{Ed}}{W_{bot}} + \frac{N_{Ed}}{A_c}$$

Due to the pre-stress the axial force is always compressive. Now for each limit state the highest stress can be computed:

$$\sigma_{ct,quas} = \frac{M_{Ed,quas}}{W_{bot}} + \frac{N_{Ed,quas}}{A_c} = \frac{2421}{W_{bot}} + \frac{-15493}{A_t} = -2.41 \text{ MPa}$$

$$\sigma_{ct,quas} < 0.00$$

So ,the SLS-quas check is O.K.

$$\sigma_{ct,freq} = \frac{M_{Ed,freq}}{W_{bot}} + \frac{N_{Ed,freq}}{A_c} = \frac{10522}{W_{bot}} + \frac{-17899}{A_t} = -0.35 \text{ MPa}$$

$$\sigma_{ct,freq} < 1.10$$

So, the SLS-freq check is O.K.

$$\sigma_{ct,char} = \frac{M_{Ed,char}}{W_{bot}} + \frac{N_{Ed,char}}{A_c} = \frac{12896}{W_{bot}} + \frac{-18186}{A_t} = 0.34 \text{ MPa}$$

$$\sigma_{ct,char} < 1.10$$

So, the SLS-char check is O.K.

Compression checks

Next to the tension stress, the compressive stress in the bridge at t=0 should not exceed the compression strength. This check is performed in SLS-quasi permanent, because that is representative of the forces acting at t=0. The maximum compressive stress can be calculated similar like before looking at both the situation with maximum compressive force and max moment to find:

$$\sigma_c = -\frac{M_{Ed}}{W_{top}} + \frac{N_{Ed}}{A_c} = 5.68 \text{ MPa}$$

Concluding with the unity check:

$$\text{u.c}_{compr} = \frac{\sigma_c}{f_{cd}} = \frac{5.68}{23} = 0.24$$

Annex K: SLS Girder main tension stress

In this chapter the main tension stress in the girder will be calculated in accordance with NSRL1015, to limit crack formation at the haunch. The main stress will ocur just above the haunch at the inner wall of the girder and should be checked at 0.8d and 2d away from the bearing cross-sections. At x < 0.8d the forces are expected to be carried to the support directly and at x = 2d the shear force is expected to change sign. The location of the main tension stress is shown in figure 42.

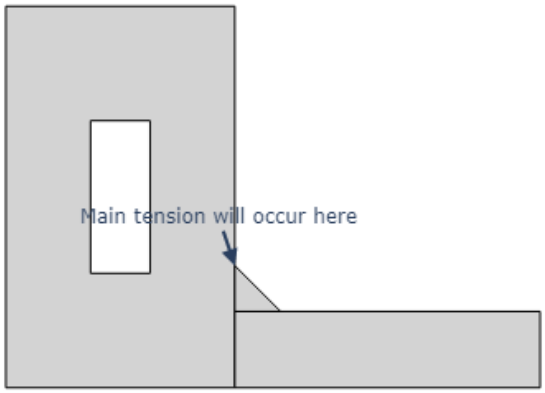

Figure 42: Location of main tension stress

The load combinations with both max V_z and max M_x and at both locations have been checked. The decisive combination is shown here at x = 1.91 m and with load combination: CO73 and effective width b_{eff} = 3692 mm. The main tension stress consists of thee components.

- σ_{xx} is the stress component caused normal force and moment by external loading and pre-stress
- σ_{zz} is the stress component caused by suspension forces and fixed end moments simillarly to how it was calculated for the stirrups
- τ is the stress component caused by torsion and mobile loads and shear force caused by external loading and pre-stress

These stresses are combined to find the main concrete tension stress.

σxx

First the stress the normal force and moment in the girder are obtained. The normal force in the girder is the normal force in the floor integrated over half the width of the floor plus the normal force in the girder. The moment M_{Ed} = 3502 kNm is obtained directly from the girder as the moment from the floor is already integrated.

$$N_{\text{tot}} = N_{\text{gir}} + N_{\text{x,floor}} = -15816 - 362 = -16179 \text{ kN}$$

The stresses due to normal force and moment can now be computed, with those stresses the stress at the haunch can be calculated. For this calculation the cross-sectional properties of half the cross-section of the whole bridge have been used to compute the stress for one girder.

$$\sigma_{\text{xx,N}} = \frac{N_{\text{tot}}}{A_{\text{bridge/2}}} = -3.32 \text{ MPa}$$

$$\sigma_{\text{xx,M}} = \frac{zM_{\text{y}}}{I_{\text{bridge/2}}} = -0.00 \text{ MPa}$$

Where z = -200 mm is the distance between the neutral line of the cross-section and the top of the haunch, such that:

$$\sigma_{\text{xx}} = \sigma_{\text{xx,N}} + \sigma_{\text{xx,M}} = -3.32 \text{ MPa}$$

σzz

σ_{zz} is caclculated similar to how the suspension and hanging forces were determined for the ULS girder calculations. From there it is obtained that N_{tot} = 193 kN. The moment is also calculated in the same way. However for the main tension stress only mobile loads should be considered as the other loads are present over the whole bridge length and will not cause the main tension stresses. In this way $M_{fixed\ end}$ = 589 kNm. The stress diagrams are shown in figure 43. Also the same reduction factor as for the stirrup calculation may be used.

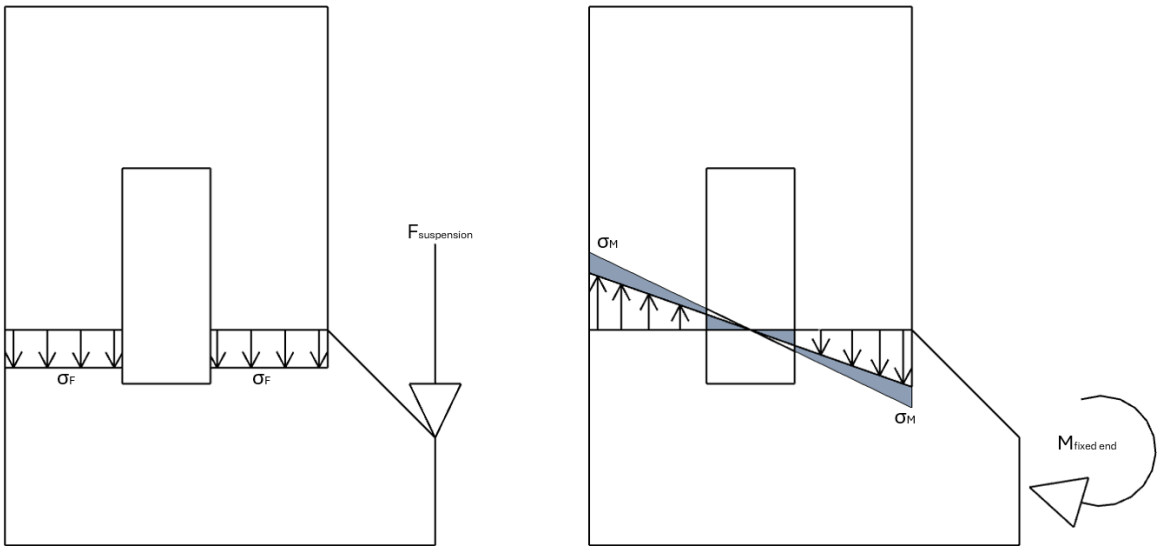

Figure 43: Stress distribution in cross-section

The stress distribution can now be calculated. For the calcualtion of the stress due to the moment the grey areas in the figure are the same. With some geometric calculations the stress can be calculated. First the stress situation without cutout is calculated. Than the area in the cutout is calculated and added to the area not in the cutout while keeping the slope the same. This way $\sigma_{zz,M}$ is obtained.

$$\sigma_{zz,M,0} = \frac{M_{\text{fixed end}}\alpha_A}{\frac{1}{6}W_{gir}^2} = 1.12\ \text{MPa}$$

$$\sigma_{zz,M} = \frac{W_{gir}\sigma_{zz,M,0}}{W_{gir} - W_{cutout} - \frac{W_{cutout}^2}{W_{gir}}} = 1.66\ \text{MPa}$$

$$\sigma_{zz,N} = \frac{N_{tot}\alpha_A}{W_{gir} - W_{cutout}} = 0.12\ \text{MPa}$$

With these results the total σ_{zz} = 1.79 MPa can be determined.

τ

τ consists of two parts, one is the shear force that causes a stress at the haunch and the other is the torsion in the girder. First the stress due to shear is calculated, using the FEM result V_{Ed} = 1679 kN.To get the shear stress at the haunch section the sectional modulus $S_{A,haunch}$ is calculated.

This is done by computing the sectional modulus of the whole cross-section and than subtracting the sectional modulus of the cutout.

With this sectional modulus the stress can be calculated using:

$$\tau_{\mathrm{V}} = \frac{V_{\mathrm{Ed}} S_{\mathrm{A,haunch}}}{I(W_{\mathrm{gir}} - W_{\mathrm{cutout}})} = 0.45 \text{ MPa}$$

The stress due to torsion can be calculated simillarly to how the torsional shear stress was calculated for the stirrups using NEN-EN 1992-1-1 using the same t_{eff} and A_k and the FEM result T_{Ed} = 503 kNm, such that:

$$\tau_{\mathrm{T}} = \frac{M_{\mathrm{Ed}}}{2A_{\mathrm{k}} t_{\mathrm{eff}}} = 0.61 \text{ MPa}$$

Now the total tau is computed as τ = 0.61 MPa

Evaluation

From all the calculated stress components the total tension stress at the haunch can be calculated.

$$\sigma_{ct} = \frac{1}{2}(\sigma_{xx} + \sigma_{zz}) + \sqrt{\frac{1}{4}(\sigma_{xx} - \sigma_{zz})^2 + \tau^2} = 0.54 \text{ MPa}$$

This stress should be lower than $0.6f_{ctd}$.

$$\text{u.c}_{\text{main tension}} = \frac{\sigma_{ct}}{0.6f_{ctd}} = \frac{0.54}{0.88} = 0.62$$

Annex L: SLS Crack width floor

This section covers the calculation of crack width in the floor both in longitudinal and transverse direction. The calculation method of NEN-EN 1992-1-1 formulas 7.8-7.9 has been used to find the maximum crack-width. According to OVS crack-width should be checked in SLS-freq.

Longitudinal

First the stress in the steel should be determined that occurs at M_{rep} = 377 kNm and N_{rep} = 70 kN. The steel stress can be determined when satisfying both ΣM = 0 and ΣN = 0. The result is calculated using an automatic algorithm and shown in figure 44 and 44.

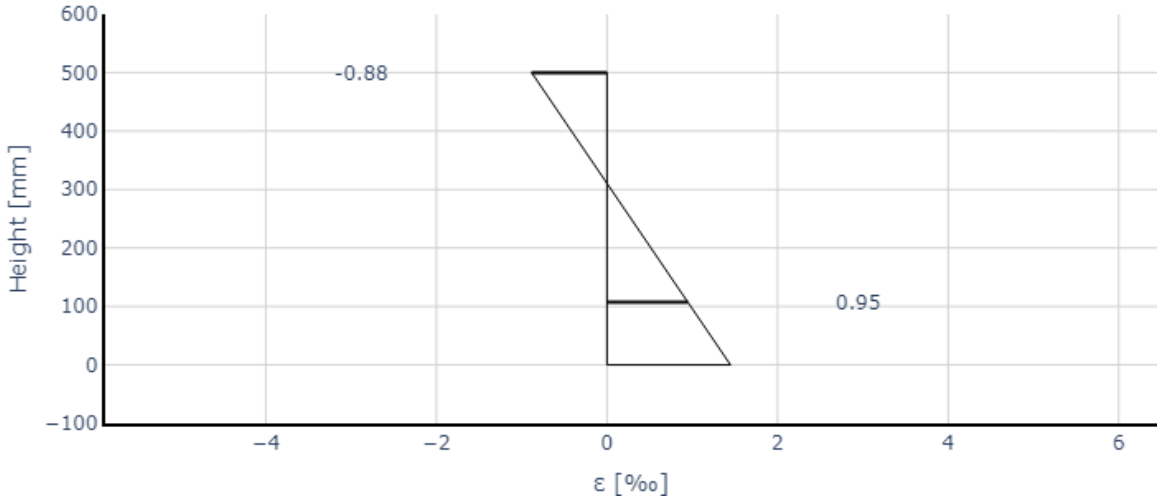

Figure 44: Strain diagram

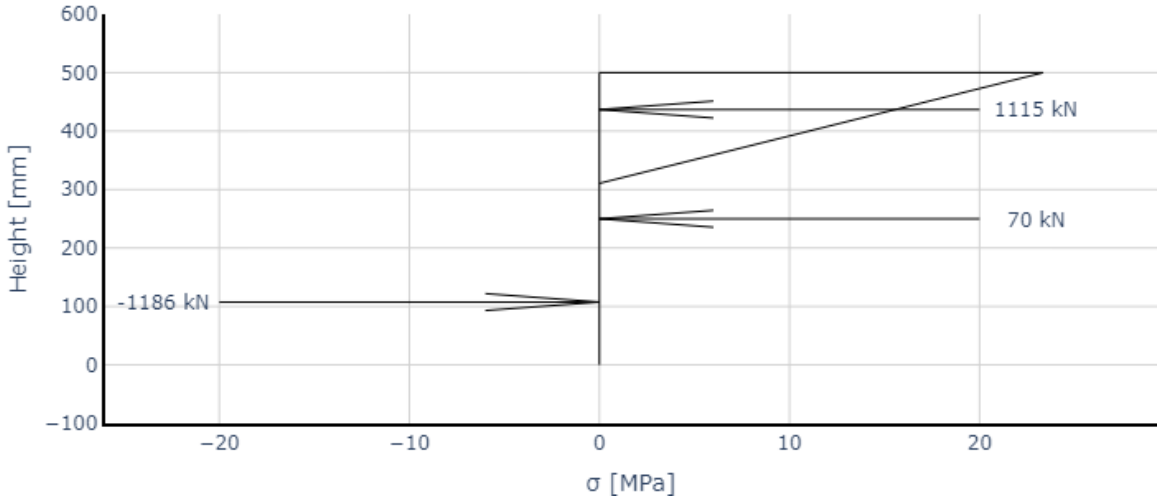

Figure 45: Stress diagram

To support these diagrams the following calculations have been made.

$$N_c = \alpha\sigma_s(\varepsilon)w_{gir}x = 1115 \text{ kN}$$

Here α = 0.50, x = 189 mm and. σ_c = 11.78 MPa at ε_c = 0.88 ‰.
The force in the steel can be calculated using:

$$N_s = A_s \cdot \sigma_s = 1186 \text{ kN}$$

Where σ_s = 199 MPa. This way both the moment and force equilibirum are statisfied knowing z = d_s - βx = 329 mm.

Now that the steel stress is known ε_{sm} - ε_{cm} can be determined with 7.9:

$$\varepsilon_{sm} - \varepsilon_{cm} = \frac{\sigma_s - k_t \frac{f_{ct,eff}}{\rho_{p,eff}}(1 + \alpha_e \rho_{p,eff})}{E_s} \geq 0.6 \frac{\sigma_s}{E_s} = 0.81 \text{ ‰}$$

Where α_e = 5 (OVS), k_t = 0.4 (long term loading) and:

$$\rho_{p,eff} = \frac{A_s}{A_{c,eff}} = 0.06$$

Where $A_{c,eff}$ = 103532 mm^2.

Also $s_{r,max}$ needs to be calculated with formula 7.11 to find the maximum crack-width.

$$s_{r,max} = k_3 c + \frac{k_1 k_2 k_4 \varnothing_{eq}}{\rho_{p,eff}} = 241 \text{ mm}$$

Where: k_1 = 0.8 assuming good bond conditions, k_3 = 3.4, k_4 = 0.425. Also:

$$\varnothing_{eq} = \frac{n_1 \varnothing_1^2 + n_2 \varnothing_2^2}{n_1 \varnothing_1 + n_2 \varnothing_2} = 18 \text{ mm}$$

And:

$$k_2 = \frac{\varepsilon_1 + \varepsilon_2}{2\varepsilon_1} = 0.50$$

Now finally w_k can be calcualted with formula 7.8:

$$w_k = s_{r,max}(\varepsilon_{sm} - \varepsilon_{cm}) = 0.20 \text{ mm}$$

To conclude with the unity check for crack-width using k_x = c / c_{nom} = 1.00:

$$\text{u.c}_{cw,y} = \frac{w_k}{k_x w_{allowed}} = \frac{0.20}{0.20} = 0.98$$

Transverse

For the transverse direction the same calculations can be made: M_{rep} = 126 kNm and N_{rep} = 56 kN. The stress and strain diagrams are shown in figure 46 and 46.

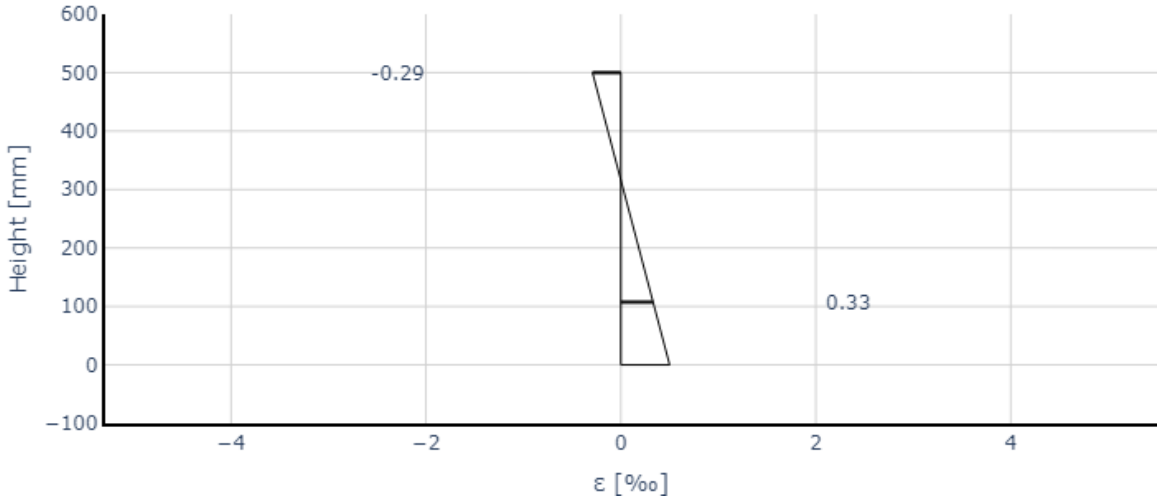

Figure 46: Strain diagram

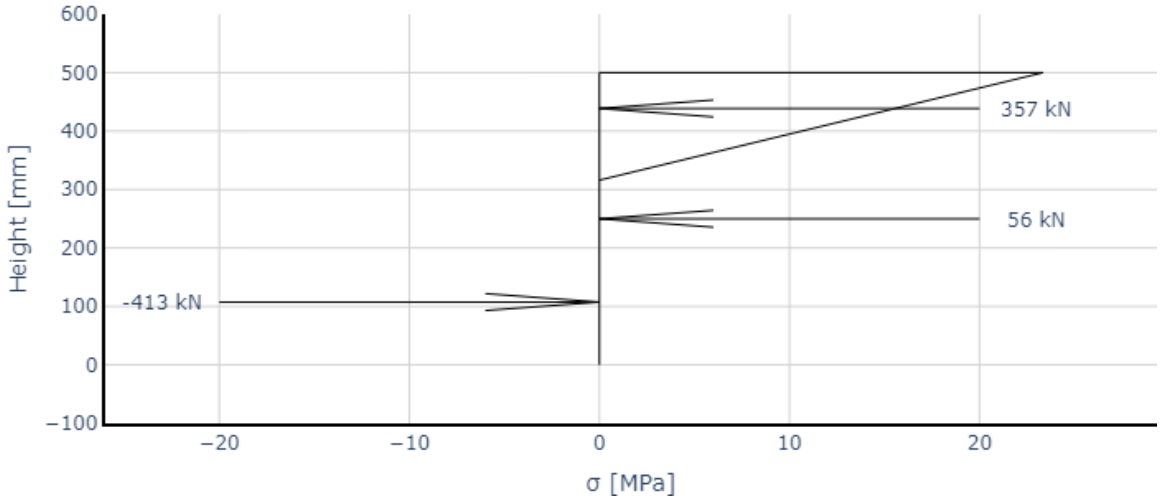

Figure 47: Stress diagram

$$N_c = \alpha \sigma_s(\varepsilon) w_{gir} x = 357 \text{ kN}$$

Here α = 0.50, x = 184 mm and. σ_c = 3.88 MPa at ε_c = 0.29 ‰.

$$N_s = A_s \cdot \sigma_s = 413 \text{ kN}$$

Where σ_s = 69 MPa. This way both the moment and force equilibirum are statisfied knowing z = d_s - βx = 331 mm.

$$\varepsilon_{sm} - \varepsilon_{cm} = \frac{\sigma_s - k_t \frac{f_{ct,eff}}{\rho_{p,eff}}(1 + \alpha_e \rho_{p,eff})}{E_s} \geq 0.6 \frac{\sigma_s}{E_s} = 0.20 \text{ ‰}$$

Where α_e = 5 (OVS), k_t = 0.4 (long term loading) and:

$$\rho_{\text{p,eff}} = \frac{A_{\text{s}}}{A_{\text{c,eff}}} = 0.06$$

Where $A_{c,eff}$ = 105367 mm^2.

And:

$$s_{\text{r,max}} = k_3 c + \frac{k_1 k_2 k_4 \varnothing_{\text{eq}}}{\rho_{\text{p,eff}}} = 242 \text{ mm}$$

Where: k_1 = 0.8 assuming good bond conditions, k_3 = 3.4, k_4 = 0.425. Also:

$$\varnothing_{\text{eq}} = \frac{n_1 \varnothing_1^2 + n_2 \varnothing_2^2}{n_1 \varnothing_1 + n_2 \varnothing_2} = 18 \text{ mm}$$

And:

$$k_2 = \frac{\varepsilon_1 + \varepsilon_2}{2\varepsilon_1} = 0.50$$

To find w_k:

$$w_{\text{k}} = s_{\text{r,max}}(\varepsilon_{\text{sm}} - \varepsilon_{\text{cm}}) = 0.05 \text{ mm}$$

To conclude with the unity check for crack-width in transverse direction using k_x = c / c_{nom} = 1.00:

$$\text{u.c}_{\text{cw,x}} = \frac{w_{\text{k}}}{k_{\text{x}} w_{\text{allowed}}} = \frac{0.05}{0.20} = 0.24$$

Appendix E: Calculation report reduced width

Calculation report super structure concrete through girder bridge

Table of contents

1. Introduction

1.1 Cross-section

The cross-section of the bridge is given in figure 1.

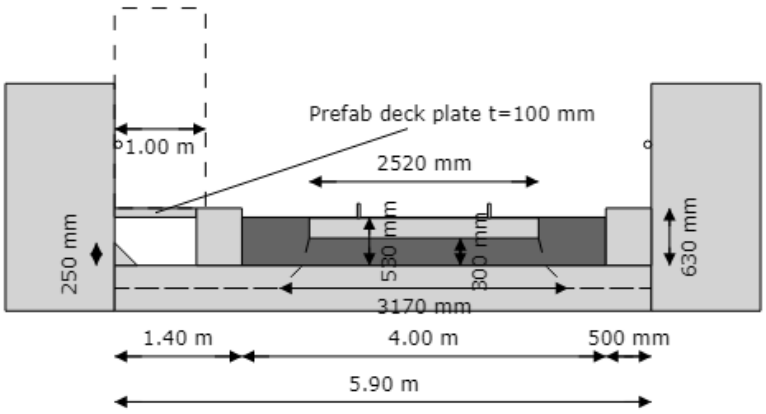

Figure 1: Cross-section of the through girder bridge

1.2 Length profile

The length profile of the bridge is given in figure 2.

Figure 2: Length profile of the through girder bridge

1.3 Aim of the report

The aim of this report is to calculate and optimize the reinforcement and pre-stressing of the super structure of a concrete through girder bridge in preliminary design phase. For this report a parametric design tool has been used to optimize the design and to make use of the automatic calculations.

2. Boundary conditions

2.1 Norms and guidelines

The most important norms and guidelines are listed below, however the applied norms are not limited to those listed.

- NEN-EN 1990-1-1:2019: Basis of structural design + NB
- NEN-EN 1991-1-4:2011: Actions on structures - General actions - Wind actions + NB
- NEN-EN 1991-2:2015: Actions on structures - Traffic loads on bridges + NB
- NEN-EN 1992-1-1:2011: Design of concrete structures - General rules and rules for buildings + NB
- NEN-EN 1992-2:2011: Design of concrete structures - Concrete bridges - Design and detailing rules + NB
- OVS00030-6-V005: Ontwerpvoorschrift kunstwerken - deel 6 - Aanvullingen en wijzigingen op NEN-EN normen
- OVS00030-1-V004: Ontwerpvoorschrift kunstwerken - deel 1 - Kunstwerken voor spoorverkeer
- RTD 1001 Richtlijnen Ontwerp Kunstwerken (ROK) 2.0
- NS Richtlijn 1015 1.3 Uitgangspunten van het ontwerp van trogbruggen

2.2 References

The references and techincal information used in this report is listed below.

- European Tehcnincal Assessment ETA-06/0147 (BBR VT CONA CMI)
- Table technical data pre-stressing strands Netherlands voorspanstaal.nl
- Product specification sheaths Tension Technology Martin

2.3 Calculation software

The following software is used for the creation of this report.

- Dlubal RFEM 6.07
- Python 3.10.8

2.4 Materials

This chapter will provide an overview of the used materials for the design.

2.4.1 Concrete

Concrete of strenght class C35/45 with the following parameters, according to NEN-EN 1992-1-1 table 3.1, are used for the design:

- f_{ck}: 35 MPa
- f_{ctm}: 3.2 MPa
- E_{cm}: 34 GPa (uncracked)
- γ_M: 1.5
- v: 0.2 (uncracked)

2.4.2 Steel

Reinforcement steel of strenght class FeB500 with the following parameters is used for the design:

- f_{yk}: 500 MPa
- f_{yd}: 434 MPa
- E_s: 210 GPa

2.4.3 Pre-stress steel

Pre-stressing steel of strenght class FeP1860 with the following parameters is used for the design:

- f_{pk}: 1860 MPa
- $f_{p,0.1,k}$: 1600 MPa
- E_p: 195 GPa

2.4.3 Pre-stress system

The design makes use of a BBR VT CONA CMI prestressing system internal post-tensioning system with cables and a duct of:

- $n_{strands}$: 22
- $\varnothing_{strands}$: 15.7 mm

The pre-stress ducts used are of type: STB-100x109x0.40 as described in the product specification of TTM

The filling degree of the pre-stress duct thus becomes: 0.54.

2.5 Environmental classes

In table 1 the environmental classes and crack width requirements have been summarized. The design life of all train bridges is 100 years and the crack width

requirement and the environmental classes have been decided by OVS-00030-6 and NEN-EN 1992-1-1.

Structural element	Environmental class	$c_{nom,reinf}$ mm	c_{app} mm	$c_{nom,p}$ mm	w_{max} mm
Girder	XC4, XD3, XF4, XA2	55.0	60.0	70.0	0
Top of deck	XC4, XD3, XF4, XA2	55.0			0.2
Bottom of deck	XC4, XD3, XF4, XA2	55.0			0.2

Table 1: Durability factors

2.6 Loads

The loads working on the super structure of the bridge will be summarized here. For the complete calculation of the loads please refer to annex B. Also the load combinations considered are summarized in annex C.

2.6.1 Permanent loads

LC1.1 Self-Weight

The self-weight of the structure is calculated automatically calculated by RFEM.

LC1.2 Permanent loads train

Other permanent loads that are considered are due to the infrastructure on the bridge for the trains. The loads are visualised in figure 3.

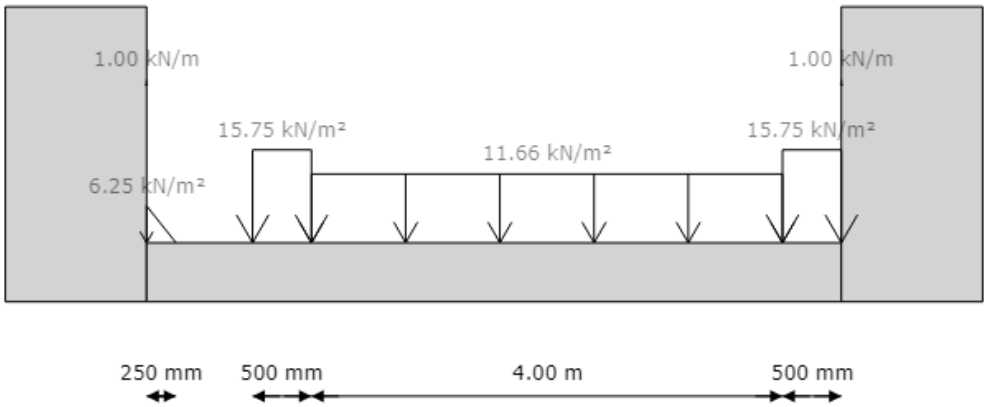

Figure 3: Permanent loads

LC2 Prestressing

For the calculation of the pre-stress forces and losses please refer to annex B. Figure 4 shows the pre-stress profile and figure 5 shows the resulting forces.

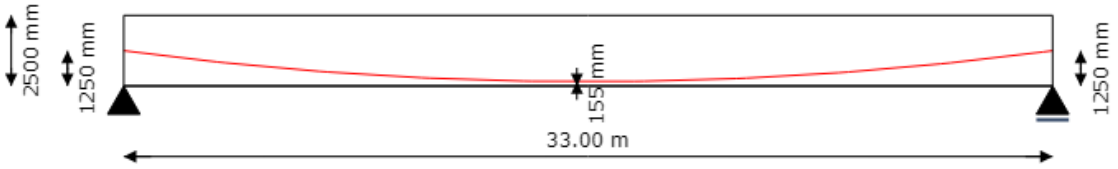

Figure 4: Pre-stress profile

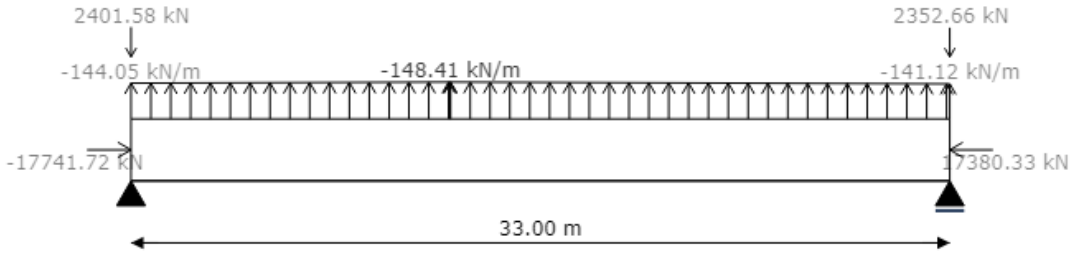

Figure 5: Pre-stress loads

LC3 Setting
Because a single span statically determined bridge is considered, settings will not cause loads.

2.6.2 Variable loads

LC4 Other variable loads
Variable loads on the passing path are considered as per NEN-EN 1991-2.

- $Q_{passing\ path}$: 5 kN/m^2

Snow loads are not considered because these will be inisgnificant compared to the train loads.

LC5 Braking loads and LC6 Accelerating loads
Brake and accelerating forces are not considered for the super structure as these will be mostly important for the substructure.

LC7 Wind loads
Windloads are calculated using NEN-EN 1991-1-4, for the complete calculation please refer to Annex B.

The decisive loads F_{wk} and the reduced F_{wk}^{**} that are considered are given below. The loads in x-direction are modelled as line loads acting on the wall of the structure, while the loads in z direction are considered as distributed loads over the whole area of the bridge.

- $q_{wk,x}$: 17.03 kN/m
- $q_{wk,x}^{**}$: 12.23 kN/m
- $p_{wk,z}$: 1.44 kN/m^2
- $p_{wk,z}^{**}$: 1.03 kN/m^2

LC8 Temperature loads
Temperature loads have not yet been incorporated in the design.

LC9.1.1 Train loads model LM71 M

The position of the train load model LM71 from NEN-EN 1991-2 is automatically calculated using influence lines. Also the effective width over which the load may be spread is calculated:

$$W_{\text{load}} = l_{\text{sleeper}} + 2 \cdot (\frac{t_{\text{bal}}}{4} + \frac{h_{\text{fl}}}{2}) = 2520 + 2 \cdot (75.0 + 250.0) = 3170 \text{ mm}$$

It is assumed that the point loads in the middle of this load model can be evenly distributed over the whole area. The loads resulting in the highest moment from LM71 are shown in figure 6:

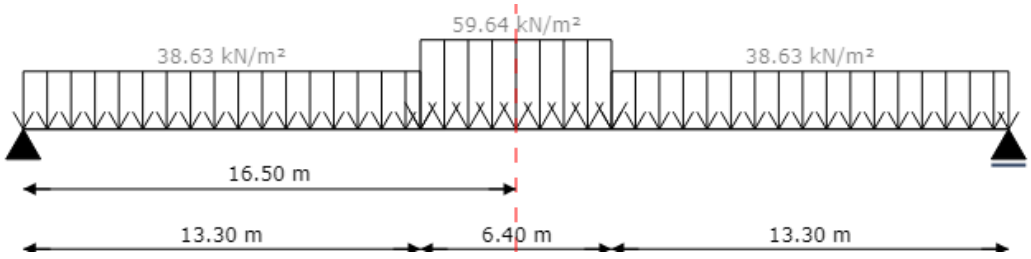

Figure 6: Load model LM71, max moment

LC9.1.2 Train loads model LM71 V

The loads resulting in the highest shear force from LM71 are shown in figure 7:

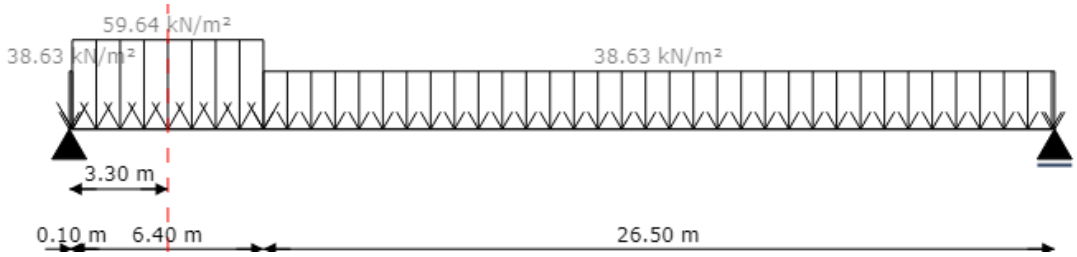

Figure 7: Load model LM71, max shear force

LC9.2.1 Train loads model SW/0 M

Because a single span bridge is designed load model SW/0 is not considered.

LC9.3.1 Train loads model SW/2 M

The position of the train load model SW/2 from NEN-EN 1991-2 is automatically calculated using influence lines. The effective width is the same as before. The loads resulting in the highest moment from SW/2 are shown in figure 8:

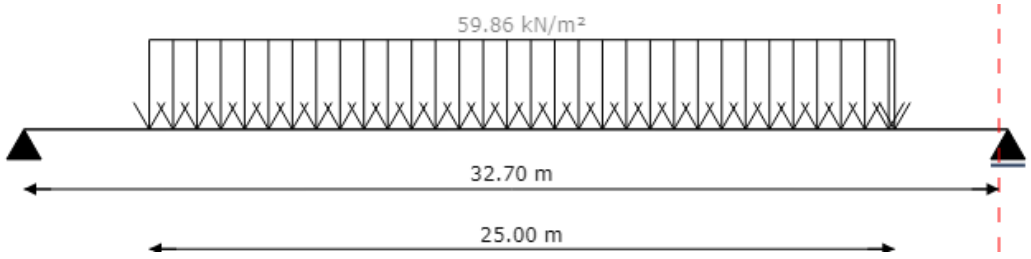

Figure 8: Load model LM71, max moment

LC9.3.2 Train loads model SW/2 V

The loads resulting in the highest shear force from SW/2 are shown in figure 9:

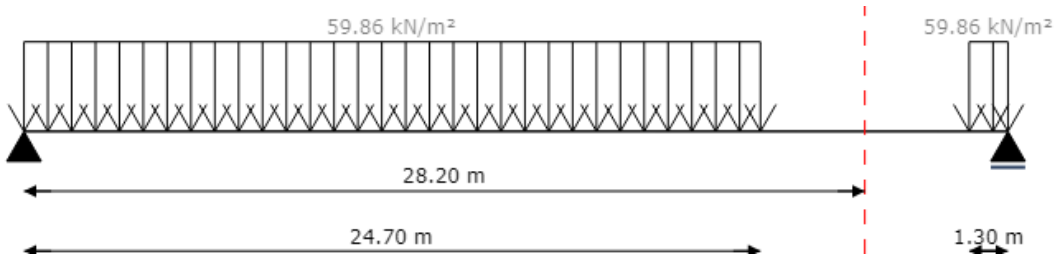

Figure 9: Load model LM71, max shear force

2.6.3 Special loads

LC10.1 Train loads tilting and LC10.2 Rerailing loads

These load cases have not been implemented yet. Also centrifugal force is not considered because the bridge is straight.

3. Calculations

For the pre-stress and reinforcement layouts of the design please refer to annex B.

3.1 Modelling and loadtransfer

As mentioned before the FEM model is build in RFEM. The principal cross-section in RFEM is shown in figure 10. In the following paragraphs the most important elements of the model will be explained.

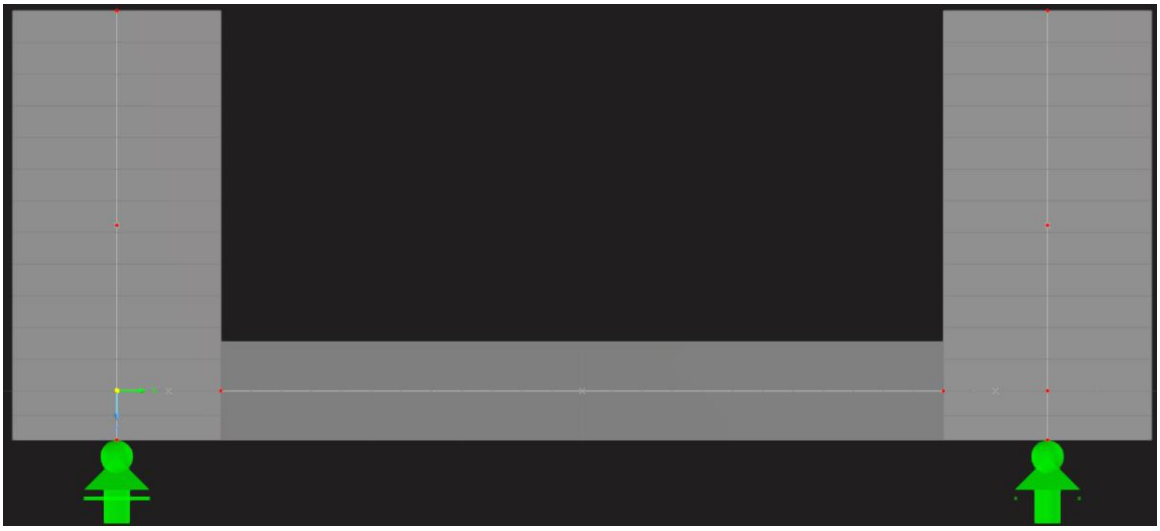

Figure 10: Principal cross-section in RFEM

3.2.1 Girders

The girders are modelled as vertical planar 2D plate elements with a uniform thickness that transfer moments and membrane forces. This way the homogenous en isotropic behaviour of the girder is correctly modelled. The target mesh size for the elements is 0.25 m.

3.2.2 Floor

The floor is modelled simillarly as the girders. For the floor again a vertical planar 2D plate element with a uniform thickness that transfer moments and membrane forces is used. For the floor also a mesh size of 0.25 m is used.

3.2.3 Connection floor-girder

The floor and girders are connected via a rigid planar surface with zero mass density such that the self-weight is not doubled in this area. By making sure this surface connects the floor and the girder the connection correctly models the bahaviour of load transfer between these elements. Figure 11 shows how the elements are modelled by side view.

Figure 11: Side view of the surface elements in RFEM

3.2.4 Supports

The model has 4 supports all of them restricting movement in z-direction and none of them restricting rotation. Figure 12 shows how the supports of the model are ordered and in which direction they allow for translation.

Figure 12: Top view of the support directions

3.2.5 Result beams

To transfer the loads of the 2D elements of the girders into 1D internal forces to be used for evaluation result beams are used. These beams cover the surface elements and integrate the internal forces to 1D internal forces.

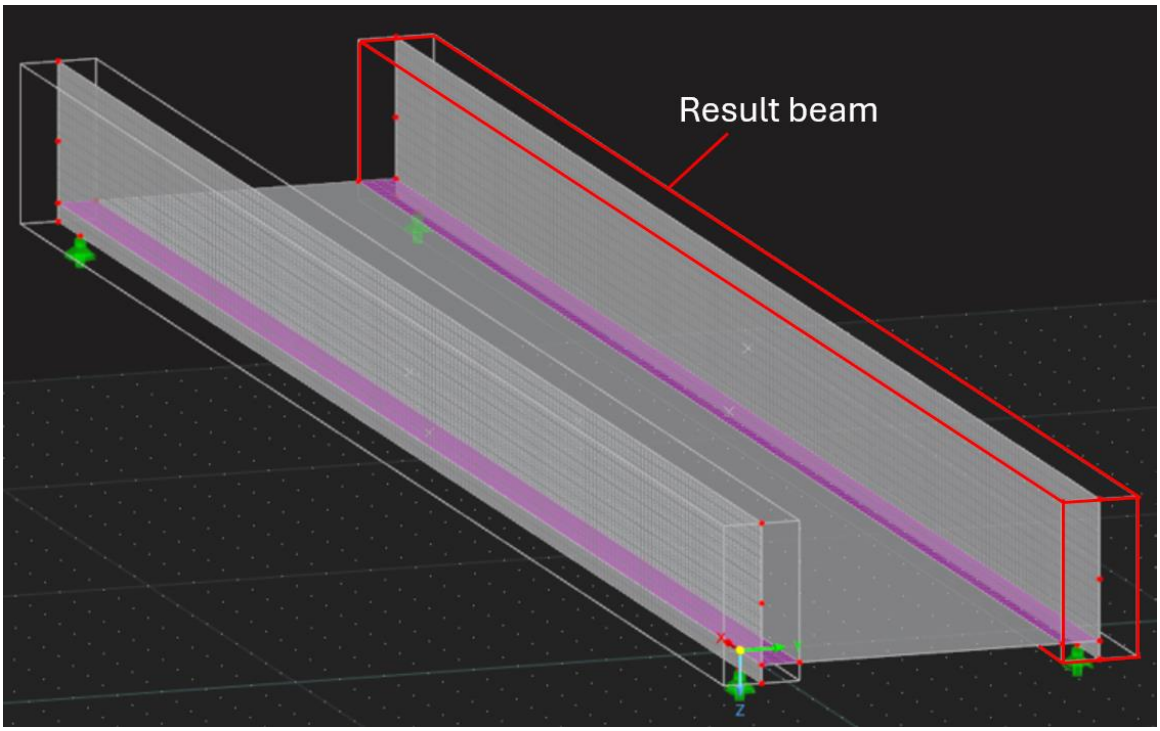

Figure 13: Result beam in model

3.2 Calculations girder

This paragraph outlines the results of the calculations made for the girder. The reinforcement and pre-stress layout can be found in annex B.

3.2.1 Ultimate limit state

These calculations can be found in Annex E and F. The longitudinal and stirrups reinforcement has been checked according to NEN-EN 1992-1-1. The stirrups have been divided into three regions, each having a different purpose for the type of load they carry. Next to that the longitudinal reinforcement is tested both for capacity and for max compression zone height according to NEN-EN 1992-1-1 6.1 (9). To achieve this the pre-stress has been ficticiously reduced to 44 % such that only the part of the pre-stress that is needed to carry the load remains. With this case the compression zone height is checked.

The results are summarized in table 2.

	Symbol	Value	Limit value	Result
Longitudinal reinforcement torsion	$u.c_{sl,T}$	$A_{sl,T,req}$ = 9218 mm^2	$A_{sl,T}$ = 10455 mm^2	0.88
Stirrup horizontal reinforcement	$u.c_{sw,T,hor}$	$A_{sw,T,hor,req}$ = 228 mm^2	$A_{sw,T}$ = 565 mm^2	0.40
Stirrup zone I reinforcement	$u.c_{sw,I}$	$A_{sw,I,req}$ = 503 mm^2	A_{sw} = 565 mm^2	0.89

Stirrup zone II reinforcement	$u.c_{sw,II}$	$A_{sw,II,req}$ = 761 mm^2	A_{sw} = 905 mm^2	0.84
Stirrup zone III reinforcement	$u.c_{sw,III}$	$A_{sw,III,req}$ = 2166 mm^2	A_{sw} = 2234 mm^2	0.97
Moment reinforcement	$u.c_{M,gir}$	M_{Ed} = 19577 kNm	M_{Rd} = 36590 kNm	0.54
Increased moment reinforcement	$u.c_{M,rot}$	$M_{Ed,rot}$ = 29712 kNm	$M_{Rd,rot}$ = 29909 kNm	0.99
Compression zone height	$u.c_{x,rot}$	x_u = 919 mm	$x_{u,allowed}$ = 932 mm	0.99

Table 2: Calculation results girder ULS

3.2.2 Serviceability limit state

This section covers the SLS calculations for the girder. Both the compressive and tension stresses in the concrete have been checked in annex J. The tension stresses have been checked according to the requirements of the OVS and the compressive stress has been checked at t=0. Next to that the main tension stress just above the haunch at the inner wall of the girder has also been checked in accordance with NSRL1015. This stress is built up out of three stres components σ_{xx}, σ_{zz} and τ and they are calculated in annex K.

The results are summarized in table 3.

	Symbol	Value	Limit value	Result
Tension stress SLS-quas		$\sigma_{ct,quas}$=-2.80 MPa	$\sigma_{ct,quas,allowed}$=0.00 MPa	O.K.
Tension stress SLS-freq		$\sigma_{ct,freq}$=-0.89 MPa	$\sigma_{ct,freq,allowed}$=1.10 MPa	O.K.
Tension stress SLS-char		$\sigma_{ct,char}$=-0.04 MPa	$\sigma_{ct,char,allowed}$=1.10 MPa	O.K.
Compressive stress	$u.c_{compr}$	σ_c=6.12 MPa	f_{cd}=23 MPa	0.26
Main tension stress	$u.c_{main\ tension}$	σ_{ct}=0.80 MPa	$0.6f_{ctd}$=0.88 MPa	0.91

Table 3: Calculation results floor SLS

3.3 Calculations floor

This paragraph outlines the results of the calculations made for the floor.

3.3.1 Ultimate limit state

The ULS calculations for the floor are conducted using NEN-EN 1992-1-1. Reinforcement in both x and y direction is applied en checked in annex G.

The results are summarized in table 4.

	Symbol	Value	Limit value	Result
Longitudinal reinforcement	$u.c_{M,floor,y}$	M_{Ed}=549 kNm	M_{Rd}=867 kNm	0.63
Transverse reinforcement	$u.c_{M,floor,x}$	M_{Ed}=206 kNm	M_{Rd}=220 kNm	0.94

Table 4: Calculation results floor ULS

3.3.2 Servicability limit state

The SLS calculations for the floor are conducted using NEN-EN 1992-1-1. Annex L outlines how the crack-width has been calculated.

The results are summarized in table 5.

	Symbol	Value	Limit value	Result
Crack-width longitudinal	$u.c_{cw,y}$	w=0.18 mm	$w_{allowed}$=0.20 mm	0.92
Crack-width transverse	$u.c_{cw,x}$	w=0.05 mm	$w_{allowed}$=0.20 mm	0.24

Table 5: Calculation results floor ULS

3.4 Other calculations

This paragraph outlines the results of the other calculations.

3.3.1 Ultimate limit state

Longitudinal shear between the girder and the floor has ben checked in annex H according to NEN-EN 1992-1-1 6.2.4.Next to that splitting reinforcement at the ends of the deck has also been calculated in annex I using a strut and tie model
The results of these calculations have been summarized in table 6.

	Symbol	Value	Limit value	Result
Longitudinal shear	$u.c_{l,s}$	v_{Ed}=0.56 MPa	kf_{ctd}=0.59 MPa	0.95
Splitting reinforcement	$u.c_{spl}$	σ_{spl}=401 MPa	f_{yd}=434 MPa	0.92

Table 6: Calculation results other calculations ULS

3.3.2 Servicability limit state

The maximum displacement is calculated with the FEM model is 28.2 mm. The by OVS required camber is 33.0 mm, this means that the pre-camber of the bridge should be 61.2 mm

4. Results

Based on the internal forces from the 3D FEM model of the design model, the reinforcement and prestressing of the superstructure of the trough bridge have been determined. The structure has been checked for strength and durability in a preliminary design stage. The geometry and reinforcement is summarized in appendix A and B.

4.1 Points of attention

- This report is made for a preliminary design, further detailling is needed to complete the design.
- Temperature loads are not considered in this report.
- This bridge has not been tested in FAT.
- Splitting reinforcement for the introduction of the pre-stressing has not been designed.
- No calculations for detailing around the supports have been made.
- It is essential for the design that the bridge is correctly protected from stray currents by isolation of the clearway in accordance with OVS.

Annex A: Geometry and effective width

Cross-sectional properties

The calculation of certain cross-sectional parameters is displayed below.

$$A = 2 \cdot h_{\text{gir}} \cdot W_{\text{gir}} + h_{\text{fl}} \cdot W_{\text{fl}} + a_{\text{vou}}^2 = 9.01\ \text{m}^2$$

$$z_{\text{neutral,axis}} = \frac{2 \cdot A_{\text{gir}} \cdot z_{\text{gir}} + A_{\text{fl}} \cdot z_{\text{fl}} + 2 \cdot A_{\text{vou}} \cdot z_{\text{vou}}}{A} = 0.918\ \text{m}$$

$$I = 2 \cdot (I_{\text{girder}} + A_{\text{girder}} \cdot a_{\text{girder}}^2) + I_{\text{fl}} + A_{\text{fl}} \cdot a_{\text{fl}}^2 + 2 \cdot (I_{\text{vou}} + A_{\text{vou}} \cdot a_{\text{vou}}^2) = 5.175\ \text{m}^4$$

The cross-section for including the max effective width is shown in figure 14.

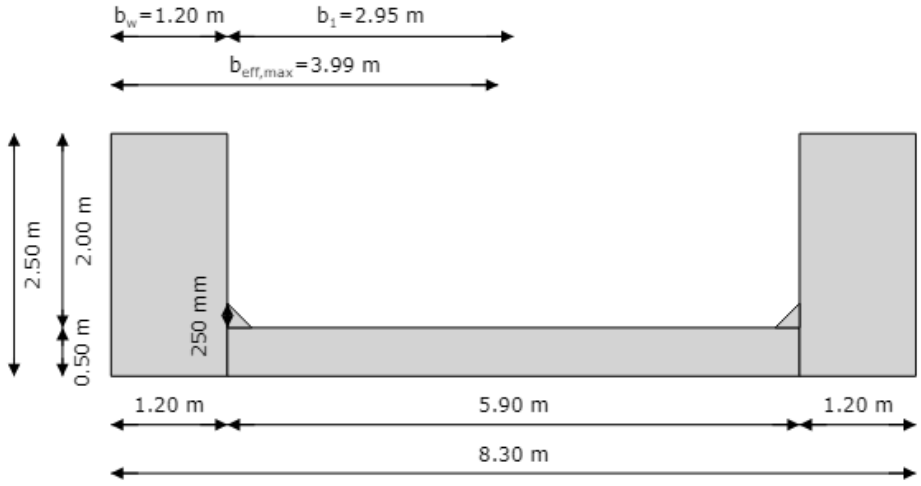

Figure 14: Cross-section including maximum effective width

The effective width over the length of the bridge is shown in figure 15

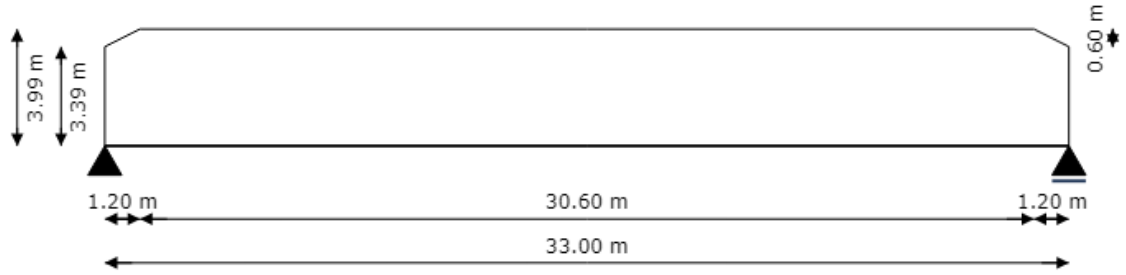

Figure 15: Length profile with effective width of the through girder bridge

The effective width is calculated via NEN-EN 1992-2. First the l_0/b_i ratio can be calculated as: 33/2.95=11.19.
Referencing this ratio in figure 16, it is found that the ratio b_{eff}/b_i for S_s should be: 0.74 and for S_v: 0.95. The effective width can be calculated accordingly.

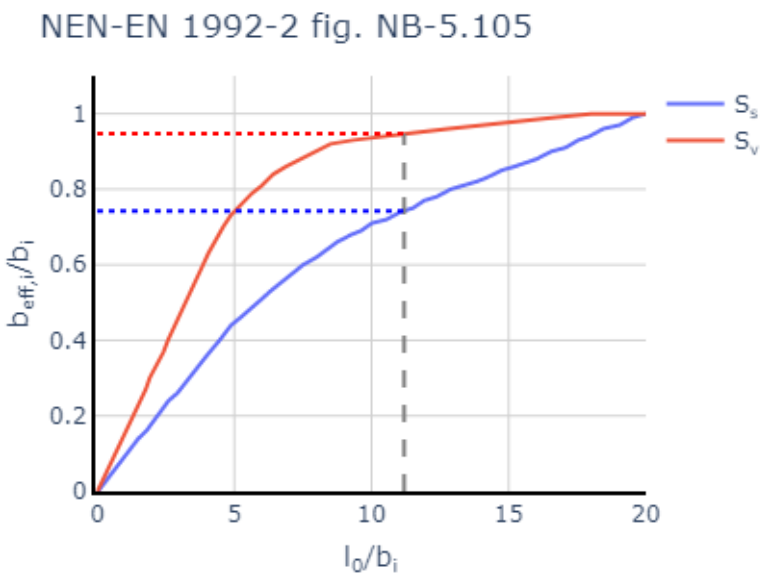

Figure 16: NEN-EN 1992-2 fig. NB.5-105 and the effective width ratio's

Train infrastructure

The geometry of the train infrastructure in the cross-section should also be determined in accordance with OVS00030-6-V005 and OVS00030-1-V004.
Sleepers are 2520x260x121 mm based on OVS6 article 6.3.6.2 and on the fact that a UIC-54 rail has a height of 159 mm, they have a spacing of 600 mm according to NEN-EN 1991-2 fig. 6.5.
The thickness of the ballast layer is 300.0 mm and the thickness of the deck plate for the passing path is 100 mm. The width of this passing path is 1 m according to OVS1 article 3.3.3 and it should be atleast 2.4 m out of the center of the rails knowing no high-speed trains will cross this bridge.
The derailment guards should be placed at least 2 m out of the center of the rails according to OVS1 article 4.1.4.1 and the width of the derailment guard is 500 mm to accomodate the reinforcement needed for big impacts. The height of these guards should at least be 100 mm above the top of the rail.
For design purposes the height of the ballast bed should be from the top of the deck to the top of the rails - 150 mm with a volumetric of 22 kN/m^3 according to OVS-6 article 5.2.3.
Using these rules the cross-section with train infrastructure in the report is designed.

Annex B: Pre-stress and reinforcement

Pre-stress

The pre-stress layout at midspan is shown in 17. This system uses 5 cables per girder.

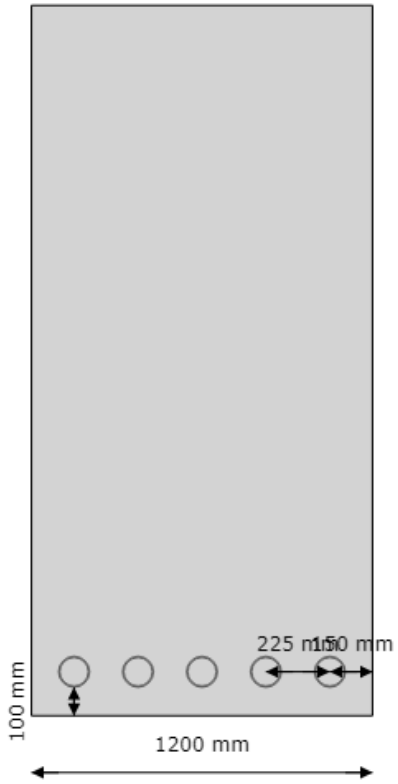

Figure 17: Pre-stress layout

- R: 124 m
- A_P: 16500 mm^2
- $d_{P,mid}$: 2345 mm
- $\sigma_{Pi,max}$: 1427 MPa
- $\sigma_{Pw,max}$: 1118 MPa
- $c_{P,min}$: 70 mm
- $c_{P,app}$: 100 mm

Girder reinforcement

The reinforcement layout of the girder is shown in 18.

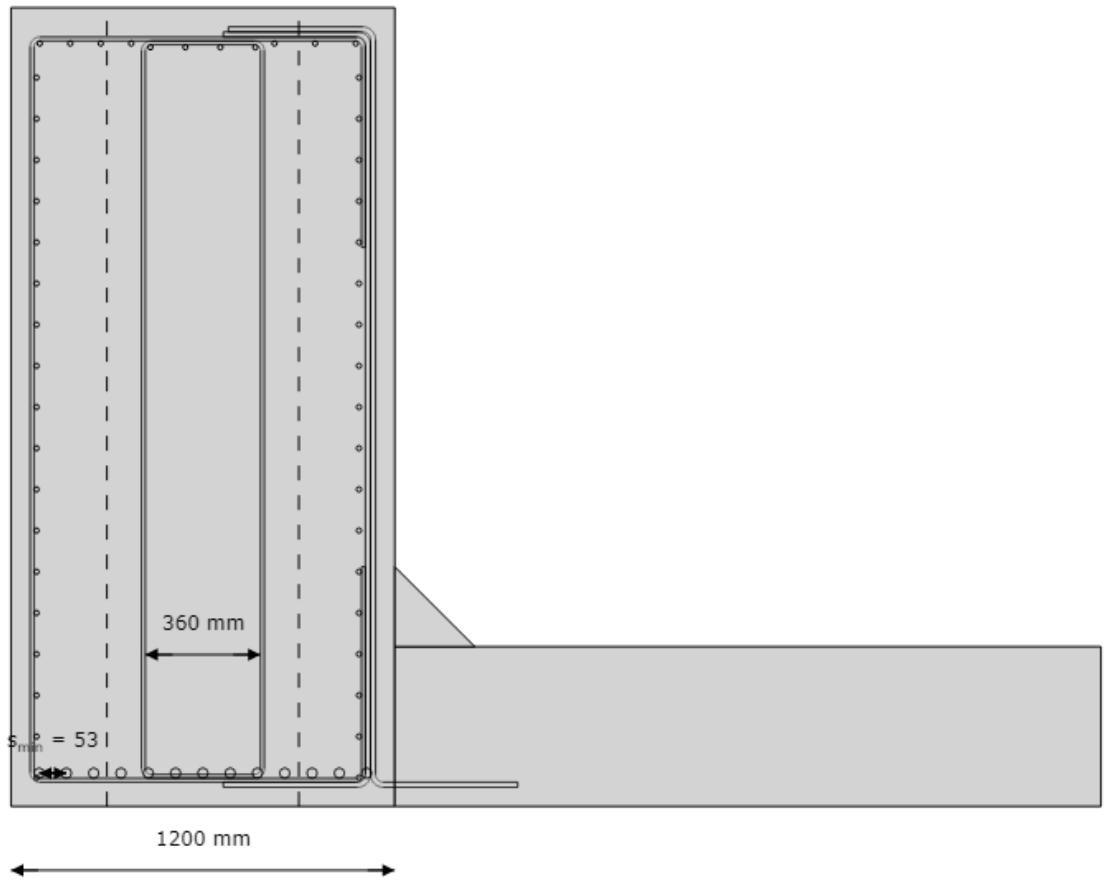

Figure 18: Girder reinforcement layout

Main longitudinal reinforcement:

- $\varnothing_{sl}$: 32 mm
- A_{sl}: 20910 mm^2
- d_{sl}: 2396 mm

Longitudinal reinforcement for torsional resistance:

- $\varnothing_{sl,T}$: 16 mm
- $s_{sl,T}$: 130 mm
- $A_{sl,T}$: 10455 mm^2

Stirrups:

- $\varnothing_{sw,C}$: 12 mm
- $s_{sw,C}$: 200 mm
- $\varnothing_{sw,mid}$: 12 mm
- $s_{sw,mid}$: 250 mm
- $\varnothing_{sw,inverted\ C}$: 16 mm
- $s_{sw,inverted\ C}$: 180 mm
- $\varnothing_{sw,Z}$: 16 mm
- $s_{sw,Z}$: 180 mm
- $A_{sw,I}$: 565 mm^2
- $A_{sw,II}$: 905 mm^2
- $A_{sw,III}$: 2234 mm^2

Cover:

- c_{min}: 55 mm
- c_{app}: 60 mm

The stirrup reinforcement is divided in three different areas. Area I serves as torsional and shear forces reinforcement, area II serves for shear reinforcement and area III serves for both shear and torsional reinforcement and also carries the loads from the suspension forces from the floor.
Due to the limitation is NEN-EN 1992-1-1, the maximum spacing of the stirrups in the girder is 500 mm. This requirement is fulfilled

Floor reinforcement

The reinforcement layout of the floor in y-direction is shown in 19. The reinforcement in x-direction is shown in the transverse direction.

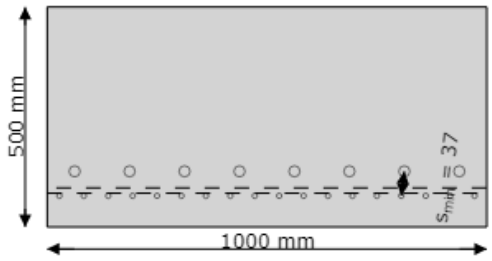

Figure 19: Floor reinforcement layout

Longitudinal reinforcement y-direction:

- $\varnothing_{1,y}$: 12 mm
- $s_{1,y}$: 56 mm
- $\varnothing_{2,y}$: 25 mm
- $s_{2,y}$: 125 mm
- $A_{sl,y}$: 5963 mm^2
- $d_{sl,y}$: 392 mm

Longitudinal reinforcement x-direction:

- $\varnothing_{1,x}$: 12 mm
- $s_{1,x}$: 91 mm
- $A_{sl,x}$: 1244 mm^2
- $d_{sl,x}$: 417 mm

Cover:

- c_{min}: 55 mm
- c_{app}: 55 mm

Splitting reinforcement

The splitting reinforcement at the ends of the span has also been calculated. The layout for both ends of the bridge is:

- $\varnothing_{spl}$: 32 mm
- n_{spl}: 9
- A_{spl}: 7238 mm^2

Annex C: Loads

LC1.2 Permanent loads train

This section will feature the calculation of the additional permanent loads

- Weight haunches

The additional load of the haunches which are not modelled in SCIA as structural elements is calculated with:

$$Q_{\text{haunch}} = h_{\text{haunch}} \cdot \gamma_{\text{concrete}} = h_{\text{haunch}} \cdot 25$$

Because the haunchs have a slope of 1:1 and the max height of 250.0 mm, this leads to the loads represented in the report.

- Weight derailment guard

The additional load of the derailment guards is calculated as:

$$Q_{\text{derailment guard}} = h_{\text{derailment guard}} \cdot \gamma_{\text{concrete}} = 630.0 \cdot 25 = 15.75 \text{ kN/m}^2$$

- Weight ballastbed

The additional load of the ballast bed is calculated as:

$$Q_{\text{ballast bed}} = h_{\text{ballast bed}} \cdot \gamma_{\text{concrete}} = 530.0 \cdot 25 = 11.66 \text{ kN/m}^2$$

With these calculations the loads shown in the report have been calculated.

LC2 Prestressing

The tendon profile of the prestress is given in figure 20.

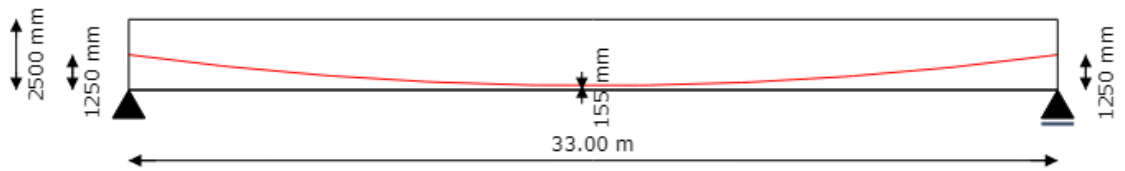

Figure 20: Prestress tendon profile

The tendon profile is given by:

$$y = 4.08 \cdot 10^{-6}x^2 + -0.13x + 1250;\ R = 124\ \text{m}$$

In addition to this the vertical displacement of the cable Δz due to the stressing of the cable is calculated with a maximum of 18 mm due as prescribed by ROK

First the maximum force should be determined. From a simple calculation it follows that the maximum pre-stressing force is limited by the material properties rather than by the maximum pre-stressing force that will yield a positive moment at t=0 when only the self-weight and the prestressing force will be acting on the bridge:

$$\frac{N_\text{P}}{A} - \frac{M_\text{P}}{W_\text{top}} + \frac{M_\text{sw}}{W_\text{top}} > 0;\ N_\text{P} = \sigma_\text{P} A_\text{P}$$

Using:

$$M_\text{P} = \frac{1}{2} \cdot N_\text{P}(e_1 + e_2) + \frac{N_\text{P} l^2}{8R}$$

$$M_\text{sw} = \frac{1}{8} \cdot A\gamma_\text{conc} l^2$$

$$A_\text{P} = A_\text{strand} n_\text{strands} n_\text{cable} = 150 \cdot 22 \cdot 5 = 16500\ \text{mm}^2$$

It can be concluded that $\sigma_{\text{PM0,max}}$=2538 MPa, which is much higher than the limit given by:

$$\sigma_{\text{PM0,max}} = \min(0.75 \cdot f_\text{pk}, 0.85 \cdot f_{\text{p0.1k}}) = \min(0.75 \cdot 1860, 0.85 \cdot 1600) = 1360\ \text{MPa}$$

The maximum stress during tensioning is:

$$\sigma_{\text{PMi,max}} = \min(0.8 \cdot f_\text{pk}, 0.9 \cdot f_{\text{p0.1k}}) = \min(0.8 \cdot 1860, 0.9 \cdot 1600) = 1440\ \text{MPa}$$

These two stresses are the basis for the pre-stress loss calculations. For these calculations the following losses are considered:

- Friction losses

The prestressing system makes use of a Steel strip sheath with: k=0.005 rad/m and μ=0.18 rad^{-1} following from European Technical Assessment ETA-06/0147. The friction losses over the length profile can be calculated using:

$$F = F_0 e^{-\mu(\theta + k \cdot x)}$$

Where θ is the sum of the angular displacements over the distance x, irrespective of direction or sign. The pre-stressing steel is stressed first from the left side and than from the right side. Now σ_{PMi} can be calculated.

- Wedge set

The wedge set for the pre-stressing system is assumed to be 7 mm because of the ROK. How this loss is spread over the length of the bridge is calculated by discretizing the length of the bridge into many small dx's. For the each dx and $\Delta\sigma_{slip}$ the total Δl is calculated using:

$$\Delta l = \frac{\Delta\sigma_{\text{slip}}}{E_{\text{P}}} \cdot \Delta x$$

Using a smart optimization algorithm the actual stress losses can be calcualted by finding the $\Delta\sigma_{slip}$ values such that ΣΔl=7 mm using the follwing rule.

$$\Delta\sigma_{\text{slip},x=i+1} = \max(\Delta\sigma_{\text{slip},x=i} - \max(2(\sigma_{\text{PMi},x=i} - \sigma_{\text{PMi},x=i+1}),0),0)$$

- Creep loss

The creep loss can be calculated assuming: t=36500 days, t_0=10 days and RH=65 %. The calculation from Annex B of NEN-EN 1992-1-1 can be used to calculate the creep coefficient:

$$\alpha_1 = \left(\frac{35}{f_{\text{cm}}}\right)^{0.7} = 0.87;\ \alpha_2 = \left(\frac{35}{f_{\text{cm}}}\right)^{0.2} = 0.96;\ \alpha_3 = \left(\frac{35}{f_{\text{cm}}}\right)^{0.5} = 0.90$$

$$h_0 = \frac{2A_{\text{c}}}{u} = \frac{2 \cdot 9012500}{25600} = 704\ \text{mm}$$

Where u is the perimeter of the cross-section of the bridge.

$$\begin{aligned}\beta_{\text{H}} &= \min(1.5(1 + (0.012\text{RH})^{18})h_0 + 250\alpha_3, 1500\alpha_3) \\ &= \min(1.5(1 + (0.012 \cdot 65)^{18})704 + 226, 1353) = 1294\end{aligned}$$

$$\beta_{\text{c}}(t, t_0) = \left(\frac{t - t_0}{\beta_{\text{H}} + t - t_0}\right)^{0.3} = \left(\frac{36500 - 10}{1294 + 36500 - 10}\right)^{0.3} = 0.99$$

$$\beta(t_0) = \frac{1}{0.1 + t_0^{0.20}} = \frac{1}{0.1 + 10^{0.20}} = 0.59$$

$$\beta(f_{\text{cm}}) = \frac{16.8}{\sqrt{f_{\text{cm}}}} = \frac{16.8}{\sqrt{43}} = 2.56$$

$$\phi_{\text{RH}} = \alpha_2(1 + \alpha_1 \cdot \frac{1 - \text{RH}/100}{0.1h_0^{\frac{1}{3}}}) = 0.96(1 + 0.87 \cdot \frac{1 - 0.65}{0.19}) = 1.29$$

$$\phi_0 = \phi_{\text{RH}}\beta(f_{\text{cm}})\beta(t_0) = 1.29 \cdot 2.56 \cdot 0.59 = 1.96$$

Using these parameters the creep coefficient can be calculated. Using the creep coefficient and the aforementioned first estimate of steel stress the creep strain can be calculated:

$$\phi(t, t_0) = \phi_0\beta_{\text{c}}(t, t_0) = 1.96 \cdot 0.99 = 1.94$$

$$E_{\text{c}} = 1.05E_{\text{cm}};\ \sigma_{\text{c}} = \sigma_{\text{P}} \cdot \frac{A_{\text{P}}}{A_{\text{c}}}$$

$$\varepsilon_{\text{cc}}(\infty, t_0) = \phi(\infty, t_0) \cdot \frac{\sigma_{\text{c}}}{E_{\text{c}}} = 1.94 \cdot \frac{7}{35700} = 0.443\ ‰$$

- Drying shrinkage loss

Drying shrinkage ε_{cd} strain can also be calculated via NEN-EN 1992-1-1. Cement of class N is used or this design giving α_{ds1}=4 and α_{ds2}=0.12, also f_{cmo}=10 MPa and RH_0=100 %. Now $\varepsilon_{cd,0}$ can be calculated:

$$\beta_{\text{RH}} = 1.55(1 - (\frac{RH}{RH_0})^3) = 1.55(1 - (\frac{65}{100})^3) = 1.12$$

$$\varepsilon_{\text{cd,0}} = 0.85((220 + 110\alpha_{\text{ds1}}) \cdot \exp(-\alpha_{\text{ds2}} \cdot \frac{f_{\text{cm}}}{f_{\text{cmo}}})) \cdot 10^{-6} \cdot \beta_{\text{RH}}$$
$$= 0.85((220 + 110 \cdot 4) \cdot \exp(-0.12 \cdot \frac{43}{10})) \cdot 10^{-6} \cdot 1.12 = 376.50 \cdot 10^{-6}$$

The value of k_h can be found in table 3.3 and is 0.70. Now the final drying shrinkage can be calculated:

$$\varepsilon_{\text{cd},\infty} = k_{\text{h}} \cdot \varepsilon_{cd,0} = 0.423\ ‰$$

- Autognenous shrinkage loss

This loss can be also be calculated using NEN-EN 1992-1-1 and follows quite straightforwardly from:

$$\varepsilon_{\text{ca}}(\infty) = 2.5(f_{\text{ck}} - 10) \cdot 10^{-6} = 2.5(35 - 10) \cdot 10^{-6} = 0.062\ ‰$$

- Relaxation loss

The final considered pre-stress loss is relaxation loss. With ρ_{1000}=2.5 % this can be calculated, again using NEN-EN 1992-1-1 formula 3.29 and using pre-stress strands of class 2 as presribed by ROK. For this calculation the length of the bridge is again discretized such that for all dx:

$$\Delta\sigma_{PR} = 0.66\sigma_{Pi}\rho_{1000}e^{9.1\mu}\left(\frac{t}{1000}\right)^{0.75(1-\mu)} \cdot 10^{-5}$$

Using:

$$\mu = \frac{\sigma_{Pi}}{f_{pk}}$$

The maximum relaxation loss $\Delta\sigma_{PR,max}$ ilustratively is computed as 60.9 MPa, assuming t=500000 h using 3.3.2 (8).

Incorporating all these losses in the internal stress of the pre-stress tendon over the length of the bridge, figure 21 can be plotted finalizing the prestress losses.

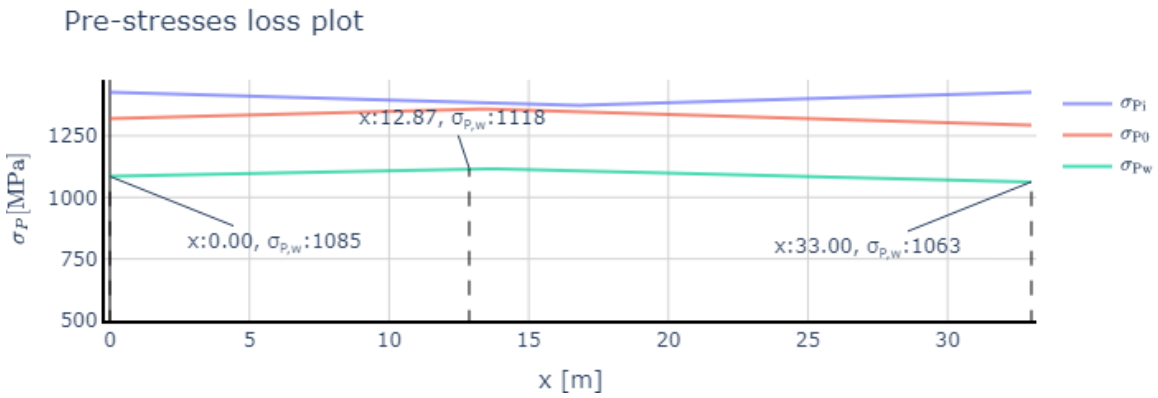

Figure 21: The prestress stresses over the length profile of the bridge.

Combining this loss plot and the pre-stress profile from figure 21 the loads shown in the report will be found

LC7.1 Wind loads

This section covers the calculations made for the windloads on the bridge in accordance with NEN-EN 1991-1-4.

The bridge is located in windarea I, and has terrain category 0. Next to that it is important to note that the free height of the bridge to ground level is 6 m.
Refering to NEN-EN 1991-1-4 some values for the variables can already be determined:

- The height of the traffic band $h_{traffic}$=4 m
- Wind direction factor c_{dir}=1.00 (NB. 4.2 (2))
- Seasonal factor c_{season}=1.00 (NB. 4.2 (2))
- Annual exceedance probability p=0.01 (NB. 4.2 (2))
- Orographic factor c_0=1 (4.3.1 (1), assumption)
- Maximum height for these calculations z_{max}=200 m (NB. 4.3.2 (1))
- Turbulence factor k_l=1 (NB. 4.4 (1))
- Volumetric weight of air ρ=1.25 kg/m^3 (NB. 4.5 (1))
- Reduced fundamental base wind speed $v^{**}_{b,0}$=25 m/s (NB. 8.1 (5))
- Building factor $c_s c_d$=1 (8.2 (1))
- Force coefficient z-direction $c_{f,z}$=1 (NB. 8.3.3 (1))

Now the steps outlined in NEN-EN 1991-1-4 + NB can be followed to calculate the windloads on the bridge.
The total height of the bridge can be calculated according to 8.3.1 (1):

$$d_{\text{tot}} = \max(h_{\text{girder}}, h_{\text{floor}} + t_{\text{ballast}} + h_{\text{sleeper}} + h_{\text{rail}} + h_{\text{traffic}}) \\ = \max(2.50, 0.50 + 1.01 + 0.22 + 0.16 + 4.00) = 5.19 \text{ m}$$

$c_{b,0}$=29.5 m/s can be found in table NB.1 and the values for K=0.200 and n=0.5 can be found in table NB.2. After that c_{prob} can be calculated:

$$c_{\text{prob}} = \left(\frac{1 - K \cdot \ln(-\ln(1-p))}{1 - K \cdot \ln(-\ln(0.98))}\right)^n = \left(\frac{1 - 0.200 \cdot \ln(-\ln(1-0.01))}{1 - 0.200 \cdot \ln(-\ln(0.98))}\right)^{0.5} = 1.04$$

Base wind speed v_b=30.64 m/s can now be calculated via 4.1 and 4.2:

$$v_{\text{b}} = c_{\text{dir}} \cdot c_{\text{season}} \cdot v_{\text{b,0}} \cdot c_{\text{prob}}$$

For the calculation of the reduced windspeed F^{**}_w, $v^{**}_{b,0}$=25.00 m/s should be used for calculating the windspeed and the resulting forces.
z_{min}=1.000 m and z_0=0.005 m can now be gathered from NB.3 - 4.1, such that k_r can be calculated with NB form 4.5:

$$k_{\text{r}} = 0.19 \cdot \left(\frac{z_0}{0.05}\right)^{0.07} = 0.19 \cdot \left(\frac{0.005}{0.05}\right)^{0.07} = 0.16$$

The reference height for the wind forces is taken as z = h_{ground}+0.5h_{girder}=6.00+0.5*2.50 = 7.25 m.

The roughness factor and additionally the average windspeed can now be calculated using formula 4.4.

$$c_{\mathrm{r}}(z) = k_{\mathrm{r}} \cdot \ln(\frac{z}{z_0}) = 0.16 \cdot \ln(\frac{7.25}{0.01}) = 1.18$$

$$v_{\mathrm{m}}(z) = c_{\mathrm{r}}(z) c_0(z) v_{\mathrm{b}} = 1.18 \cdot 1.00 \cdot 30.64 = 36.06\ \mathrm{m/s}$$

In similar fashion the turbulence intensity factor $\mathrm{l_v}$ can be calculated based on form. 4.7.

$$l_{\mathrm{v}}(z) = \frac{k_{\mathrm{l}}}{c_0(z) \cdot \ln(\frac{z}{z_0})} = \frac{1.00}{1.00 \cdot \ln(\frac{7.25}{0.01})} = 0.14$$

The base hydrostatic pressure $\mathrm{q_b}$ can be calculated using formula 4.10 and the following extreme hydrostatic pressure $\mathrm{q_p}$ from 4.8.

$$q_{\mathrm{b}} = \frac{1}{2} \cdot \rho v_{\mathrm{b}}^2 = \frac{1}{2} \cdot 1.25 \cdot 30.64^2 = 0.59\ \mathrm{kN/m^2}$$

$$q_{\mathrm{p}} = (1 + 7 l_{\mathrm{v}}(z)) \frac{1}{2} \cdot \rho v_{\mathrm{m}}(z)^2 = (1 + 7 \cdot 0.14) \cdot \frac{1}{2} \cdot 1.25 \cdot 36.06^2 = 1.59\ \mathrm{kN/m^2}$$

The wind load factor in x direction $\mathrm{c_{f,x}}$ can now be determined to be 2.06 following from fig. 8.3. $\mathrm{A_{ref,x}}$, $\mathrm{A_{ref,z}}$ can be determined by fig. 8.3 and fig. 8.6 respectively.

$$A_{\mathrm{ref,x}} = d_{\mathrm{total}} \cdot l_{\mathrm{bridge}}$$

$$A_{\mathrm{ref,x}} = b_{\mathrm{total}} \cdot l_{\mathrm{bridge}}$$

Finally the wind forces can be calculated using formula 5.3. The loads calculated from this formula are presented in the report. The loads denoted with ** represent reduced loads calculated with $\mathrm{v^{**}_{b,0}}$.

$$F_{\mathrm{w},i} = c_{\mathrm{s}} c_{\mathrm{d}} \cdot c_{\mathrm{f},i} \cdot q_{\mathrm{p}}(z_{\mathrm{e}}) A_{\mathrm{ref},i}$$

LC9.1.1 Train loads model LM71 M

This section covers the calculations made for the train load model LM71 in accordance with NEN-EN 1992-1. The load model as given in the eurocode is shown in figure 22.

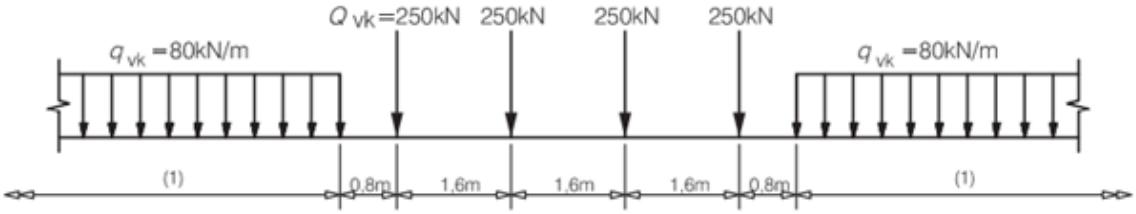

Figure 22: Load model LM71 as given in NEN-EN 1992-1

These loads need to be multiplied with α which is 1.21 according to the national annex and dynamic factor Φ_2 for carefully maintained rail. This factor can be calculated via formula 6.4 from NEN-EN 1991-2 where L_Φ can be calculated as twice the span of the deck from table 6.2 4.3.

$$\Phi_2 = \min(\max(\frac{1.44}{\sqrt{L_\Phi} - 0.2} + 0.82; 1); 1.67) = 1.27$$

The loads may be divided by the effective with over which they are spread, which is calculated in the main report. Next to that the point loads in the middle are assumed to be evenly destributed for middle part of the load.

The position of the load on the bridge has been choossen by running an influence line analysis which shows the position of the load which gives the highest possible moment at mid-span given in figure 23. Next to that also an excentricity e calculated with NEN-EN 1991-2 figure 6.3 is introduced for the LM71 loads. However the effect of this excentricity is not significant.

$$e = \frac{r}{18} = \frac{1435}{18} = 79.7 \text{ mm}$$

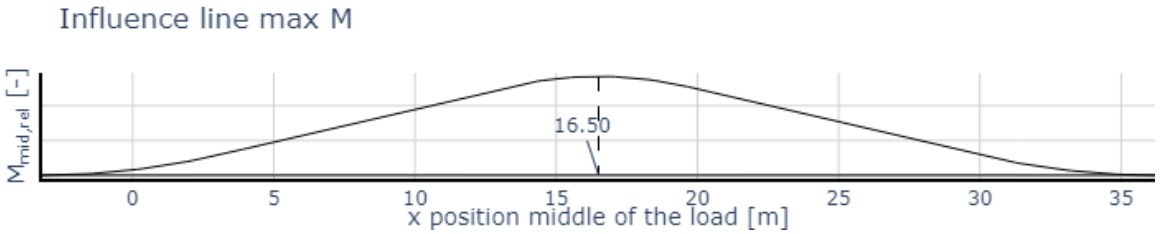

Figure 23: Influence line LM71 load model for the bridge, maximum moment

LC9.1.2 Train loads model LM71 V

The load resulting in the highest shear force is calculated in the same manner and results in the following influence line 24.

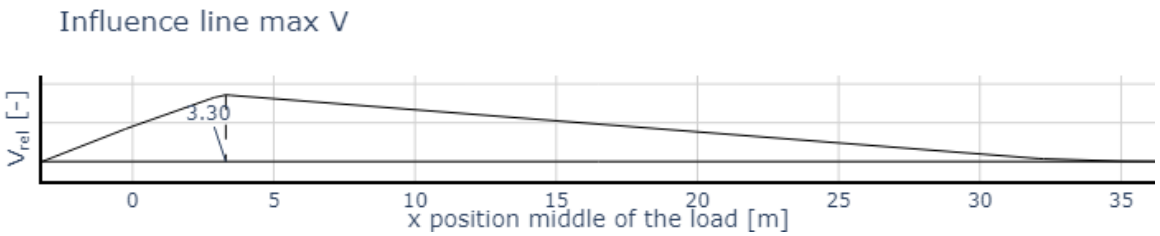

Figure 24: Influence line LM71 load model for the bridge, maximum shear force

LC9.3.1 Train loads model SW/2 M

This section covers the calculations made for the train load model SW/2 in accordance with NEN-EN 1992-1. The load model as given in the eurocode is shown in figure 25.

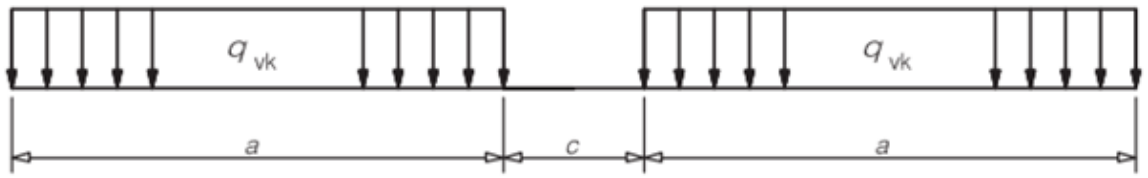

Figure 25: Load model SW as given in NEN-EN 1992-1

The values of a, c and q_{vk} are given as 25 m, 7 m, 150 kN/m respectively. Loads for SW/2 should not be multiplied with factor α and dynamic factor Φ_2.
Just like before these loads are spread over the effective width and the position has once again been choossen using influence lines. Figure 26 shows the influence line for max mid-span moment for this load model.

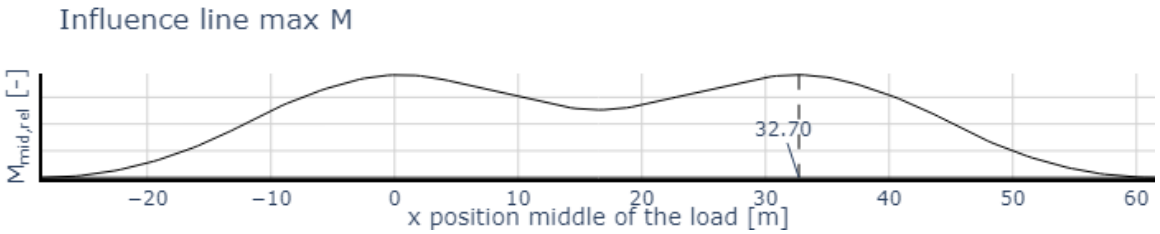

Figure 26: Influence line SW/2 load model for the bridge, maximum moment

LC9.3.2 Train loads model SW/2 V

In the same manner the influence line for the maximum shear force is displayed in figure 27.

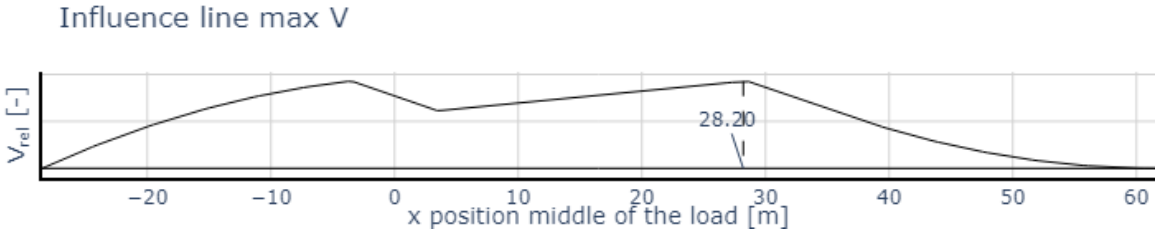

Figure 27: Influence line SW/2 load model for the bridge, maximum shear force

Annex D: Load combinations

The limit states ULS, SLS-Characteristic, SLS-Frequent, SLS-Quasi Permanent are considered in the FEM model.
The decisive load combination for ULS is the least favourable of NEN-EN 1990 form. 6.10a, 6.10b:

$$\sum_{j\geq 1} \gamma_{G,j} G_{k,j} + \gamma_P P + \gamma_{Q,1} \Psi_{0,1} Q_{k,1} + \sum_{i>1} \gamma_{Q,i} \Psi_{0,i} Q_{k,i}$$

$$\sum_{j\geq 1} \xi_j \gamma_{G,j} G_{k,j} + \gamma_P P + \gamma_{Q,1} Q_{k,1} + \sum_{i>1} \gamma_{Q,i} \Psi_{0,i} Q_{k,i}$$

For SLS-Characteristic the desicive load combination is governed by 6.14b:

$$\sum_{j\geq 1} G_{k,j} + P + Q_{k,1} + \sum_{i>1} \Psi_{0,i} Q_{k,i}$$

And for SLS-Frequent the desicive load combination is governed by 6.15b:

$$\sum_{j\geq 1} G_{k,j} + P + \Psi_{1,1} Q_{k,1} + \sum_{i>1} \Psi_{2,i} Q_{k,i}$$

Finally for SLS-Quasi Permanent the desicive load combination is governed by 6.16b:

$$\sum_{j\geq 1} G_{k,j} + P + \sum_{i\geq 1} \Psi_{2,i} Q_{k,i}$$

For the load combinations it is important to note that the bridge is CC3 and it only features one rail, the gamma factors are shown in table 7

$\gamma_{G,j,sup}$ 6.10a	1.40
$\gamma_{G,j,sup}$ 6.10b	1.25
$\gamma_{G,j,inf}$	0.90
$\gamma_{G,i}$ Train load gr16, gr17, gr26, gr27	1.25
$\gamma_{G,i}$ Train load other groups	1.50
$\gamma_{G,i}$ Wind load	1.65
$\gamma_{G,i}$ Other variable loads	1.65

Table 7: γ factors from NEN-EN 1990 Table NB.17

The Ψ factors from NEN-EN 1990 table A2.3 can be translated to the different limit states as shown in tables 8 - 11:

	LM71				SW/2	
Load combination	gr11	gr12	gr13	gr14	gr16	gr17
LC1 Permanent loads	1.00					
LC4 Other variable loads	0.80					
LC7.1 Wind loads	0.75			0.75		
LC7.2 Reduced wind loads	1.00			1.00		
LC9.1.1 Train loads model LM71 M	0.80		0.40			
LC9.3.1 Train loads model SW/2 M					0.80	

Table 8: Ψ factors for form. 6.10a

	LM71				SW/2		Wind			
Load combination	gr11	gr12	gr13	gr14	gr16	gr17	gr11	gr12	gr14	gr15
LC1 Permanent loads	1.00									
LC4 Other variable loads	0.80									
LC7.1 Wind loads	0.75			0.75			1.00			
LC7.2 Reduced wind loads	1.00			1.00			1.00			
LC9.1.1 Train loads model LM71 M	1.00		0.50				0.80		0.40	
LC9.3.1 Train loads model SW/2 M					1.00					

Table 9: Ψ factors for form. 6.10b and 6.14b

	LM71				SW/2		Wind	Wind deflection			
Load combination	gr11	gr12	gr13	gr14	gr16	gr17	force	gr11	gr12	gr14	gr15
LC1 Permanent loads	1.00										
LC4 Other variable loads											
LC7.1 Wind loads							0.50				
LC7.2 Reduced wind loads											
LC9.1.1 Train loads model LM71 M	0.80		0.40					1.00		0.50	
LC9.3.1 Train loads model SW/2 M					0.80						

Table 10: Ψ factors for form. 6.15b

Load combination	Quasi-permanent
LC1 Permanent loads	1.00
LC4 Other variable loads	
LC7.1 Wind loads	
LC7.2 Reduced wind loads	
LC9.1.1 Train loads model LM71 M	
LC9.3.1 Train loads model SW/2 M	

Table 11: Ψ factors for form. 6.16b

From these factors the decisive load combinations can be summarized as shown in tables 12 - 16. The wind and train loads are exclusive load cases, meaning that e.g. both wind loads can not be present at the same time.

Load combination	gr11 LM71	gr16 SW/2	gr17 SW/2
LC1 Permanent loads	1.40		
LC4 Other variable loads	1.32		
LC7.1 Wind loads	1.24		
LC7.2 Reduced wind loads	1.65		
LC9.1.1 Train loads model LM71 M	1.20		
LC9.3.1 Train loads model SW/2 M		1.00	

Table 12: ULS 6.10a

Load combination	gr11 LM71	gr16 SW/2	gr17 SW/2	gr11 Wind
LC1 Permanent loads	1.25			
LC4 Other variable loads	1.32			
LC7.1 Wind loads	1.24			1.65
LC7.2 Reduced wind loads	1.65			1.65
LC9.1.1 Train loads model LM71 M	1.50			1.20
LC9.3.1 Train loads model SW/2 M		1.25		

Table 13: ULS 6.10b

Load combination	gr11 LM71	gr16 SW/2	gr17 SW/2	gr11 Wind
LC1 Permanent loads	1.00			
LC4 Other variable loads	0.80			
LC7.1 Wind loads	0.75			1.00
LC7.2 Reduced wind loads	1.00			1.00
LC9.1.1 Train loads model LM71 M	1.00			0.80
LC9.3.1 Train loads model SW/2 M		1.00		

Table 14: SLS 6.14b

Load combination	gr11 LM71	gr16 SW/2	gr17 SW/2
LC1 Permanent loads	1.00		
LC4 Other variable loads			
LC7.1 Wind loads			
LC7.2 Reduced wind loads			
LC9.1.1 Train loads model LM71 M	0.80		
LC9.3.1 Train loads model SW/2 M		0.80	

Table 15: SLS 6.15b

Load combination	Quasi-permanent
LC1 Permanent loads	1.00
LC4 Other variable loads	
LC7.1 Wind loads	
LC7.2 Reduced wind loads	
LC9.1.1 Train loads model LM71 M	
LC9.3.1 Train loads model SW/2 M	

Table 16: SLS 6.16b

Annex E: ULS Girder stirrup calculations

This section will feature the calculation of the stirrups of the girder in ULS. The angle of θ is 21.8°.

Torsion

The decisive torsional moment T_{Ed} in the beam follows from the FEM results and is: 1278 kNm.
For determining the shear stresses the effective width t_{eff} should first be calculated according to NEN-EN 1992-1-1 figure 6.11:

$$t_{\text{eff}} = \min(W_{\text{gir}} \cdot 0.5; \frac{A_{\text{gir}}}{u_{\text{gir}}}) = 117 \text{ mm}$$

Where u_{gir}=7400 mm, is the perimeter of the girder.

With the effective effective width A_k as described in NEN-EN 1992-1-1 figure 6.11 can be calculated.

$$A_{\text{k}} = (h_{\text{gir}} - t_{\text{eff}}) \cdot (W_{\text{gir}} - t_{\text{eff}}) = 2580139 \text{ mm}^2$$

The required area of longitudinal reinforcement required for this torsion $A_{sl,T,req}$ can be calculated with formula 6.28.

$$A_{\text{sl,T,req}} = \frac{u_{\text{k}} T_{\text{Ed}} \cot(\theta)}{2 A_{\text{k}} f_{\text{yd}}} = 9218 \text{ mm}^2$$

Using u_k = 6462 mm, the perimeter of A_k.
The shear stress τ_T due to torsion can be calculated using formula 6.26.

$$\tau_{\text{T}} = \frac{T_{\text{Ed}}}{2 A_{\text{k}} t_{\text{eff}}} = 2.11 \text{ MPa}$$

Using these results and formula 6.27 an equivalent shear force $V_{Ed,T}$ on the vertical ribs can be calculated.

$$V_{\text{Ed,T}} = \tau_{\text{T}} t_{\text{eff}} z_{\text{y}} = 590 \text{ kN}$$

Using z_y=h_{gir}-t_{eff}=2383 mm.
Finally the required shear reinforcement for torsion in the vertical ($A_{sw,T}$) and horizontal ($A_{sw,T,hor}$) stirrups parts can be calculated using 6.8.

$$A_{\text{sw,T,req}} = \frac{V_{\text{Ed,T}}}{z f_{\text{yd}} \cot(\theta)} = 249 \text{ mm}^2$$

$$A_{\text{sw,T,hor,req}} = \frac{T_{\text{Ed}}}{2 A_{\text{k}} f_{\text{yd}} \cot(\theta)} = 228 \text{ mm}^2$$

Shear

The decisive shear force V_{Ed} in the beam follows from the FEM results and is: 3002 kN. Continuing from the torsion results, the maxium shear force in a wall with thickness t_{eff} in the cross-section can be calculated. It is assumed that 60% of the shear force will be transfered by the middle stirrup and the other 40% will be distributed to the outside walls, where the shear is also present:

$$V_{\text{Ed,max}} = V_{\text{Ed}} \cdot 0.2 + V_{\text{Ed,T}} = 1190376 \text{ kN}$$

To check if calculated stirrups are needed the check $V_{Ed,max} < V_{Rd,c}$ using formula 6.4:

$$V_{\text{Rd,c}} = \frac{Ib_{\text{w}}}{S}\sqrt{f_{\text{ctd}}^2 + \alpha_{\text{l}}\sigma_{\text{cp}}f_{\text{ctd}}} = 487860 \text{ kN}$$

Where α_l=1 and σ_P is calculated as:

$$\sigma_{\text{cp}} = \frac{\sigma_{\text{Pw}}A_{\text{P}}}{A_{\text{gir}}} = 6.10 \text{ MPa}$$

From this we can conclude that $V_{Ed,max} > V_{Rd,c}$ and the assumption that stirrups are needed is justified. The required stirrup area per zone can be calculated, again using 6.8:

$$A_{\text{sw,I,req}} = \frac{0.2V_{\text{Ed}}}{zf_{\text{yd}}\cot(\theta)} = 254 \text{ mm}^2$$

$$A_{\text{sw,II,req}} = \frac{0.6V_{\text{Ed}}}{zf_{\text{yd}}\cot(\theta)} = 761 \text{ mm}^2$$

$$A_{\text{sw,III,req}} = \frac{0.2V_{\text{Ed}}}{zf_{\text{yd}}\cot(\theta)} = 254 \text{ mm}^2$$

Suspension force and fixed end moment

For the calculation of the hanging moment and suspension forces NSRL1015 is used as guideline. The suspension force and fixed end moment of the floor acting on the girder cause tension stresses in the cross-section as shown in figure 28.

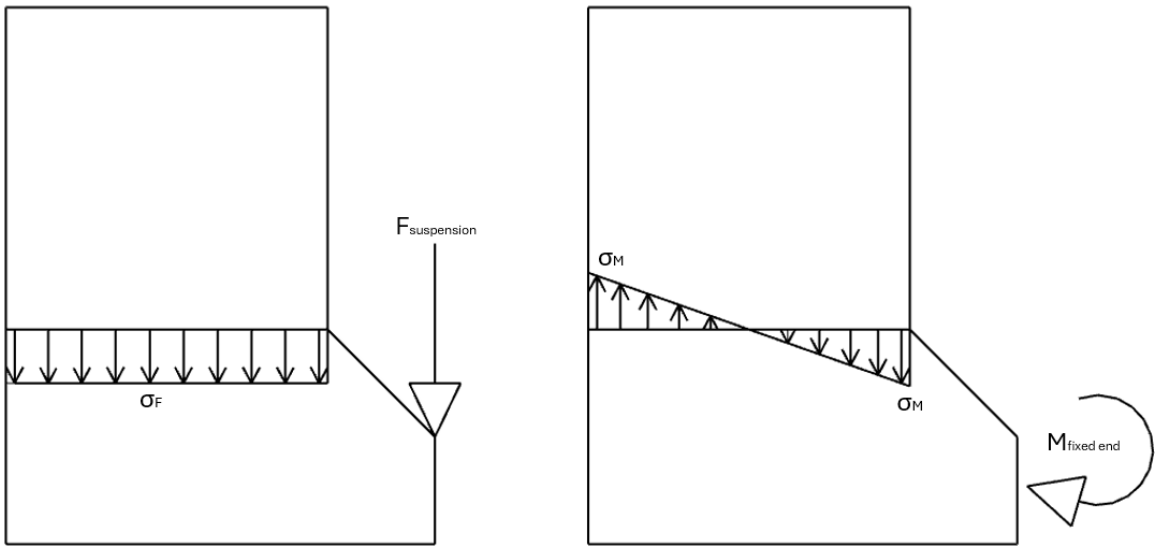

Figure 28: Stress distribution in cross-section

These stresses need to resisted by stirrups in the girder. Because the critical line for the connection of the girder and the floor is along the top of the haunch. This way only the load that needs to be carried by the top part of the girder needs to be accounted for because this needs to be carried to the top part of the cross-section. This is translated to a reduction factor based on the area of the cross-section, as described in NSRL1015.

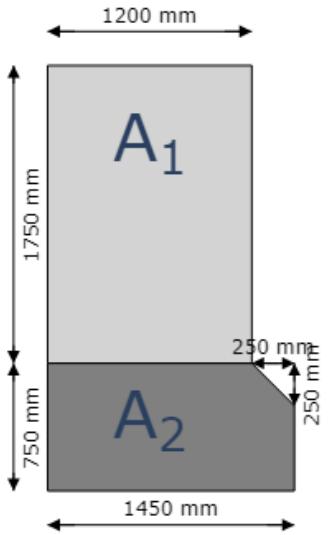

Figure 29: Area's used for reduction factor

$$\alpha_A = \frac{A_1}{A_1 + A_2} = \frac{2100000}{3156250} = 0.67$$

For the maximum suspension force acting on a girder it should be incorporated that the decisive train load SW/2 does not act in the middle of the floor, rather at x = 3.4 m, as shown in figure 30. This means that this load should be distributed to the right girder for the maximum resulting force.

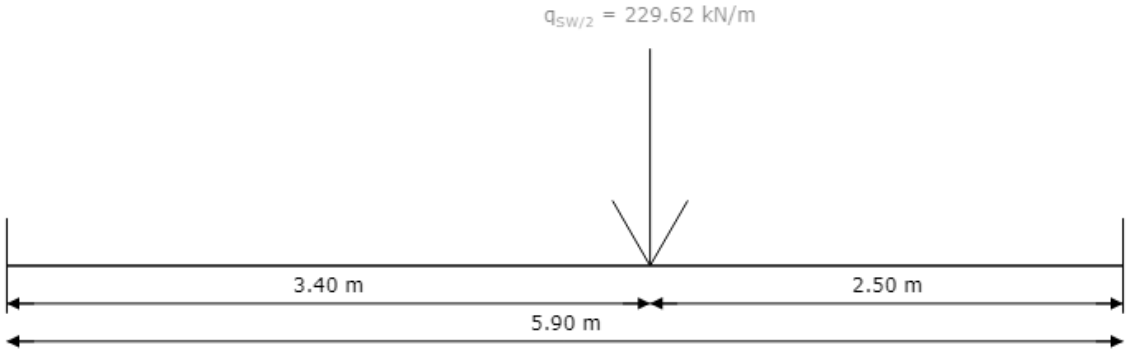

Figure 30: Position of the train load as seen on the cross-section of the floor

$$q_{\text{SW/2}} = 150\alpha\phi_2 = 150 \cdot 1.21 \cdot 1.27 = 230 \text{ kN/m}$$

$$F_{\text{SW/2}} = \frac{q_{\text{SW/2}}a}{a + 2 \cdot \frac{1}{2} \cdot 2.50}\frac{3.40}{5.90} = 120 \text{ kN/m}$$

Using the length of the load model SW/2 a = 25 m. The self-weight of the bridge and dead loads of the train infrastructure can be divided by 2 to find F_G = 73 kN/m. Incorporating the load factors to find the suspension force:

$$F_{\text{sus}} = \max(1 \cdot F_{\text{SW/2}} + 1.4 \cdot F_{\text{G}}; 1.25 \cdot F_{\text{SW/2}} + 1.25 \cdot F_{\text{G}}) = 241 \text{ kN/m}$$

The fixed end moment can be calculated using the structural model in figure 30, conservatively assuming fully clamped boundary conditions.

$$M_{\text{SW/2}} = \frac{q_{\text{SW/2}} \cdot 3.4^2 \cdot 2.5}{5.9} = 392 \text{ kNm/m}$$

Next to that the suspension force also causes a moment:

$$M_{\text{sus}} = F_{\text{G}} \cdot \frac{1}{2} W_{\text{girder}} = 62 \text{ kNm/m}$$

The maximum fixed end moment can now be calculated as:

$$M_{\text{fix}} = \max(1 \cdot M_{\text{SW/2}} + 1.4 \cdot M_{\text{sus}}; 1.25 \cdot M_{\text{SW/2}} + 1.25 \cdot M_{\text{sus}}) = 241 \text{ kNm/m}$$

The required area of the reinforcement can now be calculated according to the stresses shown in figure 28.

$$A_{\text{sw,F}} = \frac{\alpha_{\text{A}} F_{\text{sus}}}{f_{\text{yd}}} = 370 \text{ mm}^2$$

$$A_{\text{sw,M}} = \frac{\alpha_{\text{A}} M_{\text{fix}}}{z f_{\text{yd}}} = 1294 \text{ mm}^2$$

Using z = 0.9W_{gir} the total additional required area of stirrups in zone III can be calculated.

$$A_{\text{sw,III,req}} = A_{\text{sw,F}} + A_{\text{sw,M}} = 1663 \text{ mm}^2$$

Evaluation

The unity checks per zone of stirrups can now be calculated.

$$u.c_{sl,T} = \frac{A_{sl,T,req}}{A_{sl,T}} = \frac{9218}{10455} = 0.88$$

$$u.c_{sw,T,hor} = \frac{A_{sl,T,hor,req}}{A_{sl,T,hor}} = \frac{228}{565} = 0.40$$

$$u.c_{sw,I} = \frac{A_{sl,I,req}}{A_{sl,I}} = \frac{503}{565} = 0.89$$

$$u.c_{sw,II} = \frac{A_{sl,II,req}}{A_{sl,II}} = \frac{761}{905} = 0.84$$

$$u.c_{sw,III} = \frac{A_{sl,III,req}}{A_{sl,III}} = \frac{2166}{2234} = 0.97$$

Please note that the required longitudinal reinforcement for torsion at the bottom of the cross-section is added to the longitudinal reinforcement for moment and normal force.

Annex F: ULS Girder cross-section calculations

This section will feature the calculation for the girder in ULS. The decisive moment for the girder M_{Ed} = 19577 kNm.

Cross-sectional analysis

To calculate the moment resistance the stress and strain diagrams of the cross-section need to be determined. This is done with an automatic algorithm that solves the force equilibrium ΣF_h = - N_c + N_c + F_{Pw} + ΔF_P = 0 to find figures 31 and 32.

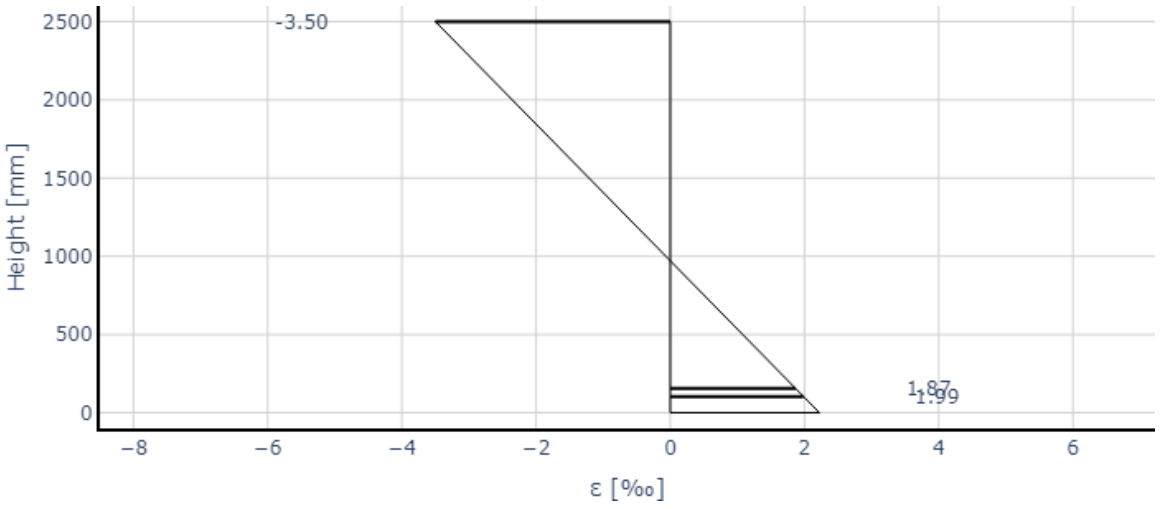

Figure 31: Strain diagram

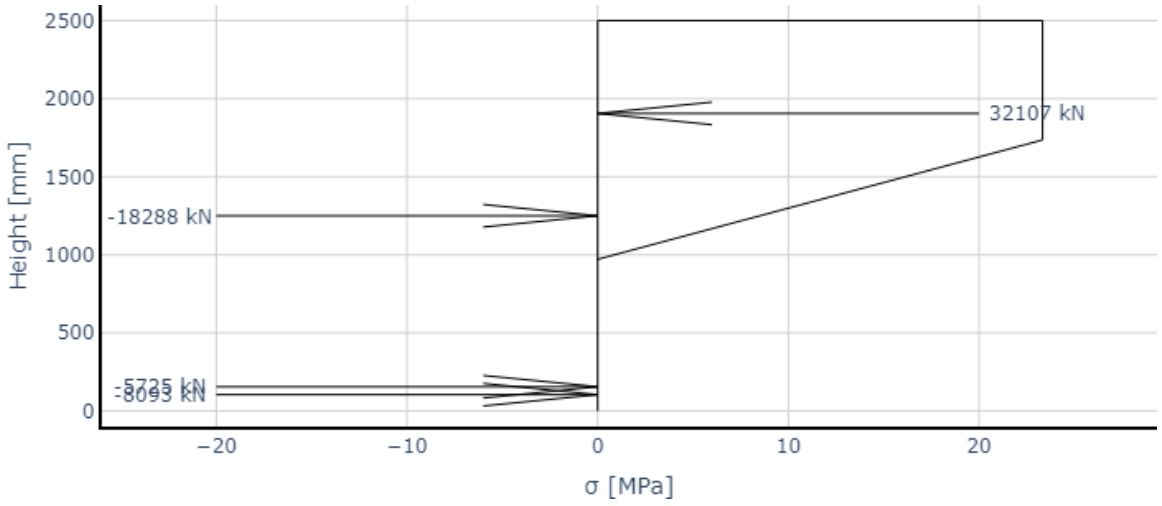

Figure 32: Stress diagram

To justify these diagrams the following calculations are made.

$$N_c = \alpha f_{cd} w_{gir} x_u = 32107 \text{ kN}$$

Here α = 0.75 and x_u = 1529 mm.
The force in the steel can be calculated using:

$$N_s = A_s \cdot \min(E_s \varepsilon_s; f_{yd}) = 8093 \text{ kN}$$

Where the area of longitudinal reinforcement required for torsion $A_{sl,T,req}$ = 1494.7565266736788 mm² is subtracted from A_s and:

$$\varepsilon_s = \varepsilon_{cu} \frac{d_s - x_u}{x_u} = 1.99 \text{ ‰}$$

Using ε_{cu} = 3.50‰.
For the prestress force both the pre-stress force F_{Pw} and the force induced by the strain in the pre-stress ΔF_P are important. First F_{Pw} is calculated:

$$F_{Pw} = \sigma_{Pw} A_P = 18288 \text{ kN}$$

Now ΔF_P can be calculated:

$$\Delta\varepsilon_P = \varepsilon_{cu} \frac{d_P - x_u}{x_u} = 1.87 \text{ ‰}$$

$$\varepsilon_{P,tot} = \frac{F_{Pw}}{A_P E_P} + \Delta\varepsilon_P = 7.55 \text{ ‰}$$

$$\Delta F_{Pw} = \sigma_P(\varepsilon_P) A_P - F_{Pw} = 5725 \text{ kN}$$

Where σ_P is dependent on the strain of the pre-stress steel via the bilinear relationship\nIt can now be verfied that ΣF_h = 0. The moment resistance can now be calculated using:

$$e_{\mathrm{P}} = d_{\mathrm{P}} - \frac{1}{2}h_{\mathrm{gir}};\ e_{\mathrm{s}} = d_{\mathrm{s}} - \frac{1}{2}h_{\mathrm{gir}}$$

$$e_{\mathrm{c}} = \frac{1}{2}h_{\mathrm{gir}} - \beta x_{\mathrm{u}}$$

$$M_{\mathrm{Rd}} = N_{\mathrm{c}}e_{\mathrm{c}} + e_{\mathrm{s}}N_{\mathrm{s}} + \Delta F_{\mathrm{P}}e_{\mathrm{P}} = 36590\ \mathrm{kNm}$$

Finally the unity check can be calculated:

$$\mathrm{u.c}_{\mathrm{M,gir}} = \frac{M_{\mathrm{Ed}}}{M_{\mathrm{Rd}}} = \frac{19577}{36590} = 0.54$$

Compression zone height

NEN-EN 1992-1-1 NB 6.1 (9) describes the maximum height of the concrete compression zone of concrete girders:

$$\frac{x_u}{d} \leq \frac{500}{500 + f} = 0.33$$

Where f=1011 MPa is the weighted steel strength of the pre-stress and steel where the σ_{Pw} is subtracted from the pre-stress steel strength.
This is not satisfied as $x_u/d=0.64$.However the pre-stress can fictitiously be lowered to make sure this requirement is satisfied. It is important to note that M_{Ed} will increase when lowering pre-stress and M_{Rd} will decrease. When the pre-stress is lowered to 44 %, M_{Ed} becomes 29712 kNm. When also lowering A_P with this factor, the new distriubutions can be found:

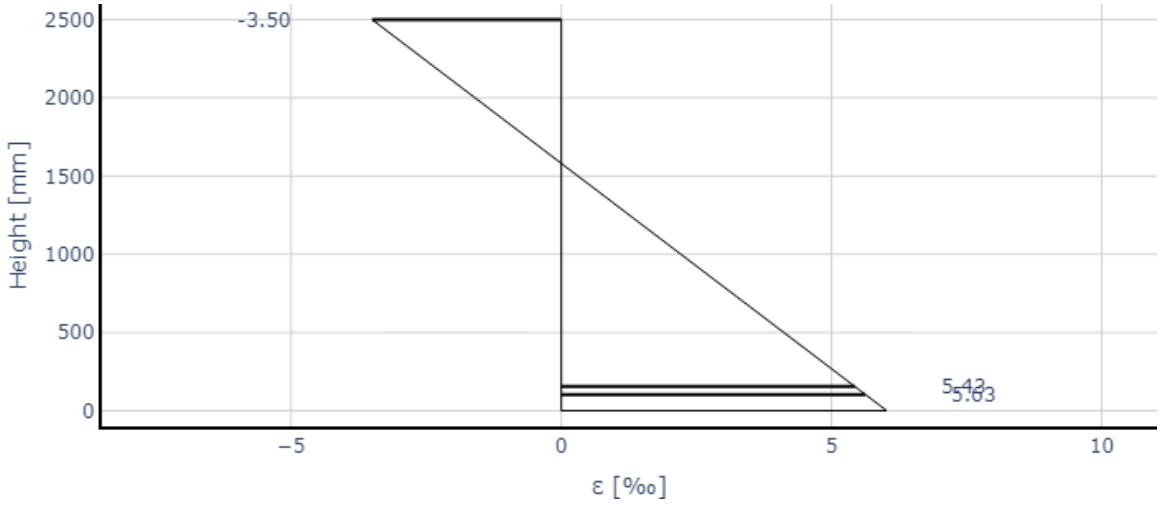

Figure 33: Strain diagram

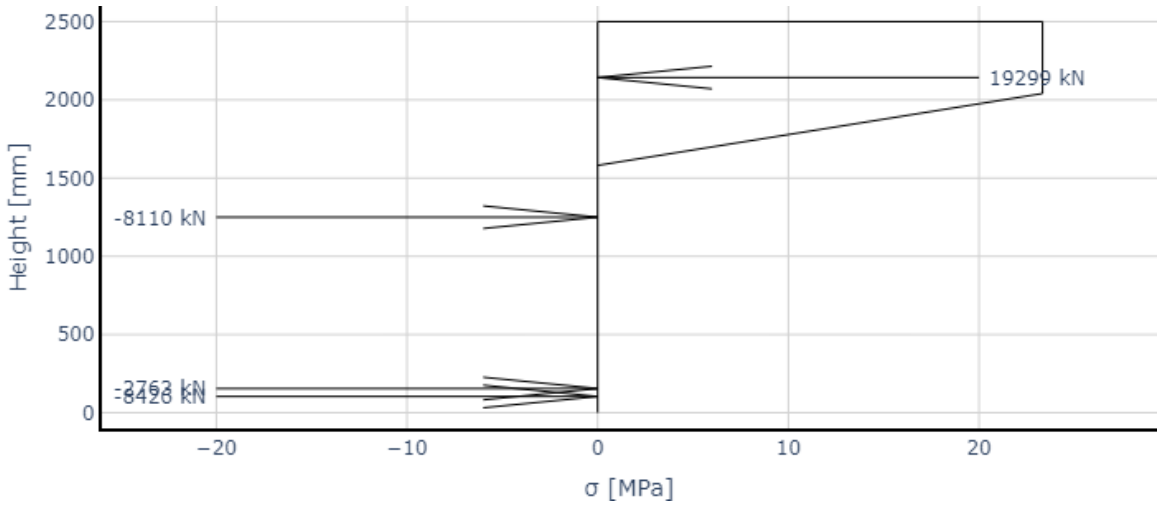

Figure 34: Stress diagram

Using the same equations as before it is obtained that:

$$M_{\text{Rd}} = N_{\text{c}} e_{\text{c}} + e_{\text{s}} N_{\text{s}} + \Delta F_{\text{P}} e_{\text{P}} = 29909 \text{ kNm}$$

Resulting in:

$$\text{u.c}_{\text{M,rot}} = \frac{M_{\text{Ed}}}{M_{\text{Rd}}} = \frac{29712}{29909} = 0.99$$

Also the maximum height of the compression zone is now sufficient:

$$\frac{x_{\text{u}}}{d} \leq \frac{500}{500 + f} = 0.39$$

$$0.39 \leq 0.39$$

Annex G: ULS Floor cross-section calculations

In this chapter the ULS calculations for the floor will be displayed.

y-direction

The decisive moment in the floor is at midspan: $M_yD+ = 549$ kNm/m. Again the stress-strain distribution can be determined given in figure 35 and 36, making sure that $\Sigma F_h = 0$.

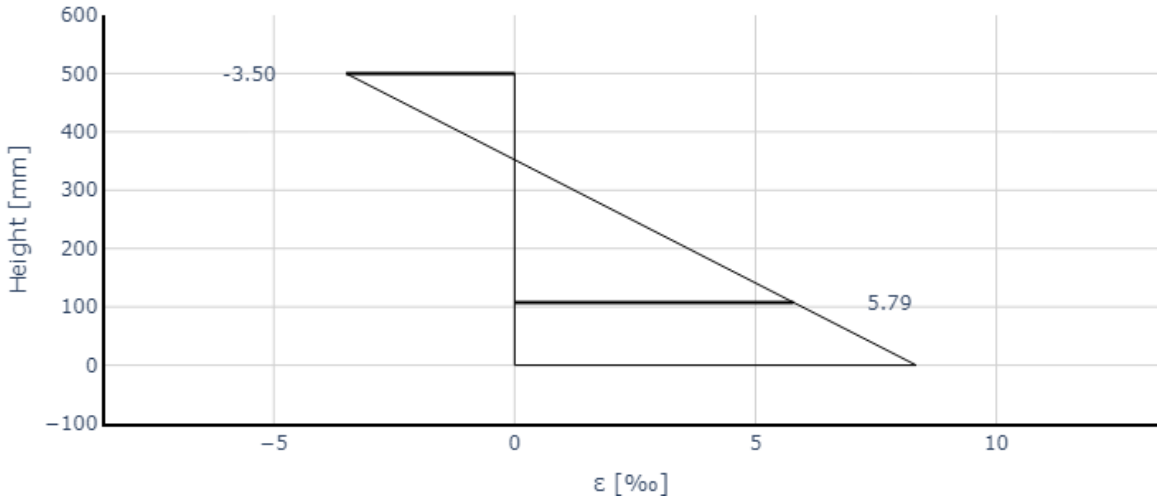

Figure 35: Strain diagram

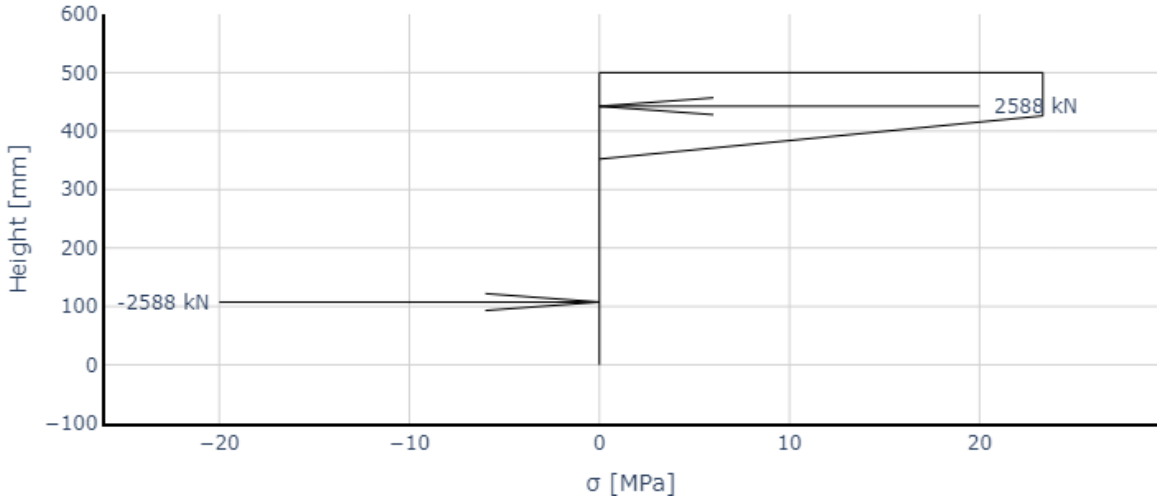

Figure 36: Stress diagram

The calculations for these diagrams are given below.

$$N_c = \alpha f_{cd} w_{gir} x_u = 2588 \text{ kN}$$

Here α = 0.75 and x_u = 148 mm.
The force in the steel can be calculated using:

$$N_s = A_s \cdot \min(E_s \varepsilon_s; f_{yd}) = 2588 \text{ kN}$$

Where:

$$\varepsilon_s = \varepsilon_{cu} \frac{d_s - x_u}{x_u} = 5.79\ ‰$$

Using ε_{cu} = 3.50‰.
The moment capacity can be calculated using:

$$M_{Rd} = N_s z = 867\ \text{kNm}$$

Using $z = d_s - \beta x_u$.
Finally the unity check can be calculated:

$$\text{u.c}_{M,floor,y} = \frac{M_{Ed}}{M_{Rd}} = \frac{549}{867} = 0.63$$

x-direction

This whole calculation can be repeated for the reinforcement in longitudinal directon: M_xD+ = 206 kNm/m. be determined given in figure 37 and 38, making sure that ΣF_h.

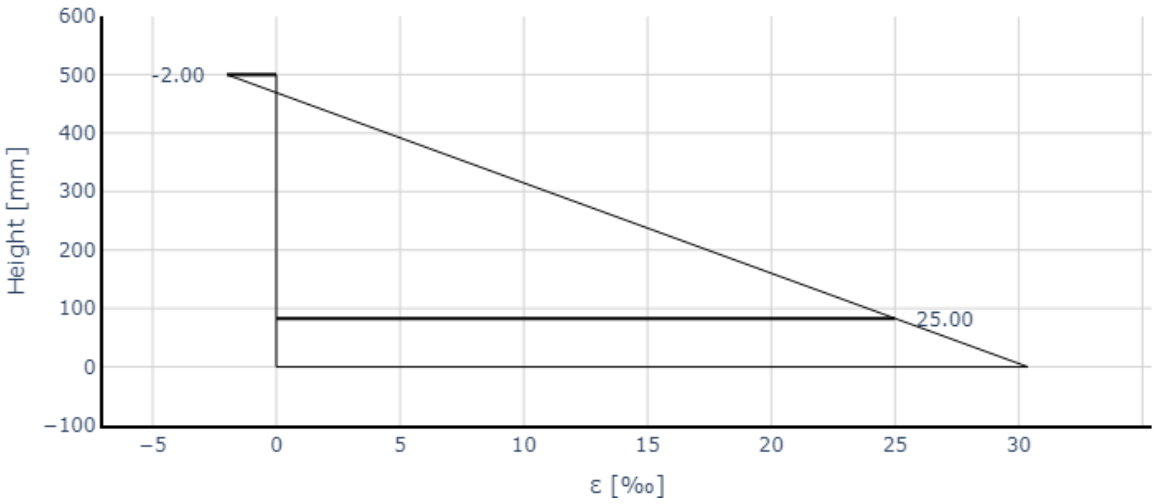

Figure 37: Strain diagram

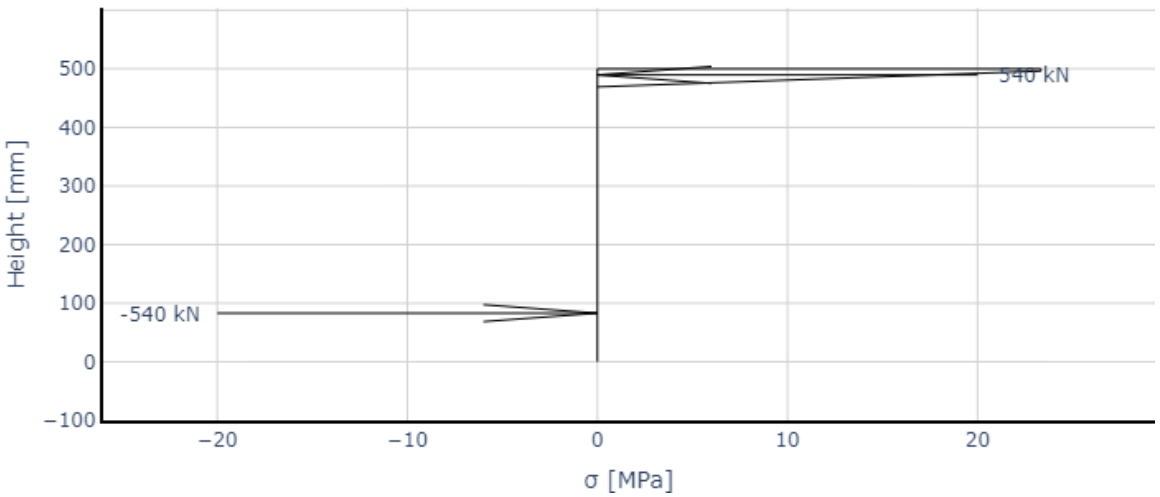

Figure 38: Stress diagram

The calculations for these diagrams are given below.

$$N_c = \alpha f_{cd} w_{gir} x_u = 540 \text{ kN}$$

Here α = 0.75 and x_u = 31 mm.
The force in the steel can be calculated using:

$$N_s = A_s \cdot \min(E_s \varepsilon_s; f_{yd}) = 540 \text{ kN}$$

Where:

$$\varepsilon_s = \varepsilon_{cu} \frac{d_s - x_u}{x_u} = 25.00 \text{ ‰}$$

Using ε_{cu} = 2.00‰.
The moment capacity can be calculated using:

$$M_{Rd} = N_s z = 220 \text{ kNm}$$

Using $z = d_s - \beta x_u$
Finally the unity check can be calculated:

$$\text{u.c}_{M,floor,y} = \frac{M_{Ed}}{M_{Rd}} = \frac{206}{220} = 0.94$$

Annex H: ULS Longitudinal shear calculations

In this chapter the ULS calculations for the longitudinal shear between the floor and the girder will be described according to the calculation method of NEN-EN 1992-1-1 6.2.4. This method calculates the longitudinal shear as:

$$v_{Ed} = \frac{\Delta F_d}{h_f \Delta x} = 0.56 \text{ MPa}$$

The maximum value that may be assumed for Δx is half the distance between the cross-section where the moment is 0 and the cross-section where the moment is at a maximum (6.2.4 (3)). In this case this means that Δx half the length of the span of the bridge. The other parameters are summarized in figure 39:

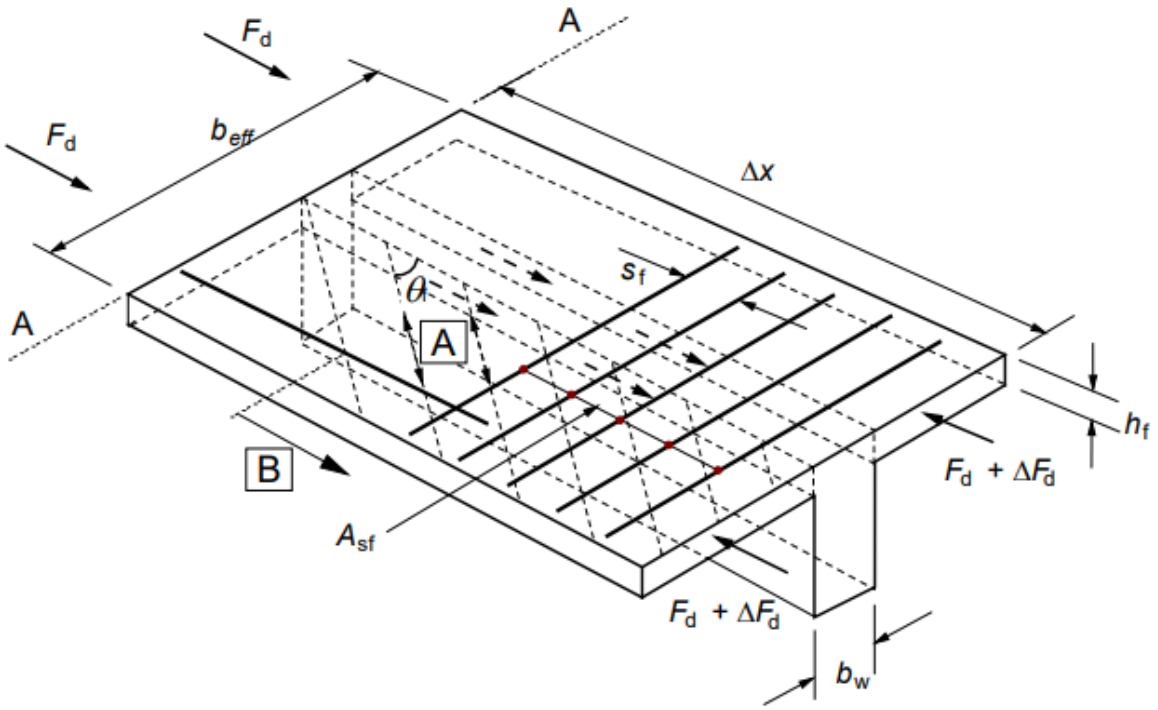

Figure 39: NEN-EN 1992-1-1 figure 6.7

The figure shows a T-girder however for a trough girder bridge one flange can be ignored. To obtain the maximum shear stress calculated above an automatic algorithm was used to find Δx = 0.25 m and ΔF_d = 70 kN, between the sections at x = 7.00 m and x = 7.25 m. The forces are obtained by integrated the 2D forces of the floor over the effective width of the floor on one side. To check if reinforcement is required the following check is performded:

$$v_{Ed} < k f_{ctd}; 0.56 < 0.59$$

This check is O.K. so no reinforcement is needed.

Annex I: ULS Splitting forces ends of deck

In this chapter the ULS calculations for the splitting reinforcement at the ends of the deck will be performed. A tension force in the ends of the deck is introduced due to the introduction of the prestress as shown in figure 40:

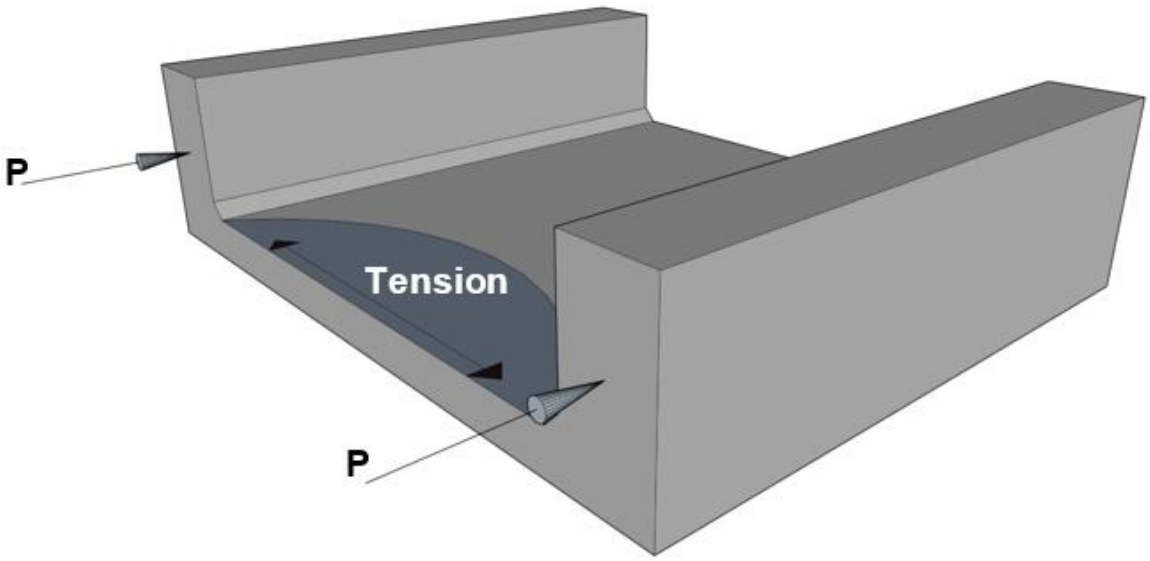

Figure 40: Splitting forces at the ends of the deck

To reinforce the bridge against these tension stresses, extra reinforcement is needed. The required reinforcement is calculated using a strut and tie model. First the equivalent stress in the whole bridge in the bernouilli zone at x = 4150 mm due to pre-stress is calculated.

$$\sigma_{\text{eq}} = \frac{2F_P}{A_{\text{P}}} = 3.86 \text{ MPa}$$

Using this stress the force in the girders and beam can be calculated:

$$F_{\text{floor/}} = \frac{1}{2}\sigma_{\text{eq}} A_{\text{floor}} = 5689 \text{ kN}$$

$$F_{\text{girder}} = \sigma_{\text{eq}} A_{\text{girder}} = 11571 \text{ kN}$$

With these values the STM shown in figure 41 can be obtained:

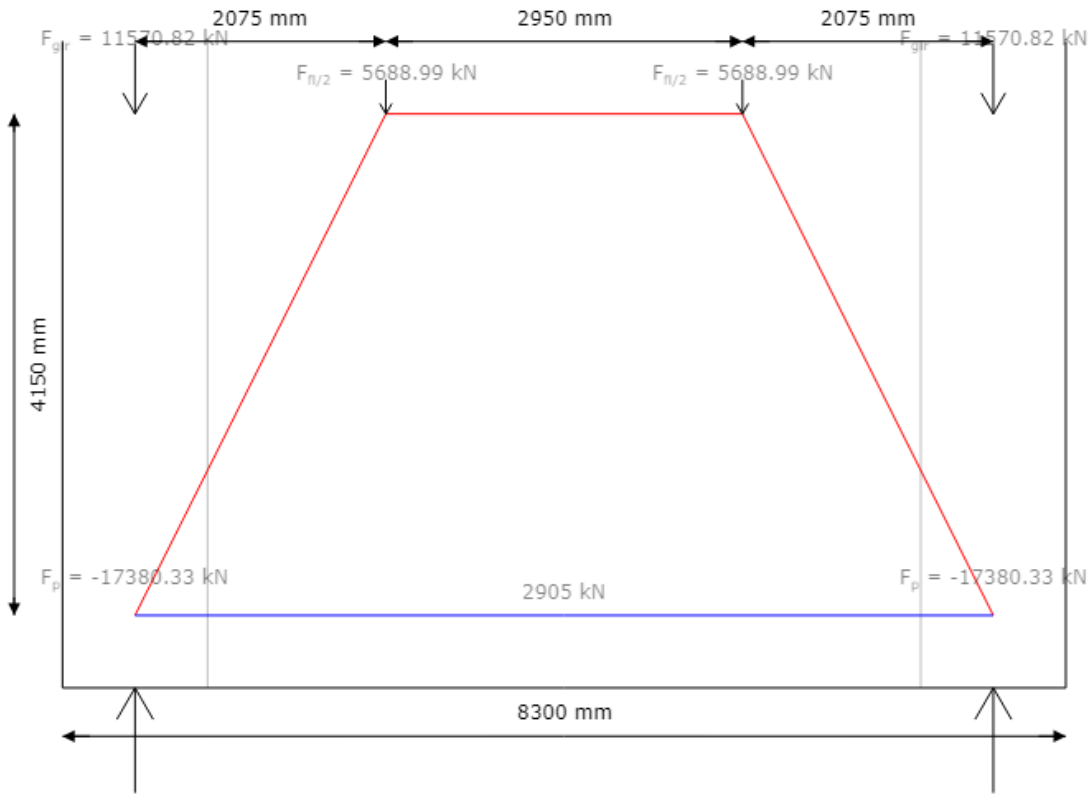

Figure 41: Strut and tie model splitting reinforcement

With the calculated force the stress in the splitting reinforcement can be calculated knowing that the designed splitting reinforcement is 9⌀32:

$$\sigma_{\text{spl}} = \frac{F_{\text{spl}}}{A_{\text{spl}}} = \frac{2904758}{7238} = 401 \text{ MPa}$$

Now the unity check can be calculated:

$$\text{u.c}_{\text{spl}} = \frac{\sigma_{\text{spl}}}{f_{\text{yd}}} = \frac{401}{434} = 0.92$$

Annex J: SLS Girder stress checks

This annex will show two SLS stresses checks for the girder.

Tension checks

The first check is an extra check required by OVS00030-6 as an amendment to NEN-EN 1992-1-1 7.3.1, which requires that:

1. In SLS-quasi: $\sigma_{ct} < 0$
2. In SLS-freq: $\sigma_{ct} < 0.5\, f_{ctk,0.05}$ and $\sigma_{ct} < 0.5\, f_{ctk,0.05}$
3. In SLS-char: $\sigma_{ct} < 0.5\, f_{ctk,0.05}$ and $\sigma_{ct} < 0.5\, f_{ctk,0.05}$

These stresses can be calculated using:

$$\sigma_{ct} = \frac{M_{Ed}}{W_{bot}} + \frac{N_{Ed}}{A_c}$$

Due to the pre-stress the axial force is always compressive. Now for each limit state the highest stress can be computed:

$$\sigma_{ct,quas} = \frac{M_{Ed,quas}}{W_{bot}} + \frac{N_{Ed,quas}}{A_c} = \frac{1856}{W_{bot}} + \frac{-15565}{A_t} = -2.80 \text{ MPa}$$

$$\sigma_{ct,quas} < 0.00$$

So ,the SLS-quas check is O.K.

$$\sigma_{ct,freq} = \frac{M_{Ed,freq}}{W_{bot}} + \frac{N_{Ed,freq}}{A_c} = \frac{8893}{W_{bot}} + \frac{-18236}{A_t} = -0.89 \text{ MPa}$$

$$\sigma_{ct,freq} < 1.10$$

So, the SLS-freq check is O.K.

$$\sigma_{ct,char} = \frac{M_{Ed,char}}{W_{bot}} + \frac{N_{Ed,char}}{A_c} = \frac{11397}{W_{bot}} + \frac{-18403}{A_t} = -0.04 \text{ MPa}$$

$$\sigma_{ct,char} < 1.10$$

So, the SLS-char check is O.K.

Compression checks

Next to the tension stress, the compressive stress in the bridge at t=0 should not exceed the compression strength. This check is performed in SLS-quasi permanent, because that is representative of the forces acting at t=0. The maximum compressive stress can be calculated similar like before looking at both the situation with maximum compressive force and max moment to find:

$$\sigma_c = -\frac{M_{Ed}}{W_{top}} + \frac{N_{Ed}}{A_c} = 6.12 \text{ MPa}$$

Concluding with the unity check:

$$\text{u.c}_{compr} = \frac{\sigma_c}{f_{cd}} = \frac{6.12}{23} = 0.26$$

Annex K: SLS Girder main tension stress

In this chapter the main tension stress in the girder will be calculated in accordance with NSRL1015, to limit crack formation at the haunch. The main stress will ocur just above the haunch at the inner wall of the girder and should be checked at 0.8d and 2d away from the bearing cross-sections. At x < 0.8d the forces are expected to be carried to the support directly and at x = 2d the shear force is expected to change sign. The location of the main tension stress is shown in figure 42.

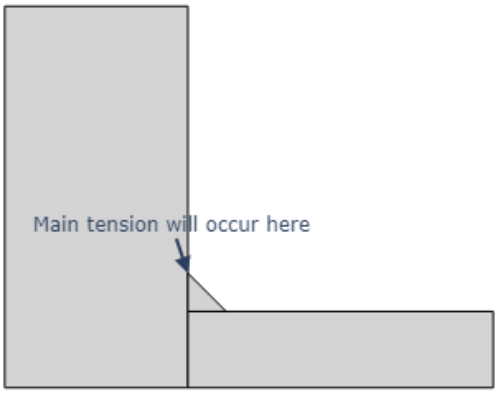

Figure 42: Location of main tension stress

The load combinations with both max V_z and max M_x and at both locations have been checked. The decisive combination is shown here at x = 1.90 m and with load combination: CO73 and effective width b_{eff} = 3392 mm. The main tension stress consists of thee components.

- σ_{xx} is the stress component caused normal force and moment by external loading and pre-stress
- σ_{zz} is the stress component caused by suspension forces and fixed end moments simillarly to how it was calculated for the stirrups
- τ is the stress component caused by torsion and mobile loads and shear force caused by external loading and pre-stress

These stresses are combined to find the main concrete tension stress.

σxx

First the stress the normal force and moment in the girder are obtained. The normal force in the girder is the normal force in the floor integrated over half the width of the floor plus the normal force in the girder. The moment M_{Ed} = 3354 kNm is obtained directly from the girder as the moment from the floor is already integrated.

$$N_{\text{tot}} = N_{\text{gir}} + N_{\text{x,floor}} = -15795 - 667 = -16461 \text{ kN}$$

The stresses due to normal force and moment can now be computed, with those stresses the stress at the haunch can be calculated. For this calculation the cross-sectional properties of half the cross-section of the whole bridge have been used to compute the stress for one girder.

$$\sigma_{\text{xx,N}} = \frac{N_{\text{tot}}}{A_{\text{bridge/2}}} = -3.65 \text{ MPa}$$

$$\sigma_{\text{xx,M}} = \frac{zM_{\text{y}}}{I_{\text{bridge/2}}} = -0.00 \text{ MPa}$$

Where z = -229 mm is the distance between the neutral line of the cross-section and the top of the haunch, such that:

$$\sigma_{\text{xx}} = \sigma_{\text{xx,N}} + \sigma_{\text{xx,M}} = -3.65 \text{ MPa}$$

σzz

σ_{zz} is caclculated similar to how the suspension and hanging forces were determined for the ULS girder calculations. From there it is obtained that N_{tot} = 193 kN. The moment is also calculated in the same way. However for the main tension stress only mobile loads should be considered as the other loads are present over the whole bridge length and will not cause the main tension stresses. In this way $M_{fixed\ end}$ = 589 kNm. The stress diagrams are shown in figure 43. Also the same reduction factor as for the stirrup calculation may be used.

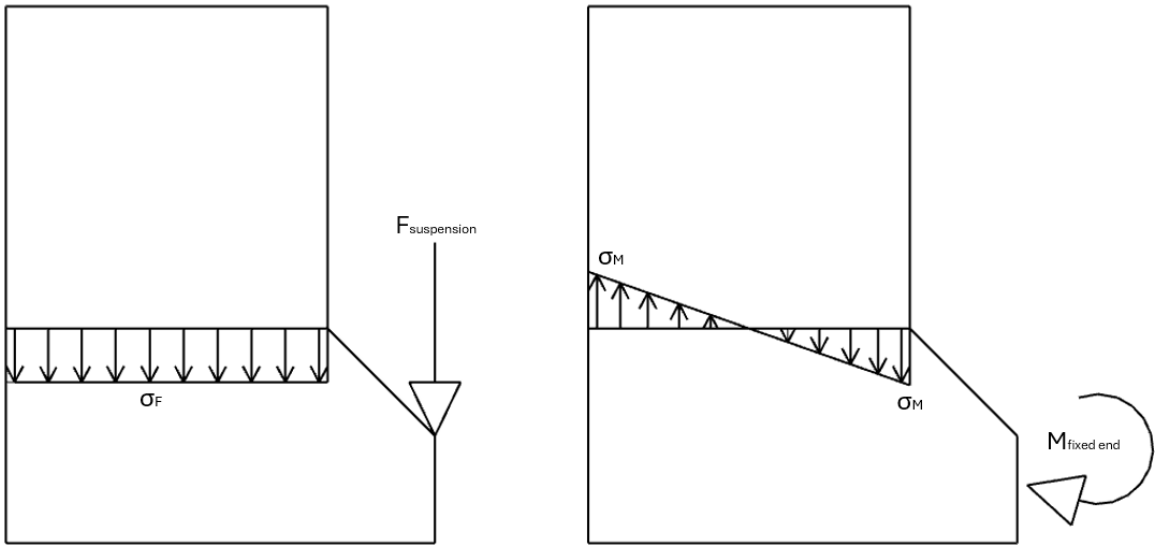

Figure 43: Stress distribution in cross-section

The stress distribution can now be calculated:

$$\sigma_{zz,M} = \frac{M_{\text{fixed end}}\alpha_A}{\frac{1}{6}W_{gir}^2} = 1.63\ \text{MPa}$$

$$\sigma_{zz,N} = \frac{N_{tot}\alpha_A}{W_{gir}} = 0.11\ \text{MPa}$$

With these results the total σ_{zz} = 1.74 MPa can be determined.

τ

τ consists of two parts, one is the shear force that causes a stress at the haunch and the other is the torsion in the girder. First the stress due to shear is calculated, using the FEM result V_{Ed} = 1386 kN.To get the shear stress at the haunch section the sectional modulus $S_{A,haunch}$ is calculated.

With this sectional modulus the stress can be calculated using:

$$\tau_V = \frac{V_{Ed} S_{A,haunch}}{I W_{gir}} = 0.43 \text{ MPa}$$

The stress due to torsion can be calculated simillarly to how the torsional shear stress was calculated for the stirrups using NEN-EN 1992-1-1 using the same t_{eff} and A_k and the FEM result T_{Ed} = 630 kNm, such that:

$$\tau_T = \frac{M_{Ed}}{2 A_k t_{eff}} = 1.04 \text{ MPa}$$

Now the total tau is computed as τ = 1.04 MPa

Evaluation

From all the calculated stress components the total tension stress at the haunch can be calculated.

$$\sigma_{ct} = \frac{1}{2}(\sigma_{xx} + \sigma_{zz}) + \sqrt{\frac{1}{4}(\sigma_{xx} - \sigma_{zz})^2 + \tau^2} = 0.80 \text{ MPa}$$

This stress should be lower than $0.6f_{ctd}$.

$$\text{u.c}_{\text{main tension}} = \frac{\sigma_{ct}}{0.6f_{ctd}} = \frac{0.80}{0.88} = 0.91$$

Annex L: SLS Crack width floor

This section covers the calculation of crack width in the floor both in longitudinal and transverse direction. The calculation method of NEN-EN 1992-1-1 formulas 7.8-7.9 has been used to find the maximum crack-width. According to OVS crack-width should be checked in SLS-freq.

Longitudinal

First the stress in the steel should be determined that occurs at M_{rep} = 359 kNm and N_{rep} = 63 kN. The steel stress can be determined when satisfying both ΣM = 0 and ΣN = 0. The result is calculated using an automatic algorithm and shown in figure 44 and 44.

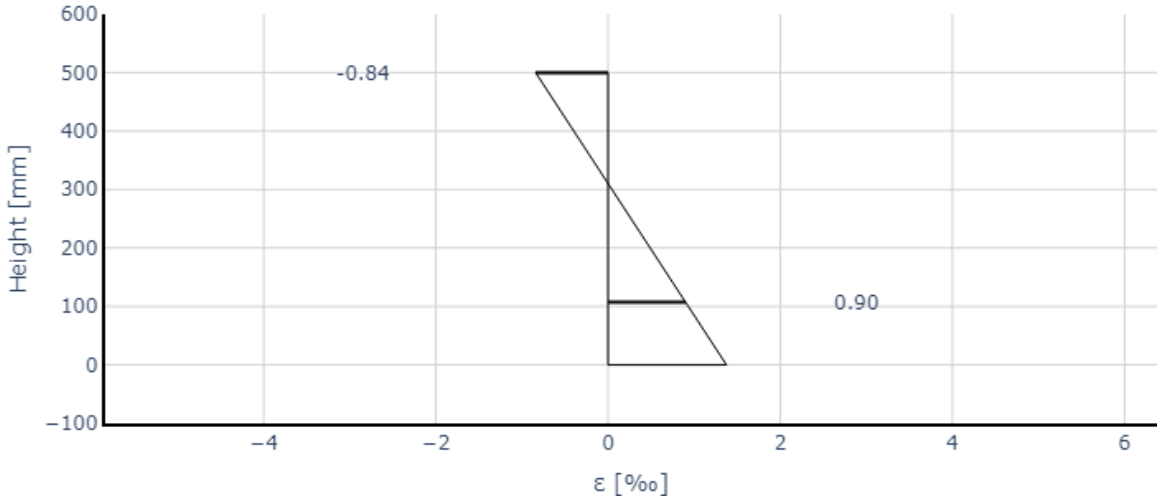

Figure 44: Strain diagram

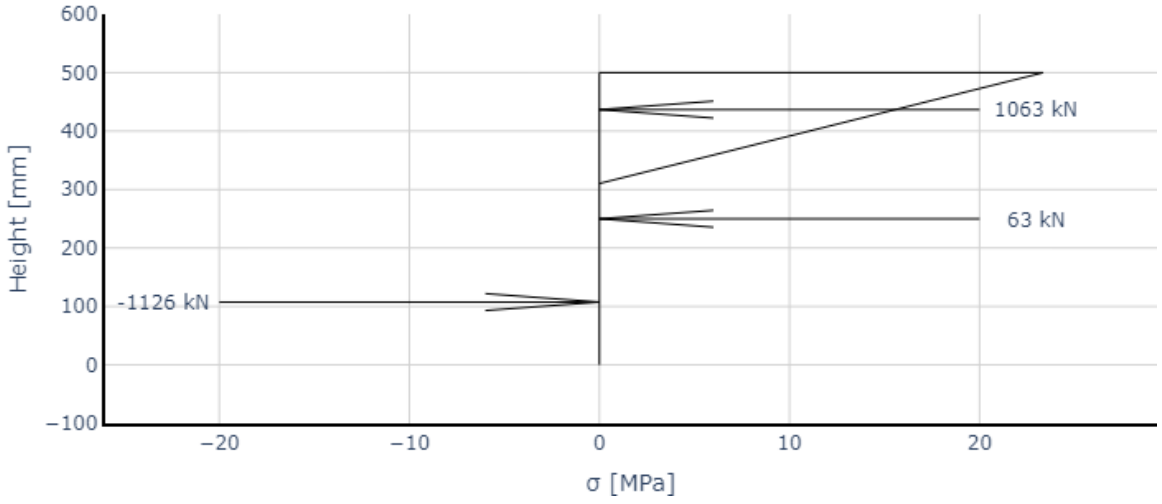

Figure 45: Stress diagram

To support these diagrams the following calculations have been made.

$$N_c = \alpha\sigma_s(\varepsilon)w_{gir}x = 1063 \text{ kN}$$

Here α = 0.50, x = 190 mm and. σ_c = 11.21 MPa at ε_c = 0.84 ‰.
The force in the steel can be calculated using:

$$N_s = A_s \cdot \sigma_s = 1126 \text{ kN}$$

Where σ_s = 189 MPa. This way both the moment and force equilibirum are statisfied knowing z = d_s - βx = 329 mm.

Now that the steel stress is known ε_{sm} - ε_{cm} can be determined with 7.9:

$$\varepsilon_{sm} - \varepsilon_{cm} = \frac{\sigma_s - k_t \frac{f_{ct,eff}}{\rho_{p,eff}}(1 + \alpha_e \rho_{p,eff})}{E_s} \geq 0.6 \frac{\sigma_s}{E_s} = 0.76 \text{ ‰}$$

Where α_e = 5 (OVS), k_t = 0.4 (long term loading) and:

$$\rho_{p,eff} = \frac{A_s}{A_{c,eff}} = 0.06$$

Where $A_{c,eff}$ = 103448 mm^2.

Also $s_{r,max}$ needs to be calculated with formula 7.11 to find the maximum crack-width.

$$s_{r,max} = k_3 c + \frac{k_1 k_2 k_4 \varnothing_{eq}}{\rho_{p,eff}} = 241 \text{ mm}$$

Where: k_1 = 0.8 assuming good bond conditions, k_3 = 3.4, k_4 = 0.425. Also:

$$\varnothing_{eq} = \frac{n_1 \varnothing_1^2 + n_2 \varnothing_2^2}{n_1 \varnothing_1 + n_2 \varnothing_2} = 18 \text{ mm}$$

And:

$$k_2 = \frac{\varepsilon_1 + \varepsilon_2}{2\varepsilon_1} = 0.50$$

Now finally w_k can be calcualted with formula 7.8:

$$w_k = s_{r,max}(\varepsilon_{sm} - \varepsilon_{cm}) = 0.18 \text{ mm}$$

To conclude with the unity check for crack-width using k_x = c / c_{nom} = 1.00:

$$\text{u.c}_{cw,y} = \frac{w_k}{k_x w_{allowed}} = \frac{0.18}{0.20} = 0.92$$

Transverse

For the transverse direction the same calculations can be made: M_{rep} = 126 kNm and N_{rep} = 47 kN. The stress and strain diagrams are shown in figure 46 and 46.

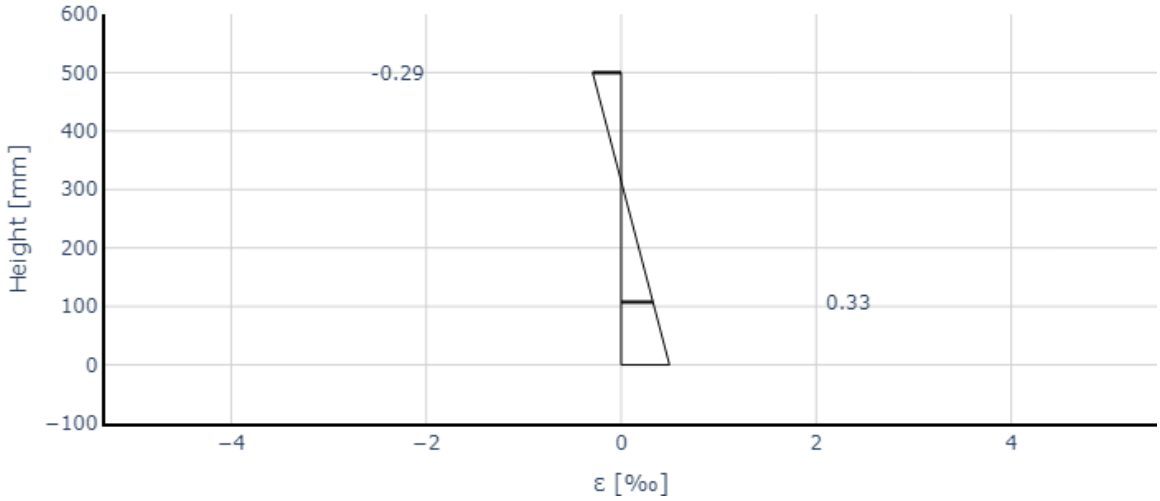

Figure 46: Strain diagram

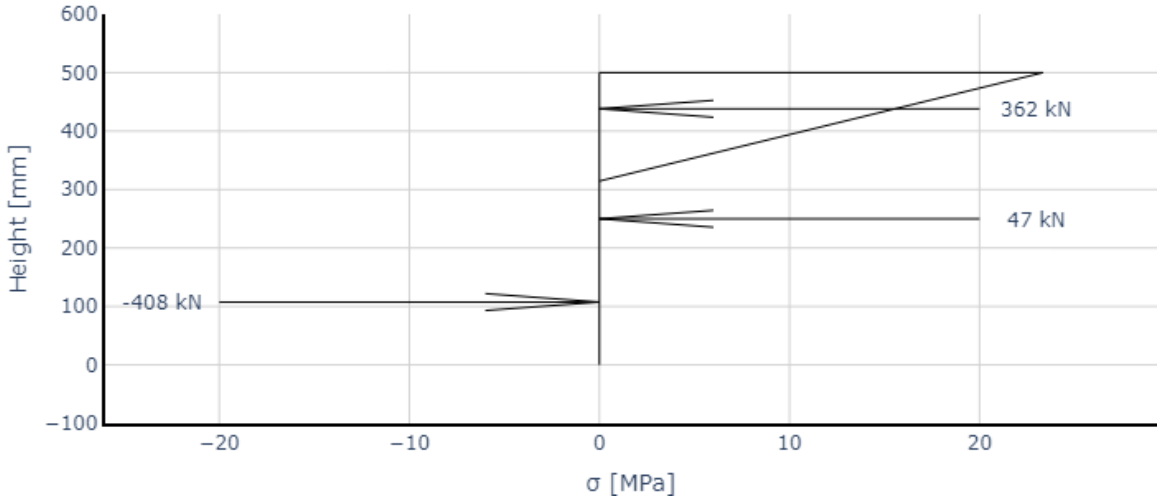

Figure 47: Stress diagram

$$N_c = \alpha \sigma_s(\varepsilon) w_{gir} x = 362 \text{ kN}$$

Here α = 0.50, x = 186 mm and. σ_c = 3.90 MPa at ε_c = 0.29 ‰.

$$N_s = A_s \cdot \sigma_s = 408 \text{ kN}$$

Where σ_s = 68 MPa. This way both the moment and force equilibirum are statisfied knowing z = d_s - βx = 331 mm.

$$\varepsilon_{sm} - \varepsilon_{cm} = \frac{\sigma_s - k_t \frac{f_{ct,eff}}{\rho_{p,eff}}(1 + \alpha_e \rho_{p,eff})}{E_s} \geq 0.6 \frac{\sigma_s}{E_s} = 0.20 \text{ ‰}$$

Where α_e = 5 (OVS), k_t = 0.4 (long term loading) and:

$$\rho_{\text{p,eff}} = \frac{A_{\text{s}}}{A_{\text{c,eff}}} = 0.06$$

Where $A_{c,eff}$ = 104829 mm^2.

And:

$$s_{\text{r,max}} = k_3 c + \frac{k_1 k_2 k_4 \varnothing_{\text{eq}}}{\rho_{\text{p,eff}}} = 242 \text{ mm}$$

Where: k_1 = 0.8 assuming good bond conditions, k_3 = 3.4, k_4 = 0.425. Also:

$$\varnothing_{\text{eq}} = \frac{n_1 \varnothing_1^2 + n_2 \varnothing_2^2}{n_1 \varnothing_1 + n_2 \varnothing_2} = 18 \text{ mm}$$

And:

$$k_2 = \frac{\varepsilon_1 + \varepsilon_2}{2\varepsilon_1} = 0.50$$

To find w_k:

$$w_{\text{k}} = s_{\text{r,max}}(\varepsilon_{\text{sm}} - \varepsilon_{\text{cm}}) = 0.05 \text{ mm}$$

To conclude with the unity check for crack-width in transverse direction using k_x = c / c_{nom} = 1.00:

$$\text{u.c}_{\text{cw,x}} = \frac{w_{\text{k}}}{k_{\text{x}} w_{\text{allowed}}} = \frac{0.05}{0.20} = 0.24$$